

2020-01-01

## Isolation And Characterization Of $\alpha$ -Gal-Containing Extracellular Vesicles (evs) From Three Major Genotypes Of Trypanosoma Cruzi: Potential Biomarkers Of Chagas Disease

Nasim Karimi Hosseini  
*University of Texas at El Paso*

Follow this and additional works at: [https://scholarworks.utep.edu/open\\_etd](https://scholarworks.utep.edu/open_etd)



Part of the [Allergy and Immunology Commons](#), [Biology Commons](#), [Immunology and Infectious Disease Commons](#), and the [Medical Immunology Commons](#)

---

### Recommended Citation

Hosseini, Nasim Karimi, "Isolation And Characterization Of  $\alpha$ -Gal-Containing Extracellular Vesicles (evs) From Three Major Genotypes Of Trypanosoma Cruzi: Potential Biomarkers Of Chagas Disease" (2020). *Open Access Theses & Dissertations*. 2986.  
[https://scholarworks.utep.edu/open\\_etd/2986](https://scholarworks.utep.edu/open_etd/2986)

This is brought to you for free and open access by ScholarWorks@UTEP. It has been accepted for inclusion in Open Access Theses & Dissertations by an authorized administrator of ScholarWorks@UTEP. For more information, please contact [lweber@utep.edu](mailto:lweber@utep.edu).

ISOLATION AND CHARACTERIZATION OF  $\alpha$ -GAL-CONTAINING  
EXTRACELLULAR VESICLES (EVS) FROM THREE MAJOR  
GENOTYPES OF *TRYPANOSOMA CRUZI*: POTENTIAL  
BIOMARKERS OF CHAGAS DISEASE

NASIM KARIMI HOSSEINI  
Doctoral Program in Bioscience

APPROVED:

---

Igor C. Almeida, D.Sc., Chair

---

Siddhartha Das, Ph.D.

---

Charles T. Spencer, Ph.D.

---

Sukla Roychowdhury, Ph.D.

---

Chuan Xiao, Ph.D.

---

Stephen L. Crites, Jr., Ph.D.  
Dean of the Graduate School

Copyright ©

by

Nasim Karimi Hosseini

2020

## **Dedication**

I dedicate my dissertation to my dear family, my sister Negin, my mom Maryam, and my dad Mahmoud, and to my dearest husband, Neftali.



ISOLATION AND CHARACTERIZATION OF  $\alpha$ -GAL-CONTAINING  
EXTRACELLULAR VESICLES (EVS) FROM THREE MAJOR  
GENOTYPES OF *TRYPANOSOMA CRUZI*: POTENTIAL  
BIOMARKERS OF CHAGAS DISEASE

by

NASIM KARIMI HOSSEINI, AAC, BSc, MSc

DISSERTATION

Presented to the Faculty of the Graduate School of  
The University of Texas at El Paso  
in Partial Fulfillment  
of the Requirements  
for the Degree of

DOCTOR OF PHILOSOPHY

Department of Biological Sciences  
THE UNIVERSITY OF TEXAS AT EL PASO  
May 2020

## ACKNOWLEDGEMENTS

I would like to firstly thank Dr. Igor C. Almeida, my mentor, for supporting me throughout my Ph.D. I would like to thank my committee members as well, Dr. Charles T. Spencer, Dr. Siddhartha Das, Dr. Sukla Roychowdhury, and Dr. Chuan Xiao in this process. I would also like to thank my advocate Dr. Marc B. Cox, and Dr. Almeida's previous and current students specially Susana Portillo and Maria Tays Mendes for their great help and support. I would like to thank Biological Science staff, faculty, and core facilities.

Also, I would like to acknowledge the BBRC, the National Institute on Minority Health and Health Disparities (NIMHD: Grant no. 2G12MD007592), The Frank B. Cotton Trust Scholarship, and The Allien and Paul C. Davidson Scholarship for their financial support.

Last but not least, I would like to greatly thank my amazing husband, Neftali, who has been there for me throughout this journey and has been extremely supportive and patient with me perusing my Ph.D. I would like to thank my sister Negin, my mom Maryam, and my dad Mahmoud, for encouraging me not only during my Ph.D., but my undergraduate and graduate studies, and my whole life.

## ABSTRACT

Chagas disease (ChD) is a neglected tropical disease (NTD) caused by the protozoan parasite, *Trypanosoma cruzi*. It is transmitted by the insect-vector triatomine (popular known as kissing bug), blood transfusion, organ transplantation, congenitally, and contaminated foods and juices. *T. cruzi* has evolved several strategies to invade the host cells, including the release extracellular vesicles (EVs), which assist pathogen survival and its replication within the host. *T. cruzi* is covered with highly glycosylated surface molecules such as glycoproteins and glycolipids, which are shown to be involved in the interaction with host immune cells. These molecules are highly immunogenic and reactive with chronic patients' sera, eliciting a strong anti-parasitic immune response, which includes the production of the highly abundant, immunodominant, and protective anti- $\alpha$ -Gal antibodies, which are critical for controlling the parasitemia in the chronic phase of ChD.  $\alpha$ -Gal-Containing glycoconjugates are also released through EVs from the parasite, indicating therefore that these vesicles might play an important role in persistence of *T. cruzi* in the mammalian host and evasion from host immunity. Our **first hypothesis** is that *T. cruzi* virulence factors released in extracellular vesicles (EVs) are highly antigenic and reactive with sera from chronic Chagas disease (ChD) patients and could be used as biomarkers for reliable diagnosis of ChD. Our **second hypothesis** is that major *T. cruzi* virulence factors (e.g., proteins and glycoproteins) and bioactive molecules (e.g., lipids) are differentially secreted in EVs from major parasite genotypes with distinct virulence and pathogenic traits (**Specific Aim 1**). Our **third hypothesis** is that *T. cruzi* EVs from major parasite genotypes could differentially modulate host-cell infection rate in vitro in a dose- and time-dependent manner (**Specific Aim 2**). In order to address the first and second hypotheses, TCT-Secr,  $\alpha$ -Gal-enriched EVs ( $\alpha$ -Gal(+) TCT-EVs) and  $\alpha$ -Gal-depleted EVs ( $\alpha$ -Gal(-) TCT-EVs) present in the TCT-Secr, from different parasite

genotypes and strains, will be tested against ChD human serum pool (ChHSP), normal human serum pool (NHSP), and anti  $\alpha$ -Gal Abs for the reactivity against these sera. We will then perform proteomic and lipidomic analysis of TCT-Secr,  $\alpha$ -Gal(+) TCT-EVs and  $\alpha$ -Gal(-) TCT-EVs from different parasite genotypes and strains to study the protein and lipid composition of these fractions (**Specific Aim 1**). Thereafter, to address the third hypothesis, we will measure the *T. cruzi* infection *in vitro* (% of infected cells, and number of the parasites per infected cells) with different parasite genotypes and strains, after pre-treatment of the cells with TCT-Secr and TCT-EVs (**Specific Aim 2**). Here, we have observed that TCT-Secr and TCT-EVs derived from *T. cruzi* infective forms from three major genotypes are highly enriched with  $\alpha$ -Gal epitopes, and are highly reactive with chronic ChD. We have been able to successfully purify and enrich these epitopes ( $\alpha$ -Gal(+) TCT-EVs) by performing immunoaffinity chromatography (IAC) utilizing a lectin which specifically binds to  $\alpha$ -Gal epitopes. These purified  $\alpha$ -Gal(+) fractions showed high reactivity with Ch anti  $\alpha$ -Gal Ab in comparison with the fractions ( $\alpha$ -Gal(-)) depleted of the  $\alpha$ -Gal epitopes. The proteomic analysis of the TCT-Secr and TCT-EVs has shown that the parasites release various *T. cruzi* surface glycosylphosphatidylinositol (GPI)-anchored glycoproteins such as mucins of the TcMUC II family, *trans*-sialidases (TS), mucin-associated surface proteins (MASP), GP63, and other glycoproteins that are involved in invasion of host cells and evasion from the host immune system. The proteomic analysis of  $\alpha$ -Gal(+) TCT-EVs showed that TcMUCII mucins are a major component of those EVs. TcMUCII mucins have been previously shown to be  $\alpha$ -galactosylated. The  $\alpha$ -Gal(-) TCT-EVs, on the other hand, were enriched with the glycoproteins previously known to contain little or no  $\alpha$ -Gal epitopes such as TS, MASP, and GP63 families. Furthermore, we have found various lipid species involved in the parasite's virulence in the TCT-Secr and TCT-EVs, such as plasmalogens (various ether-phosphatidylcholine (PCE) and ether-

phosphatidylethanolamine (PEe) species), as well as *lyso*-phosphatidylcholine (LPC). Plasmalogens are known to be involved in membrane bending and EV fusion, and LPCs are known to have platelet-activating factor (PAF)-like activity, which could be involved in pathophysiology of ChD. Finally, we have observed a significant increase in host-cell infection rate as well in the number of parasites per cell after pre-treatment with TCT-Secr. Taken together, our results strongly indicate that the TCT-EVs could function as a mechanism of immune evasion, by capturing the highly abundant anti- $\alpha$ -Gal antibodies, and as virulence factor, by making the cells more susceptible to infection.

# TABLE OF CONTENTS

ACKNOWLEDGEMENTS .....	v
ABSTRACT .....	vi
TABLE OF CONTENTS .....	ix
LIST OF TABLES .....	xiv
LIST OF FIGURES .....	xv
CHAPTER 1: GENERAL INTRODUCTION.....	1
1.1. Chagas Disease and <i>Trypanosoma cruzi</i> .....	1
1.2. <i>T. cruzi</i> genotypes .....	4
1.3. Extracellular vesicles (EVs) .....	6
1.4. <i>T. cruzi</i> extracellular vesicles (EVs) .....	8
1.5. Hypothesis, Significance, and Specific Aims.....	14
CHAPTER 2: TCT-EVS AS DIAGNOSTIC BIOMARKERS .....	18
2.1. Introduction: <i>T. cruzi</i> Highly Immunogenic Surface Glycoproteins .....	18
2.2. Materials and Methods.....	18
2.2.1. Mammalian cell culture .....	18
2.2.2. Parasite culture, and isolation and storage of trypomastigote-derived secretome (TCT-Secr) and TCT-extracellular vesicles (TCT-EVs).....	19
2.2.3. Fractionation of TCT-Secr by Size-Exclusion Chromatography (SEC) .....	20
2.2.4. Bicinchoninic Acid (BCA) Protein Assay .....	21
2.2.5. Immunoblotting the TCT-Secr with IB4-lectin, and purified Ch anti- $\alpha$ -Gal Abs .....	21
2.2.6. Silver staining .....	22
2.2.7. Affinity chromatography using immobilized <i>Bandeiraea simplicifolia</i> isolectin 4 (IB4)-lectin for enrichment of $\alpha$ -Gal-containing TCT-EVs .....	23
2.2.8. Analysis of TCT-Secr with Ch and NHS sera .....	24
2.3. Results.....	27
2.3.1. TCT-EVs were detected through NTA in TCT-Secr and -80 showed to be the most suitable storage temperature for them .....	27
2.3.2. Fractionation of TCT-Secr by SEC and BCA analysis .....	30

2.3.3. The peaks of TCT-Secr proteins were shown to be between fractions 17 and 25 of SEC .....	31
2.3.4. TCT-Secr showed high reactivity with ChD serum .....	32
2.3.5. TCT-Secr derived from different batches of Y, Col and CLB showed high reactivity with ChD serum .....	33
2.3.6. TCT-Secr derived from Col, Y, and CLB showed high reactivity with ChD serum after being stored at -80° C compared to freshly isolated TCT-Secr .....	35
2.3.7. SEC-fractionated TCT-EVs derived from Col, Y and CLB showed the highest reactivity with ChD serum from fractions 12 to 20 .....	36
2.3.8. Reactivity of TCT-Secr with ChHSP in Col, Y and CLB strains is in great part due to $\alpha$ -Gal glycotopes .....	38
2.3.9. Purified $\alpha$ -Gal-containing TCT-EVs showed distinguishable profile in NTA than the total TCT-Secr .....	39
2.4. Discussion and Future Work .....	42
CHAPTER 3: PROTEOMIC ANALYSIS OF <i>T. CRUZI</i> -DERIVED EVS .....	44
3.1. Introduction: <i>T. cruzi</i> Surface Proteins .....	44
3.2. Materials and Methods .....	46
3.2.1. Mammalian cell culture .....	46
3.2.2. Parasite culture, and isolation and storage of extracellular vesicles (EVs) .....	46
3.2.3. BCA Protein Assay .....	47
3.2.4. Western blotting the TCT-Secr with IB4-lectin, and purified Ch anti $\alpha$ -Gal Ab .....	47
3.2.5. Silver staining .....	48
3.2.6. Affinity chromatography using immobilized IB4-lectin for enrichment of $\alpha$ -Gal-containing TCT-EVs .....	49
3.2.7. Protein digestion and proteomic analysis of EV samples .....	49
3.3. Results .....	50
3.3.1. Strong binding of TCT-Secr derived from Col, Y and CLB was shown with purified Ch anti $\alpha$ -Gal Ab and IB4-lectin in western blot .....	50
3.3.2. Purified $\alpha$ -Gal-containing TCT-EVs showed distinguishable profile in NTA than the total TCT-Secr .....	54
3.3.3. Proteomic analysis of the TCT-Secr and TCT-EVs derived from Y, Col and CLB strains show TcMUC II, MASP, TS, and other EV-associated proteins .....	55
3.3.4. Proteomic analysis of the TCT-Secr and TCT-EVs $\alpha$ -Gal+ and $\alpha$ -Gal-derived from Col, and Y strains show consistency with previous results .....	61
3.4. Discussion and Future Work .....	63

CHAPTER 4: LIPIDOMIC ANALYSIS OF <i>T. CRUZI</i> -DERIVED EVS .....	75
4.1. Introduction: Lipid composition in <i>T. cruzi</i> .....	75
4.2. Materials And Methods.....	76
4.2.1. Mammalian cell culture .....	76
4.2.2. Parasite culture, and isolation and storage of extracellular vesicles (EVs).....	76
4.2.3. BCA Protein Assay .....	77
4.2.4. Fractionation of TCT-Secr by Size-Exclusion Chromatography (SEC) .....	77
4.2.5. Analysis of SEC fractionated-TCT-Secr with Ch and NHS sera, as well as Anti $\alpha$ -Gal Ab .....	77
4.2.6. Affinity chromatography using immobilized IB4-lectin for enrichment of $\alpha$ -Gal-containing TCT-EVs .....	78
4.2.7. Lipid extraction .....	78
4.2.8. Structural characterization of negatively charged lipid species by tandem electrospray ionization-linear ion trap-mass spectrometry (ESI-LIT-MS) .....	79
4.3. Results .....	80
4.3.1. SEC fractions 2 to 5 of TCT-Secr were chosen as pre-enriched $\alpha$ -Gal+ fractions before performing IB4-lectin column .....	80
4.3.2. Lipidomic analysis showed various lipid classes in TCT-Secr derived from Col, Y and CLB .....	84
4.3.3. Various lysophosphatidylcholine, and Plasmalogen species have been isolated from TCT-Secr derived from Col, Y and CLB .....	86
4.3.4. Various further negatively charged lipid classes have been isolated in TCT- Secr, being significantly higher in TCT-Secr derived from CLB compared to Col and Y. ....	88
4.3.5. Further negatively charged lipid classes have been isolated in TCT-Secr derived from Col, Y and CLB, including Cholesterol Sulfate and Fatty acids ..	91
4.4. Discussion and future work .....	92
CHAPTER 5: INFECTION ASSAY AFTER TREATMENT WITH TCT-SECR/ EVS.....	96
5.1. Introduction: <i>T. cruzi</i> -derived EVs effect on parasitic infection.....	96
5.2. Materials And Methods.....	97
5.2.1. Mammalian cell culture .....	97
5.2.2. Parasite culture, and isolation of extracellular vesicles (EVs).....	98
5.2.3. BCA Protein Assay .....	98
5.2.4. Infection assay after treatment with TCT-Secr derived from Col, Y and CLB.....	98



5.3. Results .....	100
5.3.1. Treatment with TCT-Secr increased the infection (% of parasitemia) with <i>T. cruzi</i> respective strains .....	100
5.3.2. Treatment with TCT-Secr increased the number of the parasites per infected cells after infection with <i>T. cruzi</i> respective strains .....	103
5.3.3. Infection with live-CFSE stained TCT is promising for stablishing HCI protocol for <i>T. cruzi</i> infection assay .....	105
5.4. Discussion and future work .....	107
6. REFERENCES .....	109
7. LIST OF APPENDICES .....	138
Appendix A: Proteins identified in the TCT-Secr from Col, Y, and CLB strains. Values are expressed as average of normalized weighted spectrum counts. ....	138
Appendix B: TcMUC II family members identified in the TCT-Secr and IB-4 lectin column fractions, $\alpha$ -Gal(-) and $\alpha$ -Gal(+), from <i>T. cruzi</i> Col strain. Values are expressed as average of normalized weighted spectrum counts. ....	188
Appendix C: MASP family members identified in the TCT-Secr and in the IB4-lectin column fractions, $\alpha$ -Gal(-) and $\alpha$ -Gal(+), from <i>T. cruzi</i> Col strain. Values are expressed as average of normalized weighted spectrum counts. ....	190
Appendix D: TS Family Members identified in TCT-Secr and in the IB4-lectin column fractions, $\alpha$ -Gal(+) and $\alpha$ -Gal(-), from Col strain. Values are expressed as average of normalized weighted spectrum counts. ....	198
Appendix E: GP63 family members Identified in the TCT-Secr and IB-4 lectin column fractions, $\alpha$ -Gal(-) and $\alpha$ -Gal(+), from <i>T. cruzi</i> Col strain. Values are expressed as average of normalized weighted spectrum counts. ....	209
Appendix F: : TcMUC II family members identified in the TCT-Secr and IB-4 lectin column fractions, $\alpha$ -Gal(-) and $\alpha$ -Gal(+), from <i>T. cruzi</i> Y strain. Values are expressed as average of normalized weighted spectrum counts. ....	211
Appendix G: MASP family members identified in the TCT-Secr and in the IB4-lectin column fractions, $\alpha$ -Gal(-) and $\alpha$ -Gal(+), from <i>T. cruzi</i> Y strain. Values are expressed as average of normalized weighted spectrum counts. ....	215
Appendix H: TS Family Members identified in TCT-Secr and in the IB4-lectin column fractions, $\alpha$ -Gal(-) and $\alpha$ -Gal(+), from Y strain. Values are expressed as average of normalized weighted spectrum counts. ....	223
Appendix I: GP63 family members identified in the TCT-Secr and in the IB4-lectin column fractions, $\alpha$ -Gal(-) and $\alpha$ -Gal(+), from <i>T. cruzi</i> Y strain. Values are expressed as average of normalized weighted spectrum counts. ....	232

Appendix J: : TcMUC II family members identified in the TCT-Secr and IB-4 lectin column fractions, $\alpha$ -Gal(-) and $\alpha$ -Gal(+), from <i>T. cruzi</i> CLB strain. Values are expressed as average of normalized weighted spectrum counts. ....	234
Appendix K: MASP family members identified in the TCT-Secr and in the IB4-lectin column fractions, $\alpha$ -Gal(-) and $\alpha$ -Gal(+), from <i>T. cruzi</i> CLB strain. Values are expressed as average of normalized weighted spectrum counts. ....	237
Appendix L: TS Family Members identified in TCT-Secr and in the IB4-lectin column fractions, $\alpha$ -Gal(-) and $\alpha$ -Gal(+), from CLB strain. Values are expressed as average of normalized weighted spectrum counts. ....	241
Appendix M: GP63 family members identified in the TCT-Secr and in the IB4-lectin column fractions, $\alpha$ -Gal(-) and $\alpha$ -Gal(+), from <i>T. cruzi</i> CLB strain. Values are expressed as average of normalized weighted spectrum counts. ....	242
VITA.....	243

## LIST OF TABLES

<b>Table 3.1.</b> Proteases and peptidases identified by proteomic analysis in the total TCT-Sec, and flow-through and eluate fractions from the IB4-lectin column. ....	<b>Page 53</b>
--	----------------

## LIST OF FIGURES

<b>Figure 1.1.</b> <i>T. cruzi</i> life cycle. ....	<b>Page 3</b>
<b>Figure 1.2.</b> Estimated geographical distribution of <i>T. cruzi</i> DTUs I-VI. ....	<b>Page 5</b>
<b>Figure 1.3.</b> Schematic representation of three major types of extracellular vesicles: exosomes, ectosomes, and apoptotic bodies. ....	<b>Page 8</b>
<b>Figure 1.4.</b> Transmission electron (TEM), scanning (SEM), and atomic force microscopy (AFM) of <i>T. cruzi</i> trypomastigote EVs (TCT-EVs). ....	<b>Page 12</b>
<b>Figure 1.5.</b> <i>T. cruzi</i> extracellular vesicles from noninfective and infective insect-derived developmental forms. Upper panel. <b>Page 13</b>	
<b>Figure 2.1.</b> Preparation and analysis of TCT-Secr and TCT-EVs. ....	<b>Page 26</b>
<b>Figure 2.2.</b> NTA analysis of EVs derived from CLB <i>T. cruzi</i> trypomastigote. ....	<b>Page 28</b>
<b>Figure 2.3.</b> NTA analysis of EVs derived from <i>T. cruzi</i> trypomastigote after storing them at 4, -20, and -80°C. <b>Page 29</b>	
<b>Figure 2.4.</b> Protein concentration in 20 fractions and left-over proteins of the columns, after fractionation of EVs measured by BCA. ....	<b>Page 30</b>
<b>Figure 2.5.</b> Protein concentration in 20 fractions and left-over proteins of the columns, after fractionation of EVs measured by BCA. ....	<b>Page 31</b>
<b>Figure 2.6.</b> Protein concentration measured by BCA in fractions and leftover proteins from the Sepharose Cl-4B column, after fractionation of EVs. ....	<b>Page 32</b>
<b>Figure 2.7.</b> CL-ELISA reactivity of ChHSP and NHSP to TCT-Secr derived from Colombiana (Col) and Y strains. ....	<b>Page 33</b>
<b>Figure 2.8.</b> CL-ELISA reactivity of ChHSP and NHSP to various batches of TCT-Secr derived from of Y, Col and CLB. ....	<b>Page 34</b>
<b>Figure 2.9.</b> CL-ELISA reactivity of ChHSP and NHSP to TCT-Secr that were freshly isolated on the same day compared to TCT-Secr stored at -80°C (derived from of Col, Y, and CLB). ....	<b>Page 36</b>
<b>Figure 2.10.</b> BCA (A), and CL-ELISA reactivity of IB4-lectin (B), ChHSP (C), and NHSP (B,C) to TCT-Secr, derived from of Col, Y, and CLB, and fractionated by SEC. ....	<b>Page 37</b>
<b>Figure 2.11.</b> Reactivity of TCT-Secr from Col, Y and CLB strains to ChHSP and NHSP, following treatment with $\alpha$ -galactosidase. ....	<b>Page 38</b>
<b>Figure 2.12.</b> NTA analysis of TCT-Secr and EVs from Col, Y and CLB strains after being subjected to immunoaffinity chromatography. ....	<b>Page 40</b>
<b>Figure 2.13.</b> Reactivity of EL and FT fractions after IB4-lectin purification, against Ch anti- $\alpha$ -Gal. ....	<b>Page 41</b>
<b>Figure 3.1.</b> Schematic representation of <i>T. cruzi</i> trypomastigote surface coat and its GPI-anchored glycoconjugates. ....	<b>Page 45</b>
<b>Figure 3.2.</b> Blotting with IB4 Lectin and Ch anti- $\alpha$ -Gal, as well as staining with Silver stain. ....	<b>Page 52</b>
<b>Figure 3.3.</b> NTA analysis of TCT-Secr and TCT-EVs from Col, Y and CLB strains after being subjected to immunoaffinity chromatography. ....	<b>Page 54</b>
<b>Figure 3.4.</b> Proteomic analysis of TCT-Secr from Col, Y, and CLB strains. ....	<b>Page 56</b>

<b>Figure 3.5.</b> Heat map of 1,000 most abundant proteins found in the TCT-Secr of Col, Y, and CLB strains (zoomed in Figure 3.3). .....	<b>Page 57</b>
<b>Figure 3.6.</b> Proteomic analysis of TCT-Secr and IB4-lectin-purified TCT-EVs from <i>T. cruzi</i> Colombiana (Col) strain. ....	<b>Page 58</b>
<b>Figure 3.7.</b> Proteomic analysis of TCT-Secr and IB4-lectin-purified TCT-EVs from <i>T. cruzi</i> Y strain. .	<b>Page 59</b>
<b>Figure 3.8.</b> Proteomic analysis of TCT-Secr and IB4-lectin-purified TCT-EVs from <i>T. cruzi</i> Luc. CL Brener clone. ....	<b>Page 60</b>
<b>Figure 3.9.</b> Proteomic analysis of TCT-Secr, $\alpha$ -Gal(+) and $\alpha$ -Gal(-) derived from Col, and Y strains. ..	<b>Page 62</b>
<b>Figure 4.1.</b> Protein concentration measured by BCA in TCT-Secr fractioned by SEC. ....	<b>Page 81</b>
<b>Figure 4.2.</b> NTA analysis of SEC-derived TCT-Secr fractions 2 to 5 (isolated from Y strain) before being subjected to CL-ELISA and immunoaffinity chromatography in order to detect and enrich $\alpha$ -Gal epitopes.	<b>Page 82</b>
<b>Figure 4.3.</b> Detecting $\alpha$ -Gal enriched fractions in SEC Fractionated TCT-Secr by CL-ELISA prior to IB4-lectin chromatography. ....	<b>Page 83</b>
<b>Figure 4.4.</b> Various lipid classes have been detected in TCT-Secr derived from Col, Y and CLB TCTs.	<b>Page 85</b>
<b>Figure 4.5.</b> Various lysophosphatidylcholine species (LPCs) have been detected in TCT-Secr derived from Col, Y and CLB TCTs. ....	<b>Page 87</b>
<b>Figure 4.6.</b> Various Plasmalogen species (PEe and PCe species) have been detected in TCT-Secr derived from Col, Y and CLB TCTs. ....	<b>Page 88</b>
<b>Figure 4.7.</b> Various lipid classes have been detected in TCT-Secr, significantly higher in CLB-derived TCT-Secr in comparison with Col- and Y-derived TCT-Secr. ....	<b>Page 90</b>
<b>Figure 4.8.</b> Further lipid classes have been detected in TCT-Secr derived from Col, Y and CLB TCTs.	<b>Page 91</b>
<b>Figure 5.1.</b> Pre-treatment with TCT-Secr prior to <i>T. cruzi</i> infection resulted in increase in or of parasitemia (or increase in number of intracellular parasites or amastigotes). ....	<b>Page 101</b>
<b>Figure 5.2.</b> Infection with Col and Y strains. ....	<b>Page 102</b>
<b>Figure 5.3.</b> Pre-treatment with TCT-Secr prior to <i>T. cruzi</i> infection resulted in increase in or of number of the parasites per infected cells. ....	<b>Page 104</b>
<b>Figure 5.4.</b> Infection with parasites pre-stained with CFSE. ....	<b>Page 106</b>

## CHAPTER 1: GENERAL INTRODUCTION

### 1.1. CHAGAS DISEASE AND *TRYPANOSOMA CRUZI*

*Trypanosoma cruzi* is a protozoan parasite and the causative agent of Chagas disease (ChD), which is a neglected tropical disease affecting 21 countries in endemic areas in Latin America. Approximately, 6-8 million people are affected by ChD (Rassi, Rassi et al. 2010, Schmunis and Yadon 2010), and the number of cases reported has been increasing in nonendemic regions, such as the United States, Canada, Europe, Australia, and Japan mainly due to globalization and increased migratory movement (Bern and Montgomery 2009, Coura and Vinas 2010, Schmunis and Yadon 2010).

*Trypanosoma cruzi* is transmitted through the feces of infected hematophagous insect-vector (triatomine or reduviid bug, commonly known as kissing bug) during the blood meal, blood transfusion, organ transplantation, congenitally and consumption of contaminated food or drink (Schmunis and Yadon 2010, Sanchez and Ramirez 2013). The initial phase of infection will last for 4–8 weeks; however, the chronic phase may persist for the whole host's lifespan (Dias, Laranja et al. 1956, Committee 2002). The disease usually has an asymptomatic acute phase or may show a self-limiting illness with fever. Symptoms appear between one and two weeks after the infection, or up to a few months after infected blood being transfused (Rassi, Rassi et al. 2010). Acquired immunity controls the disease; however, 30%-40% of the patients go to a symptomatic chronic phase, developing heart disease and/or gastro-intestinal complications (Viotti, Vigliano et al. 2006). It causes 12,000-50,000 deaths per year due to heart failure and over 100 million people are under risk of infection. There are only two drugs available for ChD (nifurtimox and benznidazole) which are >90% effective during acute phase, and 60-80% effective during its

chronic phase. However, nifurtimox is not FDA-approved and benznidazole has recently been approved by FDA (Morrow 2017). There is no human vaccine available for ChD, despite many experimental attempts in the last several years (Bivona, Alberti et al. 2020).

There are four developmental stages in *T. cruzi* life cycle which are two stages present in the hematophagous insect vector (triatomine or reduviid bug) and two in the mammalian host (**Figure 1.1**). Epimastigotes are noninfective, replicative forms present in the vector's gut and they later differentiate into metacyclic trypomastigotes, which are nonreplicative, infective forms transmitted to mammals by the insect's excreta or through the oral route (Tyler and Engman 2001, Yoshida, Tyler et al. 2011). It has been shown that the levels of the circulating bloodstream trypomastigotes in ChD patients can vary from pediatric patients, from 1,000 parasites/ml to less than 1 parasite/ml, to 1,400 parasites/ml in reactivated ChD patients co-infected with HIV (Duffy, Bisio et al. 2009). Both parasite and host factors have influence on the disease's presentation, progression and differences in organ involvement (Dutra and Gollob 2008).

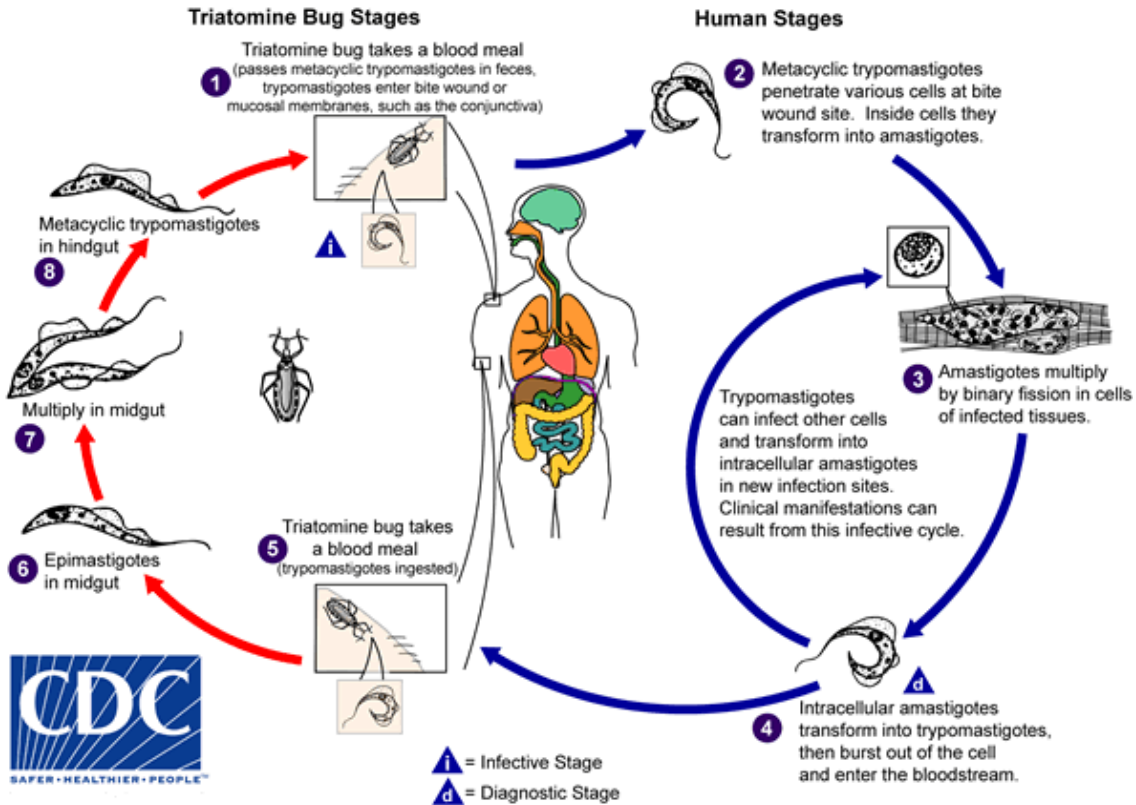


**Figure 1.1. *T. cruzi* life cycle.** An infected triatomine insect vector, known as kissing bug, takes a blood meal and defecates and trypomastigotes will be released in the feces near the site of the bite wound. Trypomastigotes enter the host via the wound or through intact mucosal membranes, such as the conjunctiva (1). The trypomastigotes invade cells near the site of inoculation inside the host, where they differentiate into intracellular amastigotes (2). The amastigotes multiply by binary fission (3) and differentiate into trypomastigotes, and then will be released into blood as bloodstream trypomastigotes (4). Trypomastigotes infect varieties of cells and transform into intracellular amastigotes in new infection sites. Replication resumes only when the parasites enter another cell or are ingested by another vector. The cycle continues by kissing bug feeding on human or animal blood that contains circulating parasites (5). The ingested trypomastigotes transform into epimastigotes in the vector’s midgut (6). The parasite multiplies and differentiates in the midgut (7) and differentiates into infective metacyclic trypomastigotes in the hindgut (8). Figure taken, and text modified and adapted from the CDC website (<https://www.cdc.gov/parasites/chagas/biology.html>).



## **1.2. *T. CRUZI* GENOTYPES**

Seven distinct discrete typing units (DTUs) (DTU I-VI and Tcbat) have been revealed in *T. cruzi* by multilocus genotyping, which partitioned from the two major subdivisions of DTU I and DTU II, identifiable by common genetic, immunological, geographical, or molecular markers (Tibayrenc 1998, Zingales, Andrade et al. 2009, Zingales, Miles et al. 2012, Zingales 2018, Jimenez, Jaimes et al. 2019) (**Figure 1.2**). DTU II was further split into five DTUs (IIa-e) based on congruent phylogenetic data from multilocus enzyme electrophoresis (MLEE) and random amplified polymorphic DNA (RAPD) markers (Brisse, Barnabe et al. 2000, Brisse, Verhoef et al. 2001). DTU I corresponds to *T. cruzi* I group and DTU IIb corresponds to *T. cruzi* II group, as recommended by original expert committee in 1990 (Brisse, Barnabe et al. 2000, Falla, Herrera et al. 2009). Recent studies show that four subdivisions have emerged within DTU I as well (Herrera, Bargues et al. 2007, Falla, Herrera et al. 2009), nevertheless they have been integrated into the nomenclature revision. On the other hand, it has been previously shown that the six DTUs have various geographical distribution as well as clinical symptoms (Zingales, Miles et al. 2012) (**Figure 1.2**). Therefore, it is important to study these DTUs in order to come to a more comprehensive and integrated approaches to understand the diverse *T. cruzi* virulence and ChD pathology.

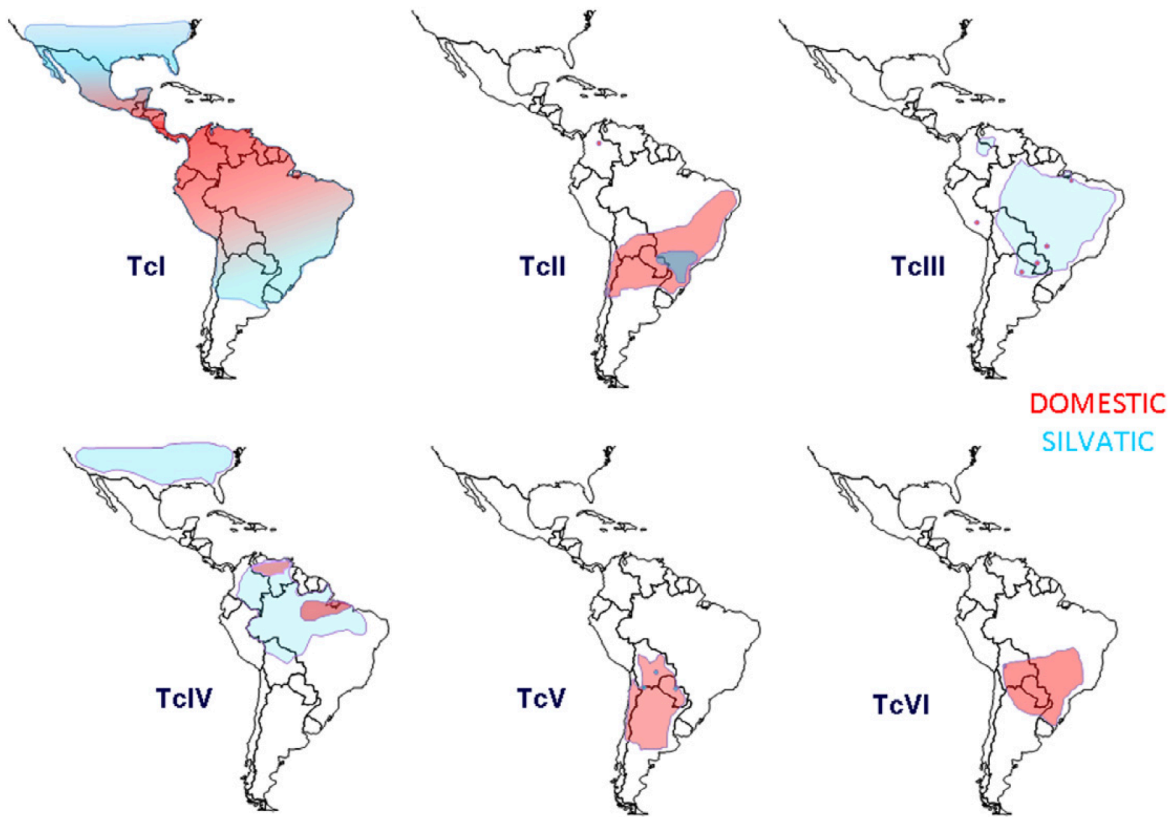


**Figure 1.2. Estimated geographical distribution of *T. cruzi* DTUs I-VI.** The geographical distribution of the seventh genotype, Tcbat, has not been included in this figure. However, this newest DTU has been reported in Colombia and Brazil associated to anthropogenic deaths (Jimenez, Jaimes et al. 2019). Figure taken from (Zingales, Miles et al. 2012).

### **1.3. EXTRACELLULAR VESICLES (EVs)**

Extracellular vesicles (EVs), which are secreted by both prokaryotic and eukaryotic cells, are small lipid vesicles which comprise proteins, nucleic acids, and small metabolites, which are essential for cell communication (Pilzer, Gasser et al. 2005, Ratajczak, Wysoczynski et al. 2006, Silverman, Clos et al. 2010, Raposo and Stoorvogel 2013, Turturici, Tinnirello et al. 2014, Kalra, Drummen et al. 2016) (**Figure 1.3**). EVs are favorable sources for being diagnostic markers due to their characteristics, and they have been referred to as biomarker “treasure chests” (Duijvesz, Luider et al. 2011). EVs can have their effect either locally or in distant tissues, depending on the targeted cell, in a paracrine or endocrine signaling manner. It has been shown that EVs released from infected cells with virus, bacteria, fungi or parasites play a crucial role in vast varieties of biochemical modifications in the host and pathogen such as modulating the immune system. Although in the early 80’ it was thought that exosomes were used as elements to excrement the waste materials in reticulocytes (Harding, Heuser et al. 2013), however they have been shown to have the ability of immune response stimulation or tolerance induction, as well as antigen presentation (Bobrie, Colombo et al. 2011, Chaput and Thery 2011). Thus, these traits make them attractive potential biomarkers for disease diagnosis and treatment follow-up.

Although EVs are heterogeneous in size and originally the term exosome was used for vesicles sized from 40 to 1000 nm (Trams, Lauter et al. 1981); however, based on their biogenesis, they are categorized into three different groups which are: exosomes (40–100 nm) with cup-shaped morphology (Raposo, Nijman et al. 1996), formed by exocytic fusion of multivesicular bodies (MVBs); ectosomes (100–1000 nm) or plasma membrane-derived EVs (microparticles) with heterogeneous morphology, formed by budding directly from the plasma membrane; and apoptotic bodies (1-4  $\mu$ m) with heterogeneous morphology (Holme, Solum et al. 1994, Hess, Sadallah et al.

1999, Cocucci, Racchetti et al. 2009, Gyorgy, Szabo et al. 2011, Raposo and Stoorvogel 2013, Turturici, Tinnirello et al. 2014, Kalra, Drummen et al. 2016) (**Figure 1.3**).

The origin of the exosomes is endocytic and it is released to the medium by fusing MVBs, which are formed via endosomal and lysosomal compartments, with the cell plasma membrane (Fevrier and Raposo 2004). MVBs play a role in obsolete proteins eradication, however, they could be also released into extracellular space which will result in having effect on potential cell to cell communication (van Niel, Porto-Carreiro et al. 2006). On the other hand, microvesicles are released by the plasma membrane budding, and apoptotic bodies are formed by nucleus condensation and segregation as well as the damage and blebbing of the plasma membrane (Akers, Gonda et al. 2013). EVs, although they have small size, they comprise of various molecules including lipids, proteins, different RNAs, ssDNA, as well as metabolites. It is suggested that the prototypical exosomes can have 100 and 10000 proteins and nucleotides respectively, as their internal volume of an exosome can range between 20 and 90 nm<sup>3</sup> (Vlassov, Magdaleno et al. 2012), which suggests larger content in the case of ectosomes and apoptotic bodies with relatively bigger size. EVs can be transferred through parasite–parasite, parasite–host cell, or host cell–host cell interaction, between the host cells and the parasites (Marcilla, Martin-Jaular et al. 2014, de Pablos Torro, Retana Moreira et al. 2018).

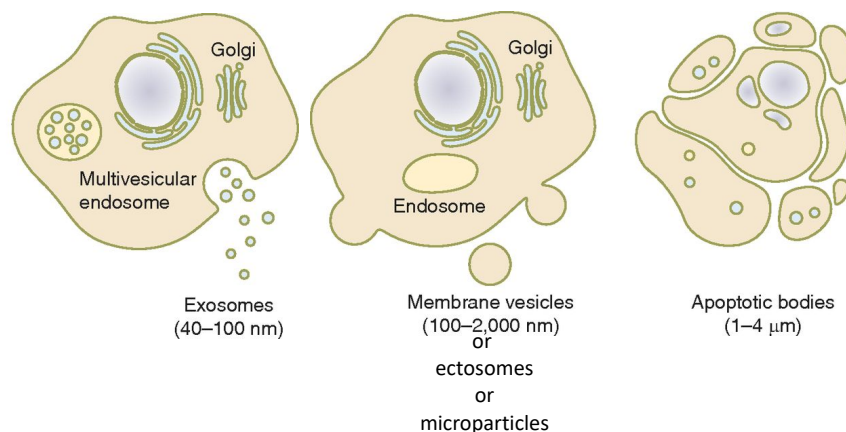


**Figure 1.3. Schematic representation of three major types of extracellular vesicles: exosomes, ectosomes, and apoptotic bodies.** Figure modified from (Turturici, Tinnirello et al. 2014).

#### **1.4. *T. CRUZI* EXTRACELLULAR VESICLES (EVs)**

The biology of *T. cruzi* EVs and their role in invading innate immunity has been studied in the past few years (Marcilla, Martin-Jaular et al. 2014, de Pablos Torro, Retana Moreira et al. 2018). *T. cruzi* is capable of secreting extracellular vesicles (EVs) to the extracellular milieu (**Figures 1.4 and 1.5**) (reviewed in (Pilzer, Gasser et al. 2005, Marcilla, Martin-Jaular et al. 2014)). These EVs are crucial for parasite-host interaction via promoting the pathogen replication within the host and its survival. EVs are able to directly interact with host target cells, induce long-distance impact on the immune system of the host, as well as promoting the life-cycle transition of the parasite itself (Trocoli Torrecilhas, Tonelli et al. 2009, Marcilla, Martin-Jaular et al. 2014).

In this trypanosome, the secreted EVs were shown for first time by da Silveira *et al.* (da Silveira, Abrahamsohn et al. 1979), in the noninfective insect-vector stage of the parasite, epimastigote. It was also shown by this group that epimastigote-derived EVs were enriched with glycoconjugates as previously demonstrated (Alves and Colli 1975), which later on, these molecules were characterized to be the major glycoproteins (mucins) (Acosta-Serrano, Almeida et al. 2001, Buscaglia, Campo et al. 2006, Mendonca-Previato, Penha et al. 2013), glycolipids

(lipopeptidophosphoglycan-LPPG or glycoinositolphospholipids-GIPLs (de Lederkremer and Colli 1995) and glycopeptides (NETNES) (Macrae, Acosta-Serrano et al. 2005) in *T. cruzi* surface.

The infective host-cell-derived trypomastigotes, were shown to be secreting these EVs as well (Goncalves, Umezawa et al. 1991), in various parasite strains. Studies on labelled EVs revealed that Tc-85 which is a trans-sialidase (TS)/gp85 glycoprotein superfamily member, is involved in the parasite-host cell adhesion, as well as parasite invasion (Schenkman, Eichinger et al. 1994, Frasch 2000, Alves and Colli 2008), and is found in EVs as their major component. Moreover, previous research has shown that trypomastigote-derived EVs size ranged from 20 to 80 nm in diameter which resembles the size of the exosomes, and their expression of TC-85 shown to be from parasite's flagellar pocket (Ouaissi, Dubremetz et al. 1990). Furthermore, it was also shown that flagellar calcium-binding protein (FCaBP) which is one of the major *T. cruzi* flagellar antigens (24-kDa), is secreted in trypomastigote-derived EVs, from the plasma membrane and flagellar pocket (Ouaissi, Aguirre et al. 1992). Overall, according to the reports above, the importance of the EVs shed from *T. cruzi* is clearly pointed out, as a novel mechanism that parasite uses in order to present or deliver its major antigens to the host cells.

Both noninfective epimastigote and infective metacyclic trypomastigote insect-derived stages of *T. cruzi* secrete EVs in a constitutive manner (Bayer-Santos, Aguilar-Bonavides et al. 2013). These authors observed two major populations of EV: exosomes (25-150 nm diameter; mean ~80 nm) and ectosomes (50-250 nm diameter; mean ~140 nm). Electronic microscopy analysis showed ectosomes originated from the plasma membrane, whereas exosomes originated from multivesicular bodies (MVBs) and were secreted into medium through the flagellar pocket of both stages. These two types of EV populations were enriched by differentiation ultracentrifugation, giving rise to mainly ectosomes after 2 h at 100,000 g (V2 fraction) and

exosomes after 16 h at 100,000 g (V16 fraction). The final supernatant fraction, mostly devoid of EVs, was named VF (vesicle-free). By proteomic analysis, a differential protein enrichment was observed in ectosomes and exosomes (V2 and V16, respectively), as well as in the VF fraction. Interestingly, the main plasma membrane glycoproteins (mucin, MASP, TS, GP82, and GP63) and acylated and proteins (flagellar calcium-binding, FCaBP), which are major virulence factors, were found in the ectosomal (V2) fraction, whereas metabolic and structural proteins were found in the exosomal (V16) fraction. On the other hand, the VF fraction contained mainly proteases and peptidases, such as cruzipain, calpain-like cysteine peptidase, and peptidase M20/M25/M40, proteins/enzymes involved in carbohydrate, nucleic acid, lipid, and amino acid metabolism, and proteins that had lost their GPI-anchoring (e.g., soluble GP82) (Bayer-Santos, Aguilar-Bonavides et al. 2013).

TS is responsible for transferring SA to the TcMUC II mucin *O*-glycans (reviewed by (Schenkman, Eichinger et al. 1994, Buscaglia, Campo et al. 2006)). However, it was shown by Lantos et al. (2016) that  $\alpha$ -Gal-containing TcMUC II mucin-rich domains on the plasma membrane do not colocalize with TS-containing domains (Lantos, Carlevaro et al. 2016). Moreover, both TS and mucins seemed to be shed in cargo carriers, assumed to be EVs (Lantos, Carlevaro et al. 2016). TcMUC II Mucins are, therefore, acceptors of both SA and  $\alpha$ -Gal residues, which are known to be involved parasite protection from host immune system, and pathogenesis (Buscaglia, Campo et al. 2004, Buscaglia, Campo et al. 2006). Thus, it is important to study the distinct composition of  $\alpha$ -Gal-containing (or  $\alpha$ -Gal(+)) and TS-containing (or  $\alpha$ -Gal(-)) EVs, as well as to study their possible distinct effect on inducing infection in the host cells, in detail.

Therefore, although TCT-EVs, total secretome (TCT-Secr), and VF fraction from the infective mammal-dwelling trypomastigote stage have recently been investigated and their

proteomic composition determined by our laboratory and collaborators (Ribeiro, Vasconcellos et al. 2018) and others (Queiroz, Ricart et al. 2016, Bautista-Lopez, Ndao et al. 2017), an in-depth analysis of the EV populations (i.e.,  $\alpha$ -Gal(+) and  $\alpha$ -Gal(-)) and subpopulations therefrom, in distinct parasite genotypes and strains, is still elusive. This is, therefore, one of the major focuses of this doctoral project. We aim to characterize these  $\alpha$ -Gal(+) and  $\alpha$ -Gal(-) TCT-Secr and TCT-EVs, in order to investigate potential biomarkers for diagnosis and early assessment of chemotherapeutic outcomes of ChD, which are much needed in the clinical settings.



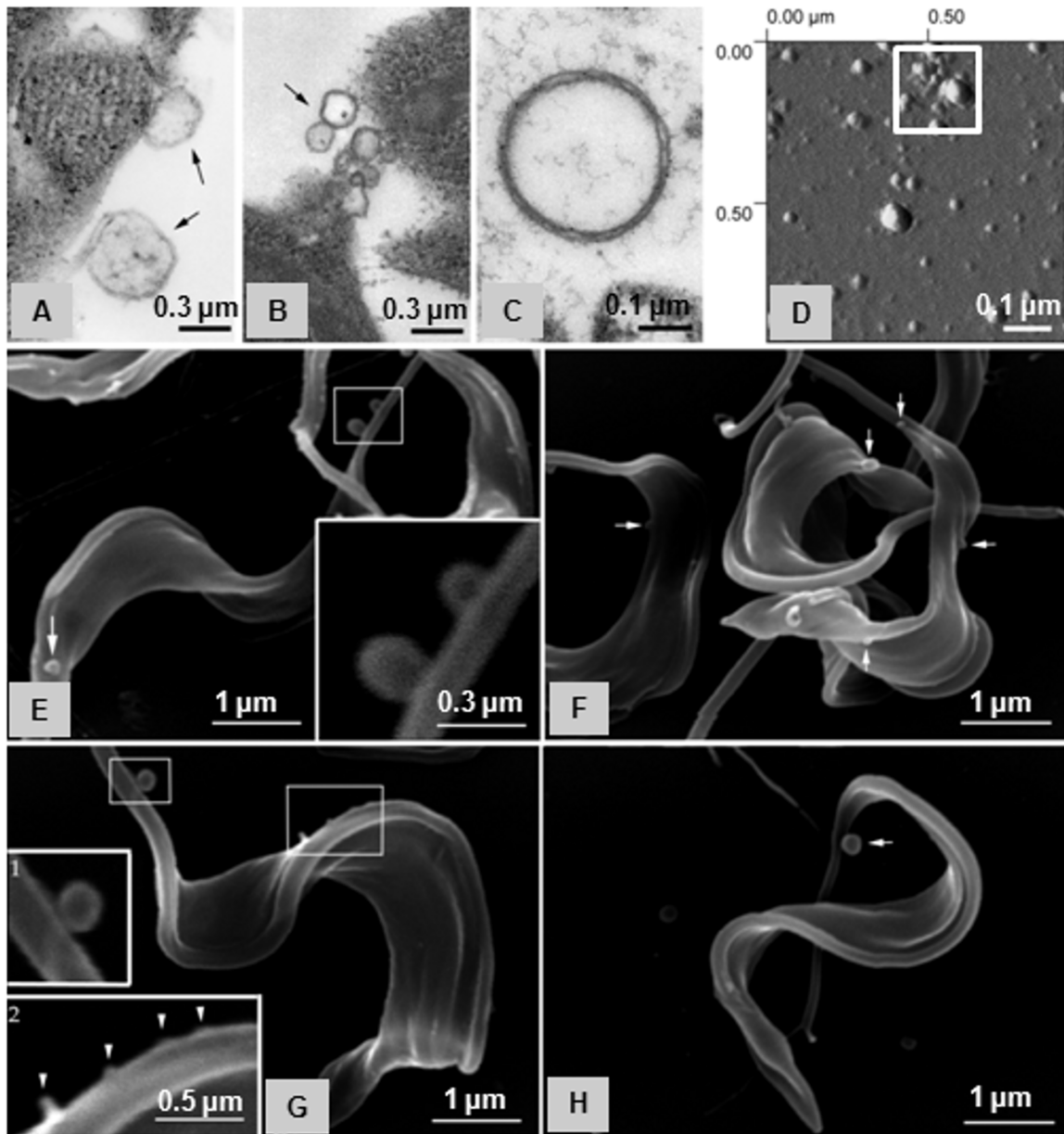


**Figure 1.4. Transmission electron (TEM), scanning (SEM), and atomic force microscopy (AFM) of *T. cruzi* trypomastigote EVs (TCT-EVs).** (A and B) TEM of trypomastigote flagellar pocket region, showing EVs being released (arrows). (C) TEM of pelleted vesicles (100,000 x g). (D) AFM of purified TCT-EVs. (E-H) SEM of trypomastigotes; EVs being released are indicated by arrows or arrow heads. E and G insets show areas on the parasite surface where the vesicles can be visualized in more detail. Scale bars are indicated. Figure taken from Torrecilhas, Almeida et al. (unpublished data).

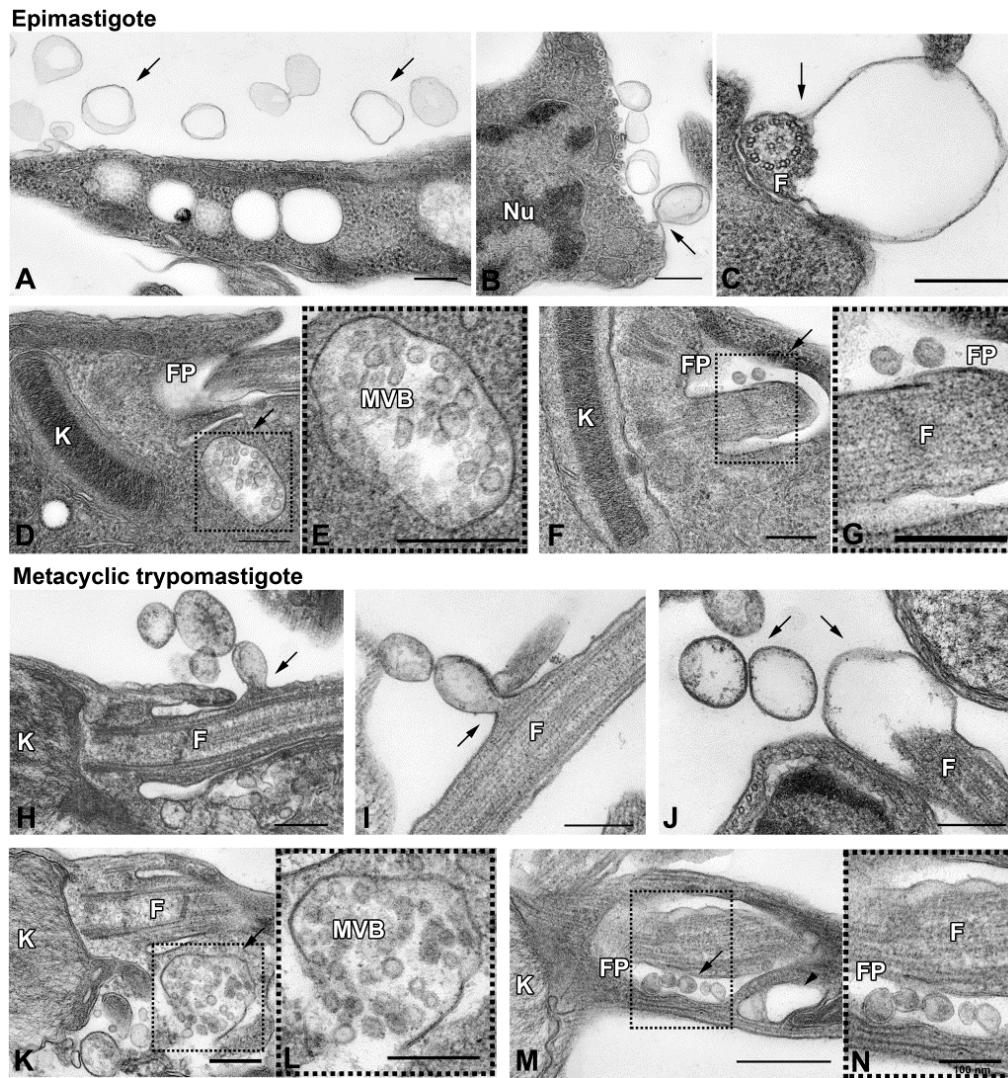


**Figure 1.5. *T. cruzi* extracellular vesicles from noninfective and infective insect-derived developmental forms.**

**Upper panel:** representative TEM images of noninfective epimastigotes releasing vesicles from the plasma membrane (A–C) and showing an MVB close to the flagellar pocket (D and E), which contains exosomes inside (F and G) (arrow). **Lower panel:** representative TEM images of infective metacyclic trypomastigote forms releasing ectosomes from the plasma membrane (H–J) and showing an MVB close to the flagellar pocket (K and L), which contains exosomes inside (M and N) (arrow). Arrowhead indicates an empty large vesicle close to the flagellar pocket that could be resultant of an MVB exocytic fusion (M). Scale bar = 250 nm, except for N (bar = 100 nm). Nu, nucleus; K, kinetoplast; F, flagellum; FP, flagellar pocket; MVB, multivesicular body. Figure and text copied or modified from (Bayer-Santos, Aguilar-Bonavides et al. 2013).

## **1.5. HYPOTHESIS, SIGNIFICANCE, AND SPECIFIC AIMS**

### **HYPOTHESES:**

It has been previously shown that trypomastigote-specific surface glycoproteins play an important role in inducing parasite-specific immune responses against the parasite (Camargo, Almeida et al. 1997, Almeida, Camargo et al. 2000, Almeida and Gazzinelli 2001, Campos, Almeida et al. 2001). Moreover, it has been shown that *T. cruzi* has surface glycoproteins and glycolipids that are conserved to the parasite and are involved in parasite's invasion and evasion, and are highly immunogenic to the mammalian including human immune cells. These molecules were shown to be released in the EVs (Bayer-Santos, Aguilar-Bonavides et al. 2013, Ribeiro, Vasconcellos et al. 2018).

We propose the following hypotheses:

1. *T. cruzi* virulence factors released in extracellular vesicles (EVs) are highly antigenic and reactive with sera from chronic Chagas disease (ChD) patients and could be used as biomarkers for reliable diagnosis of ChD.
2. Major *T. cruzi* virulence factors (e.g., proteins and glycoproteins) and bioactive molecules (e.g., lipids) are differentially secreted in EVs from major parasite genotypes with distinct virulence and pathogenic traits.
3. *T. cruzi* EVs from major parasite genotypes could differentially modulate host-cell infection rate *in vitro* in a dose- and time-dependent manner.

### **SIGNIFICANCE:**

BZN has been recently approved by FDA, but it has toxic side effects, and only less than 1% of the ChD patients are being currently treated, especially due to the lack of reliable clinical biomarkers that can assess the therapeutic outcomes (cure or failure) much earlier than the conventional serology. Thus, there is an urgent need for these biomarkers in the clinical settings of ChD.

Approximately 6-8 million people are chronically infected with *T. cruzi* in Latin America (over 100 million people under risk of infection), and 12,000-50,000 deaths occur per year due to heart failure caused by the infection (Rassi, Rassi et al. 2010). In the United States, 300,000 people are estimated to be chronically infected with the parasite. *T. cruzi*-infected bugs are found in 75% of the U.S. states (Rassi, Rassi et al. 2010). Only two drugs (nifurtimox-NFX and benznidazole-BZN) are available, with above 90% cure rate during acute phase, and 60-80% during chronic phase (BZN has been recently approved by FDA, but it has toxic side effects). Only less than 1% of the ChD patients are being currently treated, especially due to the lack of reliable clinical biomarkers that can assess the therapeutic outcomes (cure or failure) much earlier than the conventional serology. Serological diagnosis for ChD, using *T. cruzi* epimastigotes extracts as antigens shows limited specificity although it has high sensitivity in the chronic phase of the disease, and moreover, it shows low sensitivity in the acute phase and congenital infection (Villalta, Scharfstein et al. 2009, Rassi, Rassi et al. 2010). Inconclusive and doubtful results have been shown by various reports that depending on the commercial diagnostic assay that was used. Moreover, cross-reactivity with patients' sera infected with *Leishmania* spp. has been shown using serological assays for ChD (Umezawa, Nascimento et al. 1996). Therefore, urgent needs for characterizing EVs in order to find potential markers with more specificity and sensitivity in diagnostic tests arise, for early assessment of chemotherapeutic outcomes of ChD. EVs are

favorable sources for being diagnostic markers (Rassi, Rassi et al. 2010) and therefore, characterizing EVs and assessing them as a potential biomarker is the main focus of this study.

## **SPECIFIC AIMS:**

- **Specific aim 1:** Purify and molecularly and immunologically characterize EVs derived from *T. cruzi* trypomastigotes (TCT EVs) from three major parasite genotypes with distinct virulence and pathogenic traits.
  - 1.1. To purify and validate TCT EVs as potential diagnostic biomarkers for ChD.
  - 1.2. To perform a high-resolution proteomic analysis of TCT EVs.
  - 1.3. To perform a high-resolution lipidomic analysis of TCT EVs.
  
- **Specific aim 2:** Evaluate the role of TCT-EVs in the host-cell infection.
  - 2.1. Analyze the infection after treatment with the total TCT secretome and TCT EVs from different parasite genotypes, *in vitro*.

## CHAPTER 2: TCT-EVS AS DIAGNOSTIC BIOMARKERS

### 2.1. INTRODUCTION: *T. CRUZI* HIGHLY IMMUNOGENIC SURFACE GLYCOPROTEINS

The surface of *T. cruzi* is covered by immunogenic glycoconjugates like TcMUC II, which contain the trisaccharide Gal $\alpha$ (1,3)Gal $\beta$ (1,4)GlcNAc $\alpha$ , one of the immunodominant glycotopes. This trisaccharide induces high levels of protective, lytic anti- $\alpha$ -Gal antibodies in infected individuals (Almeida, Ferguson et al. 1994, Schocker, Portillo et al. 2016). The majority of the ChD patient's lytic antibodies are specific for  $\alpha$ -galactosyl-comprising epitopes (Almeida, Milani et al. 1991), which are present in the trypomastigote forms (Almeida, Ferguson et al. 1994), although they are also found in the GP72 glycoproteins in metacyclic trypomastigote forms (Travassos, Almeida et al. 1994, Allen, Richardson et al. 2013). Therefore, evaluating the reactivity of *T. cruzi*-derived EVs with ChD patients' sera could be led to the discovery of new diagnostic biomarkers. We hypothesize that TCT-EVs comprise antigenic  $\alpha$ -Gal glycotopes, which are likely expressed in TcMUC II glycoproteins and are highly reactive with ChD sera.

### 2.2. MATERIALS AND METHODS

#### 2.2.1. Mammalian cell culture

Green monkey (Rhesus) kidney LLC-MK2 epithelial cells and human osteosarcoma (U2-OS) cells were cultured in low glucose Dulbecco's Modified Eagle Medium (DMEM: Corning™ DMEM with L-Glutamine, 4.5 g/L Glucose and Sodium Pyruvate) medium with 10% fetal bovine serum (FBS: HyClone™ Fetal Bovine Serum, USDA Tested) and 1% Penicillin-Streptomycin (Corning®) at 37°C, under CO<sub>2</sub> atmosphere. The cells were sub-cultured once or twice a week in a 150, 175, and 182 cm<sup>2</sup> flask (Corning® cell culture flasks), using 1-2 ml trypsin (Corning™

0.25% trypsin, 0.1% EDTA in HBSS w/o calcium, magnesium and sodium bicarbonate) after the media being removed and the cells being washed with 5 ml of 1X phosphate buffer saline (PBS: HyClone™ phosphate-buffered saline). After cells being detached, the volume was reached to 10 ml by adding media, and the cells were transferred to a new flask and the volume reached to 20-30 ml with the media, according to the flask size. Otherwise stated, DMEM was used throughout the study for the mammalian cell and *T. cruzi* trypomastigote cultures. Parasites and mammalian cells were regularly tested for Mycoplasma (Universal Mycoplasma Detection Kit: ATCC® 30-1012K™).

### **2.2.2. Parasite culture, and isolation and storage of trypomastigote-derived secretome (TCT-Secr) and TCT-extracellular vesicles (TCT-EVs)**

Murine blood-derived trypomastigotes, and tissue culture trypomastigotes (TCTs) of Colombiana (Col), and Y strains, and red-shifted luciferase-expressing CL Brener (CLB) clone (genotypes or DTUs TcI, TcII, and TcVI, respectively) (Zingales, Andrade et al. 2009, Zingales 2018) were added to the cells at a multiplicity of infection (MOI) of 10, after the cells were at approximately 60-70% confluent. The medium was replaced with fresh media the next day, and the cells were under monitoring for approximately 5 days until the parasites start appearing in the media (the peak of the parasites was on day 7-10 depending on the parasite strain/clone, and they were harvested from the cells up to day 10-12), when the medium was daily replaced with fresh medium. The parasite-comprising supernatant (approximate numbers of 1e6, 1e7, 1e8, and 1e9) was taken from the cell flask and centrifuged for 10 min at 1,500 xg at 4°C and the supernatant was incubated for 2 h for the cell debris and amastigotes (in the pellet) to be separated from the trypomastigotes, which swam to the supernatant. The supernatant comprising the trypomastigotes was transferred to another tube and centrifuged for 10 min at 2,465 xg at 4°C, and the



trypomastigote-containing pellet was washed with 1X PBS 2x and incubated with FBS free media for 6 h for the parasites to shed vesicles, and it was centrifuged at 2,465 xg for 10 min at 4°C to separate the vesicles from the trypomastigotes. The supernatant was then filtered through 0.45- $\mu$ m syringe filter (33 mm Millipore® Millex®, PVDF Sterile Syringe Filter), using 5-ml syringe (BD), and the flow through, which is TCT-EV-rich, was stored in three conditions (4, -20, and -80°C) and analyzed by nanoparticle tracking analysis (NTA) in triplicate, after 48 h and 30 days of storage. Briefly, the samples were diluted 10x in PBS, and NTA was performed using NanoSight model LM14C (NanoSight Technology, Salisbury, United Kingdom), equipped with a green laser and a sCMOS camera (Hamamatsu Photonics K.K., Hamamatsu City, Japan). The software used for capturing and analyzing the data was the NTA 3.2, Dev Build 3.2.16. Three measurements of the same sample were performed in 20-sec acquisition times, using the default settings of the instrument. The error bars indicate the standard error of the mean. Thereafter, data were compared between the samples in order to find the suitable storage temperature for vesicles to keep their integrity. Parasites and mammalian cells were regularly tested for *Mycoplasma* (Universal Mycoplasma Detection Kit: ATCC® 30-1012K™).

### **2.2.3. Fractionation of TCT-Secr by Size-Exclusion Chromatography (SEC)**

Sepharose CL-2B (Sigma-Aldrich) (~15 ml) was let to settle in a glass beaker and storage solution was removed. Sepharose was rocked gently in 0.1 M ammonium acetate buffer (filtered through 0.22- $\mu$ m filter), and was let to settle to wash by removing the buffer (the Sepharose was let to settle and washed twice more). A 3-ml syringe tip (BD) was plugged with glass wool, and was setup on a ring stand with a waste container bellow it. The column was packed with Sepharose until the 3 ml mark and washed by passing 6 ml of the buffer through. TCT-Secr samples from Col, Y, and CLB were loaded (300  $\mu$ l) and immediately collected (each comprising 150  $\mu$ l). Once

the top of the resin was visible, 3 ml of the buffer was added to it slowly (200  $\mu$ l at a time) until all the liquid has been collected. For further analyses, samples were stored at 4°C for less than 48 h, and at -80° C for longer periods.

#### **2.2.4. Bicinchoninic Acid (BCA) Protein Assay**

Sample fractions from Col, Y, and CLB were analyzed for protein concentration by Bicinchoninic Acid Assay (BCA: Pierce™ BCA Protein Assay Kit, Thermo Fisher Scientific) according to the manufacturer. Briefly, a serial dilution of standards as well as samples were tested in duplicates in 96-well plate and incubated for 30 minutes at 37°C and the colorimetric reaction was measured at 562 nm and samples were calculated against the standard curve.

#### **2.2.5. Immunoblotting the TCT-Secr with IB4-lectin, and purified Ch anti- $\alpha$ -Gal Abs**

TCT-Secr aliquots (derived from Col, Y, and CLB: genotypes Tc I, II, and VI, respectively) were added 1% Halt™ Protease Inhibitor Cocktail (Thermo Fisher Scientific)/  $\pm$  50  $\mu$ g of N $\alpha$ -Tosyl-L-lysine chloromethyl ketone hydrochloride (TLCK: Millipore Sigma) before the storage at -80°C. Samples containing 10 and 30  $\mu$ g of protein, quantified by BCA technique (as described in the previous section in 2.4.), were applied in each lane of 4-20% Mini-PROTEIN® TGX™ Precast Protein Gels and separated. The proteins were transferred to 0.45- $\mu$ m nitrocellulose membranes (Bio-Rad) using standard wet transfer sandwich protocol (Towbin, Staehelin et al. 1992). Briefly, transfer buffer (25 mM Tris/192 mM glycine/ 0.1% sodium dodecyl sulfate (SDS), at pH 8.3) was added to the transfer tank, transfer sandwich was assembled with assuring the membrane being on the cathode and the gel on the anode, and the air bubbles being removed from the system. The proteins were transferred at 100V for 1 h, at 4°C on ice, and the membranes were blotted first with biotinylated isolectin B4 (IB4) (or GSL-1) from *Bandeiraea (Griffonia) simplicifolia* (Wood,

Kabat et al. 1979) (Vector Labs, catalog # B-1205), and then with Ch anti  $\alpha$ -Gal Abs (Almeida, Milani et al. 1991), after stripping the IB4 lectin. Briefly, membranes were blocked with Tris-buffered saline: 50 mM Tris, 150 mM NaCl (TBS)/ 1% bovine serum albumin (BSA: Fisher BioReagents™ Bovine Serum Albumin, Fraction V, heat shock-treated)/ 0.1% Tween 20 (Promega, Madison, WI: T): TBST/ 1% BSA, pH 7.6, at 4°C, overnight. The membranes were washed (all the washings were performed 3x with TBST, each time for 5 min), and incubated with 5  $\mu$ g/mL biotinylated IB4 lectin/TBST/1% BSA for 1 h. The membranes were washed, and incubated with neutravidin-horseradish peroxidase (NA-HRP, Thermo Fisher Scientific) at 1/5,000 dilution/TBST/1% BSA for 1 h, and finally CL reagent (Pierce™ ECL Western Blotting Chemiluminescent Substrate: Thermo Scientific; reagents A:B (1:1, v/v)), was added and the images were immediately taken by iBright Western Blot Imaging Systems (Thermo Scientific). All the steps after blocking were performed with gentle agitation at 400 rpm, at room temperature (rt). After the first blotting, the membrane was stripped with stripping buffer (Restore™ western Blot Stripping Buffer: Thermo Fisher Scientific), washed 5x with ultrapure water, and probed with 5  $\mu$ g Ch anti  $\alpha$ -Gal Ab/ TBST/1% BSA, and for 1 h, at 37°C. The membrane was washed 5x with TBST, and incubated with secondary antibody (anti goat-anti human biotin-conjugated IgG antibody: Thermo Fisher Scientific), at 1/10,000 dilution/ TBST/ 1% BSA for 1 h, at 37°C. Finally, following the neutravidin-horseradish peroxidase step, the immunoblotting was developed as described above.

#### **2.2.6. Silver staining**

After TCT-Secr samples were separated through precast gel (as described in 2.2.5), the proteins were stained with silver stain (Pierce™ Silver Stain for Mass Spectrometry: Thermo Fisher Scientific) according to the manufacturer's protocol. Briefly, the gel was washed with ultrapure

water for 5 minutes 2x, fixed with Fixing solution (30% ethanol, 10% acetic acid) first for 15 minutes, and then overnight. Thereafter, the gel was washed with Ethanol Wash solution (10% ethanol) for 5 minutes 2x, and then with ultrapure water for 5 minutes 2x. Afterwards, the Sensitizer Working solution (1:500 Silver Stain Sensitizer: ultrapure water) was added (prepared just before use), and the gel was incubated exactly for 1 minute, and then washed with ultrapure water for 1 minute 2x. Then the Enhancer solution (1:100 Silver Stain Enhancer: Silver Stain) was immediately added to the gel, and incubated for 5 minutes. The Developer Working solution thereafter was prepared (1:100 Silver Stain Enhancer: Silver Stain Developer), and after the gel was washed with ultrapure water for 20 seconds 2x, it was quickly added for 1 minute. The Stop solution (5% acetic acid) was immediately added to the gel after the desired bands appeared, to the existing developer working solution (to avoid excessive background spontaneously generated), and then replaced with fresh Stop solution and incubated for 10 minutes. Finally, the Stop solution was washed with ultrapure water 3x and the gel was imaged by iBright Western Blot Imaging Systems: Thermo Scientific. All the steps were performed with gentle agitation at 42 RPM, at RT.

### **3.2.7. Affinity chromatography using immobilized *Bandeiraea simplicifolia* isolectin 4 (IB4)-lectin for enrichment of $\alpha$ -Gal-containing TCT-EVs**

$\alpha$ -Gal-containing EVs were purified from the TCT-Secr, obtained from the conditioned medium of Col, Y, and CLB strains (genotypes Tc I, II, and VI, respectively) by immunoaffinity chromatography, using immobilized biotinylated *Bandeiraea simplicifolia* isolectin 4 (IB4)-lectin. Briefly, storage solution was removed by breaking off the bottom cap and spinning the column (GE Healthcare, 28903130) at 150 g at 4° C for 1 minute. The column was equilibrated with adding 400  $\mu$ l of 50 mM Tris/150 mM NaCl: TBS, at pH 7.5 and spinning the column at 150 xg at 4°C for 1 min (3x). Thereafter, the column was added 300  $\mu$ g biotinylated IB4-lectin (Sigma-Aldrich,

L2140, Vector Laboratories, B-1205-5), which was resuspended by inverting it manually, and then the column was incubated at 4°C, overnight, with slow rocking motion. Thereafter, blocking was done by adding 400 µl blocking buffer (2 mM Biotin/TBS) and mixing it by manual inversion for 5 min (2x). Column was then washed with TBS by spinning at 150 xg, at 4°C, for 1 min (3x), and TCT-Secr sample (1 mg protein total/ FBS free DMEM) was added to the column. The sample was incubated for overnight at 4°C, with slow rocking motion. Unbound flow-through (FT: α-Gal(-)) fraction was collected by spinning the column at 150 xg, at 4°C, for 1 min. The column was washed with adding 400 µl wash buffer (TBS/2 M urea, pH 7.5) and spinning at 150 xg at 4°C for 1 min (5x), and these wash (W) fractions were pooled and collected. Thereafter, the bound α-Gal epitopes were eluted (EL: α-Gal(+)) and collected from the column by adding 200 µl elution buffer (0.1 M glycine/2 M urea, pH 2.9) and centrifuging at 1,000 xg, at 4° C (3x). The EL fractions were immediately neutralized with 1 M Tris, pH 8.0. The bottom cap of the column was kept on during all the incubation steps and was kept removed during the centrifugation steps.

### **2.2.8. Analysis of TCT-Secr with Ch and NHS sera**

The TCT-Secr were analyzed with chronic ChD serum pool (ChHSP) and normal human serum pool (NHSP) by chemiluminescent ELISA (CL-ELISA: SuperSignal™ ELISA Pico Chemiluminescent Substrate) (Schocker, Portillo et al. 2016, Ortega-Rodriguez, Portillo et al. 2019). Briefly, the TCT-EV samples (at various protein concentrations) and the positive control neoglycoprotein (KM24b or NGP24b) (containing the Galα(1,3)Galβ(1,4)GlcNAcα trisaccharide conjugated via 13-atom to BSA) (Schocker, Portillo et al. 2016), at 125 ng/well. NGP24b was immobilized in 0.2 M carbonate-bicarbonate buffer (CB buffer), pH 9.6, and incubated at 4°C overnight. They were blocked with PBS/1% bovine serum albumin (BSA, Fisher BioReagents™ Bovine Serum Albumin, Fraction V, Heat Shock Treated), incubated at 37° C for 1 h, and washed

3x with 200  $\mu$ L PBS/0.05% Tween 20 (Promega, Madison, WI) (PBST). Afterwards, ChHSP and NHSP at 1:800 dilution were added, the plates were incubated at 37°C, washed 3x with PBST, incubated with secondary antibody (goat anti-human biotin-conjugated IgG antibody: Thermo Fisher Scientific, at 1:10,000 dilution), and washed 3 times with PBST. Samples were then incubated with neutravidin horseradish peroxidase (NA-HRP: Thermo Fisher Scientific, at 1:5,000 dilution), and washed 3 times with PBST, thereafter CL-ELISA reagent (SuperSignal ELISA Pico Chemiluminescent Substrate, 1:1:8 Reagent A: Reagent B: CB buffer/0.1%BSA, v/v/v) was added and the reaction was measured by Luminoskan luminometer. The positive control was Gal $\alpha$ (1,3)Gal $\beta$ (1,4)GlcNAc $\alpha$ -BSA + ChHSP, and negative control was the same trisaccharide with the NHSP.

**Figure 2.1** summarizes the general approach used for preparation, enrichment, and proteomic analysis of TCT-Secr and TCT-EVs.

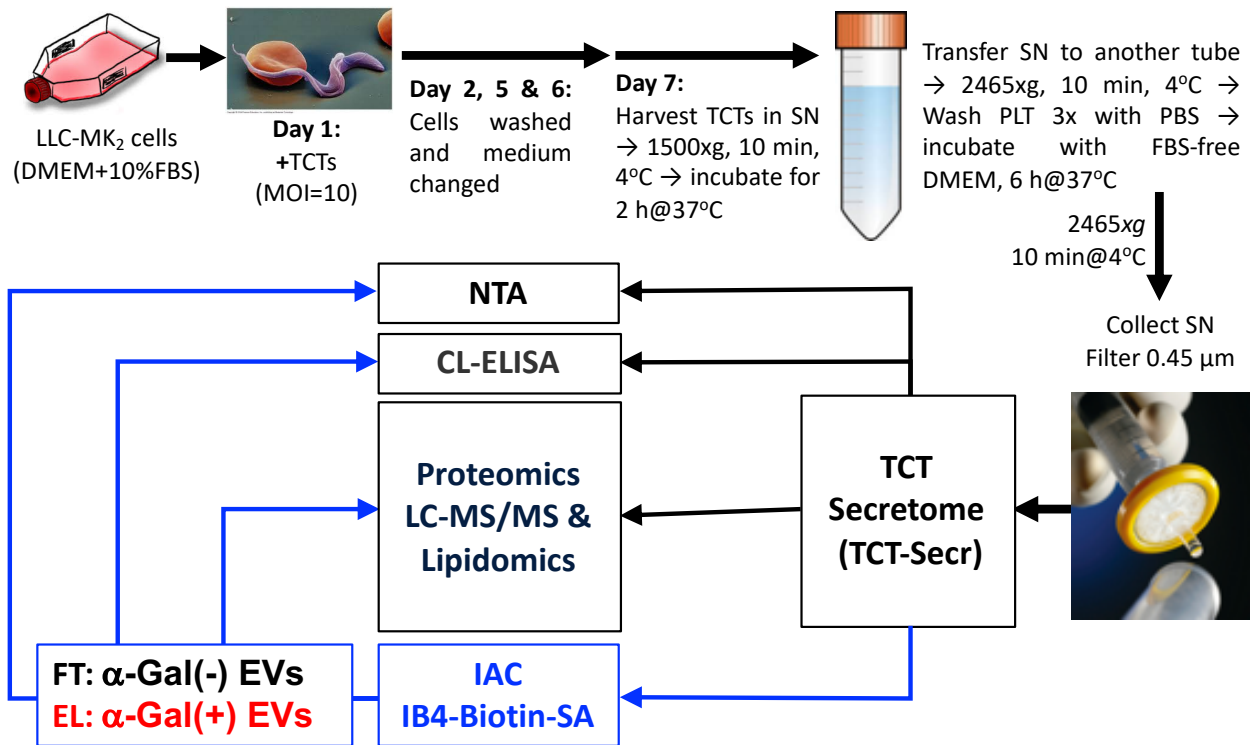


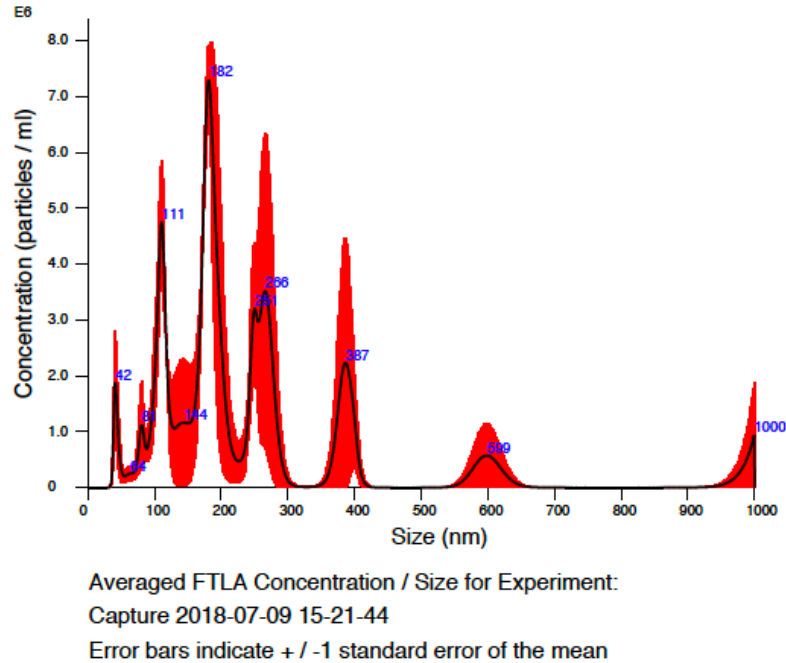
**Figure 2.1. Preparation and analysis of TCT-Sec and TCT-EVs.** Immunoaffinity chromatography (IAC) with biotinylated *Bandeiraea simplicifolia* isolectin 4 (IB4) linked to neutravidin-agarose (IB4-Biotin-SA). SN, supernatant; NTA, Nanoparticle Tracking Analysis (NanoSight); CL-ELISA, chemiluminescent ELISA; FT, flow-through; EL, eluate.

## **2.3. RESULTS**

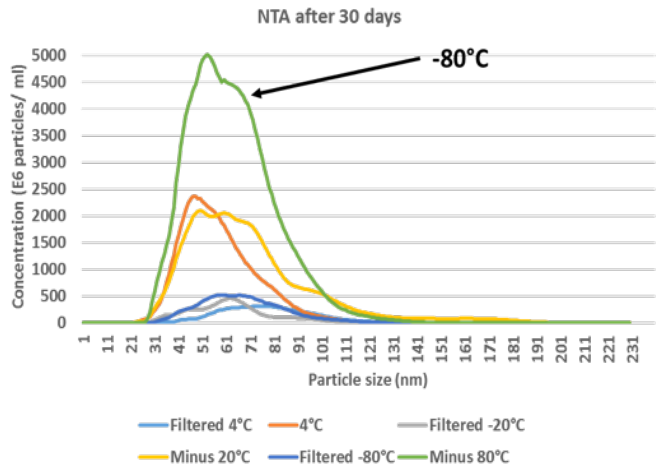
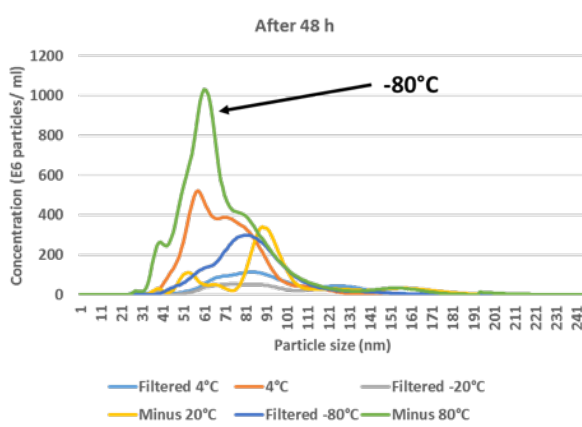
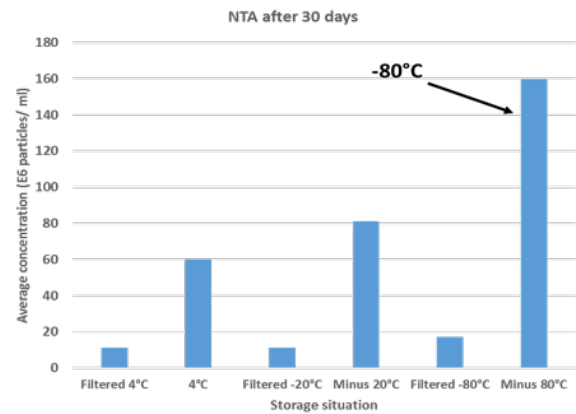
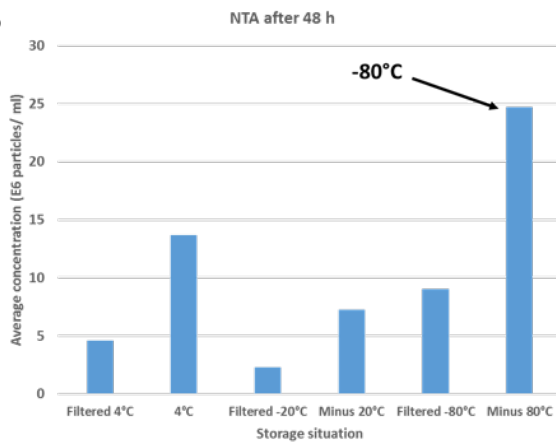
### **2.3.1. TCT-EVs were detected through NTA in TCT-Secr and -80 showed to be the most suitable storage temperature for them**

As it is shown in **Figure 2.2**, EVs were detected in TCT-Secr, derived from CLB by NTA. EVs between ~ 40 and 1,000 nm of diameter were observed in the secretome (similar data were shown in Col and Y strains). Furthermore, amongst three conditions of 4, -20, and -80°C, TCT-EVs showed the highest concentration even after 30 days of storage (**Figure 2.3**). Therefore, this condition was chosen for their storage. Moreover, it was shown that the integrity of the EVs was kept at -80°C, since the peaks showed sharper profile at this temperature and the EVs did not show aggregation as much as they did in lower temperatures (data not shown). However, for the shorter storage up to 24 h, the EVs seemed to be stable.





**Figure 2.2. NTA analysis of EVs derived from CLB *T. cruzi* trypomastigote.** Vesicles from TCT-Secr derived from Luc CLB (20X in PBS) were tracked and measured for 30 s at RT and data are analyzed with NTA software. Total concentration showed to be  $6.25 \times 10^8$  particles/mL. The size distribution of the EVs showed that exosomes (ranging from 40 nm to 100 nm) and ectosomes (ranging from 100 nm to 1000 nm) are both found in the secretome. Similar data were observed for TCT-EVs derived from Col and Y strains (not shown).

**A****B**

**Figure 2.3.** NTA analysis of EVs derived from *T. cruzi* trypomastigote after storing them at 4, -20, and -80°C.

The size distribution (A) and average concentration (B) of EVs showed that -80°C is the optimum storage temperature for EVs. The samples were diluted twice in 1X PBS.

### 2.3.2. Fractionation of TCT-Secr by SEC and BCA analysis

TCT-EVs derived from host cell-derived trypomastigote ( $2 \times 10^6$  per ml) secretome (TCT-Secr) were fractionated by SEC, using Sepharose CL-4B. Twenty fractions were collected and the left-protein of the column were tested for protein content by BCA. Little or no detectable protein content was observed in these fractions (**Figure 2.4**).

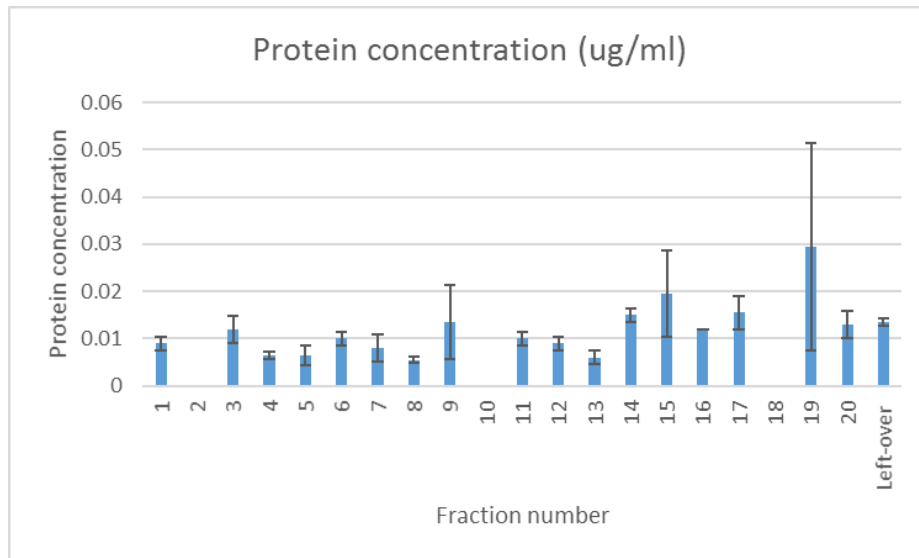


**Figure 2.4. Protein concentration in 20 fractions and left-over proteins of the columns, after fractionation of EVs measured by BCA.** The protein concentration was undetectable as the initial number of the parasites ( $2 \times 10^6$ ) was low. The results are shown in means  $\pm$  SDs of two technical replicates.

The number of parasites that EVs were derived from was increased to  $1.6 \times 10^8$ /ml, and measured for proteins as previously explained. **Figure 2.5** shows that increasing the number of the parasites significantly increased the amount of protein being detected by BCA in the TCT-EVs. However as seen in **Figure 2.5**, the peak seemed to be at around fraction 21 (between F17 to F25). Therefore, SEC was performed on TCT-Secr collecting a total of 30 fractions.

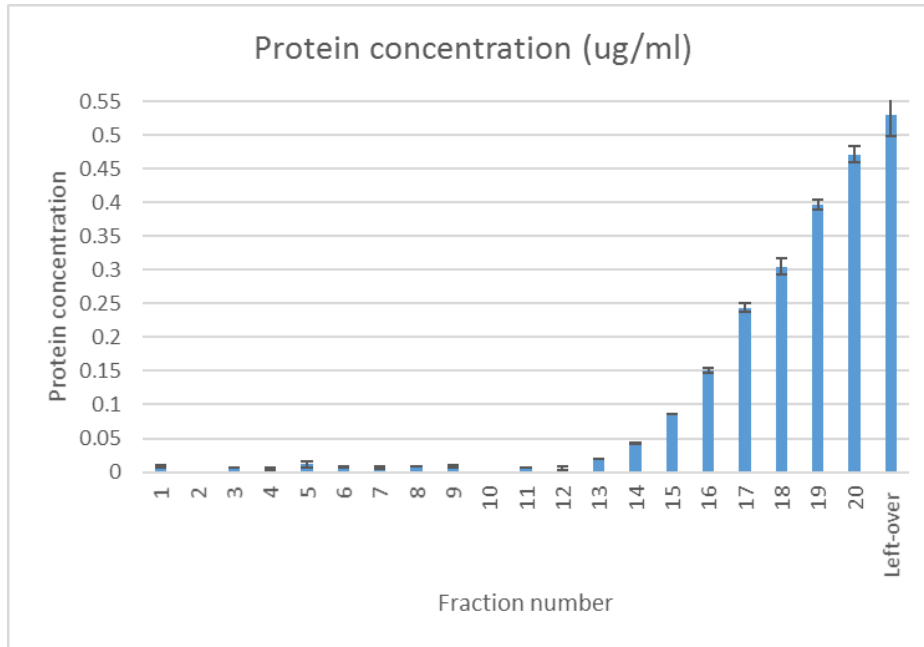


**Figure 2.5. Protein concentration in 20 fractions and left-over proteins of the columns, after fractionation of EVs measured by BCA.** The protein concentration was increased with higher number of parasites (100x more). The initial number of the parasites was increased to 1.6e8/ml. The results are shown in means  $\pm$  SDs of two technical replicates.

### **2.3.3. The peaks of TCT-Secr proteins were shown to be between fractions 17 and 25 of SEC**

The number of the initial parasites this time was increased to 7.3e8/ml. The number of the collected fractions was increased as well to 31 fractions. The protein content was determined in these fractions and leftover proteins from the column by BCA (**Figure 2.6**). As expected, a higher protein content was detected in the fractions, especially those eluting from the Sepharose CL-4B between fractions 17 and 25, which likely correspond to free proteins. Therefore, for subsequent analysis, the number of the parasites was kept at approximately 1e8, and the number of the collected fractions was kept to 30 fractions.

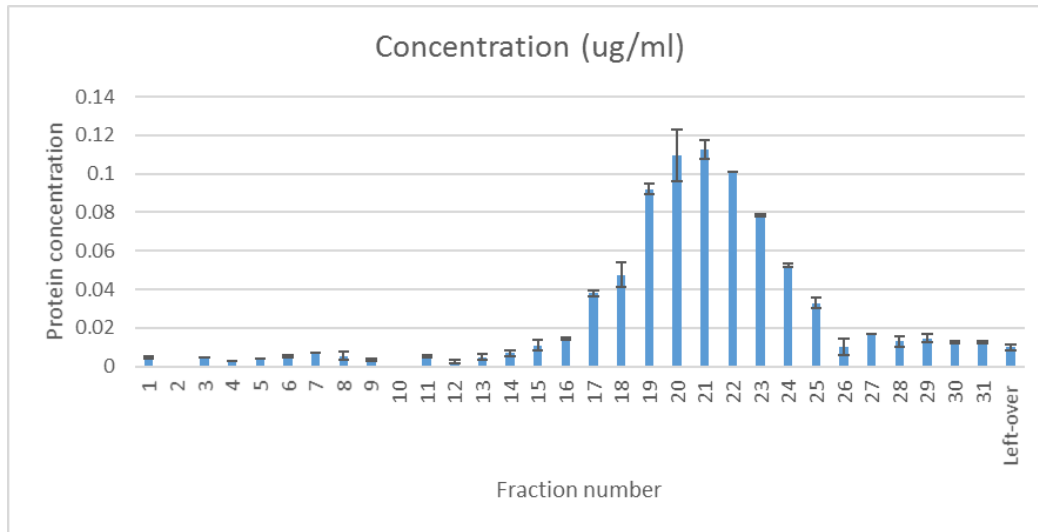


**Figure 2.6. Protein concentration measured by BCA in fractions and leftover proteins from the Sepharose CI-4B column, after fractionation of EVs.** The protein concentration increased from fraction 17 to 25 (peak at fraction 21). The initial number of the parasites was increased to  $7.3 \times 10^8$ /ml). The results are shown in means  $\pm$  SD of two technical replicates.

#### 2.3.4. TCT-Secr showed high reactivity with ChD serum

TCT-Secr (at 0.01, 0.1, 1, and 10  $\mu\text{g/ml}$ ) derived from approximately  $1 \times 10^8$  parasites/ml of Col and Y strains were analyzed by CL-ELISA against ChHSP and NHSP, at 1/100, 1/200, 1/400 and 1/800 dilutions. All four concentrations of TCT-Secr derived from these strains showed high reactivity with ChHSP (**Figure 2.7**). It was also shown in this experiment that the reactivity is dose-dependent. As it was expected, the fractions showed low reactivity with NHSP.

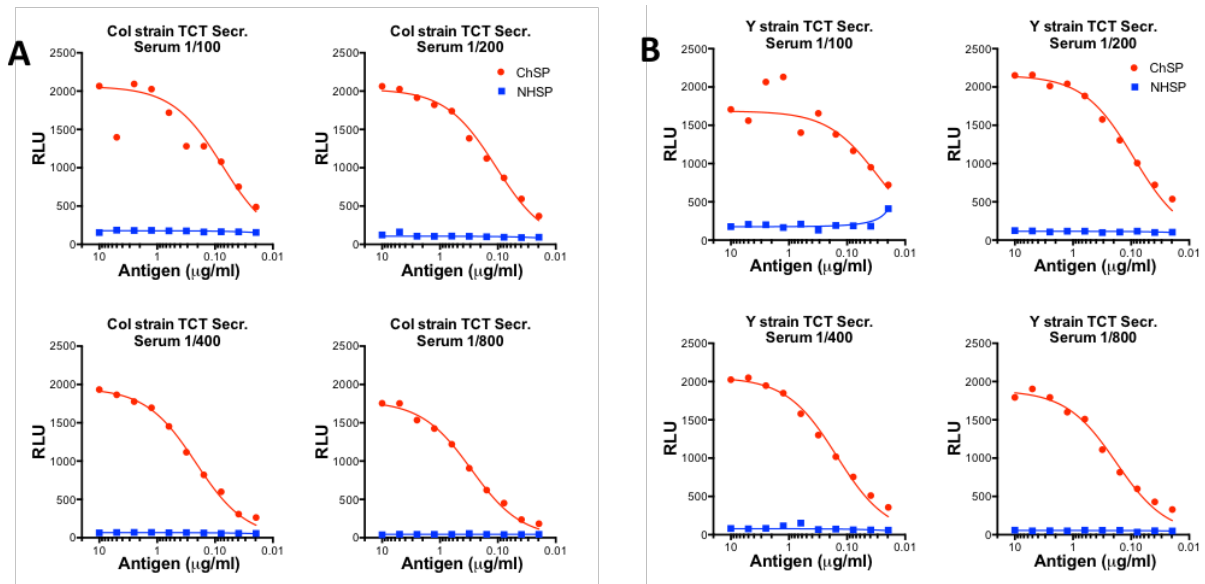


**Figure 2.7.** CL-ELISA reactivity of ChHSP and NHSP to TCT-Secr derived from Colombian (Col) and Y strains. The results show high reactivity of ChHSP to TCT-Secr from both Col (A) and Y (B) strains, at all the tested serum dilutions (1/100, 1/200, 1/400, and 1/800). The results are means  $\pm$  SD of three technical replicates.

### 2.3.5. TCT-Secr derived from different batches of Y, Col and CLB showed high reactivity with ChD serum

The concentrations of 0.1, 1 and 10  $\mu\text{g/ml}$  for the TCT-Secr, and 1/400 and 1/800 dilutions for the serum pools (ChHSP and NHSP) were selected based on the previous experiment. In this experiment, different batches/biological samples were tested (the number varies amongst the three strains, based on the availability) to see whether the reactivity with ChHSP is reproducible and consistent as well. TCT-Secr derived from approximately  $1\text{e}8/\text{ml}$  of Col, Y and CLB (3, 9, and 4 samples, respectively) were analyzed by CL-ELISA against ChHSP and NHSP. High reactivity with ChHSP was observed (Figure 2.8). As it can be observed, the reactivity within each strain is consistently Ag dose-dependent, however, the difference between Ab at 1/400 and 1/800 is

negligible. This pattern as well is followed in the majority of the fractions derived from all 3 strains/clones.

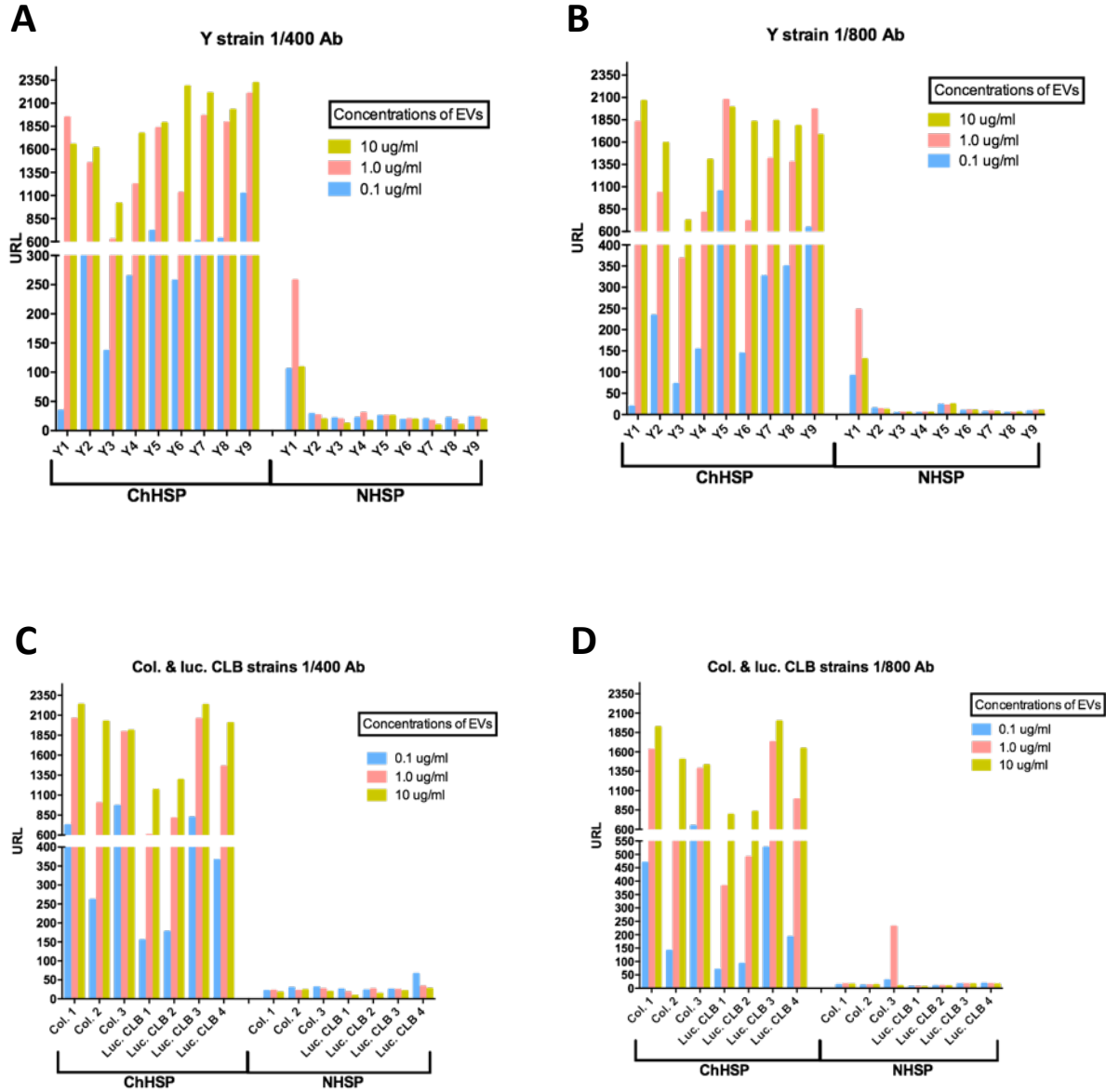


**Figure 2.8. CL-ELISA reactivity of ChHSP and NHSP to various batches of TCT-Secr derived from of Y, Col and CLB.** The results show high reactivity of Y (A and B) and Col and CLB (C and D) strains against ChHSP at both tested serum dilutions (1/400 and 1/800), and all tested TCT-Secr concentrations (0.1, 1, and 10  $\mu\text{g}/\text{ml}$ ). The results are means  $\pm$  SD of three technical replicates.

### **2.3.6. TCT-Secr derived from Col, Y, and CLB showed high reactivity with ChD serum after being stored at -80° C compared to freshly isolated TCT-Secr**

In order to assure  $\alpha$ -Gal content being conserved due to freezing and thawing in addition to the EVs integrity, we also performed CL-ELISA on TCT-Secr isolated freshly on the same day versus the isolates after being stored at -80°C for 2 to 3 months (derived from Col, Y, and CLB), against NHSP and ChHSP. Briefly, TCT-Secr samples were serially diluted in CBC starting with 10  $\mu$ g/ml for 5 dilutions, were immobilized overnight, blocked with 1% BSA/PBST for 1 hr, and incubated for 1 hr with NHSP and ChHSP (1/800) in 1% BSA/PBST. Thereafter, biotinylated goat anti-human IgG was added (1/10,000 in 1%BSA/PBST) for 1 hr, and the reactivity was detected with CL-ELISA reagent (see details in **2.2.8**). As it can be observed in **Figure 2.9**, the reactivity of TCT-Secr with ChHSP was shown (in agreement with our previous results), and moreover, there is no significant difference detected between the reactivity of freshly isolated TCT-Secr, in comparison with TCT-Secr stored at -80°C for few months. Therefore, it is assured that for further analysis, irrespective of TCT-Secr being freshly isolated, or stored at -80°C, the integrity of  $\alpha$ -Gal reactivity with ChHSP is maintained and, therefore, they could be used for further analysis.



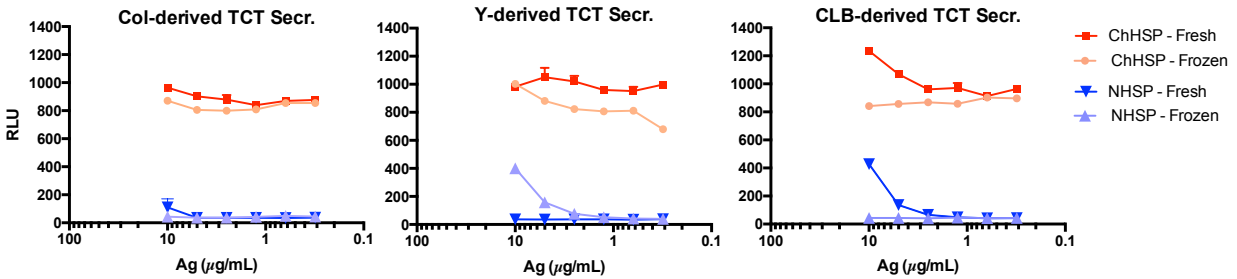


**Figure 2.9.** CL-ELISA reactivity of ChHSP and NHSP to TCT-Secr that were freshly isolated on the same day compared to TCT-Secr stored at  $-80^{\circ}\text{C}$  (derived from of Col, Y, and CLB). The results show high reactivity of TCT-Secr, regardless of being freshly isolated or stored at  $-80^{\circ}\text{C}$ , against ChHSP. The results are means  $\pm$  SD of three technical replicates.

### **2.3.7. SEC-fractionated TCT-EVs derived from Col, Y and CLB showed the highest reactivity with ChD serum from fractions 12 to 20**

After fractionating TCT-Secr derived from Col, Y and CLB by SEC, it was indicated that the reactivity of IB4-lectin and ChHSP to  $\alpha$ -Gal in TCT-Secr was shown mainly between fractions 12 and 20 (**Figure 2.10**). It was shown also that although Y strain-derived fractions showed distinct pattern compared to Col and CLB, however the latter strain/clone showed similar pattern and trend of the reactivity (**Figure 2.10.B-C**). It is noteworthy to mention that there was another peak of protein was detected by BCA between fractions 8 and 10 which was consistent amongst the 3 strains/clone (**Figure 2.10.A**).

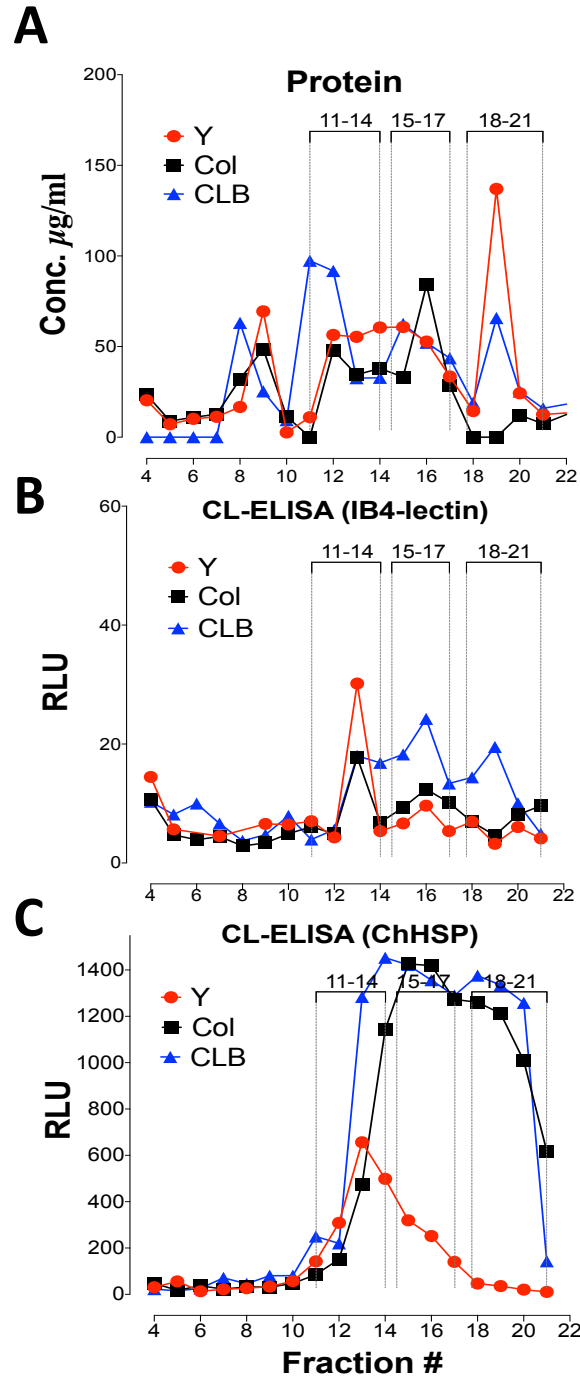


**Figure 2.10.** BCA (A), and CL-ELISA reactivity of IB4-lectin (B), ChHSP (C), and NHSP (B,C) to TCT-Sec, derived from of Col, Y, and CLB, and fractionated by SEC. The results show that protein peaks were shown between fractions 8 and 10 as well as 12 and 20 (A). Moreover, it is shown here that the highest reactivity of TCT-Sec, against IB4-lectin and ChHSP was detected between fractions 12 and 20 (B,C). The results are means  $\pm$  SD of three technical replicates.

### 2.3.8. Reactivity of TCT-Secr with ChHSP in Col, Y and CLB strains is in great part due to $\alpha$ -Gal glycotopes

*T. cruzi* expresses specific surface glycoproteins that have been shown to be conserved amongst different strains. TCT forms have  $\alpha$ -Gal glycotopes that are highly reactive with ChD patient's IgG (Almeida, Milani et al. 1991, Almeida, Ferguson et al. 1994). Here in this experiment, TCT-Secr derived from Col, Y and CLB strains were treated with 0.1 unit/ml green coffee bean  $\alpha$ -galactosidase, overnight, and then tested for reactivity with ChHSP (at 1/800 dilution). Interestingly, the reactivity dropped by 39% and 41% for Col-derived TCT-Secr at 1 and 10  $\mu$ g/ml, respectively. The reduction was also shown in Y-derived TCT-Secr to 55% and 48% at 1 and 10  $\mu$ g/ml, respectively. The reduction was also shown in Y-derived TCT-Secr to 55% and 48% at 1 and 10  $\mu$ g/ml, respectively, as well as in CLB-derived TCT-Secr to 75% and 66% at 1 and 10  $\mu$ g/ml, respectively. These data indicated that the TCT-Secr shed comprise  $\alpha$ -Gal epitopes and the reactivity to the ChHSP is in great part directed to  $\alpha$ -Gal epitopes (Figure 2.11).

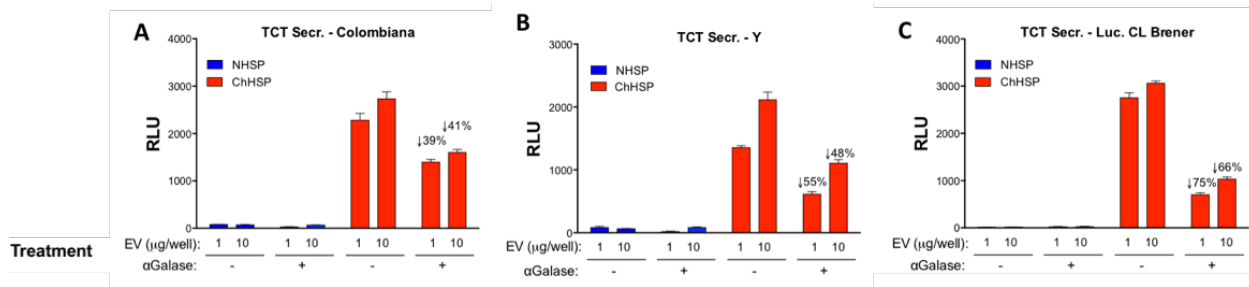


**Figure 2.11. Reactivity of TCT-Secr from Col, Y and CLB strains to ChHSP and NHSP, following treatment with  $\alpha$ -galactosidase.** A reduction of 39-75% of the reactivity to ChHSP (at 1/800 dilution) of TCT-EVs derived from Col (A), Y (B), and CLB (C) strains, at 1 and 10  $\mu$ g/ml. The results are means  $\pm$  SD of three replicates.

### **2.3.9. Purified $\alpha$ -Gal-containing TCT-EVs showed distinguishable profile in NTA than the total TCT-Secr**

In order to assess the EVs population profile (size distribution and concentration) in the TCT-Secr as well as the IB4-lectin-purified EL ( $\alpha$ -Gal(+)) and FT ( $\alpha$ -Gal(-)), NTA was performed. As it is shown in the **Figure 2.12**, EL fractions are showing a shift towards left (smaller EV size: exosomes), which is abundant between 100 and 200 nm. In other words, the exosome population was shown to be enriched in EL fractions in all the strains, and more vividly in Y strain. Furthermore, as expected, FT fractions are showing similar profile as TCT-Secr nonetheless slightly different, and they showed less homogeneity in terms of size distribution compared to EL fractions.

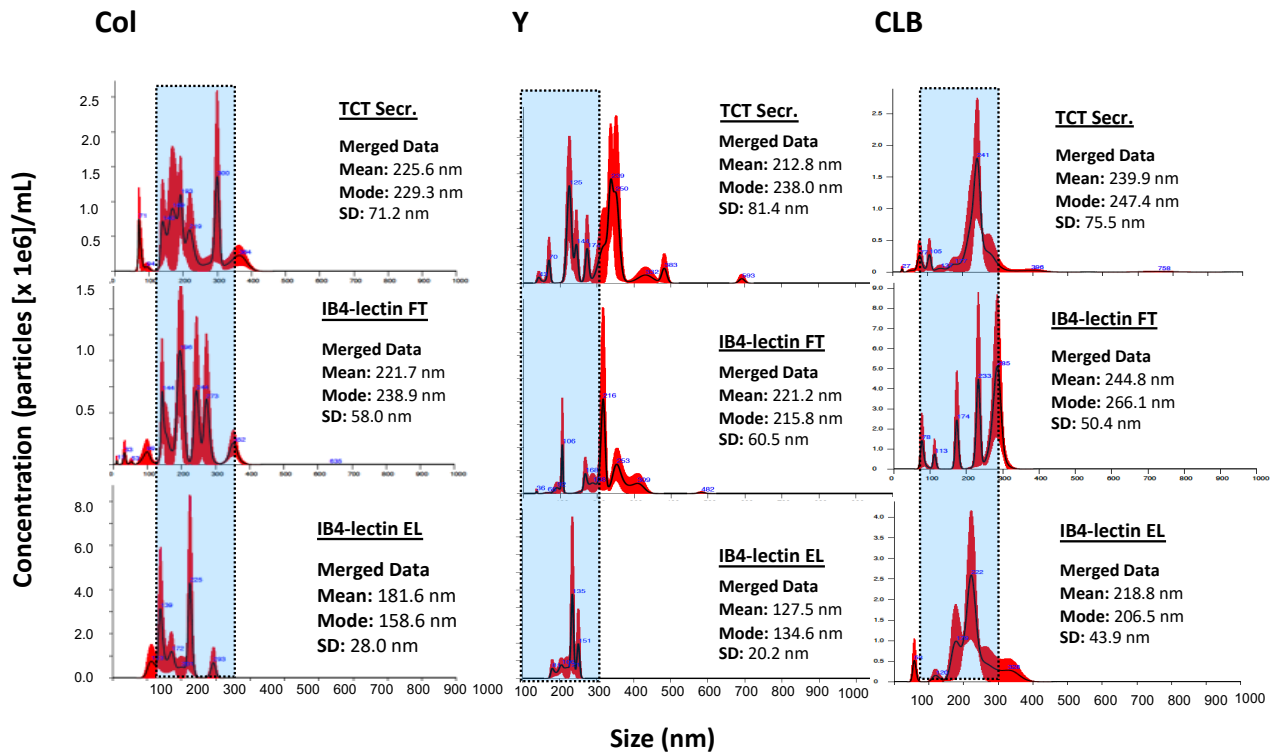


**Figure 2.12. NTA analysis of TCT-Secr and EVs from Col, Y and CLB strains after being subjected to immunoaffinity chromatography.** TCT-Secr was subjected to immunoaffinity chromatography using biotinylated IB4 lectin-neutravidin agarose and EVs size distribution and concentration were measured by NTA. The profiles of the fractions (TCT-Secr, EL and FT) show different profile for ELs compared to FTs. Nevertheless, FTs show more heterogenous population similar to TCT-Secr, unlike ELs which show more homogenous profile and enriched with more of exosomes.

Before proceeding with proteomics analysis, IB4-lectin column fractions (EL and FT) were tested for reactivity with Ch anti- $\alpha$ -Gal by CL-ELISA. As expected, clear high reactivity was observed with EL fraction in compare to FT fraction, indicating that EL fraction was highly enriched with  $\alpha$ -Gal successfully ( $\alpha$ -Gal(+)), through performing the IB4-lectin (**Figure 2.13**). The data of  $\alpha$ -Gal epitope being purified and enriched by IB4-lectin in EL fraction of is supported here as well.

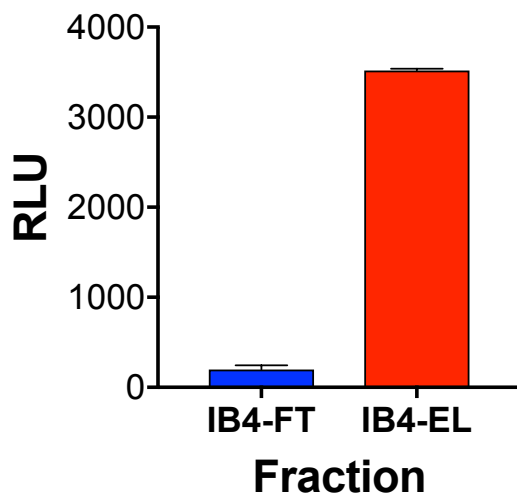


**Figure 2.13. Reactivity of EL and FT fractions after IB4-lectin purification, against Ch anti- $\alpha$ -Gal.** Y-derived EL fraction showed high reactivity with Ch anti- $\alpha$ -Gal, whereas FT which showed very little reactivity. RLU, relative luminescence units. The results are means  $\pm$  SEM of three replicates.

## 2.4. DISCUSSION AND FUTURE WORK

Chagas disease caused by *T. cruzi*, the parasite's life cycle, its vector and its pathogenesis in humans have been described more than 100 years ago by Carlos Chagas (Chagas 1909). However, the detailed mechanisms of host-parasite interaction and immune system modulation are to be elucidated. Various studies have been conducted within previous decades, on EVs in the concept of diseases, as both host and pathogen cells secrete them. One of the mechanisms by which infectious diseases evade immune system is cell-cell modulation which is facilitated by extracellular vesicles (Lovo-Martins, Malvezi et al. 2018). The role of EVs secreted by several parasites during the infection and disease progression has been recently investigated by several researchers (Beauvillain, Ruiz et al. 2007, Giri and Schorey 2008, Beauvillain, Juste et al. 2009, Schnitzer, Berzel et al. 2010, Del Cacho, Gallego et al. 2011, Cronemberger-Andrade, Aragao-Franca et al. 2014), where EVs were playing protective role. On the other hand, they have been shown in the studies on characterizing EVs released from flagellated protozoan parasites to increase the parasitemia in parasitic diseases such as *Leishmaniasis* (Silverman, Clos et al. 2010, Silverman, Clos et al. 2010). These parasites are capable of interacting with various cell types as they survive vector and the host, which leads to having EVs comprising different contents assisting parasite's biodistribution, survival, and pathogenesis (de Pablos Torro, Retana Moreira et al. 2018).

In case of *T. cruzi*, various mechanisms of EVs being releases have been described including larger EVs or ectosomes budding from plasma membrane, and smaller EVs or exosomes within the flagellar pocket which are released through MVBs being exocytosed (da Silveira, Abrahamsohn et al. 1979, Bayer-Santos, Aguilar-Bonavides et al. 2013). EVs released by the

parasite have been shown to be interfering with immune system response (Goncalves, Umezawa et al. 1991).

EVs derived from Y strain TCTs have been described by several studies (Bayer-Santos, Aguilar-Bonavides et al. 2013, Nogueira, Ribeiro et al. 2015, Clemente, Cortez et al. 2016). NanoSight analysis is a established method for assessing the size distribution of the EVs (Soo, Song et al. 2012). First, we showed the presence of EVs in TCT-Secr by NTA, and the size distribution was also determined. Although in the total secretome (TCT-Secr) we found the EVs with the mean size of 212.8 nm (larger EVs), in our  $\alpha$ -Gal(+) fractions) showed similar profile and size distribution to secretome derived from TCT (TCT-Secr). The heterogeneous population of EVs shown in the TCT-Secr in our study have been consistently shown in the previous studies as well.

Isolation of the EVs is one of the challenges in the field (They, Amigorena et al. 2006, Kalra, Simpson et al. 2012), however SEC, ultracentrifugation and affinity chromatography (Wubbolts, Leckie et al. 2003) are the common methods used for EV separation. At first, we did not see reactivity of EVs with ChHSP as it was performed in duplicates and not in triplicates (to do the screening amongst the fractions), and some of the replicates were not consistent, it can be concluded that the unexpected results could be due to technical errors. However, we showed later that they are highly enriched with molecules that are highly and specifically reactive with ChD sera in a concentration-dependent manner. These glycotopes are highly immunogenic to humans, since they are non-self and trigger high levels of trypanolytic protective Ch anti- $\alpha$ -Gal Abs (Almeida, Milani et al. 1991). They showed approximately 50% reduction of the reactivity after being treated with  $\alpha$ -galactosidase, which consolidates the presence of  $\alpha$ -Gal glycotopes. Furthermore, TCT-EVs as a diagnostic biomarker is under investigation as well as more details on how the EVs will increase the infection in vitro and hopefully *in vivo*.



## CHAPTER 3: PROTEOMIC ANALYSIS OF *T. CRUZI*-DERIVED EVS

### 3.1. INTRODUCTION: *T. CRUZI* SURFACE PROTEINS

*T. cruzi* has surface covered by GPI-anchored glycoconjugates that are shown to be conserved in different strains and genotypes (Almeida, Ferguson et al. 1994, Buscaglia, Campo et al. 2006). These molecules are composed of *O*-linked glycans that are covalently attached to a polypeptide backbone, which is anchored to the trypomastigote membrane through a GPI structure (Figure 3.1). It has been previously shown that trypomastigote-specific GPI-anchored mucin-like glycoproteins play an important role in inducing potent macrophage activation (Camargo, Almeida et al. 1997, Almeida, Camargo et al. 2000, Campos, Almeida et al. 2001). These glycoconjugates are shown to be released in the EVs (da Silveira, Abrahamsohn et al. 1979, Ouaiissi, Dubremetz et al. 1990, Goncalves, Umezawa et al. 1991, Bayer-Santos, Aguilar-Bonavides et al. 2013, Bautista-Lopez, Ndao et al. 2017, Ribeiro, Vasconcellos et al. 2018).

On the other hand, *T. cruzi* has evolved several strategies to invade the host cells including manipulating various host cell surface receptors and signaling pathways (Villalta, Scharfstein et al. 2009). The infective trypomastigotes are capable of infecting large varieties of nucleated cells in mammals (De Souza 2002). One of these mechanisms is releasing extracellular vesicles (EVs) which assists the parasite's survival and its replication within the host. *T. cruzi* releases proteins associated with EVs (Bayer-Santos, Aguilar-Bonavides et al. 2013) involved with its metabolism, and interaction with host immune cells (invasion and evasion mechanisms). Protein analysis of EVs derived from *T. cruzi* has shown that GPI-anchored mucin-like glycoproteins are released in these EVs (Agusti, Couto et al. 2000). Therefore, characterization of EVs, could be helpful towards studying the pathogenesis of the parasite, and molecules involved in it.

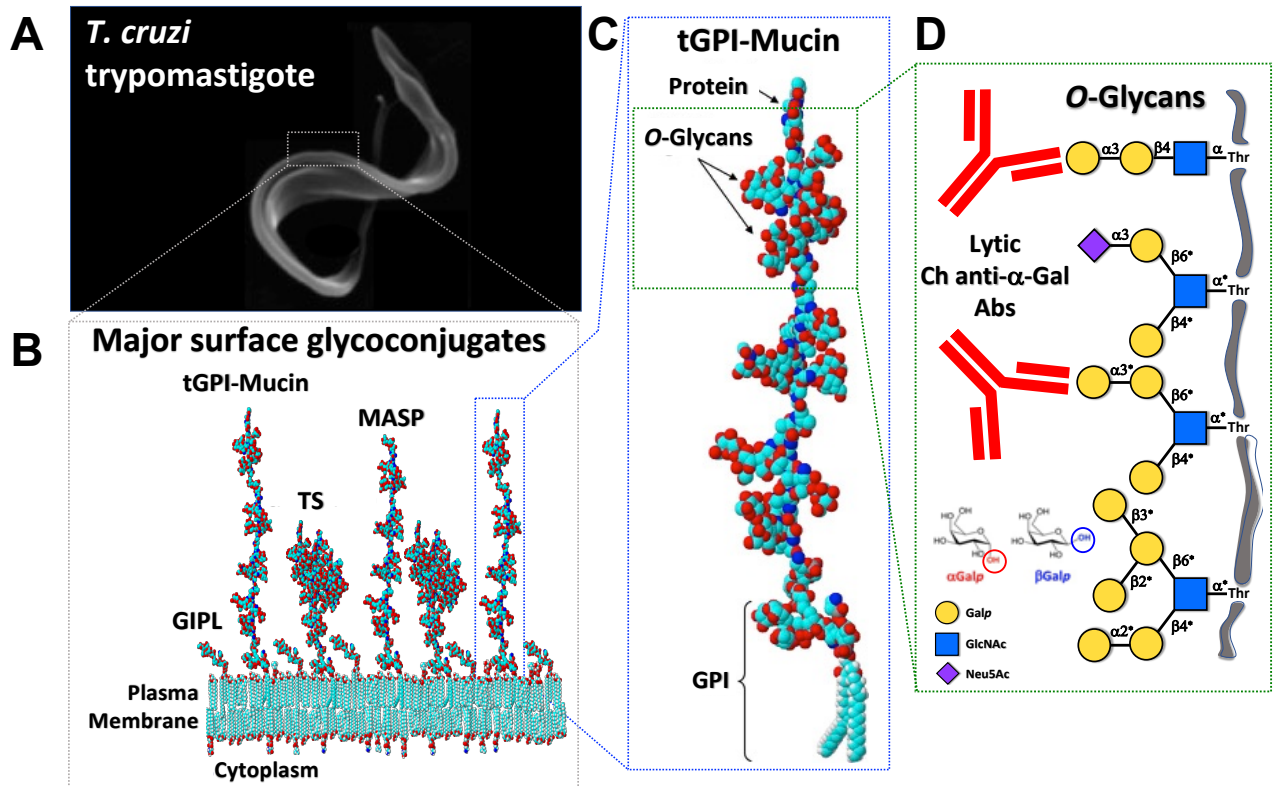


**Figure 3.1. Schematic representation of *T. cruzi* trypomastigote surface coat and its GPI-anchored glycoconjugates.** (A and B) Mammal-dwelling infective *T. cruzi* trypomastigote form contains a complex cell surface consisting of several glycoconjugates inserted into the plasma membrane via a GPI anchor (C and D) These glycoconjugates include GIPL and GPI-anchored proteins (i.e., tGPI-mucin, TS, and MASP). The major tGPI-mucin family expressed in trypomastigotes (i.e., TcMUCII) (Buscaglia, Campo et al. 2004) contains a protein core heavily glycosylated with *O*-glycans linked mostly to threonine (Thr) residues via an  $\alpha$ -*N*-acetylglucosamine ( $\alpha$ -GlcNAc). tGPI-MUCII specifically contains terminal, nonreducing  $\alpha$ -galactopyranose ( $\alpha$ -Galp) residues, which serve as the major targets for the highly abundant lytic anti- $\alpha$ -Gal Abs, produced during both the acute and chronic phases of ChD (Almeida, Milani et al. 1991, Gazzinelli, Pereira et al. 1991, Almeida, Ferguson et al. 1994). About ten percent of these *O*-glycans exists as linear trisaccharides (Gal $\alpha$ 1,3Gal $\beta$ 1,4GlcNAc $\alpha$  or Gal $\alpha$ 3LN $\alpha$ ), whereas the remaining 90% of the structures are branched and are as-yet to be structurally characterized. The hypothetical linkages (\*) of the branched *O*-glycans are based on partial liquid chromatography-tandem mass spectrometry (LC-MS/MS) data analysis

following beta-elimination and permethylation of tGPI-mucin-derived *O*-glycans (Ortega-Rodriguez and Almeida, unpublished data). Text and figure taken and modified from (Ortega-Rodriguez, Portillo et al. 2019).

## **3.2. MATERIALS AND METHODS**

### **3.2.1. Mammalian cell culture**

LLC-MK2 and U2-OS cells were cultured in low glucose DMEM with 10% FBS/ Penicillin-Streptomycin as was previously described in **2.2.1** at 37°C, under CO<sub>2</sub> atmosphere, and were sub-cultured once or twice a week Trypsin.

### **3.2.2. Parasite culture, and isolation and storage of extracellular vesicles (EVs)**

The parasite culture and TCT-Secr isolation was performed after optimization of the storage temperature and parasite number (as described in **2.2.2**). The parasite-comprising supernatant (from 1e8 parasites) was taken from the cell flask and was centrifuged for 10 minutes at 1,500 xg, at 4° C, and the supernatant was incubated for 2 h for the cell debris and amastigotes (in the pellet) to be separated from the trypomastigotes (by them swimming to the supernatant). The supernatant (which has the trypomastigotes) was transferred to another tube and centrifuged for 10 minutes at 2,465 xg at 4° C, and the trypomastigote-containing pellet was washed twice with 1X PBS and incubated with FBS free media for 6 h for the parasites to shed vesicles, and it was centrifuged at 2,465 xg for 10 minutes at 4° C to separate the vesicles from the trypomastigotes. The supernatant was filtered through 0.45-µm syringe filter and the flow through which is TCT EV-comprising conditioned medium, and analyzed by nanoparticle tracking analysis (NTA), in triplicate. Three measurements of the same sample were performed in 20-sec intervals, using the default settings of the instrument. The error bars indicate the standard error of the mean.

### **3.2.3. BCA Protein Assay**

TCT-Secr derived from Col, Y, and CLB TCTs were analyzed for protein concentration by BCA according to the manufacturer as described earlier (2.2.4).

### **3.2.4. Western blotting the TCT-Secr with IB4-lectin, and purified Ch anti $\alpha$ -Gal Ab**

TCT-Secr aliquots (derived from Col, Y, and CLB) were added 1% Halt™ Protease Inhibitor Cocktail (Thermo Fisher Scientific)/  $\pm$  50  $\mu$ g N $\alpha$ -Tosyl-L-lysine chloromethyl ketone hydrochloride (TLCK: Millipore Sigma) before the storage at -80°C. Samples containing 10 and 30  $\mu$ g of protein, quantified by BCA technique (as described in 2.4.), were applied in each lane of 4-20% Mini-PROTEIN® TGX™ Precast Protein Gels, and separated and transferred to 0.45  $\mu$ m nitrocellulose membranes using standard wet transfer sandwich protocol (Towbin, Staehelin et al. 1992). Briefly, transfer buffer (25 mM Tris/192 mM glycine/0.1% SDS, at pH 8.3) was added to the transfer tank, transfer sandwich was assembled with assuring the blot being on the cathode and the gel on the anode, and the air bubbles being removed from the system, and the proteins were transferred at 100V for 1 hr, at 4°C on ice. The membranes were blotted with IB4-lectin and then Ch anti  $\alpha$ -Gal Ab after stripping the lectin. Briefly, membranes were blocked with Tris-buffered saline: 50 mM Tris, 150 mM NaCl (TBS)/ 1% bovine serum albumin (BSA: Fisher BioReagents™ Bovine Serum Albumin, Fraction V, Heat Shock Treated)/ 0.1% Tween 20 (Promega, Madison, WI: T), pH at 7.6, at 4° C overnight. They were washed (all the washings were performed 3x with TBST, each time 5 minutes), and incubated with 5  $\mu$ g of IB4-lectin/ TBST/ 1% BSA for 1 hr. The membranes were washed, and incubated with secondary antibody (anti goat-anti human biotin-conjugated IgG antibody: Thermo Fisher Scientific, at 1/10,000 dilution/ TBST/ 1% BSA for 1 hr. Thereafter, they were washed and incubated with Neutravidin Horse Radish Peroxidase (HRP: Thermo Fisher Scientific) at 1/5000 dilution/ TBST/ 1% BSA for 1 hr, and finally CL reagent

(Pierce<sup>TM</sup> ECL Western Blotting Chemiluminescent Substrate: Thermo Scientific), at 1:1 Reagent A: Reagent B was added and the images were taken d by iBright Western Blot Imaging Systems: Thermo Scientific. All the steps after blocking were performed with gentle agitation at 42 RPM, at RT. After the first blotting, the membrane was stripped with stripping buffer (Restore<sup>TM</sup> western Blot Stripping Buffer: Thermo Fisher Scientific), and was probed with 5 µg of Ch anti α-Gal Ab/ TBST/1% BSA, and the immunoblotting was performed as described in this section.

### **3.2.5. Silver staining**

After TCT-Secr prep samples were separated through precast gel (as described in **2.8**), the proteins were stained with silver stain (Pierce<sup>TM</sup> Silver Stain for Mass Spectrometry: Thermo Fisher Scientific) according to the manufacturer's protocol. Briefly, the gels were washed with ultrapure water for 5 minutes 2x, fixed with fixing solution (30% ethanol, 10% acetic acid) first for 15 min, and then overnight. Thereafter, the gel was washed with ethanol wash solution (10% ethanol) for 5 min 2x, and then with ultrapure water for 5 min 2x. Afterwards, the sensitizer working solution (1:500 Silver Stain Sensitizer: ultrapure water) was added (prepared just before use) and the gel was incubated exactly for 1 minute, and then washed with ultrapure water for 1 minute 2x. Then the enhancer solution (1:100 Silver Stain Enhancer: Silver Stain) was immediately added to the gel, and incubated for 5 min. The developer working solution thereafter was prepared (1:100 Silver Stain Enhancer: Silver Stain Developer), and after the gel was washed with ultrapure water for 20 sec 2x, it was quickly added to the gel for 1 min. The stop solution (5% acetic acid) was immediately added after the desired bands appeared, to the existing developer working solution (to avoid excessive background being generated), and then replaced with fresh stop solution and incubated for 10 min. Finally, the stop solution was washed with ultrapure water 3x and the gel

was imaged by iBright Western Blot Imaging Systems: Thermo Scientific. All the steps were performed with gentle agitation at 42 rpm, at rt.

### **3.2.6. Affinity chromatography using immobilized IB4-lectin for enrichment of $\alpha$ -Gal-containing TCT-EVs**

$\alpha$ -Gal-containing EVs were purified from the TCT-Secr, obtained from the conditioned medium of Col, Y, and CLB strains by affinity chromatography, using IB4-lectin as described in **3.2.7**. Briefly, the TCT-Secr sample (1 mg protein) was redissolved in TBS buffer, and applied to a column after the storage buffer was removed (**3.2.7**) with biotinylated IB4 lectin immobilized to Neutravidin HP SpinTrap. Unbound flow-through (**FT**) fraction was collected. The column was then washed with wash buffer, and a wash (**W**) fraction was collected.  $\alpha$ -Gal-Positive molecules were eluted with elution buffer (**EL**), and immediately neutralized with 1 M Tris, pH 8.0.

### **3.2.7. Protein digestion and proteomic analysis of EV samples**

The EV samples from Y, Colombiana (Col) and luciferase-expressing CL Brener were separately pooled together and concentrated 5X, digested through trypsin digestion. Briefly, 40  $\mu$ g of protein was resuspended in 8 M urea, reduced with 5 mM dithiothreitol (DTT), alkylated with iodoacetamide (IAA), and digested using trypsin through Filter-Aided Sample Prep (FASP) kit (Expedeon, San Diego, CA). Peptides were eluted from the filter with 0.1% formic acid (FA) and the samples were then dried in a vacuum centrifuge (CentriVap Concentrator, Labconco) and were run through mass-spectrometry (MS) for proteins associated with the respective *T. cruzi* strains.

After the peptide digestion, 5  $\mu$ L was loaded onto a 25 cm in house packed pre-equilibrated 5  $\mu$ m porous silica AQUA C18 (Phenomenex) New Objective Picotip Emitter column, with 5% solvent B (90% acetonitrile, 0.1% formic acid) 95% solvent A (100% water, 0.1% formic acid) for 10 minutes with at flow rate of 0.4 mL min<sup>-1</sup>. The elution gradient ramped from 10% to 35% solvent B over 85 minutes, followed by a 5-minute ramp to 95% solvent B. A plateau was maintained at 95% solvent B for 9 minutes, then a sharp decrease to equilibration conditions for 1 minute, followed by a 20-minute equilibration for subsequent sample injections. A top-10 peak analysis was performed on a Q Exactive Plus Hybrid Quadrupole-Orbitrap Mass Spectrometer (Thermo Scientific) with the full scan set to a 70,000 resolution with an AGC target set to 3e6; dd-MS2 resolution at 17,500 with a 1e5 AGC target. The Q Exactive Plus was equipped with a Nanospray Flex Ion Source (Thermo Scientific).

### **3.3. RESULTS**

#### **3.3.1. Strong binding of TCT-Secr derived from Col, Y and CLB was shown with purified Ch anti- $\alpha$ -Gal Ab and IB4-lectin in western blot**

Western blotting of TCT-Secr proteins, derived with Col, Y, and CLB strains being probed with Ch anti  $\alpha$ -Gal Ab and IB4-lectin, showed strong binding with both anti  $\alpha$ -Gal Ab and IB4-lectin. The pattern of  $\alpha$ -Gal-containing glycoproteins which behave like tGPI-mucins and form a smear (ranging from approximately 60 to 110 kDa in the case of *T. cruzi* TCT-Secr), is further supported by silver staining. Nevertheless, within the smear, stronger bands were noticeable in silver staining, with the sizes of 65 and 95 kDa in Col and Y strain-derived. It is noteworthy to mention that when the sample preps are added TLCK additional to Halt Proteinase inhibitor

cocktail in order to prevent protein degradation by protease(s), it was shown that the degradation was less observed in the lanes loaded with samples added TLCK, and the bands/ smears were stronger (**Figure 3.2**). Therefore, for the further analysis, samples were stored with both 1% Halt Proteinase inhibitor cocktail and 50 µg/ml of TLCK being added to them.

Silver staining of TCT-Secr protein samples derived from Col, Y, and CLB strains and separated on the SDS gel showed strong bands with approximately 100 kDa, and smears from 50 to 65 kDa (**Figure 3.2**). Moreover, two less strong bands appeared with the sizes of approximately 175 kDa and 200 kDa. Immunoblotting of TCT-Secr proteins samples probed with Ch anti  $\alpha$ -Gal Ab and IB4-lectin, showed strong binding with both anti  $\alpha$ -Gal Ab and IB4-lectin (**Figure 3.2**). The pattern of *T. cruzi*  $\alpha$ -Gal-containing glycoproteins which behave like tGPI-mucins and form a smear (ranging from approximately 60 to 110 kDa), is clearly shown here. It is noteworthy to mention that as protein degradation by protease(s)/ peptidases(s) have been observed in our earlier proteomics analysis (**Table 3.1**), when solely Halt proteinase inhibitor cocktail was added to the TCT-Secr, therefore, TLCK with more effective inhibition ability (specially on trypsin and trypsin-like enzymes) was added to the samples to maintain the protein integrity. As shown in **Figure 3.2**, in TCT-Secr samples with TLCK added additional to Halt Proteinase inhibitor cocktail, less degradation was observed and the bands/ smears were stronger, especially in the lanes with 30 µg/ lane of protein. Therefore, for the further analysis, samples were stored with both 1% Halt Proteinase inhibitor cocktail and 50 µg of TLCK being added to them.



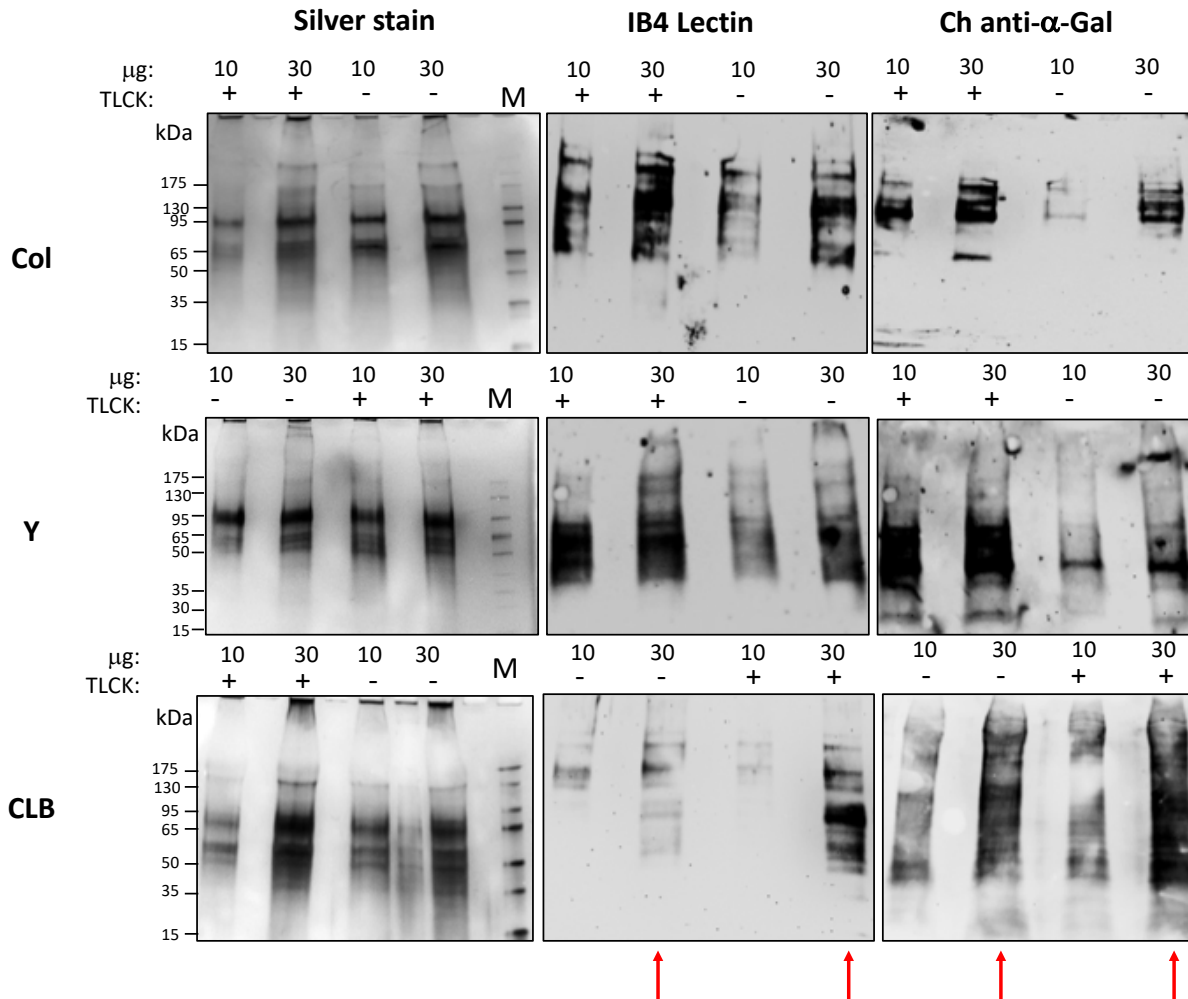


**Figure 3.2. Blotting with IB4 Lectin and Ch anti- $\alpha$ -Gal, as well as staining with Silver stain.** Col, Y, and CLB TCT-Secr blotting with IB4 Lectin and Ch anti- $\alpha$ -Gal, and stained with Silver stain. Trypomastigote secretome was added Halt Proteinase inhibitor cocktail with, and without TLCK before storage. Col-Strain trypomastigote secretome contains serine protease(s) that degrade the  $\alpha$ -Gal-containing glycoproteins that behave like tGPI-mucins (red arrows), which are inhibited when protease/ proteinase inhibitor is added to the sample, specially, in 10  $\mu$ g lane.

**Table 3.1. Proteases and peptidases identified by proteomic analysis in the total TCT-Sec, and flow-through and eluate fractions from the IB4-lectin column.**

#	Protein Name	Accession Number	TCT Total Secr	Flow Through	Elute
<b>PEPTIDASES</b>					
261.1	Aminopeptidase OS=Trypanosoma cruzi Dm28c	V5BSI2_TRYCR	0.4	0.0	0.0
49	Aminopeptidase OS=Trypanosoma cruzi Dm28c	V5BWE3_TRYCR	4.4	12.1	0.0
185	Aminopeptidase, putative OS=Trypanosoma cruzi (strain CL Brener) GN=Tc00.1047053504153.140 PE=4 SV=1	Q4E2R9_TRYCC	0.7	1.5	0.0
261.2	Aminopeptidase, putative OS=Trypanosoma cruzi (strain CL Brener) GN=Tc00.1047053508153.60 PE=4 SV=1	Q4E686_TRYCC	0.4	0.0	0.0
71	Aminopeptidase, putative OS=Trypanosoma cruzi (strain CL Brener) GN=Tc00.1047053511051.70 PE=4 SV=1	Q4D5P1_TRYCC	7.3	0.0	3.1
129	Calpain cysteine peptidase, putative (Fragment) OS=Trypanosoma cruzi (strain CL Brener) GN=Tc00.1047053511441.10 PE=3 SV=1	Q4CS87_TRYCC	5.1	0.0	0.0
251.1	Calpain-like cysteine peptidase, putative OS=Trypanosoma cruzi (strain CL Brener) GN=Tc00.1047053506983.39 PE=4 SV=1	Q4CYU3_TRYCC	0.4	0.0	0.0
251.2	Calpain-like cysteine peptidase, putative OS=Trypanosoma cruzi (strain CL Brener) GN=Tc00.1047053508675.29 PE=4 SV=1	Q4D066_TRYCC	0.4	0.0	0.0
143	Calpain-like cysteine peptidase, putative OS=Trypanosoma cruzi (strain CL Brener) GN=Tc00.1047053508999.190 PE=3 SV=1	Q4E0D8_TRYCC	4.4	0.0	0.0
99	Carboxypeptidase OS=Trypanosoma cruzi PE=3 SV=1	A0A1B1R0V7_TRYCR	0.0	4.5	2.1
261	Group of Aminopeptidase OS=Trypanosoma cruzi Dm28c GN=TCDM_00251	V5BSI2_TRYCR (+1)	0.7	0.0	0.0
<b>PROTEASES</b>					
262.1	ATP-dependent Clp protease subunit OS=Trypanosoma cruzi Dm28c GN=TCDM_12171	V5AYJ4_TRYCR	0.4	0.0	0.0
183	ATP-dependent Clp protease subunit, heat shock protein 78, putative OS=Trypanosoma cruzi (strain CL Brener) GN=Tc00.1047053508737.100	Q4DTH5_TRYCC	0.0	0.0	2.1
59	Surface protease GP63, putative OS=Trypanosoma cruzi (strain CL Brener) GN=Tc00.1047053506289.210	Q4DVY4_TRYCC	4.4	10.6	0.0

### 3.3.2. Purified $\alpha$ -Gal-containing TCT-EVs showed distinguishable profile in NTA than the total TCT-Secr

In order to assess the EVs population profile (size distribution and concentration) in the TCT-Secr as well as the  $\alpha$ -Gal(+) (EL) and  $\alpha$ -Gal(-) (FT), NTA was performed. The data of  $\alpha$ -Gal being purified is supported with NTA as it is shown in **Figure 3.3**. As it is shown in the figure, EL fractions are showing a shift towards left (smaller EV size: exosomes) which is abundant between 100-200 nm. In other words, the exosome population was shown to be enriched in EL fractions in all the strains, and more vividly in Y strain. Furthermore, as expected, FT fractions are showing similar profile as TCT-Secr nonetheless slightly different, and they showed less homogeneity in terms of size distribution compared to EL fractions.

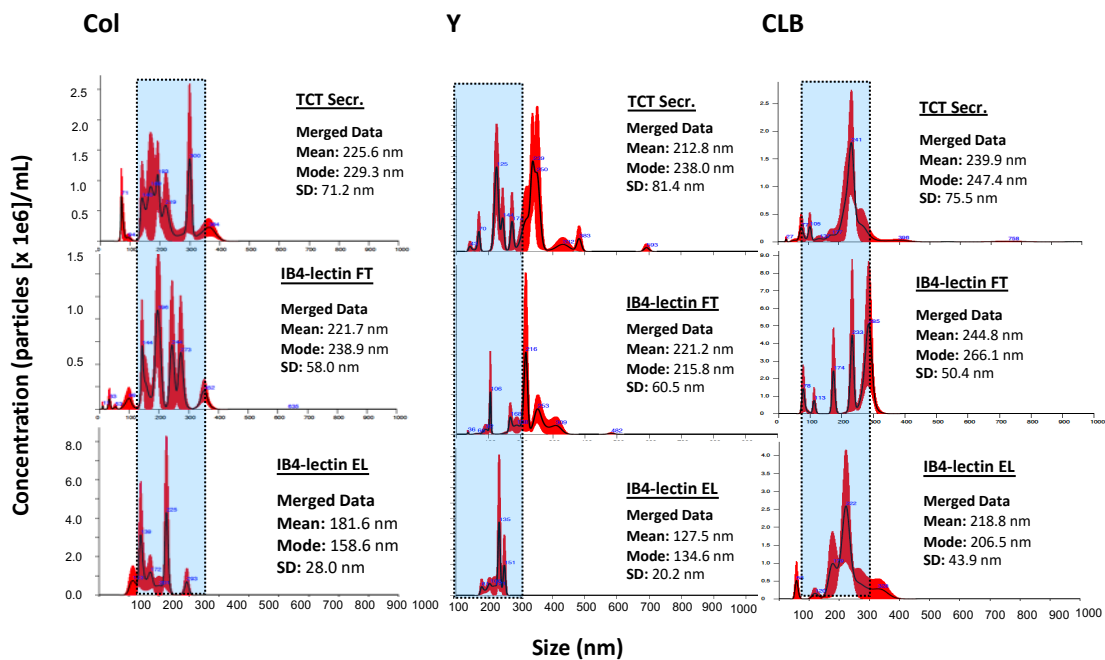


**Figure 3.3.** NTA analysis of TCT-Secr and TCT-EVs from Col, Y and CLB strains after being subjected to **immunoaffinity chromatography**. TCT-Secr was subjected to immunoaffinity chromatography using biotinylated IB4 lectin-neutravidin agarose and EVs size distribution and concentration were measured by NTA. The profiles of the fractions (TCT-Secr, EL and FT) show different profile for ELs compared to FTs. Nevertheless, FTs show more

heterogenous population similar to TCT-Secr, unlike ELs which show more homogenous profile and enriched with more of exosomes.

### **3.3.3. Proteomic analysis of the TCT-Secr and TCT-EVs derived from Y, Col and CLB strains show TcMUC II, MASP, TS, and other EV-associated proteins**

*T. cruzi* GPI-anchored proteins such as TcMUC II and MASP are crucial for parasite invasion and evasion (Almeida and Gazzinelli 2001, Ropert, Ferreira et al. 2002, Nardy, Luiz da Silva Filho et al. 2013) (**Figure 3.1**). These parasites also use its TS enzyme to acquire sialic acid residues from host glycoconjugates and transfer to GPI-mucins, to be able to escape from being recognized by the host immune system (Nardy, Luiz da Silva Filho et al. 2013, da Fonseca, da Costa et al. 2019), which has an important implication during the disease acute phase (Tribulatti, Mucci et al. 2005). Moreover, EVs from *T. cruzi*, comprise several parasite's virulence factors, including peptidases that are able to digest different peptides (Alvarez, Niemirowicz et al. 2012, Bayer-Santos, Aguilar-Bonavides et al. 2013, Marcilla, Martin-Jaular et al. 2014). Since secreting vesicles are known to be crucial for the parasite like other eukaryotes, it is important to test if those surface markers on the parasite are secreted in the vesicles. A vast array of surface markers in the EVs derived from the parasites (Col, Y, and CLB) was found by proteomic analysis (**Figure 3.4-5**). It was shown also that there are more common expressed proteins between Y and CLB but not Col. We have found various *T. cruzi* specific surface markers being secreted in the EVs including Tc-MUC II, MASP, and TS families, which supports the previous research showing these crucial molecules of the parasite being exchanged through EVs.

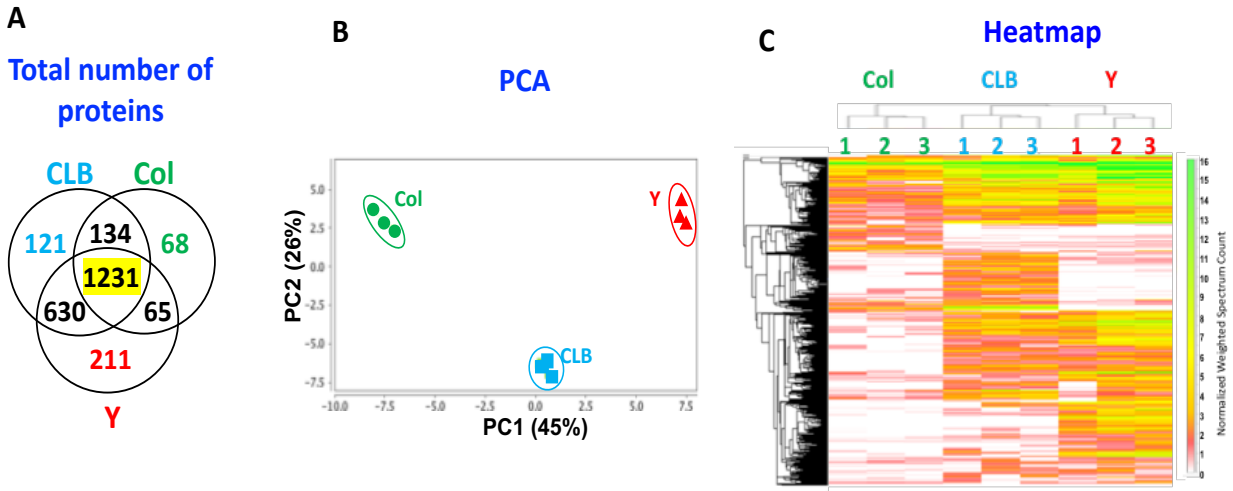


**Figure 3.4. Proteomic analysis of TCT-Secr from Col, Y, and CLB strains.** (A) Venn diagram of proteins identified in TCT-Secr of Col, Y, and CLB. (B) Principal component analysis (PCA) of proteins of TCT-Secr of Col, Y, and CLB. (C) Heat map of 1,000 most abundant proteins found in the TCT-Secr of the three strains (human and bovine contaminants were excluded as well). For each strain, five biological replicates were combined, concentrated by freeze-drying, and digested via FASP-trypsin. The heat map graph was plotted using Scaffold perSPECTives.

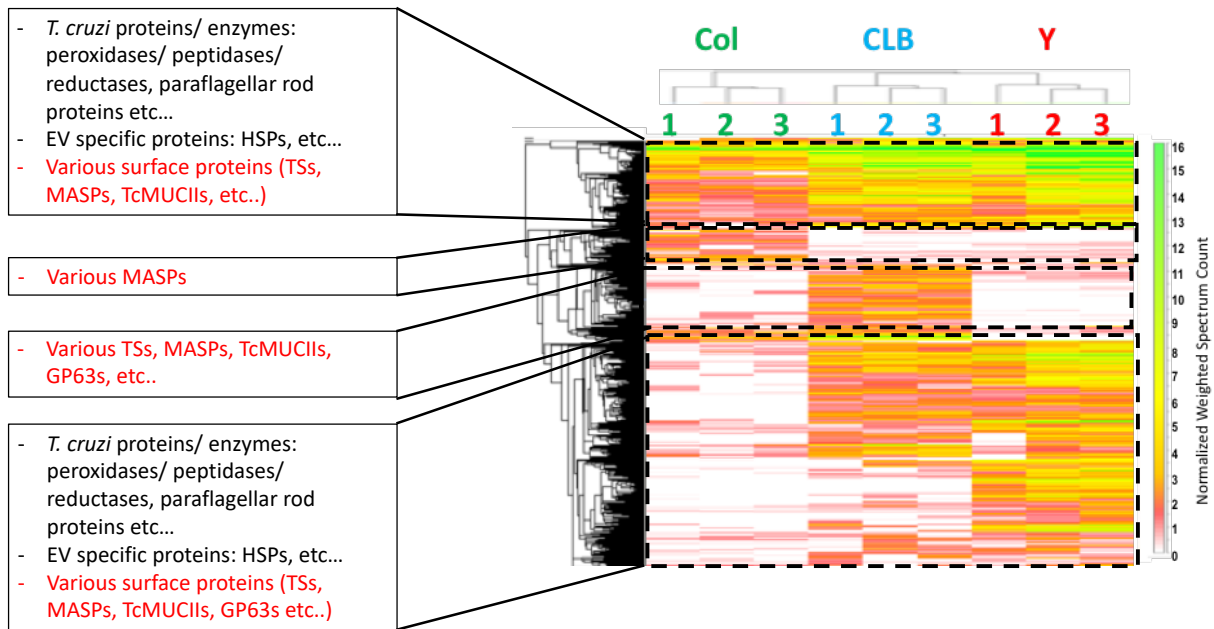


**Figure 3.5. Heat map of 1,000 most abundant proteins found in the TCT-Secr of Col, Y, and CLB strains (zoomed in Figure 3.3).** Heat map of 1,000 most abundant proteins found in the TCT-Secr of the three strains show various *T. cruzi*-isolated (including pathogenic surface proteins), and EV-specific proteins. Human and bovine contaminants were excluded as well. For each strain, five biological replicates were combined, concentrated by freeze-drying, and digested via FASP-trypsin. The heat map graph was plotted using Scaffold perSPECTives.

A subset of highly enriched  $\alpha$ -Gal(+) glycoproteins, particularly TcMUCII mucins, was obtained in the EL fraction from the IB4-lectin column in Col, and Y strains as well as CLB clone (Figures 3.6-8). Mucins of the TcMUC II family have been described as the main  $\alpha$ -Gal-containing glycoproteins of *T. cruzi* TCTs (Almeida, Ferguson et al. 1994, Buscaglia, Campo et al. 2004). On the other hand,  $\alpha$ -Gal- fraction comprised of MASP, TS, and GP63 glycoprotein families which are known to be having no or very less  $\alpha$ -Gal epitopes.  $\alpha$ -Gal-containing fraction obtained by IB4-lectin immune-purification from TCT-Secr seem to be devoid of these latter group

of glycoproteins (MASP, TS, and GP63), indicating that the  $\alpha$ -Gal-enriched TCT-EVs have a distinct protein profile. These results are in agreement with previous work that proposed distinct regions and biogenesis for  $\alpha$ -Gal(-) and  $\alpha$ -Gal(+) glycoproteins, and it has been described that they are not located on the same plasma membrane regions (e.g. for Tc-MUC and TS: (Lantos, Carlevaro et al. 2016).

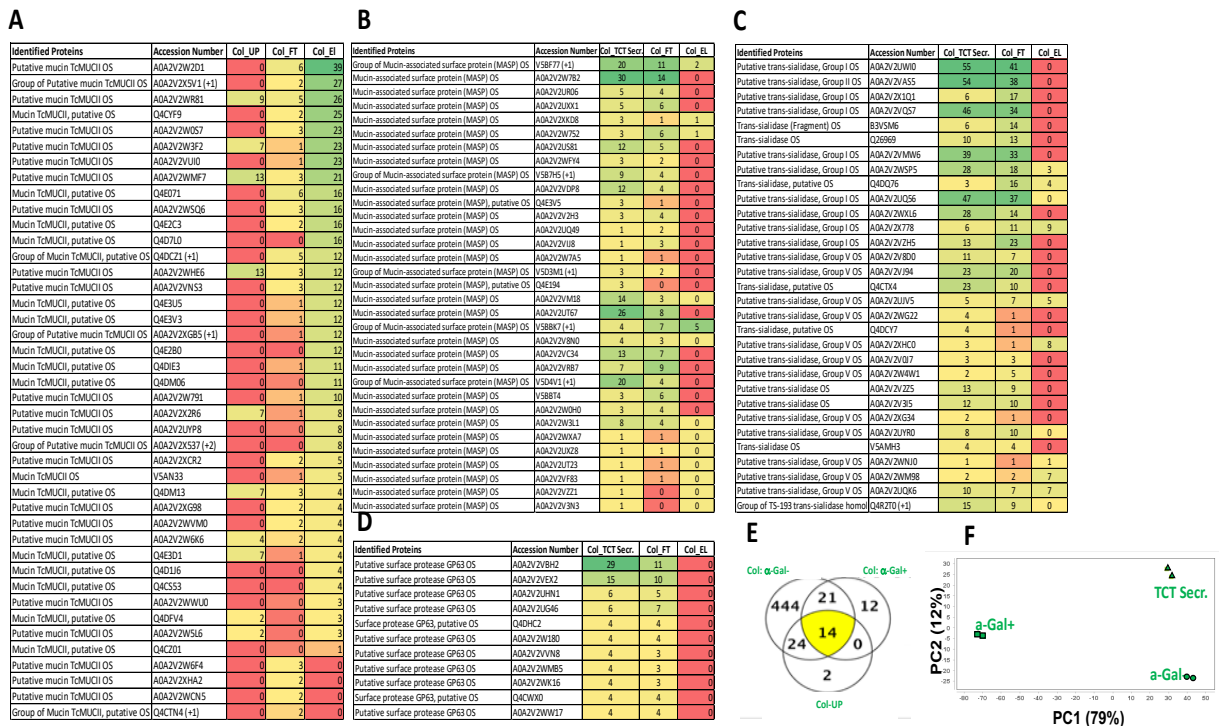


**Figure 3.6. Proteomic analysis of TCT-Secr and IB4-lectin-purified TCT-EVs from *T. cruzi* Colombiana (Col) strain.** (A) TcMUC mucins, particularly members of the TcMUC II family, are the main  $\alpha$ -Gal-containing glycoproteins eluted from the immobilized IB4 lectin column. (B-D) MASPs, TS, and GP63 proteins found in the TCT-Secr but not in the IB4-EL fraction. This indicates that they do not have  $\alpha$ -Gal residues in their composition. (E) Venn diagram and (F) principal component analysis (PCA) of proteins identified in TCT-Secr,  $\alpha$ -Gal(-) and  $\alpha$ -Gal(+) fractions. Numbers in the last two columns of each table represent the total spectral count for the protein identified by LC-MS/MS. The results represent five biological replicates being combined, concentrated by 10-kDa filter, and digested via FASP-trypsin.

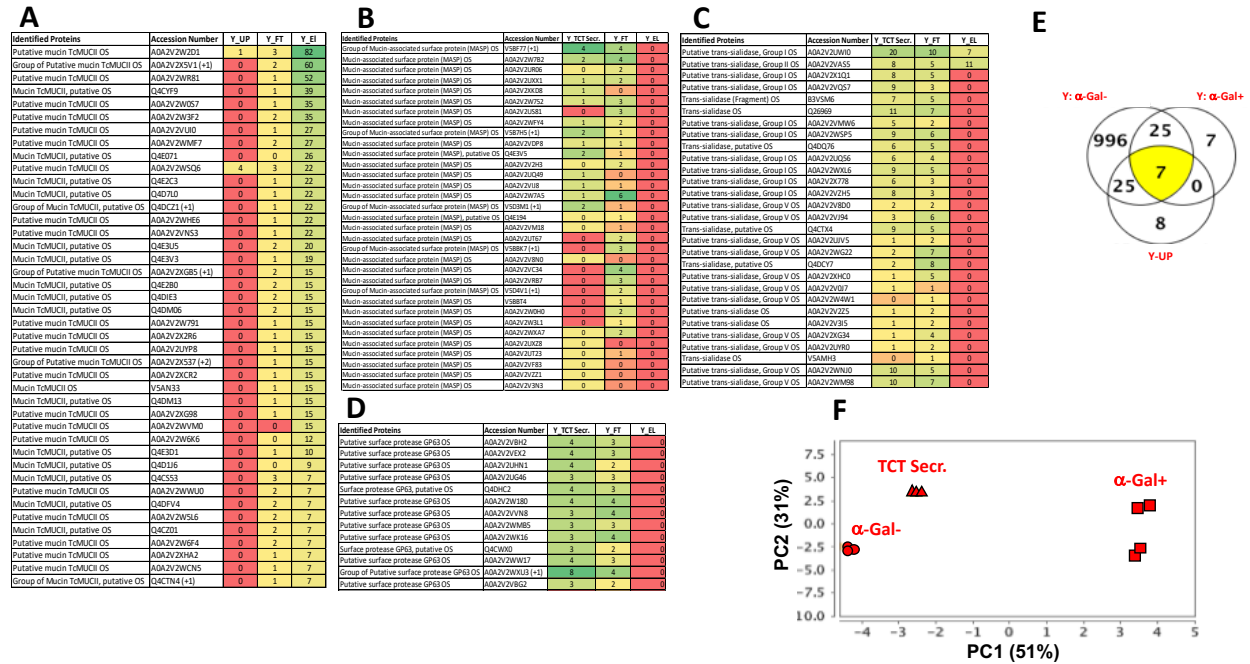


**Figure 3.7. Proteomic analysis of TCT-Secr and IB4-lectin-purified TCT-EVs from *T. cruzi* Y strain. (A)** TcMUC mucins, particularly members of the TcMUC II family, are the main  $\alpha$ -Gal-containing glycoproteins eluted from the immobilized IB4 lectin column. **(B-D)** MASPs, TS, and GP63 proteins found in the TCT-Secr however not in the IB4-EL fraction. This indicates that they do not have  $\alpha$ -Gal residues in their composition. **(E)** Venn diagram and **(F)** principal component analysis (PCA) of proteins identified in TCT-Secr,  $\alpha$ -Gal(-) and  $\alpha$ -Gal(+) fractions. Numbers in the last two columns of each table represent the total spectral count for the protein identified by LC-MS/MS. The results represent five biological replicates being combined, concentrated by 10 kDa filter, and digested via FASP-trypsin.





### **3.3.4. Proteomic analysis of the TCT-Secr and TCT-EVs $\alpha$ -Gal+ and $\alpha$ -Gal- derived from Col, and Y strains show consistency with previous results**

In this experiment, we performed proteomic analysis as explained earlier in this chapter (2.2.7), however on TCT-Secr,  $\alpha$ -Gal(+) and  $\alpha$ -Gal(-) only derived from Col, and Y strains (based on availability). Consistent with previous results,  $\alpha$ -Gal(+) fractions in both Col- and Y-derived TCT-Secr showed distinct profiles compared to  $\alpha$ -Gal(-) fractions as well as unpurified TCT-Secr derived from Col and Y strains, shown by NTA (**Figures 3.3 and 3.9**). We also showed that  $\alpha$ -Gal(-) fractions showed more similarities with respective of protein distribution profile to total TCT-Secr, in agreement with previous results in which we showed similar EV size and profile distribution between these two fractions, by NTA (**Figures 3.3 and 3.9.A**).

We showed here that the majority of the proteins in TCT-Secr were depleted into FT fractions after IB4-lectin purification (total protein: 517 and 1068, TCT-Secr: 40 and 40, and FT: 503 and 1053 in Col- and Y-derived samples, **Figures 3.9.B-C**). It is noteworthy to mention that the total amount of proteins was shown to be approximately double in Y strain-derived TCT-Secr compared to Col-derived TCT-Secr. Furthermore, EL or  $\alpha$ -Gal(+) fractions showed to have respectively 47 and 39 in Col- and Y-secretome, which shows higher enrichment in Col-derived purification in comparison with Y strain-derived purification, considering the total number of the proteins (ELs being approximately 3.65% and 9% of TCT-Secr respectively). This indicates that perhaps the column reached a saturation point.

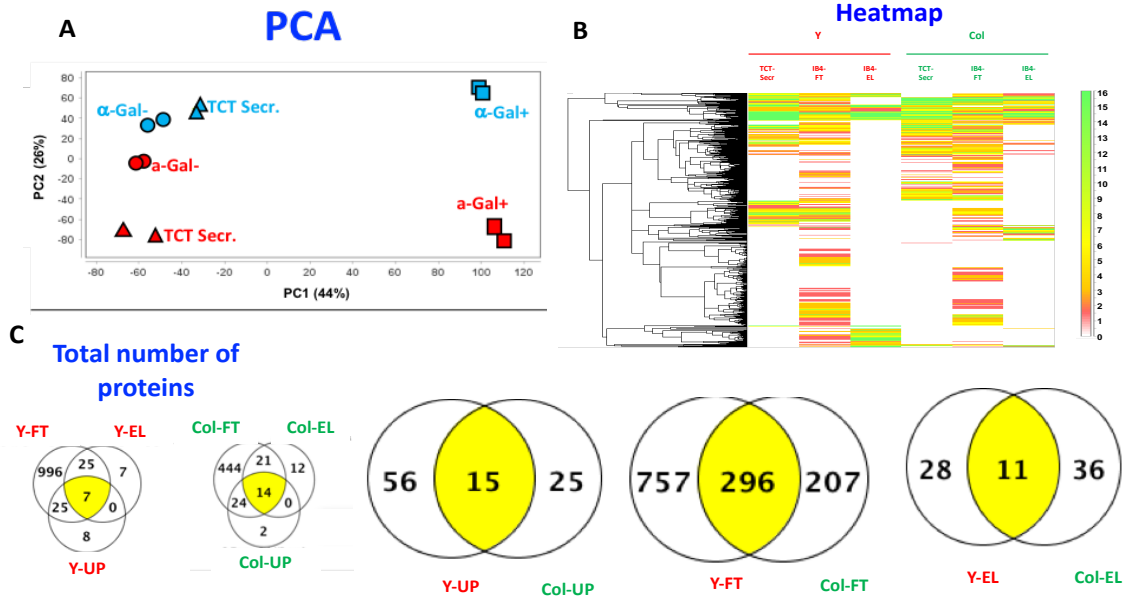


**Figure 3.9. Proteomic analysis of TCT-Secr,  $\alpha$ -Gal(+) and  $\alpha$ -Gal(-) derived from Col, and Y strains. (A)** Principal component analysis (PCA) of proteins of TCT Secr,  $\alpha$ -Gal(+) and  $\alpha$ -Gal(-) derived from Col, and Y. **(B)** Heat map of 1,000 most abundant proteins found in the TCT-Secr,  $\alpha$ -Gal(+) and  $\alpha$ -Gal(-) derived from Col and Y. Human and bovine contaminants were excluded. **(C)** Venn diagram of proteins identified in TCT-Secr,  $\alpha$ -Gal(+) and  $\alpha$ -Gal(-) derived from Col and Y.  $\alpha$ -Gal(+) and  $\alpha$ -Gal(-) derived from Col, and Y showed distinct protein profiles by performing proteomic analysis. The heat map graph was plotted using Scaffold perSPECTives.

### 3.4. DISCUSSION AND FUTURE WORK

Pathogenesis of *T. cruzi* infection involves complex interactions between the host cells and the parasite (Machado, Dutra et al. 2012), and the role of *T. cruzi* derived EVs recently has been studied on (Schorey, Cheng et al. 2015). However, detailed effects of EVs and mechanisms involved in the process amongst the various commonly infecting genotypes (Colombiana, and Y strains and CL Brener clone) are not fully understood (Coakley, Maizels et al. 2015). TCT-EVs are responsible for transferring various pathogenic factors including *T. cruzi* surface markers in the host, which will modulate immune response in favor of the parasite. Characterizing the parasite's molecules including peptides and glycopeptides released by EVs, will lead to understanding the pathogenesis of the disease and to perhaps finding a biomarker for disease diagnosis and treatment follow-up.

Proteomics has revealed the complex composition of EVs in any cell type (Choi, Kim et al. 2015). Nevertheless, various proteins in the exoproteome of *T. cruzi*, which have been shown to be responsible for the parasite's pathogenesis including invasive strategies (interacting, invading, and dysregulating host target cells e.g. macrophages), have been shown to be released in EVs (Queiroz, Ricart et al. 2016). Furthermore, stage specific surface markers such as gp90 and gp82 which are specific to metacyclic form (Teixeira and Yoshida 1986), have been found in the EVs. Other surface GPI-anchored members of the trans-sialidase family from genes gp82 and gp35/50, which are required for the parasite's ability for invading the mammalian host cells, have been found in EVs in previous research. To date, the best proteomic description provided on *T. cruzi* EVs has been performed in epimastigotes and metacyclic trypomastigotes (Bayer-Santos, Aguilar-Bonavides et al. 2013).

There are various proteins that are secreted by *T. cruzi*, which are involved in promoting host cell invasion and therefore, there are several studies been done with the focus on characterizing the parasite's excretory-secretory antigens which can be possibly vaccine candidate. One of the most promising vaccine candidate could be the primary secreted lysosomal peptidase cruzipain which plays a pivotal role in the parasite's life cycle such as triggering host arginase (Rodriguez-Morales, Monteon-Padilla et al. 2015). Moreover, a novel trans-sialidase-based immunogen could confer protection in a later *Trypanosoma cruzi* challenge, through influencing on cell populations involved in immune control, specially reducing myeloid suppressor cells (Prochetto, Roldan et al. 2017). Base on the previous research, the major glycoproteins (35-50 kDa) on the insect-derived stage (epimastigotes) are mucin-like glycoproteins, active and inactive trans-sialidases, NETNES (a major complex glycoprotein, which has 13 amino acids: AQENETNESGSID (Macrae, Acosta-Serrano et al. 2005), mucin-associated surface proteins (MASPs), peptidases such as gp63-like metalloprotease, and the cysteine proteinase cruzipain's isoforms (Schenkman, Eichinger et al. 1994, Macrae, Acosta-Serrano et al. 2005, Buscaglia, Campo et al. 2006, De Pablos, Gonzalez et al. 2011, Giorgi and de Lederkremer 2011, Goldenberg and Avila 2011, Alvarez, Niemirowicz et al. 2012, De Pablos and Osuna 2012). In this insect-specific stage of *T. cruzi*, the coat which is formed by 76 glycoproteins and glycoinositolphospholipid (GIPLs) protects them from protease enzymes inside the insect's intestinal tract (Kollien, Schmidt et al. 1998). It also supports survival of metacyclic trypomastigotes during the vector-born transmission, as well as gastric mucosa penetration of mammalian host (Yoshida, Tyler et al. 2011). However, amount of GIPLs drastically changes in metacyclic trypomastigotes (Golgher, Colli et al. 1993), and the expression of stage-specific

antigens including gp90 and gp82 which mediate adhesion and infection of vertebrate host cells, will be induced (Yoshida, Tyler et al. 2011).

As it was shown here, amongst three tested conditions, EVs derived from *T. cruzi* trypomastigotes showed the highest concentration even after 30 days of storage, although after 30 days, it was demonstrated that EVs seemed to be aggregated at all three temperatures, which makes these conditions not suitable for storing the EVs in order to do functional analysis. Moreover, it was shown by our results that EVs were detected between fractions 17 and 25 (21 being the pick). It also has been shown that the EVs derived from 2e6/ml did not show the detectable amount of EVs, and as it was again tested on higher number of parasites, it showed higher number of vesicles though in higher fractions. The results were repeated in order to collect more fractions to achieve the pick of EVs in the fractions, as well as to eliminate the FBS as the given sample was incubated in media with 10% FBS added to it, and consistently proteins were detected in EVs.

It is very crucial to test if those surface markers on the parasite are secreted in the vesicles. We showed vast varieties of surface markers in the EVs derived by various strains of the parasites by proteomic analysis (total of approximately 1,400 proteins). A subset of highly enriched  $\alpha$ -Gal(+) glycoproteins, including TcMUC II mucins, was obtained in the elute (EL) fraction from biotinylated IB-lectin-neutravidin-agarose. TcMUCII has been described as the main  $\alpha$ -Gal-containing glycoprotein of *T. cruzi* TCTs (Buscaglia et al., JBC 2004). It was shown also that there are more common expressed proteins between Y and Lu. CLB but not Col. Moreover, lipidomic, and glycomic analysis on EVs derived from *T. cruzi* strains are under investigation.

Furthermore, we observed a distinguishable profile/size in the EVs from EL (purified  $\alpha$ -Gal-containing TCT-Secr) in comparison with FT. This was enriched with TS glycoproteins, and they had very low reactivity with Ch anti- $\alpha$ -Gal Abs, indicating that these glycoproteins contain

few or no a-Gal glycotopes. This is agreement with the Lantos et al. (2016), who showed that a-Gal-positive plasma membrane domains do not colocalize with TS-positive domains (Lantos, Carlevaro et al. 2016).

## CHAPTER 4: LIPIDOMIC ANALYSIS OF *T. CRUZI*-DERIVED EVS

### 4.1. INTRODUCTION: LIPID COMPOSITION IN *T. CRUZI*

*T. cruzi* GPI-anchors which contain an alkylacyl moiety with an unsaturated fatty acid (FA), C18:1 or C18:2, are shown to highly induce proinflammatory cytokines (Almeida, Camargo et al. 2000). Although EVs secreted by *T. cruzi* are enriched with proteins associated with lipid rafts (GPI-anchored proteins) (They, Regnault et al. 1999, Wubbolts, Leckie et al. 2003), exosomes regardless of the source of secretion comprise of lipids such as cholesterol, sphingomyelin, hexosylceramides, phosphatidylcholine and phosphatidylethanolamine, as well as ceramides (Agusti, Couto et al. 2000, Wubbolts, Leckie et al. 2003, Laulagnier, Motta et al. 2004, Subra, Laulagnier et al. 2007, Trajkovic, Hsu et al. 2008, Brouwers, Aalberts et al. 2013). Platelet-activating factor (PAF), which induces its activity (platelet aggregation) via a PAF-specific receptor (PAFR), is known as a potent intracellular lipid mediator and a second messenger (Gazos-Lopes, Oliveira et al. 2014), and associated with platelet reactivity and chances of acquiring acute coronary diseases being increased (Kabbani, Watkins et al. 2001).

It has been shown that a bioactive lysophosphatidylcholine (*sn*-1-C18:1-LPC) synthesized by mammalian-specific stages of *T. cruzi* (trypomastigotes and intracellular amastigotes) and shows PAF-like activity (Gazos-Lopes, Oliveira et al. 2014). It also has been shown previously that the PC species with PAF-like activity were able to induce the differentiation of epimastigotes into metacyclic trypomastigotes in *T. cruzi in vitro* (Gomes, Monteiro et al. 2006). Although other few LPC species have been isolated from *T. cruzi* such as C16:0-LPC, C18:0-LPC, and C18:2-LPC, they have not shown any PAF-like activity. However, LPCs in general, have been shown to elicit intracellular signals (Ogita, Tanaka et al. 1997), as well as cytokine secretion mediation



(Huang, Schafer-Elinder et al. 1999). *T. cruzi*-isolated C18:1-LPC unlike C16:0-LPCs and C18:0-LPCs, showed to be capable of inducing rapid and receptor-mediated oxidative burst by generating reactive oxygen species in neutrophils (Ojala, Hirvonen et al. 2007). EVs derived from *T. cruzi* have shown to comprise C18:1-LPC as well.

On the other hand, ether-linked PCs showed to be important as reservoirs in inflammatory cells for key lipid mediators (Chilton, Fonteh et al. 1996), and in particular, PMEs or Plasmalogens (ether-linked phosphatidylethanolamine: PEE, and ether-linked phosphatidylcholine: PCE species) are shown to facilitate membrane bending and EVs fusion and release. Previous studies have shown that these are released by *T. cruzi* parasite (Longo, Nakayasu et al. 2013), as well as they are shed in EVs secreted by the parasite (Agusti, Couto et al. 2000). Therefore, as it is essential to investigate the detailed lipid composition released by the *T. cruzi* parasite through EVs, in this chapter, we aimed to look at the lipid classes and lipid species released into EVs by the parasites.

## **4.2. MATERIALS AND METHODS**

### **4.2.1. Mammalian cell culture**

LLC-MK2 and U2-OS cells were cultured in low glucose DMEM with 10% FBS/ Penicillin-Streptomycin as was previously described in 2.2.1 at 37°C, under CO<sub>2</sub> atmosphere, and were sub-cultured once or twice a week Trypsin.

### **4.2.2. Parasite culture, and isolation and storage of extracellular vesicles (EVs)**

The parasite culture and TCT-Secr isolation was performed (as described in 2.2.2.), and TCT-Secr was isolated from TCTs derived from Col, Y, and CLB *T. cruzi* strains/ clone (from 1e8 parasites). TCT-Secr isolates (10 isolates) were pooled by using 10 kDa filter tubes (10x to 15x), from each strain, and after measuring the protein concentration by BCA, were washed in 0.1 mM

of ammonium acetate 3x, and finally resuspended in 0.1 mM ammonium acetate. NTA analysis was performed on the samples in order to analyze the EV size distribution (see section 2.2.2).

#### **4.2.3. BCA Protein Assay**

TCT-Secr derived from Col, Y, and CLB TCTs were analyzed for protein concentration by BCA according to the manufacturer as described earlier (2.2.4).

#### **4.3.4. Fractionation of TCT-Secr by Size-Exclusion Chromatography (SEC)**

TCT-Secr was loaded onto Sepharose CL-2B column and fractionated through SEC (2.3.2). Briefly, the resin was washed in 0.1 M ammonium acetate 3x. A 3 ml syringe tip was plugged with glass wool, and was setup on a ring stand with a waste container below it. The column was packed with Sepharose until 3 ml mark and washed by passing 6 ml of the buffer through. TCT-Secr samples from Col, Y and CLB were loaded (300  $\mu$ l) and immediately collected (each comprising 150  $\mu$ l). Once the top of the resin was visible, 3 ml of the buffer was added to it slowly (200  $\mu$ l at a time) until all the liquid has been collected. The samples were stored at -80° C for further analysis.

#### **4.2.5. Analysis of SEC fractionated-TCT-Secr with Ch and NHS sera, as well as Anti $\alpha$ -Gal Ab**

CL-ELISA was performed afterwards on SEC fractionated TCT-Secr fractions 2 through 7 (which showed the highest content of proteins) out of 15 fractions, in order to detect the fractions with highest enrichment of  $\alpha$ -Gal epitopes, prior to performing IB4-lectin. Briefly, fractions were immobilized (10% of the sample volume: ~15  $\mu$ l) in CBC overnight, blocked with 1% BSA/PBST for 1 hr, and incubated for 1 hr with NHSP and ChHSP (1/800), as well as anti  $\alpha$ -Gal Ab at 5

µg/ml (in 1% BSA/PBST). Thereafter, biotinylated goat anti human IgG was added (1/10000 in 1%BSA/PBST) for 1 hr, and the reactivity was detected with CL-ELISA reagent (see details in **2.2.8**).

#### **4.2.6. Affinity chromatography using immobilized IB4-lectin for enrichment of $\alpha$ -Gal-containing TCT-EVs**

$\alpha$ -Gal-containing EVs were obtained from the conditioned medium of Col, Y, and CLB strains, and were purified from the 10 kDa-pooled TCT-Secr by affinity chromatography, using IB4-lectin (after pooling the pre-enriched  $\alpha$ -Gal+ fractions from SEC by performing CL-ELISA: see **4.2.5**) as described in **3.2.7**. Briefly, the TCT-Secr sample (70% of the total pooled TCT-Secr) was re-dissolved in TBS buffer, and applied to a column with biotinylated IB4 lectin immobilized to Neutravidin HP SpinTrap, after the storage buffer was removed (**3.2.7**). Unbound flow-through fraction (**FT**) was collected. The column was then washed with wash buffer, and a wash fraction (**W**) was collected.  $\alpha$ -Gal-Positive molecules were eluted with elution buffer and elute fraction (**E**) was collected, and immediately neutralized with 1 M Tris.

#### **4.2.7. Lipid extraction**

$\alpha$ -Gal+ (EL) and  $\alpha$ -Gal- (FT) fractions derived from Col-, Y- and CLB-isolated TCT-Secr, as well as unpurified TCT-Secr and TCT Lysate (Lys.: extracted through 3 cycles of freezing and thawing by N<sub>2</sub>) were freeze-dried, and subjected to Folch's partition (Folch, Lees et al. 1957, Gazos-Lopes, Oliveira et al. 2014). Briefly, the samples were resuspended in HPLC-grade water. They were then transferred to Pyrex culture tubes with polytetrafluoroethylene (PTFE)-lined screw caps and HPLC-grade chloroform and methanol were added to each sample, maintaining the final ratio of chloroform/methanol/water (C/M/W) of 1:2:0.8 (v/v/v). The samples were mixed

thoroughly by utilizing vortex for 2 minutes, and then centrifuged at 1,800 g for 15 minutes at room temperature. The supernatants were then transferred to PTFE-lined Pyrex glass tubes, and the pellets were dried by using constant N<sub>2</sub> flow. The dried pellets were extracted 3x with C/M at 2:1 ratio (v/v) and 2x with C/M/W at 1:2:0.8 ratio (v/v/v), and the supernatants were pooled together and dried. Thereafter, first, samples were dissolved in C/M/W at 4:2:1.5 ratio (v/v/v) and then mixed thoroughly using vortex for 5 minutes, and finally centrifuged at 1,800 g for 15 minutes at room temperature. The lower phase (organic) and the upper phase (aqueous) were separated in PTFE-lined Pyrex glass tubes after centrifugation. The lower phase was then washed 2x with freshly prepared upper phase, dried using constant N<sub>2</sub> steam, and stored at -80°C for further analysis.

#### **2.4.8. Structural characterization of negatively charged lipid species by tandem electrospray ionization-linear ion trap-mass spectrometry (ESI-LIT-MS)**

Folch's lower phases of the samples were dissolved in MS-grade methanol (5 mM LiOH), and were directly injected at 300 nL per minute, by chip-based infusion using a TriVersa NanoMate nanoelectrospray source (Advion, Ithaca, NY), into an LTQXL ESI-linear ion trap-MS (ESI-LIT-MS: Thermo Fisher Scientific), in negative-ion mode. 0.01 kV and 0.03  $\mu$ A were set as the source voltage and current respectively; capillary voltage was set at 36 V and the temperature was set at 150°C; and tube lens voltage was set at 145 V. Select ions were subjected to sequential tandem fragmentation (MS<sub>n</sub>) by collision-induced dissociation (CID). Full-scan (MS) spectra were collected at the 400–1000 m/z range. Tandem mass fragmentation was performed using normalized collision energies of 35, 40, and 45 for MS<sub>2</sub>, MS<sub>3</sub>, and MS<sub>4</sub>, respectively. The resulting spectra were compared to the aforementioned phospholipid standards, as well as to

previously described results. The analysis of detected lipids was performed utilizing MS-DIAL program.

### **4.3. RESULTS**

#### **4.3.1. SEC fractions 2 to 5 of TCT-Secr were chosen as pre-enriched $\alpha$ -Gal+ fractions before performing IB4-lectin column**

In order to perform IB4-lectin chromatography to acquire  $\alpha$ -Gal+ and  $\alpha$ -Gal- fractions prior to lipid analysis, it was important to pre-enrich the  $\alpha$ -Gal epitopes, as it is more challenging to investigate lipid composition compared to protein composition. In order to do so, TCT-Secr derived from Y strain *T. cruzi* TCTs were fractionated by SEC to 15 fractions, and protein concentration and  $\alpha$ -Gal reactivity were measured in the fractions. The results showed that the protein was mainly detected in fractions 2 to 6 (**Figure 4.1**), with the high protein content being detected in fractions 2 through 5. Therefore, we proceeded with CL-ELISA with SEC-derived TCT-Secr fractions of 2 to 7 in order to detect the fractions with the highest  $\alpha$ -Gal content through their reactivity with anti  $\alpha$ -gal Ab and ChHSP.

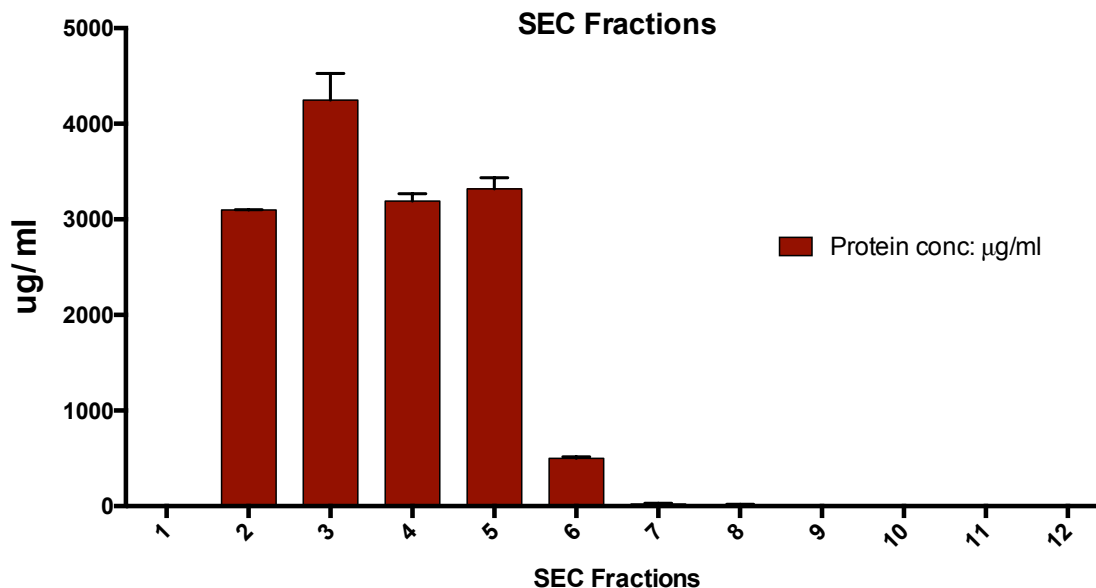


**Figure 4.1. Protein concentration measured by BCA in TCT-Secr fractioned by SEC.** The protein content is mainly detected between fractions 2 and 5. The results are shown in means  $\pm$  SD of two technical replicates.

Moreover, NTA also was performed to show the profile and size distribution of EVs in these fractions (**Figure 4.2**). Various EV populations were shown in the SEC-fractionated Y strain-derived TCT-Secr fractions. Heterogeneous population of EVs were shown mainly in fractions 2, 3 and 5, whereas fraction 4 showed more homogeneous population. It is noteworthy to mention that fractions 2 and 5 showed a shift towards larger size EVs ( $> 300$  nm), in comparison with fractions 3 and 4 which has smaller populations (100 nm - 300 nm, and  $< 100$  nm).

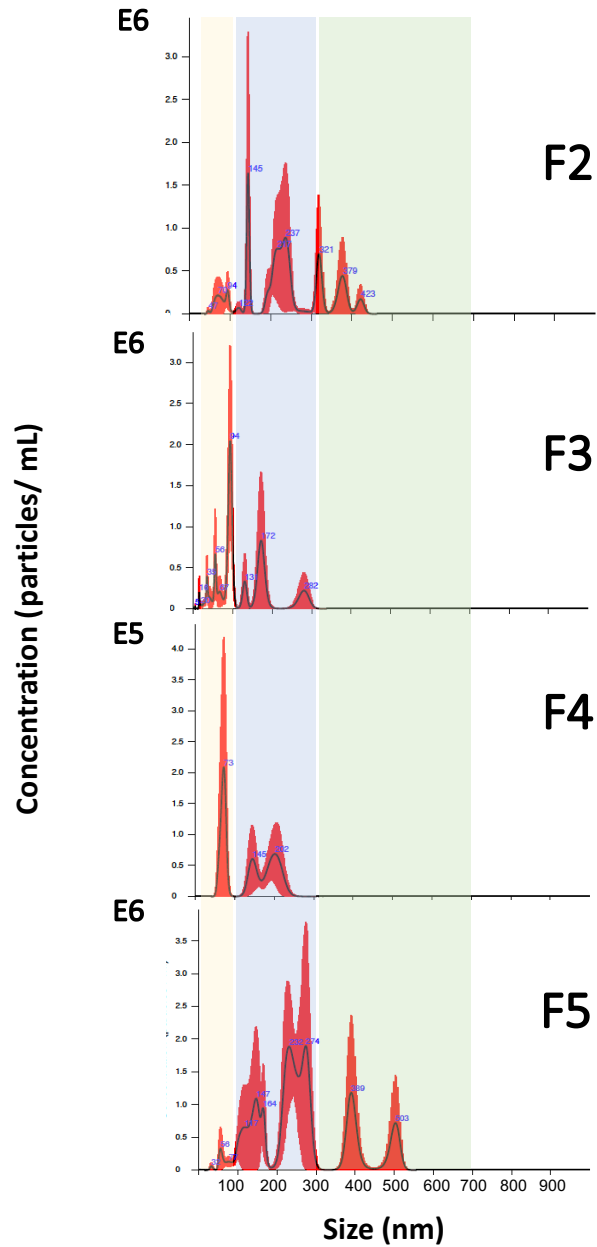


**Figure 4.2.** NTA analysis of SEC-derived TCT-Secr fractions 2 to 5 (isolated from Y strain) before being subjected to CL-ELISA and immunoaffinity chromatography in order to detect and enrich  $\alpha$ -Gal epitopes. TCT-Secr derived from Y strain was fractionated through SEC and EVs size distribution and profile were measured by NTA. The results show heterogeneous population of EVs in fractions 2 to 5.

Furthermore, after performing CL-ELISA on TCT-Secr fractions collected through SEC, the results showed that fractions 2 to 5 had the highest reaction with anti  $\alpha$ -Gal Ab and Ch serum pool (**Figure 4.3**). The fractions showed no to very low reactivity with NHSP (negative control). Therefore, prior to performing IB4-lectin chromatography in order to acquire  $\alpha$ -Gal+ (EL) and  $\alpha$ -Gal- (FT) fractions, TCT-Secr derived from Col, Y, and CLB after being pooled  $\sim 10\times$  by utilizing 10 kDa filter tubes, were fractionated through SEC and fractions 2-5 were only selected and pooled for IB4-lectin column.

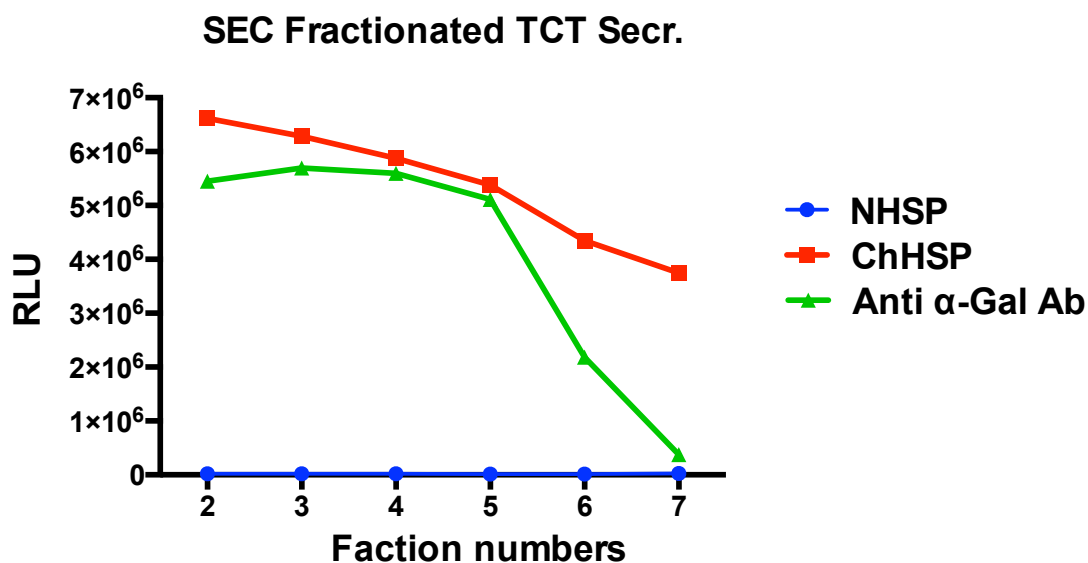


**Figure 4.3. Detecting  $\alpha$ -Gal enriched fractions in SEC Fractionated TCT-Secr by CL-ELISA prior to IB4-lectin chromatography.** CL-ELISA was performed with  $\sim 10\%$  of each SEC-isolated TCT-Secr fractions against NHSP, ChHSP, and anti  $\alpha$ -Gal Ab. Fractions 2 through 5 showed to have the highest reactivity with ChHSP and anti  $\alpha$ -Gal Ab, therefore chosen to be pooled for IB4-lectin column chromatography prior to lipid analysis.



### **4.3.2. Lipidomic analysis showed various lipid classes in TCT-Secr derived from Col, Y and CLB**

It has been described by previous research that various lipid classes have been isolated from both vector and host specific stages of *T. cruzi* (epimastigotes and trypomastigotes respectively) (Diaz de Toranzo, Castro et al. 1988, Gazos-Lopes, Oliveira et al. 2014). They have been described to have important role in activating innate and adaptive immune responses in the host. EVs derived from *T. cruzi* TCTs showed by previous studies to comprise various lipid classes that have been isolated from *T. cruzi* parasite. Here, we show that in negative ion mode analysis, various negatively-charged lipid classes have been detected in Col-, Y-, and CLB-derived TCT-Secr (**Figure 4.4**), which is in agreement with previous studies. As our control, we have included Y strain-derived TCT Lys. (not included in the graphs in order to have less ambiguity in the comparison amongst the TCT-Secr samples), and the majority of the lipid classes that are found in Y strain TCTs were isolated from TCT-Secr derived from Col, Y, and CLB with the exception of few LPCs, PCs and PEs. It is noticeable that CLB-derived TCT-Secr in the majority of the cases in general showed the highest lipid content. As could be seen in the figure, those include various PCs, LPCs, and PIs.

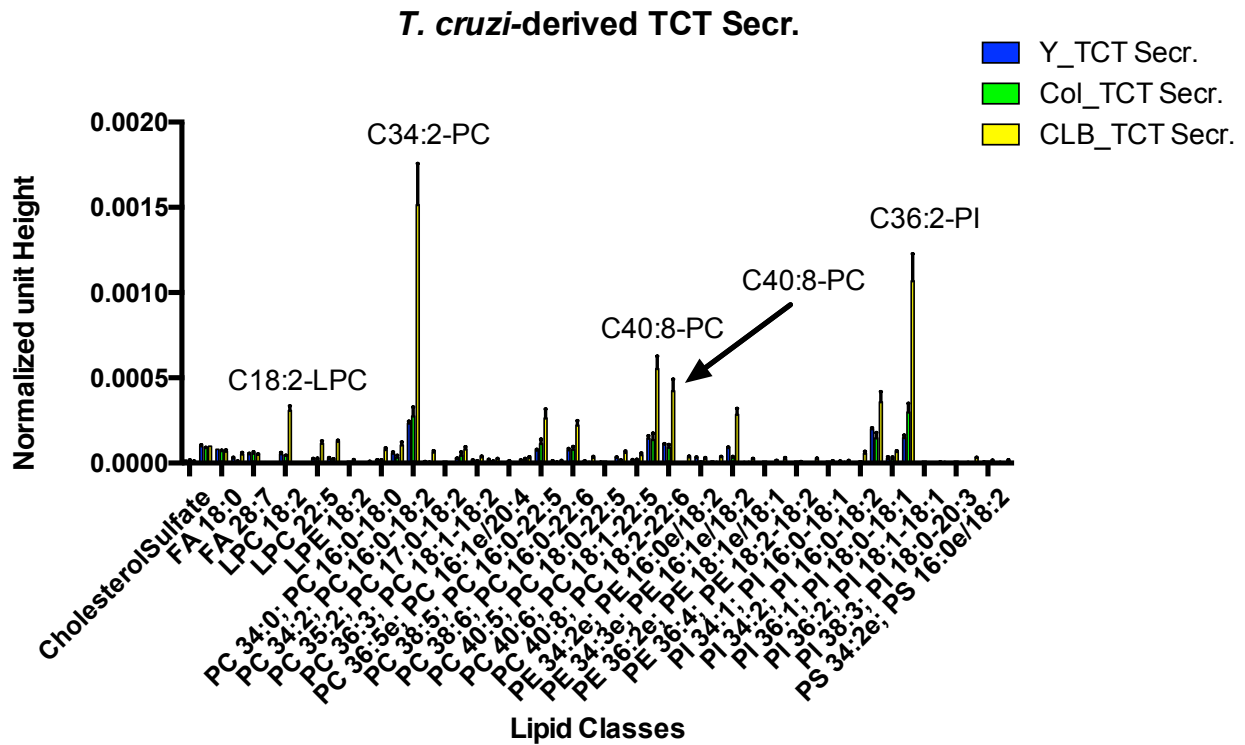


**Figure 4.4.** Various lipid classes have been detected in TCT-Secr derived from Col, Y and CLB TCTs. Various lipid classes have been detected by negative ion mode lipidomic analysis. CLB-derived TCT-Secr showed the highest lipid content in most of the lipid classed (labeled in the figure). The results are normalized according to unit peak height. LPC: lysophosphatidylcholine; PC: phosphatidylcholine; PI: phosphatidylinositol.

### **4.3.3. Various lysophosphatidylcholine, and Plasmalogen species have been isolated from TCT-Secr derived from Col, Y and CLB**

Previous studies have shown that lysophosphatidylcholine species (LPCs) are important in activation of immune response in TLR dependent manner, and they have platelet activating (PAF)-like factor activity which could be involved in pathophysiology of Chagas disease such as increased platelet aggregation related to myocarditis, focal ischemia, and myonecrosis (Tanowitz, Burns et al. 1990, Tanowitz, Kirchhoff et al. 1992, Carod-Artal, Vargas et al. 2005, Mukherjee, Machado et al. 2011, Gazos-Lopes, Oliveira et al. 2014). Furthermore, PMEs or plasmalogens (ether-linked phosphatidylethanolamine (PEe), and ether-linked phosphatidylcholine (PCe) species) are shown to facilitate membrane bending and EVs fusion and release (Longo, Nakayasu et al. 2013). Here, we show that TCT-Secr derived from Col, Y and CLB TCTs are enriched in lipid classes such as LPCs and PMEs (**Figures 4.5-6**). Although TCT-Secr derived from all 3 strains mainly showed LPC species C18:0, C18:2, C20:4, C22:5, and C22:6, however, CLB-derived TCT-Secr showed to comprise significantly higher LPC species in comparison with the TCT-Secr derived from the other 2 strains, Col and Y (**Figure 4.5**).

Moreover, we show that various plasmalogen species (both PEe and PCe species) were detected in TCT-Secr derived from the 3 *T. cruzi* strains/ clone (**Figure 4.6.A**). With respect of PEe species, few of them were observed abundantly in comparison with other species which included C16:0e/C18:2, C16:1e/C18:1, C16:1e/C18:2, and C18:1e/C18:2. It is worth mentioning that the species in this class as well showed significantly higher content in CLB-derived TCT-Secr, in comparison with Col- and Y-derived TCT-Secr. Furthermore, with regards to PCe class, one species was detected in the TCT-Secr derived from 3 strains/ clone (C16:1e/20:4) as could be

observed in **Figure 4.6.B**. This species was detected higher in TCT-Secr derived from Col, in comparison with TCT-Secr derived from Y and CLB, however this difference was not statistically significant.

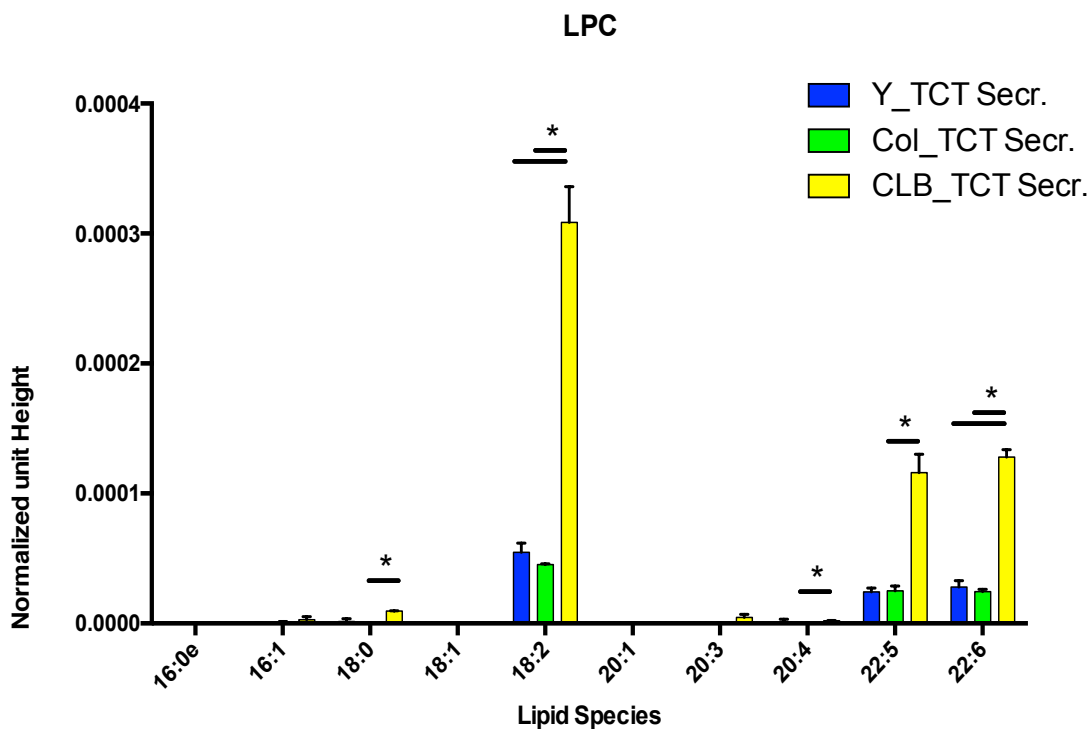


**Figure 4.5. Various lysophosphatidylcholine species (LPCs) have been detected in TCT-Secr derived from Col, Y and CLB TCTs.** Various LPC species have been detected by negative ion mode analysis in TCTs. CLB-derived TCT-Secr showed significantly higher LPC composition compared to Col- and Y-derived TCT-Secr. The results are normalized according to unit peak height. LPC: lysophosphatidylcholine.

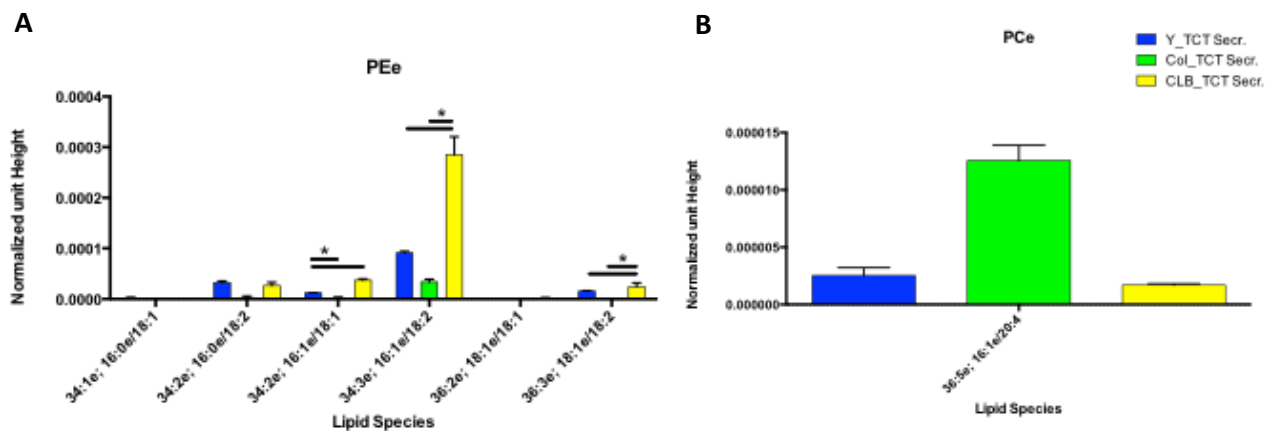


**Figure 4.6. Various Plasmalogen species (PEe and PCe species) have been detected in TCT-Secr derived from Col, Y and CLB TCTs.** Various Plasmalogens have been detected by negative ion mode lipidomic analysis. CLB- and Col-derived TCT-Secr showed the highest content (which was statistically significant in case of CLB-) in most of the PEe and PCe species respectively, in comparison with the other strain(s)/ clone. The results are normalized according to unit peak height. PEe: ether-linked phosphatidylethanolamine; PCe: ether-linked phosphatidylcholine.

#### **4.3.4. Various further negatively charged lipid classes have been isolated in TCT-Secr, being significantly higher in TCT-Secr derived from CLB compared to Col and Y.**

In addition to the lipid classes/ species have been mentioned previously in the chapter, further negatively charged lipid classes have been detected in TCT-Secr, which are significantly higher in CLB-derived TCT-Secr in comparison with Col- and Y-derived TCT-Secr (**Figure 4.7**). These include various species in Lysophosphatidylethanolamine (LPE), ether-linked lysophosphatidylethanolamine (LPEe), phosphatidylethanolamine (PE), phosphatidylcholine (PC), phosphatidylinositol (PI), ether-linked phosphatidylinositol (PIe), and Phosphatidylglycerol (PG), ether-linked Phosphatidylserine (PSe) classes. Among the above classes, although as far as

some lipid species (LPE species: **Figure 4.7.A.** and some other species in other lipid classes) that TCT-Secr derived from CLB showed significantly higher content than Col- or Y-derived TCT-Secr), majority of the lipid classes showed significantly higher content in CLB-derived TCT-Secr compared to both Col- and Y-derived TCT-Secr (LPEe, PE, PC, PI, PIe, PG, and PSe: **Figure 4.7.B-H**). As can be observed in the figure, Y strain-derived TCT-Secr following by CLB-derived TCT-Secr showed the highest content of the majority of the lipid classes, in comparison with Col-derived TCT-Secr which was significant with regards to PG and PSe (**Figure 4.7.G-H**). It also is worth mentioning that in LPE and PI classes however (**Figure 4.7. A & C**), majority of the species were detected more in Col-derived TCT-Secr in compared to Y- and CLB-derived TCT-Secr

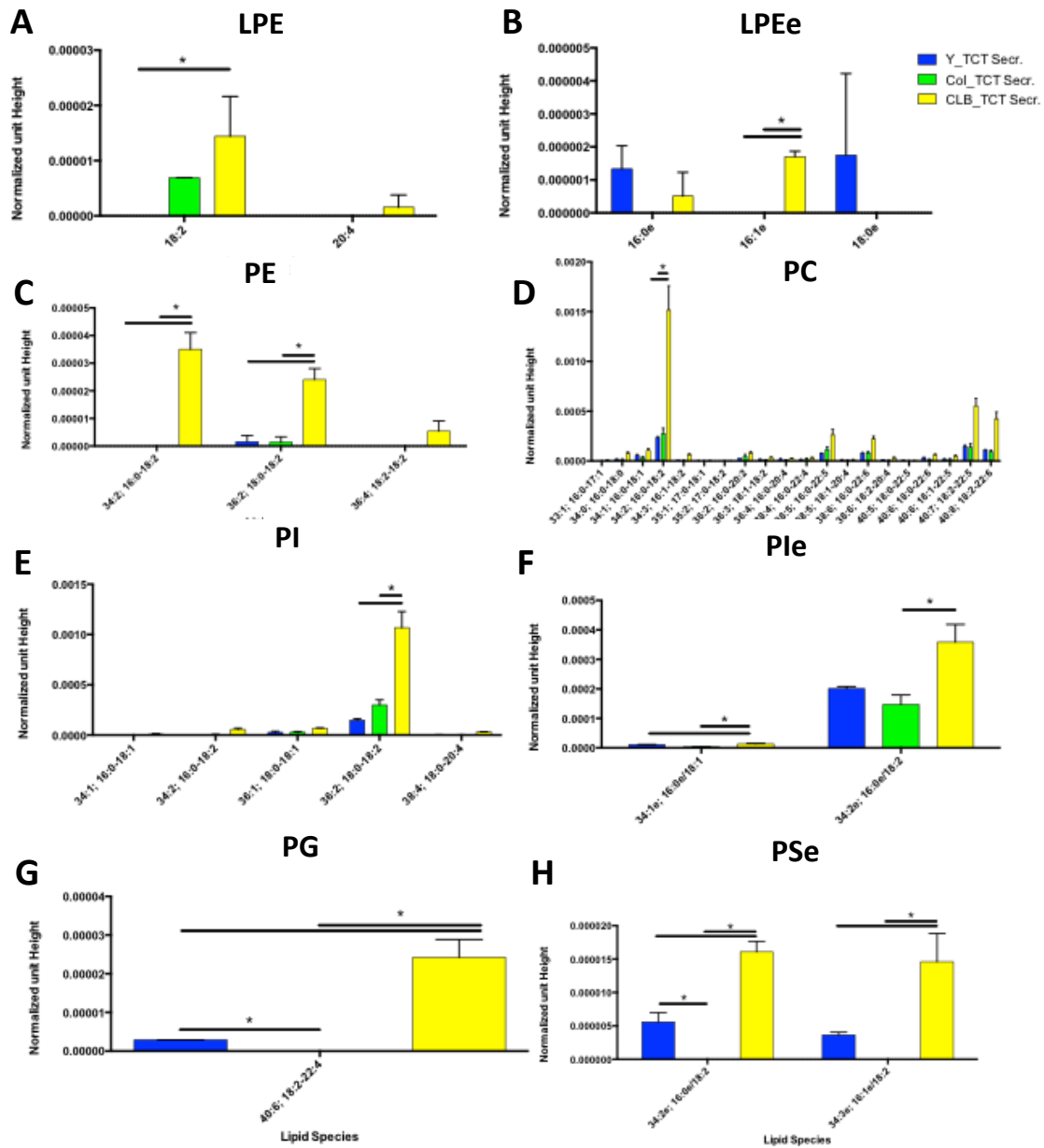


**Figure 4.7. Various lipid classes have been detected in TCT-Secr, significantly higher in CLB-derived TCT-Secr in comparison with Col- and Y-derived TCT-Secr** Various lipid classes have been detected by negative ion mode lipidomic analysis. CLB-derived TCT-Secr showed significantly highest lipid content in most of the lipid classes. The results are normalized according to unit peak height. LPE: lysophosphatidylethanolamine; LPEe: ether linked lysophosphatidylethanolamine; PE: phosphatidylethanolamine; PC: phosphatidylcholine; PI: phosphatidylinositol; Ple: ether-linked phosphatidylinositol; PG: Phosphatidylglycerol; PSe: ether-linked Phosphatidylserine.

#### 4.3.5. Further negatively charged lipid classes have been isolated in TCT-Secr derived from Col, Y and CLB, including Cholesterol Sulfate and Fatty acids

In addition to previous results in this chapter, we have shown other classes of lipids including Cholesterol Sulfate and Fatty acids (FAs) in TCT-Secr derived from Col, Y, and CLB *T. cruzi* strains/ clone TCTs (**Figure 4.8**). As it could be observed in the figure, Cholesterol Sulfate was found in both Col- and Y derived TCT-Secr with negligible differences in amount, in comparison with CLB-derived TCT-Secr (**Figure 4.8.A**). We also detected FAs species in TCT-Secr derived from TCTs of all 3 strains/ clone of the parasite (**Figure 4.8.B**). We show here that the majority of the FA species are found with minor differences in terms of content amongst the TCT-Secr derived from Col, Y and CLB, with the exception of C22:6 which showed to be higher in CLB-derived TCT-Secr followed by Y-derived TCT-Secr.

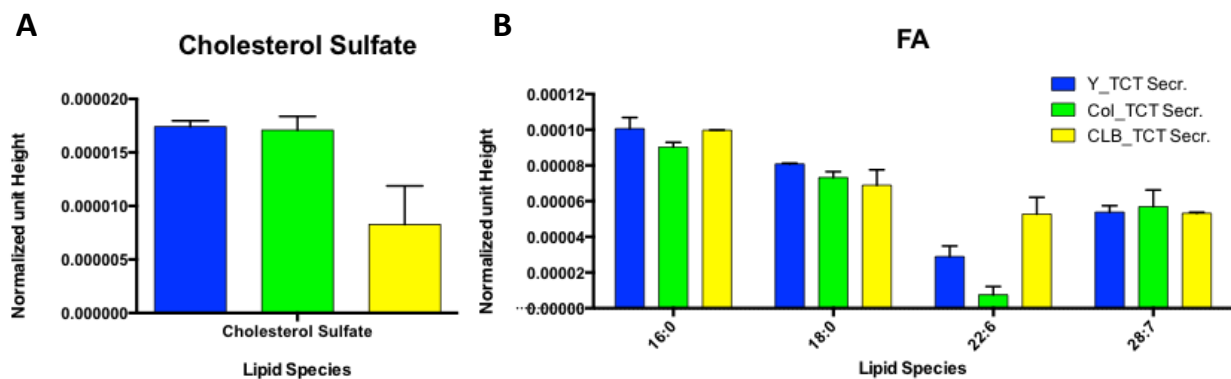


**Figure 4.8.** Further lipid classes have been detected in TCT-Secr derived from Col, Y and CLB TCTs. Further lipid classes such as Cholesterol Sulfate as well as Fatty acids (FAs) have been detected by negative ion mode lipidomic analysis. TCT-Secr derived from all strains/ clone contained approximately same amount of these 2 lipid classes. The results are normalized according to unit peak height. FA: Fatty acid.



#### 4.4. DISCUSSION AND FUTURE WORK

One of the major pathologies associated with Chagas disease is myocarditis and vasculitis which is accompanied by inflammatory mediators including cytokines, chemokines, phospholipids and glycolipids being increased (Ropert, Almeida et al. 2001, Mukherjee, Machado et al. 2011, Machado, Dutra et al. 2012). Moreover, as other pathological symptoms due to the disease, increase in platelets' aggregation, myonecrosis, focal ischemia are observed in both acute and chronic phases of the disease (Tanowitz, Burns et al. 1990, Carod-Artal, Vargas et al. 2005, Mukherjee, Machado et al. 2011). Cardiomyopathy is linked with the majority of the chronic cases which is the leading cause of death amongst parasitic diseases in Latin America (Hotez, Bottazzi et al. 2008, Machado, Dutra et al. 2012).

It has been shown by previous studies that Trypanosomatid parasites such as *leishmania spp.*, *T. brucei* and *T. cruzi* synthesize PC and LPC species (comprising of more than 50% of the total lipid composition in the latter organism) (Werbovetz and Englund 1996, Agusti, Couto et al. 2000, Richmond, Gibellini et al. 2010). Lipid mediators (Aliberti, Machado et al. 1999, Freire-de-Lima, Nascimento et al. 2000, Talvani, Machado et al. 2002, Gomes, Monteiro et al. 2006, Ashton, Mukherjee et al. 2007) and particularly LPCs (Mesquita, Carneiro et al. 2008, Silva-Neto, Carneiro et al. 2012) have been investigated in experimental models in ChD, and the latter have been shown to be capable of inducing various cellular activities such as TLR-2 dependent signal induction (Buwitt-Beckmann, Heine et al. 2005), depending on its length and its acyl-chain unsaturation degree (Ojala, Hirvonen et al. 2007, Riederer, Ojala et al. 2010, Rao, Riederer et al. 2013).

PAF (1-O-alkyl-2-acetyl-*sn*-glycero-3-phosphocholine) which has a similar structure to LPC (Smith, Hou et al. 2008), is synthesized by various cells including platelets, neutrophils, lymphocytes and macrophages, and shows strong various physiological and pathophysiological

activities such as inflammation and allergy (Honda, Ishii et al. 2002, Kasperska-Zajac, Brzoza et al. 2008). It has been previously shown by Gomes *et al.* in 2006 that C18:1-LPC synthesized by *T. cruzi* shows platelet-aggregating activity, similar to PAF (Gomes, Monteiro et al. 2006).

On the other hand, ether-linked PCs showed to be important as reservoirs in inflammatory cells for the key lipid mediators (Chilton, Fonteh et al. 1996), and specifically PMEs or Plasmalogens (ether-linked phosphatidylethanolamine: PEe, and ether-linked phosphatidylcholine: PCe species) are shown to facilitate membrane bending and EVs fusion and release. Previous research groups have shown that these are released by *T. cruzi* parasite (Longo, Nakayasu et al. 2013), and they are also shed in EVs secreted by the parasite (Agusti, Couto et al. 2000). Therefore, as it is essential to investigate the detailed lipid composition released by the *T. cruzi* parasite through EVs, in this chapter, we aimed to look at the lipid classes and lipid species released into EVs by the parasites.

We showed here in our results that various LPC species including C18:1-LPC are released in TCT Sec. derived from Colombiana and Y strains, as well as CL Brener clone. We showed C18:2-LPC was the most abundant LPC species detected in TCT-Secr, which was in agreement with previous study done by our group where we showed C18:2-LPC and C18:1-LPC were the most abundant LPC species in *T. cruzi* trypomastigotes (Gazos-Lopes, Oliveira et al. 2014). We also showed that various Plasmalogen species (within PEe and PCe classes) are released in TCT-Secr as well. Interestingly, CLB-derived TCT-Secr showed to comprise the majority of the above species significantly higher, compared with Col- and CLB-derived TCT-Secr Y strain-derived TCT-Secr showed to comprise second highest LPC and Plasmalogen species compared to Col-derived TCT-Secr, however this difference was not significant in some species. As these species are directly (in case of LPCs) and indirectly (in case of Plasmalogen which help the release of

EVs) related to the pathology of the disease, they could help us better explain the pathology of the disease caused by these various strains (e.g. DTU I is majorly responsible for cardiomyopathy, DTU VI for gastrointestinal complications and DTU II for both).

Various other negatively charged lipid species were isolated from TCT-Secr derived from *T. cruzi* strains/ clone, which was highest in CLB-derived TCT-Secr (and in majority of the species in some lipid classes significantly higher), in comparison with TCT-Secr derived from other strains, followed by Y strain-derived TCT Sec. Cholesterol Sulfate was the only class isolated the highest from Col-derived TCT-Secr compared to Y- and CLB-derived TCT-Secr

We are to be the first here, to show a detailed investigation on lipid composition in TCT-Secr derived from 3 major DTUs of *Trypanosoma cruzi*, and to show CLB (clone of DTU VI)-derived TCT-Secr contains significantly higher lipid species amongst the others (Col and Y, belonging to DTUs I and II respectively). The relationship between these findings and the pathology of the disease caused by either of these strains, including host inflammatory response and possible down- or up-regulation in genes involved in pro- and anti-inflammatory markers production by host cells involving EVs, remains to be studied. Also, as it has been shown that PAF-treated *T. cruzi* induced higher infectivity in mouse macrophages compared to none-treated parasites (Gomes, Monteiro et al. 2006), studying the effect of TCT-Secr derived from the majorly infectious DTUs of *T. cruzi* would help better understand the involvement of the lipid species mentioned above that are released into EVs, in the pathogenesis of the parasite.

Moreover, as we have not been able to analyze the aqueous phase of the Folch's extraction (which reveals mostly GIPLs, PIs and IPCs), this part will remain to be investigated for the future, as species such as diacyl-PC and sphingomyelin (SM) have been shown to be isolated from various stages of the parasite (Gazos-Lopes, Oliveira et al. 2014). Also, we showed in previous chapters,

IB4-lectin fractions ( $\alpha$ -Gal+ or EL, and  $\alpha$ -Gal- or FT) showed to display distinct protein composition, reactivity profile with ChD patients' sera, and EVs size and profile distribution which was in agreement with previous research indicating distinct regions for different GPI-anchored protein specially  $\alpha$ -Gal+ and  $\alpha$ -Gal- on the surface of the parasite (Lantos, Carlevaro et al. 2016). Thus, it will be helpful to study the lipid composition in these 2 fractions and any possible relationship between their lipid composition and other characteristics of them such as protein composition etc. and functional analysis of them, to further understand the pathogenesis of ChD caused by this protozoan parasite.

## CHAPTER 5: INFECTION ASSAY AFTER TREATMENT WITH TCT- SECR/ EVS

### 5.1. INTRODUCTION: *T. CRUZI*-DERIVED EVS EFFECT ON PARASITIC INFECTION

Infection with *T. cruzi* parasite results in innate and specific immune response being elicited, with inflammation being observed particularly in cardiac tissues (Teixeira, Gazzinelli et al. 2002). In the initial stages of the infection, innate immunity is mainly responsible for the control of the parasitemia by activation of various cell types such as NK cells and macrophages, and production of cytokines (Tarleton 2007). In the acute phase of *T. cruzi* infection, upon recognition of parasite by TLRs expressed on macrophages, it will result in induction of TNF- $\alpha$  and IL-12 production which will lead to activation of NK cells and lymphocytes to secrete IFN- $\gamma$  (Costa, Torres et al. 2006, Dutra, Menezes et al. 2014). Thereafter, intracellular growth of the parasites is controlled via macrophage activation by IFN-  $\gamma$ , through NO production by iNOS as well as reactive oxygen species (Camargo, Almeida et al. 1997, Costa, Torres et al. 2006, Gutierrez, Mineo et al. 2009). NO is toxic to trypomastigotes and it also modulates effective immune response, through enhancing and regulating inflammation during infection with *T. cruzi* (Vespa, Cunha et al. 1994, Gutierrez, Mineo et al. 2009). Furthermore, at early stages of the infection with *T. cruzi*, production of pro-inflammatory cytokines such as IL-6 and TNF- $\alpha$  is crucial as they activate inflammatory cells in order to have robust T cell dependent immune response (Wirth and Kierszenbaum 1988, Munoz-Fernandez, Fernandez et al. 1992, Cunha-Neto, Nogueira et al. 2009). Also, increase in IL-10 production in the acute phase of *T. cruzi* infection has been shown to result in increase of the infection (Reed, Brownell et al. 1994).

*T. cruzi*-derived EVs have been shown to play a crucial role in parasite pathogenesis and immune response modulation against the parasite (Cestari, Ansa-Addo et al. 2012, Ramirez, Deolindo et al. 2017). Furthermore, it has been shown that EV cargo can be transferred from parasites to parasites and infected host cells, and can facilitate the stage transition of epimastigotes to trypomastigotes, and increase the infectivity (Garcia-Silva, das Neves et al. 2014). It was shown by Trocoli-Torrecilhas *et al* in 2009 that treatment of mice with *T. cruzi* Y strain-derived EVs 7 days before the infection resulted in parasite decreasing the mice survival and increasing the damage in their heart (Trocoli Torrecilhas, Tonelli et al. 2009). Y strain-derived EVs have shown to cause the imbalance of this cytokine's production (Lovo-Martins, Malvezi et al. 2018). It also has been shown in the previous studies that treatment with Y strain-derived EVs increased infection *in vitro* and *in vivo*, increased parasite internalization and lowered the NO production *in vivo* (Lovo-Martins, Malvezi et al. 2018).

The effect of *T. cruzi*-derived EVs, on the severity of the infection, parasitemia, parasite internalization, and immune response modulation has been shown to be strain specific (Wyllie and Ramirez 2017). Therefore, it is important to study the detailed effect(s) of TCT-Secr and TCT-EVs on parasite's infection, derived from most commonly infectious strains/ clones.

## **5.2. MATERIALS AND METHODS**

### **5.2.1. Mammalian cell culture**

LLC-MK2 and U2-OS cells were cultured in low glucose DMEM with 10% FBS/ Penicillin-Streptomycin as was previously described in **2.2.1** at 37°C, under CO<sub>2</sub> atmosphere, and were sub-cultured once or twice a week Trypsin.

### **5.2.2. Parasite culture, and isolation of extracellular vesicles (EVs)**

The parasite culture and TCT-Secr isolation was performed (as described in 2.2.2.), and TCT-Secr was isolated from TCTs derived from Col, Y, and CLB *T. cruzi* strains/ clone (from 1e8 parasites). Briefly, the parasite-comprising supernatant (from 1e8 parasites) was taken from the cell flask and was centrifuged for 10 minutes at 1,500 g at 4° C and the supernatant was incubated for 2 h for the cell debris and amastigotes (in the pellet) to be separated from the trypomastigotes (by them swimming to the supernatant). The supernatant comprising trypomastigotes was centrifuged, and the trypomastigote-containing pellet was washed 2x with 1X PBS and incubated with FBS free media for the parasites to shed vesicles, and thereafter was centrifuged to separate the vesicles from the trypomastigotes. The supernatant was filtered through 0.45 µm syringe filter and the flow through which is TCT EV-comprising conditioned medium, and analyzed by nanoparticle analysis (NTA) version 3.2 in triplicate. Three measurements of the same sample were performed in 20s using the default settings of the instrument. The error bars indicate the standard error of the mean.

### **5.2.3. BCA Protein Assay**

TCT-Secr derived from Col, Y, and CLB TCTs were analyzed for protein concentration by BCA according to the manufacturer as described earlier (2.2.4).

### **5.2.4. Infection assay after treatment with TCT-Secr derived from Col, Y and CLB**

LLC-MK2 or U2-OS cells were plated in BD Falcon 96-well bioimaging plates (BD Biosciences, Rockville, MD) at a density of  $1 \times 10^4$  cells/ well and incubated overnight at 37 °C in a 5% CO<sub>2</sub> humidified atmosphere. The media of the cells was changed and freshly prepared TCT-Secr derived from Col, Y and CLB at volumes of 5 µl, 10 µl, and 100 µl was added to the wells

accordingly. The cells were incubated for 2 and 6 h with the TCT-Secr at 37°C in a 5% CO<sub>2</sub> humidified atmosphere (in triplicates). Thereafter, the media was replaced with fresh media and the parasites at MOI of 10 were added to the respective wells and incubated for 2 hrs. Afterwards, the cells were washed with 1X PBS 2x very gently to avoid scratching the detached monolayer cells, and fresh media was added and the infected cells (along with controls: uninfected cells, and infected cells without TCT-Secr treatment) were incubated for 5 days. After the incubation time supernatant was removed and the cells were washed with 1X PBS 2x and fixed with 4% paraformaldehyde/ 1X PBS for 15 minutes at room temperature, and stained with 4',6-diamidino-2-phenylindole (DAPI: ProLong™ Gold Antifade Mountant with DAPI, Thermo Fisher Scientific) at 10 µg/ml/ 1X PBS, DRAQ5 (eBioscience™ DRAQ5™, Thermo Fisher Scientific) at 5 µg/ml/ 1X PBS, Alexa Fluor (Alexa Fluor™ 488 phalloidin, Thermo Fisher Scientific) at 0.3 Units/ 1X PBS, and CFSE (carboxyfluorescein succinimidyl ester, CellTrace™ CFSE, Thermo Fisher Scientific) at 10 µM/ 1X PBS for 1 hr according to the manufacturer. CFSE however, was added to the live trypanomastigotes before infection, and parasites were washed 3x with 1X PBS and added to respective wells. Thereafter, the wells were washed 2x with 1X PBS, and then 1X PBS was added to hydrate the wells, and the plate was sealed. Image acquisition of microplates were performed by using the In Cell Analyzer 2000 (GE Healthcare) (DO I HAVE TO MENTION BBRC IMAGING CORE FACILITY?) fluorescence bioimager system, cell count was performed by GE Investigator, and parasite count was done by counting imaged 3 fields per well × 3 wells (per treatment) with 100x magnification on GE Investigator manually from the screen. Filter set appropriate for the excitation and emission of the respective channel was selected.



## 5.3. RESULTS

### 5.3.1. Treatment with TCT-Secr increased the infection (% of parasitemia) with *T. cruzi* respective strains

As it has been shown in previous chapter, various pathogenic markers isolated from *T. cruzi* parasite have been shown to be secreted in TCT-Secr/ TCT-EVs, in agreement with previous research. Here, we tested the effect of TCT-Secr/ TCT-EVs on *T. cruzi* infection *in vitro*. In order to do so, we treated the cells with TCT-Secr with various amounts (5  $\mu$ l, 10  $\mu$ l, and 100  $\mu$ l) for 2 or 6 h prior to infection with TCT-Secr derived from respective parasite strains/ clone. In this experiment, it was shown that there was an increase in parasitemia (% of infected cells/ total cell count) after treatment with TCT-Secr, although this increase was significant only in Col. infection (**Figure 5.1**). We also showed that this increase in infection was dose-dependent (with the exception Y strain infection after treatment with 5  $\mu$ l TCT-Secr). Also, we showed that although the increase was significant in treatment with Col derived TCT-Secr, infection intensity with this strain was lower compared to Y and CLB after treatment with respective TCT-Secr (**Figure 5.1.A**). Moreover, we observed that the infection intensity after treatment with CLB-derived TCT-Secr showed to be the highest in comparison with the other strains after treatment with TCT Sec., followed by treatment with Y strain-derived TCT Sec. (**Figure 5.1.A-B**). Surprisingly, these results showed here that infection with all the parasite strains/ clone showed to be higher after TCT-Secr treatment for 2 h, in comparison with 6 h of TCT-Secr treatment.

These results above showing Col leads to higher infection (% of parasitemia) in comparison with Y strain, were further supported by the imaged intracellular amastigotes in infection induced by these two parasite strains (**Figure 5.2**).

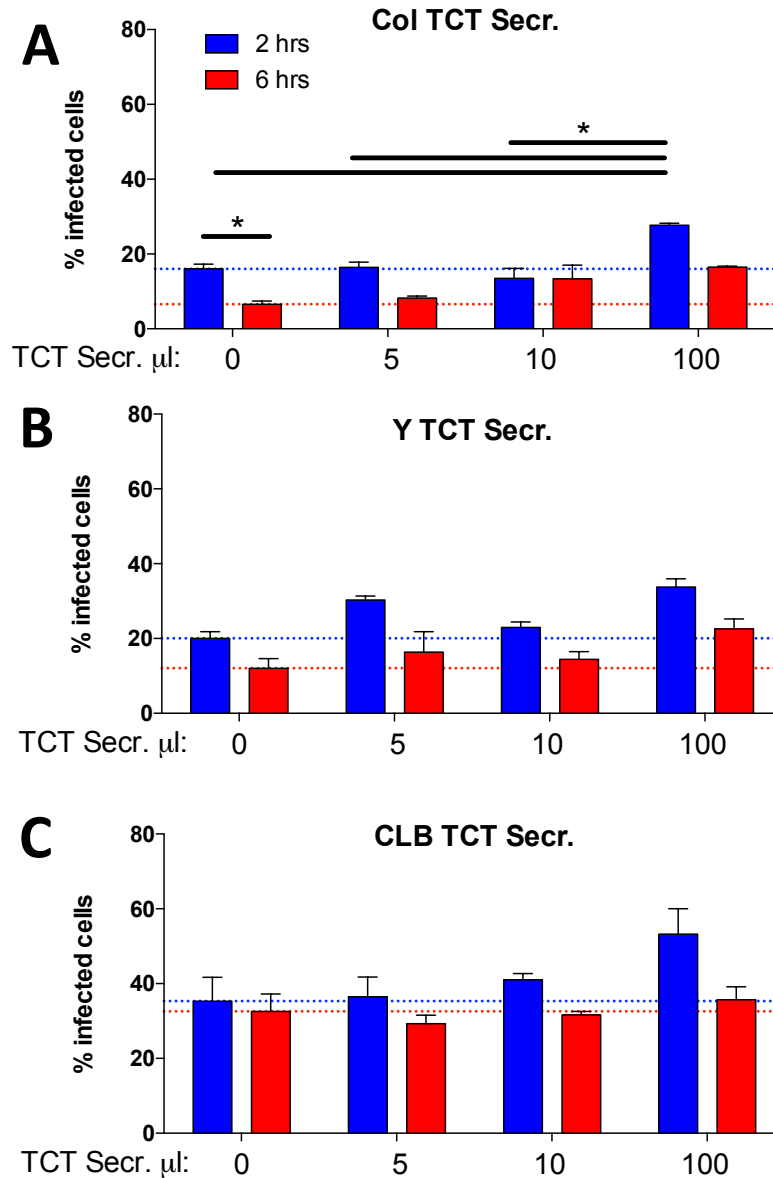


**Figure 5.1. Pre-treatment with TCT-Secr prior to *T. cruzi* infection resulted in increase in or of parasitemia (or increase in number of intracellular parasites or amastigotes).** LLC-MK2 cells were treated with 5  $\mu$ l, 10  $\mu$ l, and 100  $\mu$ l of TCT-Secr derived from parasites prior to infection with respective strain/ clone. The results show that the pretreatment with TCT-Secr resulted in increase in parasitemia (% of infection: % of infected cells/ total cell count). The results are means  $\pm$  SD of three technical replicates.

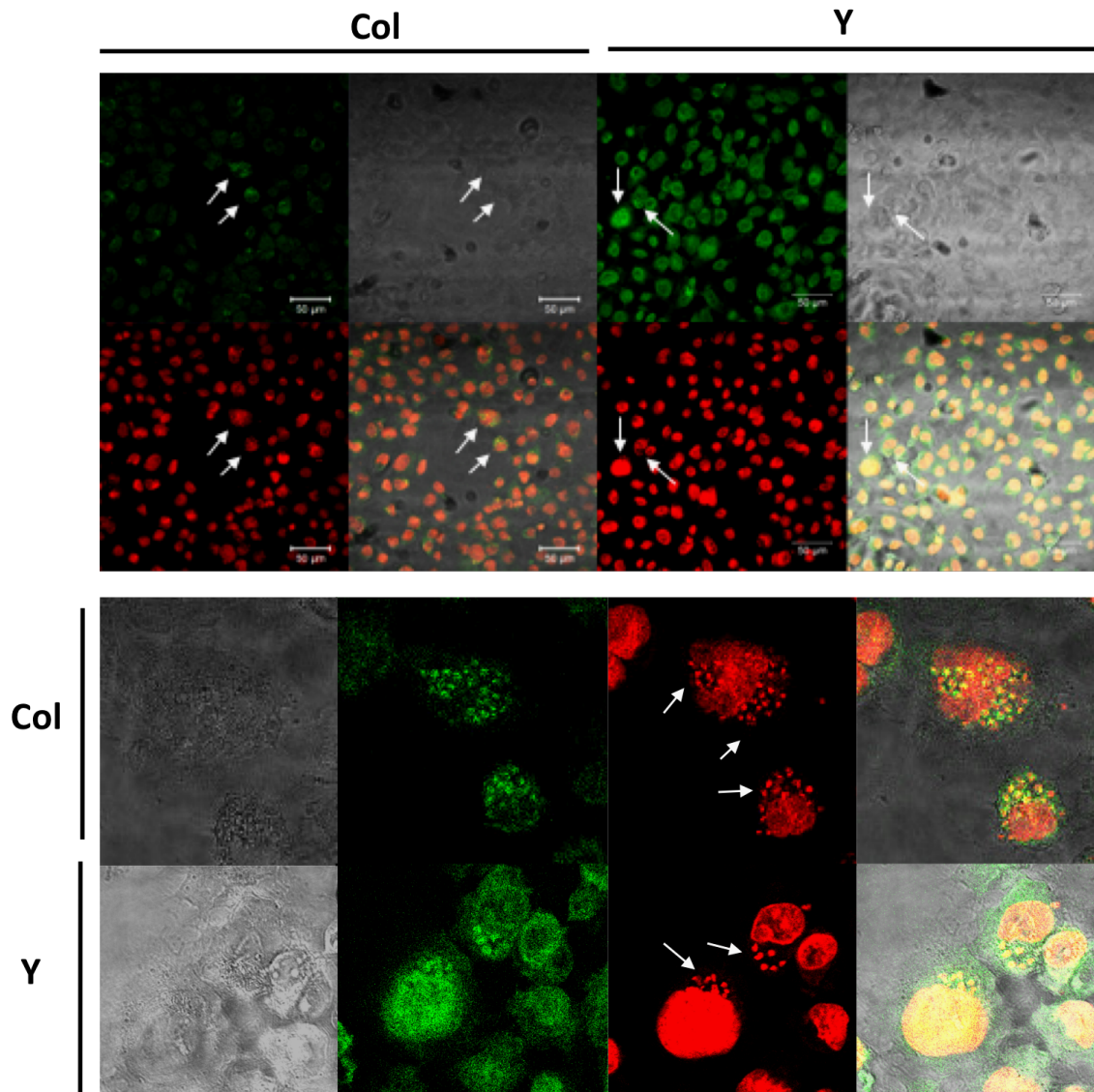


**Figure 5.2. Infection with Col and Y strains.** LLC-MK2 cells were infected with Col and Y at MOI of 10, fixed with 4% PFA, and stained with DRAQ5 (red) and Alexa Fluor (green) at 10  $\mu$ M and 0.3 Units respectively. Infection with Col strain showed to result in higher % of parasitemia compared to infection with Y strain, which is shown in upper panel, left image compared to right image. The lower panel (magnified images) clearly shows infection with Col strain causing higher % of parasitemia compared to infection with Y strain (figure above compared to lower figure).

### **5.3.2. Treatment with TCT-Secr increased the number of the parasites per infected cells after infection with *T. cruzi* respective strains**

Furthermore, it was shown by our results that number of the parasites per infected cells was increased after pre-treatment with respective TCT-Secr, and this increase was statistically significant in infection with Col and CLB strain/ clone (**Figure 5.3**). The increase of parasite number per infected cells was dose- and time- dependent, and was significantly higher after 6 h of treatment in comparison with 2 h of treatment in infection with Col strain and CLB clone (**Figures 5.3.A&C**), however not in Y strain infection (**Figure 5.3.B**). It is worth mentioning that unlike percentage of parasitemia shown in the previous section, in Col infection (**Figure 5.3.A**) intracellular parasite showed to be the highest after TCT-Secr treatment, compared to Y strain and CLB clone (**Figures 5.3.B-C**). Also, we observed that, in general, and amongst the 3 strains/ clone, infection with Col showed the highest parasite number per infected cells followed by infection with CLB. However, infection with Y strain showed the lowest infection and although a dose- and time-dependent increase was observed in parasite number per infected cell, it was not statistically significant.

On the other hand, the obstacle of counting the parasites manually and few fields per well only being included in the count, due to issues with establishing a protocol on GE Healthcare software for segmenting the cells and parasite was faced. This limited the high content imaging (HCI) of the infected cells in the assay. Also, due to the nature of LLC-MK2 cells, they showed to be not homogeneous and their cytoplasm swelled and that as well led to cell segmentation being challenging. Thus, due to the existence of these limitations in our model of high-content imaging with utilizing LLC-MK2 model and GE instrument, it was decided to use another model (U2-OS

cell line: osteoblasts), as well as the Cytation 5 instrument (Cytation™ 5 Cell Imaging Multi-Mode Reader - BioTek Instruments).

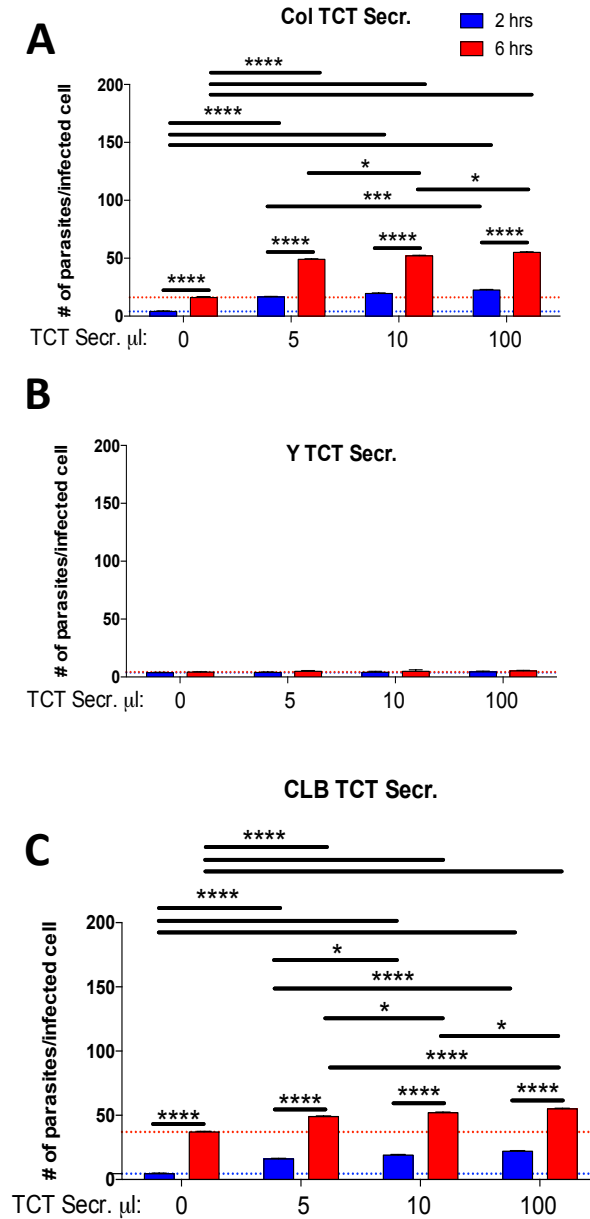


**Figure 5.3. Pre-treatment with TCT-Secr prior to *T. cruzi* infection resulted in increase in or of number of the parasites per infected cells.** LLC-MK2 cells were treated with 5  $\mu$ l, 10  $\mu$ l, and 100  $\mu$ l of TCT-Secr derived from parasite prior to infection with respective strain/ clone. The results show that the pretreatment with TCT-Secr resulted in increase in number of the parasites/ infected cells. The results are means  $\pm$  SD of three technical replicates.

### **5.3.3. Infection with live-CFSE stained TCT is promising for stabilising HCI protocol for *T. cruzi* infection assay**

In order to overcome the obstacles faced previously in the chapter, we established a protocol with pre-staining the parasites with CFSE in order to use separate fluorescent channels for counting cells and parasites (DAPI and CFSE respectively). CFSE is capable of staining the live parasites without damaging the infectivity of them. Therefore, we infected U2-OS cells with 2 different MOIs (5 and 20) for only overnight (as the dye will integrate in parasite's DNA and will lower the fluorescence intensity after second replication cycle of the parasites begins: after ~18 h). As it is illustrated in **Figure 5.4.A**, the pre-staining live parasites showed that their motility is maintained (data not shown). We also have observed that the number of the initial infection was correlated with the intracellular parasites detected after staining (**Figure 5.4.B**). Similar results were shown for Col and CLB infections. The parasites being detected through separate channel from the cells showed to be successful and promising, in order to perform HCI on infected cells in the future using Cytation 5. It was also evident that uninfected cells did not show any background (false positive), as opposed to previous protocols we have been trying to establish, and this cell line shows more homogeneity compared to the previous utilized cell line.

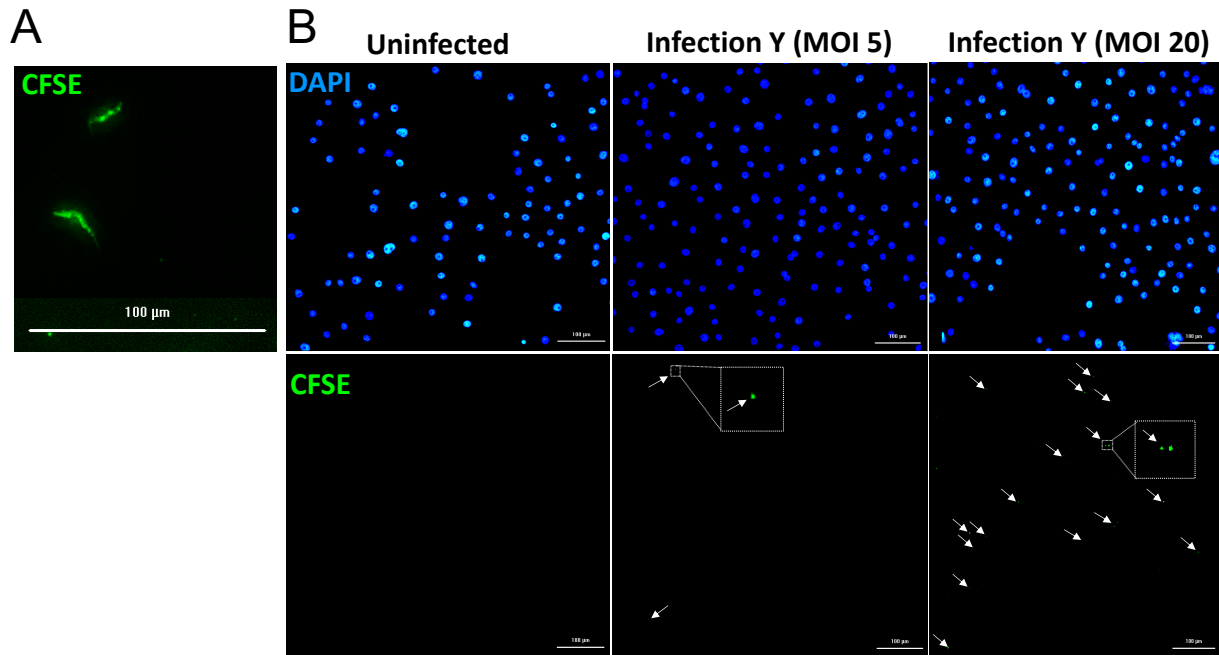


**Figure 5.4. Infection with parasites pre-stained with CFSE.** U2-OS cells were infected with Y-strain TCTs (pre-stained with CFSE, green) (A) at MOIs of 5 and 20, fixed with 4% PFA, and stained with DAPI (blue) (B). The infection rate correlated with the MOI used. Similar results were obtained in Col and CLB infections.

#### 5.4. DISCUSSION AND FUTURE WORK

The parasites-released EVs have been the focus of recent studies on protozoan parasites, and studies have shown that pre-treatment of mice infected with parasites such as *L. donovani* and *L. major*, with EVs derived from those parasites increased parasitism and edema in the mice hind legs (Silverman, Clos et al. 2010). *In vitro* studies between macrophages and *Leishmania* showed that EVs derived from the parasites induced immune response modulation in the host, as well as EVs prepared the host cells for the infection (Silverman, Clos et al. 2010). In case of *T. cruzi*-derived EVs, the effects of EVs derived from the parasite on the infection also have been shown previously (Lovo-Martins, Malvezi et al. 2018). It has been shown that pre-treatment with EVs derived from *T. cruzi* will result in increasing the parasitism as well as decrease in NO production (by downregulating iNOS expression) and TNF- $\alpha$  and IL-6 secretion, and MHC-II expressing macrophages (Trocoli Torrecilhas, Tonelli et al. 2009, Nogueira, Ribeiro et al. 2015, Lovo-Martins, Malvezi et al. 2018). It was also shown that pre-treatment with *T. cruzi*-derived EVs, has resulted in an increase in CD4<sup>+</sup> T cells, as well as IL-4, IL-12 and IL-10 production (Fernandez-Gomez, Esteban et al. 1998, Trocoli Torrecilhas, Tonelli et al. 2009).

In our study, in agreement with previous research, we showed that pre-treatment with TCT-Secr prior to *T. cruzi* parasite infection *in vitro* resulted in significant increase of parasite multiplication inside the cells after 5 days as the number of intracellular parasites increased (amastigote stage which transform to trypomastigotes after approximately 5 days). We also showed that internalization of the parasite by tissue culture-derived trypomastigotes was increased after pre-treatment with TCT-Secr derived from all Col, Y, and CLB, although this increase was not statistically significant in case of Y and CLB infection. These results are in agreement with previous data showing the importance of TCT-Secr and TCT-EVs derived from pathogens



including *T. cruzi* carrying pathogenic markers to the host cells in order to alter the mechanisms involved in host cell immune response towards to being in favor of the pathogen (increasing the infectivity, and modulating the immune response).

However, the detailed mechanisms involved in how EVs facilitate the increase of parasite internalization as well as parasite multiplication inside the cells, remain to be elucidated. Furthermore, as we showed in the previous chapters that IB4-lectin fractions ( $\alpha$ -Gal+ or EL, and  $\alpha$ -Gal- or FT) showed distinct EV profile and size distribution, proteome profile, and the profile of reactivity with ChD patients' sera, it is essential to study the effects of these distinct fractions on parasite infection. It would be more accurate and time efficient to perform these assays utilizing the newly established protocol with using live-stained TCTs with CFSE dye, and analyzing the HCI with Cytation 5. Also, the detailed mechanisms being involved in immune response and inflammatory markers production after treatment with  $\alpha$ -Gal+ and  $\alpha$ -Gal- fractions should be investigated in the future, *in vitro* and *in vivo*.

## 6. REFERENCES

- Acosta-Serrano, A., I. C. Almeida, L. H. Freitas-Junior, N. Yoshida and S. Schenkman (2001). "The mucin-like glycoprotein super-family of *Trypanosoma cruzi*: structure and biological roles." Mol Biochem Parasitol **114**(2): 143-150.
- Agusti, R., A. S. Couto, M. J. Alves, W. Colli and R. M. Lederkremer (2000). "Lipids shed into the culture medium by trypomastigotes of *Trypanosoma cruzi*." Mem Inst Oswaldo Cruz **95**(1): 97-102.
- Akers, J. C., D. Gonda, R. Kim, B. S. Carter and C. C. Chen (2013). "Biogenesis of extracellular vesicles (EV): exosomes, microvesicles, retrovirus-like vesicles, and apoptotic bodies." J Neurooncol **113**(1): 1-11.
- Aliberti, J. C., F. S. Machado, R. T. Gazzinelli, M. M. Teixeira and J. S. Silva (1999). "Platelet-activating factor induces nitric oxide synthesis in *Trypanosoma cruzi*-infected macrophages and mediates resistance to parasite infection in mice." Infect Immun **67**(6): 2810-2814.
- Allen, S., J. M. Richardson, A. Mehlert and M. A. Ferguson (2013). "Structure of a complex phosphoglycan epitope from gp72 of *Trypanosoma cruzi*." J Biol Chem **288**(16): 11093-11105.
- Almeida, I. C., M. M. Camargo, D. O. Procopio, L. S. Silva, A. Mehlert, L. R. Travassos, R. T. Gazzinelli and M. A. Ferguson (2000). "Highly purified glycosylphosphatidylinositols from *Trypanosoma cruzi* are potent proinflammatory agents." EMBO J **19**(7): 1476-1485.

Almeida, I. C., M. A. Ferguson, S. Schenkman and L. R. Travassos (1994). "Lytic anti-alpha-galactosyl antibodies from patients with chronic Chagas' disease recognize novel O-linked oligosaccharides on mucin-like glycosyl-phosphatidylinositol-anchored glycoproteins of *Trypanosoma cruzi*." Biochem J **304** ( Pt 3): 793-802.

Almeida, I. C. and R. T. Gazzinelli (2001). "Proinflammatory activity of glycosylphosphatidylinositol anchors derived from *Trypanosoma cruzi*: structural and functional analyses." J Leukoc Biol **70**(4): 467-477.

Almeida, I. C., S. R. Milani, P. A. Gorin and L. R. Travassos (1991). "Complement-mediated lysis of *Trypanosoma cruzi* trypomastigotes by human anti-alpha-galactosyl antibodies." J Immunol **146**(7): 2394-2400.

Alvarez, V. E., G. T. Niemirowicz and J. J. Cazzulo (2012). "The peptidases of *Trypanosoma cruzi*: digestive enzymes, virulence factors, and mediators of autophagy and programmed cell death." Biochim Biophys Acta **1824**(1): 195-206.

Alves, M. J. and W. Colli (1975). "Glycoproteins from *trypanosoma cruzi*: partial purification by gel chromatography." FEBS Lett **52**(2): 188-190.

Alves, M. J. and W. Colli (2008). "Role of the gp85/trans-sialidase superfamily of glycoproteins in the interaction of *Trypanosoma cruzi* with host structures." Subcell Biochem **47**: 58-69.

Ashton, A. W., S. Mukherjee, F. N. Nagajyothi, H. Huang, V. L. Braunstein, M. S. Desruisseaux, S. M. Factor, L. Lopez, J. W. Berman, M. Wittner, P. E. Scherer, V. Capra, T. M. Coffman, C. N. Serhan, K. Gotlinger, K. K. Wu, L. M. Weiss and H. B. Tanowitz (2007). "Thromboxane A2 is a key regulator of pathogenesis during *Trypanosoma cruzi* infection." J Exp Med **204**(4): 929-940.

Bautista-Lopez, N. L., M. Ndao, F. V. Camargo, T. Nara, T. Annoura, D. B. Hardie, C. H. Borchers and A. Jardim (2017). "Characterization and Diagnostic Application of *Trypanosoma cruzi* Trypomastigote Excreted-Secreted Antigens Shed in Extracellular Vesicles Released from Infected Mammalian Cells." J Clin Microbiol **55**(3): 744-758.

Bayer-Santos, E., C. Aguilar-Bonavides, S. P. Rodrigues, E. M. Cordero, A. F. Marques, A. Varela-Ramirez, H. Choi, N. Yoshida, J. F. da Silveira and I. C. Almeida (2013). "Proteomic analysis of *Trypanosoma cruzi* secretome: characterization of two populations of extracellular vesicles and soluble proteins." J Proteome Res **12**(2): 883-897.

Beauvillain, C., M. O. Juste, S. Dion, J. Pierre and I. Dimier-Poisson (2009). "Exosomes are an effective vaccine against congenital toxoplasmosis in mice." Vaccine **27**(11): 1750-1757.

Beauvillain, C., S. Ruiz, R. Guiton, D. Bout and I. Dimier-Poisson (2007). "A vaccine based on exosomes secreted by a dendritic cell line confers protection against *T. gondii* infection in syngeneic and allogeneic mice." Microbes Infect **9**(14-15): 1614-1622.

Bern, C. and S. P. Montgomery (2009). "An estimate of the burden of Chagas disease in the United States." Clin Infect Dis **49**(5): e52-54.

Bivona, A. E., A. S. Alberti, N. Cerny, S. N. Trinitario and E. L. Malchiodi (2020). "Chagas disease vaccine design: the search for an efficient *Trypanosoma cruzi* immune-mediated control." Biochim Biophys Acta Mol Basis Dis **1866**(5): 165658.

Bobrie, A., M. Colombo, G. Raposo and C. Thery (2011). "Exosome secretion: molecular mechanisms and roles in immune responses." Traffic **12**(12): 1659-1668.

Brisse, S., C. Barnabe and M. Tibayrenc (2000). "Identification of six *Trypanosoma cruzi* phylogenetic lineages by random amplified polymorphic DNA and multilocus enzyme electrophoresis." Int J Parasitol **30**(1): 35-44.

Brisse, S., J. Verhoef and M. Tibayrenc (2001). "Characterisation of large and small subunit rRNA and mini-exon genes further supports the distinction of six *Trypanosoma cruzi* lineages." Int J Parasitol **31**(11): 1218-1226.

Brouwers, J. F., M. Aalberts, J. W. Jansen, G. van Niel, M. H. Wauben, T. A. Stout, J. B. Helms and W. Stoorvogel (2013). "Distinct lipid compositions of two types of human prostasomes." Proteomics **13**(10-11): 1660-1666.

Buscaglia, C. A., V. A. Campo, J. M. Di Noia, A. C. Torrecilhas, C. R. De Marchi, M. A. Ferguson, A. C. Frasch and I. C. Almeida (2004). "The surface coat of the mammal-dwelling infective trypomastigote stage of *Trypanosoma cruzi* is formed by highly diverse immunogenic mucins." J Biol Chem **279**(16): 15860-15869.

Buscaglia, C. A., V. A. Campo, A. C. Frasch and J. M. Di Noia (2006). "Trypanosoma cruzi surface mucins: host-dependent coat diversity." Nat Rev Microbiol **4**(3): 229-236.

Buwitt-Beckmann, U., H. Heine, K. H. Wiesmuller, G. Jung, R. Brock and A. J. Ulmer (2005). "Lipopeptide structure determines TLR2 dependent cell activation level." FEBS J **272**(24): 6354-6364.

Camargo, M. M., I. C. Almeida, M. E. Pereira, M. A. Ferguson, L. R. Travassos and R. T. Gazzinelli (1997). "Glycosylphosphatidylinositol-anchored mucin-like glycoproteins isolated from Trypanosoma cruzi trypomastigotes initiate the synthesis of proinflammatory cytokines by macrophages." J Immunol **158**(12): 5890-5901.

Campos, M. A., I. C. Almeida, O. Takeuchi, S. Akira, E. P. Valente, D. O. Procopio, L. R. Travassos, J. A. Smith, D. T. Golenbock and R. T. Gazzinelli (2001). "Activation of Toll-like receptor-2 by glycosylphosphatidylinositol anchors from a protozoan parasite." J Immunol **167**(1): 416-423.

Carod-Artal, F. J., A. P. Vargas, T. A. Horan and L. G. Nunes (2005). "Chagasic cardiomyopathy is independently associated with ischemic stroke in Chagas disease." Stroke **36**(5): 965-970.

Cestari, I., E. Ansa-Addo, P. Deolindo, J. M. Inal and M. I. Ramirez (2012). "Trypanosoma cruzi immune evasion mediated by host cell-derived microvesicles." J Immunol **188**(4): 1942-1952.

Chagas, C. (1909). "Nova tripanozomiaze humana: estudos sobre a morfologia e o ciclo evolutivo do *Schizotrypanum cruzi* n. gen., n. sp., agente etiologico de nova entidade morbida do homem." Mem Inst Oswaldo Cruz **1**: 159–218.

Chaput, N. and C. Thery (2011). "Exosomes: immune properties and potential clinical implementations." Semin Immunopathol **33**(5): 419-440.

Chilton, F. H., A. N. Fonteh, M. E. Surette, M. Triggiani and J. D. Winkler (1996). "Control of arachidonate levels within inflammatory cells." Biochim Biophys Acta **1299**(1): 1-15.

Choi, D. S., D. K. Kim, Y. K. Kim and Y. S. Gho (2015). "Proteomics of extracellular vesicles: Exosomes and ectosomes." Mass Spectrom Rev **34**(4): 474-490.

Clemente, T. M., C. Cortez, S. Novaes Ada and N. Yoshida (2016). "Surface Molecules Released by *Trypanosoma cruzi* Metacyclic Forms Downregulate Host Cell Invasion." PLoS Negl Trop Dis **10**(8): e0004883.

Coakley, G., R. M. Maizels and A. H. Buck (2015). "Exosomes and Other Extracellular Vesicles: The New Communicators in Parasite Infections." Trends Parasitol **31**(10): 477-489.

Cocucci, E., G. Racchetti and J. Meldolesi (2009). "Shedding microvesicles: artefacts no more." Trends Cell Biol **19**(2): 43-51.

Committee, W. H. O. E. (2002). "Control of Chagas disease." World Health Organ Tech Rep Ser **905**: i-vi, 1-109, back cover.

Costa, V. M., K. C. Torres, R. Z. Mendonca, I. Gresser, K. J. Gollob and I. A. Abrahamsohn (2006). "Type I IFNs stimulate nitric oxide production and resistance to *Trypanosoma cruzi* infection." J Immunol **177**(5): 3193-3200.

Coura, J. R. and P. A. Vinas (2010). "Chagas disease: a new worldwide challenge." Nature **465**(7301): S6-7.

Cronemberger-Andrade, A., L. Aragao-Franca, C. F. de Araujo, V. J. Rocha, C. Borges-Silva Mda, C. P. Figueira, P. R. Oliveira, L. A. de Freitas, P. S. Veras and L. Pontes-de-Carvalho (2014). "Extracellular vesicles from *Leishmania*-infected macrophages confer an anti-infection cytokine-production profile to naive macrophages." PLoS Negl Trop Dis **8**(9): e3161.

Cunha-Neto, E., L. G. Nogueira, P. C. Teixeira, R. Ramasawmy, S. A. Drigo, A. C. Goldberg, S. G. Fonseca, A. M. Bilate and J. Kalil (2009). "Immunological and non-immunological effects of cytokines and chemokines in the pathogenesis of chronic Chagas disease cardiomyopathy." Mem Inst Oswaldo Cruz **104 Suppl 1**: 252-258.

da Fonseca, L. M., K. M. da Costa, V. S. Chaves, C. G. Freire-de-Lima, A. Morrot, L. Mendonca-Previato, J. O. Previato and L. Freire-de-Lima (2019). "Theft and Reception of Host Cell's Sialic Acid: Dynamics of *Trypanosoma cruzi* Trans-sialidases and Mucin-Like Molecules on Chagas' Disease Immunomodulation." Front Immunol **10**: 164.



da Silveira, J. F., P. A. Abrahamsohn and W. Colli (1979). "Plasma membrane vesicles isolated from epimastigote forms of *Trypanosoma cruzi*." Biochim Biophys Acta **550**(2): 222-232.

de Lederkremer, R. M. and W. Colli (1995). "Galactofuranose-containing glycoconjugates in trypanosomatids." Glycobiology **5**(6): 547-552.

De Pablos, L. M., G. G. Gonzalez, J. Solano Parada, V. Seco Hidalgo, I. M. Diaz Lozano, M. M. Gomez Samblas, T. Cruz Bustos and A. Osuna (2011). "Differential expression and characterization of a member of the mucin-associated surface protein family secreted by *Trypanosoma cruzi*." Infect Immun **79**(10): 3993-4001.

De Pablos, L. M. and A. Osuna (2012). "Multigene families in *Trypanosoma cruzi* and their role in infectivity." Infect Immun **80**(7): 2258-2264.

de Pablos Torro, L. M., L. Retana Moreira and A. Osuna (2018). "Extracellular Vesicles in Chagas Disease: A New Passenger for an Old Disease." Front Microbiol **9**: 1190.

De Souza, W. (2002). "Basic cell biology of *Trypanosoma cruzi*." Curr Pharm Des **8**(4): 269-285.

Del Cacho, E., M. Gallego, S. H. Lee, H. S. Lillehoj, J. Quilez, E. P. Lillehoj and C. Sanchez-Acedo (2011). "Induction of protective immunity against *Eimeria tenella* infection using antigen-loaded dendritic cells (DC) and DC-derived exosomes." Vaccine **29**(21): 3818-3825.

Dias, E., F. S. Laranja, A. Miranda and G. Nobrega (1956). "Chagas' disease; a clinical, epidemiologic, and pathologic study." Circulation **14**(6): 1035-1060.

Diaz de Toranzo, E. G., J. A. Castro, B. M. Franke de Cazzulo and J. J. Cazzulo (1988). "Interaction of benznidazole reactive metabolites with nuclear and kinetoplasmic DNA, proteins and lipids from *Trypanosoma cruzi*." Experientia **44**(10): 880-881.

Duffy, T., M. Bisio, J. Altcheh, J. M. Burgos, M. Diez, M. J. Levin, R. R. Favaloro, H. Freilij and A. G. Schijman (2009). "Accurate real-time PCR strategy for monitoring bloodstream parasitic loads in chagas disease patients." PLoS Negl Trop Dis **3**(4): e419.

Duijvesz, D., T. Luider, C. H. Bangma and G. Jenster (2011). "Exosomes as biomarker treasure chests for prostate cancer." Eur Urol **59**(5): 823-831.

Dutra, W. O. and K. J. Gollob (2008). "Current concepts in immunoregulation and pathology of human Chagas disease." Curr Opin Infect Dis **21**(3): 287-292.

Dutra, W. O., C. A. Menezes, L. M. Magalhaes and K. J. Gollob (2014). "Immunoregulatory networks in human Chagas disease." Parasite Immunol **36**(8): 377-387.

Falla, A., C. Herrera, A. Fajardo, M. Montilla, G. A. Vallejo and F. Guhl (2009). "Haplotype identification within *Trypanosoma cruzi* I in Colombian isolates from several reservoirs, vectors and humans." Acta Trop **110**(1): 15-21.

Fernandez-Gomez, R., S. Esteban, R. Gomez-Corvera, K. Zoulika and A. Ouaiissi (1998). "Trypanosoma cruzi: Tc52 released protein-induced increased expression of nitric oxide synthase and nitric oxide production by macrophages." J Immunol **160**(7): 3471-3479.

Fevrier, B. and G. Raposo (2004). "Exosomes: endosomal-derived vesicles shipping extracellular messages." Curr Opin Cell Biol **16**(4): 415-421.

Folch, J., M. Lees and G. H. Sloane Stanley (1957). "A simple method for the isolation and purification of total lipides from animal tissues." J Biol Chem **226**(1): 497-509.

Frasch, A. C. (2000). "Functional diversity in the trans-sialidase and mucin families in Trypanosoma cruzi." Parasitol Today **16**(7): 282-286.

Freire-de-Lima, C. G., D. O. Nascimento, M. B. Soares, P. T. Bozza, H. C. Castro-Faria-Neto, F. G. de Mello, G. A. DosReis and M. F. Lopes (2000). "Uptake of apoptotic cells drives the growth of a pathogenic trypanosome in macrophages." Nature **403**(6766): 199-203.

Garcia-Silva, M. R., R. F. das Neves, F. Cabrera-Cabrera, J. Sanguinetti, L. C. Medeiros, C. Robello, H. Naya, T. Fernandez-Calero, T. Souto-Padron, W. de Souza and A. Cayota (2014). "Extracellular vesicles shed by Trypanosoma cruzi are linked to small RNA pathways, life cycle regulation, and susceptibility to infection of mammalian cells." Parasitol Res **113**(1): 285-304.

Gazos-Lopes, F., M. M. Oliveira, L. V. Hoelz, D. P. Vieira, A. F. Marques, E. S. Nakayasu, M. T. Gomes, N. G. Salloum, P. G. Pascutti, T. Souto-Padron, R. Q. Monteiro, A. H. Lopes and I. C.

Almeida (2014). "Structural and functional analysis of a platelet-activating lysophosphatidylcholine of *Trypanosoma cruzi*." PLoS Negl Trop Dis **8**(8): e3077.

Gazzinelli, R. T., M. E. Pereira, A. Romanha, G. Gazzinelli and Z. Brener (1991). "Direct lysis of *Trypanosoma cruzi*: a novel effector mechanism of protection mediated by human anti-gal antibodies." Parasite Immunol **13**(4): 345-356.

Giorgi, M. E. and R. M. de Lederkremer (2011). "Trans-sialidase and mucins of *Trypanosoma cruzi*: an important interplay for the parasite." Carbohydr Res **346**(12): 1389-1393.

Giri, P. K. and J. S. Schorey (2008). "Exosomes derived from *M. Bovis* BCG infected macrophages activate antigen-specific CD4+ and CD8+ T cells in vitro and in vivo." PLoS One **3**(6): e2461.

Goldenberg, S. and A. R. Avila (2011). "Aspects of *Trypanosoma cruzi* stage differentiation." Adv Parasitol **75**: 285-305.

Golgher, D. B., W. Colli, T. Souto-Padron and B. Zingales (1993). "Galactofuranose-containing glycoconjugates of epimastigote and trypomastigote forms of *Trypanosoma cruzi*." Mol Biochem Parasitol **60**(2): 249-264.

Gomes, M. T., R. Q. Monteiro, L. A. Grillo, F. Leite-Lopes, H. Stroeder, A. Ferreira-Pereira, C. S. Alviano, E. Barreto-Bergter, H. C. Neto, E. S. N. L. Cunha, I. C. Almeida, R. M. Soares and A.

H. Lopes (2006). "Platelet-activating factor-like activity isolated from *Trypanosoma cruzi*." Int J Parasitol **36**(2): 165-173.

Goncalves, M. F., E. S. Umezawa, A. M. Katzin, W. de Souza, M. J. Alves, B. Zingales and W. Colli (1991). "Trypanosoma cruzi: shedding of surface antigens as membrane vesicles." Exp Parasitol **72**(1): 43-53.

Gutierrez, F. R., T. W. Mineo, W. R. Pavanelli, P. M. Guedes and J. S. Silva (2009). "The effects of nitric oxide on the immune system during *Trypanosoma cruzi* infection." Mem Inst Oswaldo Cruz **104 Suppl 1**: 236-245.

Gyorgy, B., T. G. Szabo, M. Pasztoi, Z. Pal, P. Misjak, B. Aradi, V. Laszlo, E. Pallinger, E. Pap, A. Kittel, G. Nagy, A. Falus and E. I. Buzas (2011). "Membrane vesicles, current state-of-the-art: emerging role of extracellular vesicles." Cell Mol Life Sci **68**(16): 2667-2688.

Harding, C. V., J. E. Heuser and P. D. Stahl (2013). "Exosomes: looking back three decades and into the future." J Cell Biol **200**(4): 367-371.

Herrera, C., M. D. BARGUES, A. Fajardo, M. Montilla, O. Triana, G. A. Vallejo and F. Guhl (2007). "Identifying four *Trypanosoma cruzi* I isolate haplotypes from different geographic regions in Colombia." Infect Genet Evol **7**(4): 535-539.

Hess, C., S. Sadallah, A. Hefti, R. Landmann and J. A. Schifferli (1999). "Ectosomes released by human neutrophils are specialized functional units." J Immunol **163**(8): 4564-4573.

Holme, P. A., N. O. Solum, F. Brosstad, M. Roger and M. Abdelnoor (1994). "Demonstration of platelet-derived microvesicles in blood from patients with activated coagulation and fibrinolysis using a filtration technique and western blotting." Thromb Haemost **72**(5): 666-671.

Honda, Z., S. Ishii and T. Shimizu (2002). "Platelet-activating factor receptor." J Biochem **131**(6): 773-779.

Hotez, P. J., M. E. Bottazzi, C. Franco-Paredes, S. K. Ault and M. R. Periago (2008). "The neglected tropical diseases of Latin America and the Caribbean: a review of disease burden and distribution and a roadmap for control and elimination." PLoS Negl Trop Dis **2**(9): e300.

Huang, Y. H., L. Schafer-Elinder, R. Wu, H. E. Claesson and J. Frostegard (1999). "Lysophosphatidylcholine (LPC) induces proinflammatory cytokines by a platelet-activating factor (PAF) receptor-dependent mechanism." Clin Exp Immunol **116**(2): 326-331.

Jimenez, P., J. Jaimes, C. Poveda and J. D. Ramirez (2019). "A systematic review of the *Trypanosoma cruzi* genetic heterogeneity, host immune response and genetic factors as plausible drivers of chronic chagasic cardiomyopathy." Parasitology **146**(3): 269-283.

Kabbani, S. S., M. W. Watkins, T. Ashikaga, E. F. Terrien, P. A. Holoch, B. E. Sobel and D. J. Schneider (2001). "Platelet reactivity characterized prospectively: a determinant of outcome 90 days after percutaneous coronary intervention." Circulation **104**(2): 181-186.

Kalra, H., G. P. Drummen and S. Mathivanan (2016). "Focus on Extracellular Vesicles: Introducing the Next Small Big Thing." Int J Mol Sci **17**(2): 170.

Kalra, H., R. J. Simpson, H. Ji, E. Aikawa, P. Altevogt, P. Askenase, V. C. Bond, F. E. Borrás, X. Breakefield, V. Budnik, E. Buzas, G. Camussi, A. Clayton, E. Cocucci, J. M. Falcon-Perez, S. Gabrielsson, Y. S. Gho, D. Gupta, H. C. Harsha, A. Hendrix, A. F. Hill, J. M. Inal, G. Jenster, E. M. Kramer-Albers, S. K. Lim, A. Llorente, J. Lotvall, A. Marcilla, L. Mincheva-Nilsson, I. Nazarenko, R. Nieuwland, E. N. Nolte-'t Hoen, A. Pandey, T. Patel, M. G. Piper, S. Pluchino, T. S. Prasad, L. Rajendran, G. Raposo, M. Record, G. E. Reid, F. Sanchez-Madrid, R. M. Schiffelers, P. Siljander, A. Stensballe, W. Stoorvogel, D. Taylor, C. Thery, H. Valadi, B. W. van Balkom, J. Vazquez, M. Vidal, M. H. Wauben, M. Yanez-Mo, M. Zoeller and S. Mathivanan (2012). "Vesiclepedia: a compendium for extracellular vesicles with continuous community annotation." PLoS Biol **10**(12): e1001450.

Kasperska-Zajac, A., Z. Brzoza and B. Rogala (2008). "Platelet-activating factor (PAF): a review of its role in asthma and clinical efficacy of PAF antagonists in the disease therapy." Recent Pat Inflamm Allergy Drug Discov **2**(1): 72-76.

Kollien, A. H., J. Schmidt and G. A. Schaub (1998). "Modes of association of *Trypanosoma cruzi* with the intestinal tract of the vector *Triatoma infestans*." Acta Trop **70**(2): 127-141.

Lantos, A. B., G. Carlevaro, B. Araoz, P. Ruiz Diaz, L. Camara Mde, C. A. Buscaglia, M. Bossi, H. Yu, X. Chen, C. R. Bertozzi, J. Mucci and O. Campetella (2016). "Sialic Acid Glycobiology

Unveils Trypanosoma cruzi Trypomastigote Membrane Physiology." PLoS Pathog **12**(4): e1005559.

Laulagnier, K., C. Motta, S. Hamdi, S. Roy, F. Fauvelle, J. F. Pageaux, T. Kobayashi, J. P. Salles, B. Perret, C. Bonnerot and M. Record (2004). "Mast cell- and dendritic cell-derived exosomes display a specific lipid composition and an unusual membrane organization." Biochem J **380**(Pt 1): 161-171.

Longo, L. V., E. S. Nakayasu, F. Gazos-Lopes, M. C. Vallejo, A. L. Matsuo, I. C. Almeida and R. Puccia (2013). "Characterization of cell wall lipids from the pathogenic phase of Paracoccidioides brasiliensis cultivated in the presence or absence of human plasma." PLoS One **8**(5): e63372.

Lovo-Martins, M. I., A. D. Malvezi, N. G. Zanluqui, B. F. C. Lucchetti, V. L. H. Tatakihara, P. A. Morking, A. G. de Oliveira, S. Goldenberg, P. F. Wowk and P. Pinge-Filho (2018). "Extracellular Vesicles Shed By Trypanosoma cruzi Potentiate Infection and Elicit Lipid Body Formation and PGE2 Production in Murine Macrophages." Front Immunol **9**: 896.

Machado, F. S., W. O. Dutra, L. Esper, K. J. Gollob, M. M. Teixeira, S. M. Factor, L. M. Weiss, F. Nagajyothi, H. B. Tanowitz and N. J. Garg (2012). "Current understanding of immunity to Trypanosoma cruzi infection and pathogenesis of Chagas disease." Semin Immunopathol **34**(6): 753-770.



Macrae, J. I., A. Acosta-Serrano, N. A. Morrice, A. Mehlert and M. A. Ferguson (2005). "Structural characterization of NETNES, a novel glycoconjugate in *Trypanosoma cruzi* epimastigotes." J Biol Chem **280**(13): 12201-12211.

Marcilla, A., L. Martin-Jaular, M. Trelis, A. de Menezes-Neto, A. Osuna, D. Bernal, C. Fernandez-Becerra, I. C. Almeida and H. A. Del Portillo (2014). "Extracellular vesicles in parasitic diseases." J Extracell Vesicles **3**: 25040.

Mendonca-Previato, L., L. Penha, T. C. Garcez, C. Jones and J. O. Previato (2013). "Addition of alpha-O-GlcNAc to threonine residues define the post-translational modification of mucin-like molecules in *Trypanosoma cruzi*." Glycoconj J **30**(7): 659-666.

Mesquita, R. D., A. B. Carneiro, A. Bafica, F. Gazos-Lopes, C. M. Takiya, T. Souto-Padron, D. P. Vieira, A. Ferreira-Pereira, I. C. Almeida, R. T. Figueiredo, B. N. Porto, M. T. Bozza, A. V. Graca-Souza, A. H. Lopes, G. C. Atella and M. A. Silva-Neto (2008). "Trypanosoma cruzi infection is enhanced by vector saliva through immunosuppressant mechanisms mediated by lysophosphatidylcholine." Infect Immun **76**(12): 5543-5552.

Morrow, T. (2017). "FDA Gives First-Ever Approval of Drug To Treat Chagas' Disease." Manag Care **26**(11): 38-40.

Mukherjee, S., F. S. Machado, H. Huang, H. S. Oz, L. A. Jelicks, C. M. Prado, W. Koba, E. J. Fine, D. Zhao, S. M. Factor, J. E. Collado, L. M. Weiss, H. B. Tanowitz and A. W. Ashton (2011).

"Aspirin treatment of mice infected with *Trypanosoma cruzi* and implications for the pathogenesis of Chagas disease." PLoS One **6**(2): e16959.

Munoz-Fernandez, M. A., M. A. Fernandez and M. Fresno (1992). "Synergism between tumor necrosis factor-alpha and interferon-gamma on macrophage activation for the killing of intracellular *Trypanosoma cruzi* through a nitric oxide-dependent mechanism." Eur J Immunol **22**(2): 301-307.

Nardy, A. F., J. Luiz da Silva Filho, A. R. Perez, J. de Meis, D. A. Farias-de-Oliveira, L. Penha, I. de Araujo Oliveira, W. B. Dias, A. R. Todeschini, C. G. Freire-de-Lima, M. Bellio, C. Caruso-Neves, A. A. Pinheiro, C. M. Takiya, O. Bottasso, W. Savino and A. Morrot (2013). "Trans-sialidase from *Trypanosoma cruzi* enhances the adhesion properties and fibronectin-driven migration of thymocytes." Microbes Infect **15**(5): 365-374.

Nogueira, P. M., K. Ribeiro, A. C. Silveira, J. H. Campos, O. A. Martins-Filho, S. R. Bela, M. A. Campos, N. L. Pessoa, W. Colli, M. J. Alves, R. P. Soares and A. C. Torrecilhas (2015). "Vesicles from different *Trypanosoma cruzi* strains trigger differential innate and chronic immune responses." J Extracell Vesicles **4**: 28734.

Ogita, T., Y. Tanaka, T. Nakaoka, R. Matsuoka, Y. Kira, M. Nakamura, T. Shimizu and T. Fujita (1997). "Lysophosphatidylcholine transduces Ca<sup>2+</sup> signaling via the platelet-activating factor receptor in macrophages." Am J Physiol **272**(1 Pt 2): H17-24.

Ojala, P. J., T. E. Hirvonen, M. Hermansson, P. Somerharju and J. Parkkinen (2007). "Acyl chain-dependent effect of lysophosphatidylcholine on human neutrophils." J Leukoc Biol **82**(6): 1501-1509.

Ortega-Rodriguez, U., S. Portillo, R. A. Ashmus, J. A. Duran, N. S. Schocker, E. Iniguez, A. L. Montoya, B. G. Zepeda, J. J. Olivas, N. H. Karimi, J. Alonso-Padilla, L. Izquierdo, M. J. Pinazo, B. A. de Noya, O. Noya, R. A. Maldonado, F. Torrico, J. Gascon, K. Michael and I. C. Almeida (2019). "Purification of Glycosylphosphatidylinositol-Anchored Mucins from *Trypanosoma cruzi* Trypomastigotes and Synthesis of alpha-Gal-Containing Neoglycoproteins: Application as Biomarkers for Reliable Diagnosis and Early Assessment of Chemotherapeutic Outcomes of Chagas Disease." Methods Mol Biol **1955**: 287-308.

Ouaissi, A., T. Aguirre, B. Plumas-Marty, M. Piras, R. Schoneck, H. Gras-Masse, A. Taibi, M. Loyens, A. Tartar, A. Capron and et al. (1992). "Cloning and sequencing of a 24-kDa *Trypanosoma cruzi* specific antigen released in association with membrane vesicles and defined by a monoclonal antibody." Biol Cell **75**(1): 11-17.

Ouaissi, M. A., J. F. Dubremetz, J. P. Kusnierz, J. Cornette, M. Loyens, A. Taibi, B. Marty, P. Velge, F. Rizvi and A. Capron (1990). "Trypanosoma cruzi: differential expression and distribution of an 85-kDa polypeptide epitope by in vitro developmental stages." Exp Parasitol **71**(2): 207-217.

Pilzer, D., O. Gasser, O. Moskovich, J. A. Schifferli and Z. Fishelson (2005). "Emission of membrane vesicles: roles in complement resistance, immunity and cancer." Springer Semin Immunopathol **27**(3): 375-387.

Prochetto, E., C. Roldan, I. A. Bontempi, D. Bertona, L. Peverengo, M. H. Vicco, L. M. Rodeles, A. R. Perez, I. S. Marcipar and G. Cabrera (2017). "Trans-sialidase-based vaccine candidate protects against *Trypanosoma cruzi* infection, not only inducing an effector immune response but also affecting cells with regulatory/suppressor phenotype." Oncotarget **8**(35): 58003-58020.

Queiroz, R. M., C. A. Ricart, M. O. Machado, I. M. Bastos, J. M. de Santana, M. V. de Sousa, P. Roepstorff and S. Charneau (2016). "Insight into the Exoproteome of the Tissue-Derived Trypomastigote form of *Trypanosoma cruzi*." Front Chem **4**: 42.

Ramirez, M. I., P. Deolindo, I. J. de Messias-Reason, E. A. Arigi, H. Choi, I. C. Almeida and I. Evans-Osses (2017). "Dynamic flux of microvesicles modulate parasite-host cell interaction of *Trypanosoma cruzi* in eukaryotic cells." Cell Microbiol **19**(4).

Rao, S. P., M. Riederer, M. Lechleitner, M. Hermansson, G. Desoye, S. Hallstrom, W. F. Graier and S. Frank (2013). "Acyl chain-dependent effect of lysophosphatidylcholine on endothelium-dependent vasorelaxation." PLoS One **8**(5): e65155.

Raposo, G., H. W. Nijman, W. Stoorvogel, R. Liejendekker, C. V. Harding, C. J. Melief and H. J. Geuze (1996). "B lymphocytes secrete antigen-presenting vesicles." J Exp Med **183**(3): 1161-1172.

Raposo, G. and W. Stoorvogel (2013). "Extracellular vesicles: exosomes, microvesicles, and friends." J Cell Biol **200**(4): 373-383.

Rassi, A., Jr., A. Rassi and J. A. Marin-Neto (2010). "Chagas disease." Lancet **375**(9723): 1388-1402.

Ratajczak, J., M. Wysoczynski, F. Hayek, A. Janowska-Wieczorek and M. Z. Ratajczak (2006). "Membrane-derived microvesicles: important and underappreciated mediators of cell-to-cell communication." Leukemia **20**(9): 1487-1495.

Reed, S. G., C. E. Brownell, D. M. Russo, J. S. Silva, K. H. Grabstein and P. J. Morrissey (1994). "IL-10 mediates susceptibility to *Trypanosoma cruzi* infection." J Immunol **153**(7): 3135-3140.

Ribeiro, K. S., C. I. Vasconcellos, R. P. Soares, M. T. Mendes, C. C. Ellis, M. Aguilera-Flores, I. C. de Almeida, S. Schenkman, L. K. Iwai and A. C. Torrecilhas (2018). "Proteomic analysis reveals different composition of extracellular vesicles released by two *Trypanosoma cruzi* strains associated with their distinct interaction with host cells." J Extracell Vesicles **7**(1): 1463779.

Richmond, G. S., F. Gibellini, S. A. Young, L. Major, H. Denton, A. Lilley and T. K. Smith (2010). "Lipidomic analysis of bloodstream and procyclic form *Trypanosoma brucei*." Parasitology **137**(9): 1357-1392.

Riederer, M., P. J. Ojala, A. Hrzenjak, W. F. Graier, R. Malli, M. Tritscher, M. Hermansson, B. Watzel, H. Schweer, G. Desoye, A. Heinemann and S. Frank (2010). "Acyl chain-dependent effect

of lysophosphatidylcholine on endothelial prostacyclin production." J Lipid Res **51**(10): 2957-2966.

Rodriguez-Morales, O., V. Monteon-Padilla, S. C. Carrillo-Sanchez, M. Rios-Castro, M. Martinez-Cruz, A. Carabarin-Lima and M. Arce-Fonseca (2015). "Experimental Vaccines against Chagas Disease: A Journey through History." J Immunol Res **2015**: 489758.

Ropert, C., I. C. Almeida, M. Closel, L. R. Travassos, M. A. Ferguson, P. Cohen and R. T. Gazzinelli (2001). "Requirement of mitogen-activated protein kinases and I kappa B phosphorylation for induction of proinflammatory cytokines synthesis by macrophages indicates functional similarity of receptors triggered by glycosylphosphatidylinositol anchors from parasitic protozoa and bacterial lipopolysaccharide." J Immunol **166**(5): 3423-3431.

Ropert, C., L. R. Ferreira, M. A. Campos, D. O. Procopio, L. R. Travassos, M. A. Ferguson, L. F. Reis, M. M. Teixeira, I. C. Almeida and R. T. Gazzinelli (2002). "Macrophage signaling by glycosylphosphatidylinositol-anchored mucin-like glycoproteins derived from *Trypanosoma cruzi* trypomastigotes." Microbes Infect **4**(9): 1015-1025.

Sanchez, L. V. and J. D. Ramirez (2013). "Congenital and oral transmission of American trypanosomiasis: an overview of physiopathogenic aspects." Parasitology **140**(2): 147-159.

Schenkman, S., D. Eichinger, M. E. Pereira and V. Nussenzweig (1994). "Structural and functional properties of *Trypanosoma trans-sialidase*." Annu Rev Microbiol **48**: 499-523.

Schmunis, G. A. and Z. E. Yadon (2010). "Chagas disease: a Latin American health problem becoming a world health problem." Acta Trop **115**(1-2): 14-21.

Schnitzer, J. K., S. Berzel, M. Fajardo-Moser, K. A. Remer and H. Moll (2010). "Fragments of antigen-loaded dendritic cells (DC) and DC-derived exosomes induce protective immunity against *Leishmania major*." Vaccine **28**(36): 5785-5793.

Schocker, N. S., S. Portillo, C. R. Brito, A. F. Marques, I. C. Almeida and K. Michael (2016). "Synthesis of Gal $\alpha$ (1,3)Gal $\beta$ (1,4)GlcNAc $\alpha$ -, Gal $\beta$ (1,4)GlcNAc $\alpha$ - and GlcNAc-containing neoglycoproteins and their immunological evaluation in the context of Chagas disease." Glycobiology **26**(1): 39-50.

Schorey, J. S., Y. Cheng, P. P. Singh and V. L. Smith (2015). "Exosomes and other extracellular vesicles in host-pathogen interactions." EMBO Rep **16**(1): 24-43.

Silva-Neto, M. A., A. B. Carneiro, L. Silva-Cardoso and G. C. Atella (2012). "Lysophosphatidylcholine: A Novel Modulator of *Trypanosoma cruzi* Transmission." J Parasitol Res **2012**: 625838.

Silverman, J. M., J. Clos, C. C. de'Oliveira, O. Shirvani, Y. Fang, C. Wang, L. J. Foster and N. E. Reiner (2010). "An exosome-based secretion pathway is responsible for protein export from *Leishmania* and communication with macrophages." J Cell Sci **123**(Pt 6): 842-852.

Silverman, J. M., J. Clos, E. Horakova, A. Y. Wang, M. Wiesgigl, I. Kelly, M. A. Lynn, W. R. McMaster, L. J. Foster, M. K. Levings and N. E. Reiner (2010). "Leishmania exosomes modulate innate and adaptive immune responses through effects on monocytes and dendritic cells." J Immunol **185**(9): 5011-5022.

Smith, J. C., W. Hou, S. N. Whitehead, M. Ethier, S. A. Bennett and D. Figeys (2008). "Identification of lysophosphatidylcholine (LPC) and platelet activating factor (PAF) from PC12 cells and mouse cortex using liquid chromatography/multi-stage mass spectrometry (LC/MS3)." Rapid Commun Mass Spectrom **22**(22): 3579-3587.

Soo, C. Y., Y. Song, Y. Zheng, E. C. Campbell, A. C. Riches, F. Gunn-Moore and S. J. Powis (2012). "Nanoparticle tracking analysis monitors microvesicle and exosome secretion from immune cells." Immunology **136**(2): 192-197.

Subra, C., K. Laulagnier, B. Perret and M. Record (2007). "Exosome lipidomics unravels lipid sorting at the level of multivesicular bodies." Biochimie **89**(2): 205-212.

Talvani, A., F. S. Machado, G. C. Santana, A. Klein, L. Barcelos, J. S. Silva and M. M. Teixeira (2002). "Leukotriene B(4) induces nitric oxide synthesis in Trypanosoma cruzi-infected murine macrophages and mediates resistance to infection." Infect Immun **70**(8): 4247-4253.

Tanowitz, H. B., E. R. Burns, A. K. Sinha, N. N. Kahn, S. A. Morris, S. M. Factor, V. B. Hatcher, J. P. Bilezikian, S. G. Baum and M. Wittner (1990). "Enhanced platelet adherence and aggregation



in Chagas' disease: a potential pathogenic mechanism for cardiomyopathy." Am J Trop Med Hyg **43**(3): 274-281.

Tanowitz, H. B., L. V. Kirchhoff, D. Simon, S. A. Morris, L. M. Weiss and M. Wittner (1992). "Chagas' disease." Clin Microbiol Rev **5**(4): 400-419.

Tarleton, R. L. (2007). "Immune system recognition of *Trypanosoma cruzi*." Curr Opin Immunol **19**(4): 430-434.

Teixeira, M. M., R. T. Gazzinelli and J. S. Silva (2002). "Chemokines, inflammation and *Trypanosoma cruzi* infection." Trends Parasitol **18**(6): 262-265.

Teixeira, M. M. and N. Yoshida (1986). "Stage-specific surface antigens of metacyclic trypomastigotes of *Trypanosoma cruzi* identified by monoclonal antibodies." Mol Biochem Parasitol **18**(3): 271-282.

They, C., S. Amigorena, G. Raposo and A. Clayton (2006). "Isolation and characterization of exosomes from cell culture supernatants and biological fluids." Curr Protoc Cell Biol **Chapter 3**: Unit 3 22.

They, C., A. Regnault, J. Garin, J. Wolfers, L. Zitvogel, P. Ricciardi-Castagnoli, G. Raposo and S. Amigorena (1999). "Molecular characterization of dendritic cell-derived exosomes. Selective accumulation of the heat shock protein hsc73." J Cell Biol **147**(3): 599-610.

Tibayrenc, M. (1998). "Genetic epidemiology of parasitic protozoa and other infectious agents: the need for an integrated approach." Int J Parasitol **28**(1): 85-104.

Towbin, H., T. Staehelin and J. Gordon (1992). "Electrophoretic transfer of proteins from polyacrylamide gels to nitrocellulose sheets: procedure and some applications. 1979." Biotechnology **24**: 145-149.

Trajkovic, K., C. Hsu, S. Chiantia, L. Rajendran, D. Wenzel, F. Wieland, P. Schwille, B. Brugger and M. Simons (2008). "Ceramide triggers budding of exosome vesicles into multivesicular endosomes." Science **319**(5867): 1244-1247.

Trams, E. G., C. J. Lauter, N. Salem, Jr. and U. Heine (1981). "Exfoliation of membrane ectoenzymes in the form of micro-vesicles." Biochim Biophys Acta **645**(1): 63-70.

Travassos, L. R., I. C. Almeida and H. K. Takahashi (1994). "Carbohydrate epitopes: structure, presentation and the reactivity of biological ligands. Recognition of alpha-D-GalpNAc and alpha-D-Galp conformational structures." Ci Cult J Braz Ass Adv Sc **46**: 242-248.

Tribulatti, M. V., J. Mucci, N. Van Rooijen, M. S. Leguizamon and O. Campetella (2005). "The trans-sialidase from *Trypanosoma cruzi* induces thrombocytopenia during acute Chagas' disease by reducing the platelet sialic acid contents." Infect Immun **73**(1): 201-207.

Trocoli Torrecilhas, A. C., R. R. Tonelli, W. R. Pavanelli, J. S. da Silva, R. I. Schumacher, W. de Souza, E. S. NC, I. de Almeida Abrahamsohn, W. Colli and M. J. Manso Alves (2009).

"Trypanosoma cruzi: parasite shed vesicles increase heart parasitism and generate an intense inflammatory response." Microbes Infect **11**(1): 29-39.

Turturici, G., R. Tinnirello, G. Sconzo and F. Geraci (2014). "Extracellular membrane vesicles as a mechanism of cell-to-cell communication: advantages and disadvantages." Am J Physiol Cell Physiol **306**(7): C621-633.

Tyler, K. M. and D. M. Engman (2001). "The life cycle of Trypanosoma cruzi revisited." Int J Parasitol **31**(5-6): 472-481.

Umezawa, E. S., M. S. Nascimento, N. Kesper, Jr., J. R. Coura, J. Borges-Pereira, A. C. Junqueira and M. E. Camargo (1996). "Immunoblot assay using excreted-secreted antigens of Trypanosoma cruzi in serodiagnosis of congenital, acute, and chronic Chagas' disease." J Clin Microbiol **34**(9): 2143-2147.

van Niel, G., I. Porto-Carreiro, S. Simoes and G. Raposo (2006). "Exosomes: a common pathway for a specialized function." J Biochem **140**(1): 13-21.

Vespa, G. N., F. Q. Cunha and J. S. Silva (1994). "Nitric oxide is involved in control of Trypanosoma cruzi-induced parasitemia and directly kills the parasite in vitro." Infect Immun **62**(11): 5177-5182.

Villalta, F., J. Scharfstein, A. W. Ashton, K. M. Tyler, F. Guan, S. Mukherjee, M. F. Lima, S. Alvarez, L. M. Weiss, H. Huang, F. S. Machado and H. B. Tanowitz (2009). "Perspectives on the Trypanosoma cruzi-host cell receptor interactions." Parasitol Res **104**(6): 1251-1260.

Viotti, R., C. Vigliano, B. Lococo, G. Bertocchi, M. Petti, M. G. Alvarez, M. Postan and A. Armenti (2006). "Long-term cardiac outcomes of treating chronic Chagas disease with benznidazole versus no treatment: a nonrandomized trial." Ann Intern Med **144**(10): 724-734.

Vlassov, A. V., S. Magdaleno, R. Setterquist and R. Conrad (2012). "Exosomes: current knowledge of their composition, biological functions, and diagnostic and therapeutic potentials." Biochim Biophys Acta **1820**(7): 940-948.

Werbovetz, K. A. and P. T. Englund (1996). "Lipid metabolism in Trypanosoma brucei: utilization of myristate and myristoyllysophosphatidylcholine for myristoylation of glycosyl phosphatidylinositols." Biochem J **318** ( Pt 2): 575-581.

Wirth, J. J. and F. Kierszenbaum (1988). "Recombinant tumor necrosis factor enhances macrophage destruction of Trypanosoma cruzi in the presence of bacterial endotoxin." J Immunol **141**(1): 286-288.

Wood, C., E. A. Kabat, L. A. Murphy and I. J. Goldstein (1979). "Immunochemical studies of the combining sites of the two isolectins, A4 and B4, isolated from *Bandeiraea simplicifolia*." Arch Biochem Biophys **198**(1): 1-11.

Wubbolts, R., R. S. Leckie, P. T. Veenhuizen, G. Schwarzmann, W. Mobius, J. Hoernschemeyer, J. W. Slot, H. J. Geuze and W. Stoorvogel (2003). "Proteomic and biochemical analyses of human B cell-derived exosomes. Potential implications for their function and multivesicular body formation." J Biol Chem **278**(13): 10963-10972.

Wyllie, M. P. and M. I. Ramirez (2017). "Microvesicles released during the interaction between *Trypanosoma cruzi* TcI and TcII strains and host blood cells inhibit complement system and increase the infectivity of metacyclic forms of host cells in a strain-independent process." Pathog Dis **75**(7).

Yoshida, N., K. M. Tyler and M. S. Llewellyn (2011). "Invasion mechanisms among emerging food-borne protozoan parasites." Trends Parasitol **27**(10): 459-466.

Zingales, B. (2018). "Trypanosoma cruzi genetic diversity: Something new for something known about Chagas disease manifestations, serodiagnosis and drug sensitivity." Acta Trop **184**: 38-52.

Zingales, B., S. G. Andrade, M. R. Briones, D. A. Campbell, E. Chiari, O. Fernandes, F. Guhl, E. Lages-Silva, A. M. Macedo, C. R. Machado, M. A. Miles, A. J. Romanha, N. R. Sturm, M. Tibayrenc, A. G. Schijman and M. Second Satellite (2009). "A new consensus for *Trypanosoma cruzi* intraspecific nomenclature: second revision meeting recommends TcI to TcVI." Mem Inst Oswaldo Cruz **104**(7): 1051-1054.

Zingales, B., M. A. Miles, D. A. Campbell, M. Tibayrenc, A. M. Macedo, M. M. Teixeira, A. G. Schijman, M. S. Llewellyn, E. Lages-Silva, C. R. Machado, S. G. Andrade and N. R. Sturm (2012).

"The revised *Trypanosoma cruzi* subspecific nomenclature: rationale, epidemiological relevance and research applications." Infect Genet Evol **12**(2): 240-253.

## 7. LIST OF APPENDICES

**APPENDIX A: PROTEINS IDENTIFIED IN THE TCT-SECR FROM COL, Y, AND CLB STRAINS. VALUES ARE EXPRESSED AS AVERAGE OF NORMALIZED WEIGHTED SPECTRUM COUNTS.**

<b>Identified Protein</b>	<b>Accession Number</b>	<b>TCT-Secr Col</b>	<b>TCT-Secr Y</b>	<b>TCT-Secr CLB</b>
Calmodulin (Fragment) OS	A0A0M5M222	36	17	20
CALM protein (Fragment) OS	A0A0C5AX05	29	16	17
Group of Ubiquitin-60S ribosomal protein L40 OS	RL40	25	20	16
Group of Tubulin beta chain OS	Q4DQP2	25	19	13
Group of Heat shock protein 85, putative OS	Q4CQS6	22	27	23
Group of Major paraflagellar rod OS	B5U6T6	21	31	22
Microtubule-associated protein, putative (Fragment) OS	Q4CMT2	20	7	10
Microtubule-associated protein, putative (Fragment) OS	Q4D5A7	20	6	9
Uncharacterized protein OS	V5A2J1	15	0	0
Group of Arginine kinase OS	V5BUA6	14	12	13
Heat shock protein (HSP70) OS	Q26936	13	8	9
Tubulin beta chain OS	Q4DQP2	13	9	7
Tubulin beta chain OS	Q8STF3	13	9	7

Microtubule-associated protein homolog (Fragment) OS	Q9U9R2	13	3	4
Group of Elongation factor 2, putative OS	Q4D5X0	12	15	15
Ubiquitin-60S ribosomal protein L40 OS	RL40	12	10	8
splP0CH27 IRL402_TRYCR Ubiquitin-60S ribosomal protein L40 OS	splP0CH27 IRL402	12	10	8
Surface protein TolT, putative OS	Q4CPM8	12	4	6
Tubulin alpha chain OS	Q4CLA1	11	12	12
Heat shock protein 85, putative OS	Q4CQS6	11	14	11
Heat shock protein 85, putative OS	Q4DBM7	11	14	11
Paraflagellar rod protein 3 OS	V5BDW8	11	11	10
Tryparedoxin peroxidase, putative OS	Q4CM56	11	6	9
Chaperonin HSP60, mitochondrial OS	Q4DYP5	10	8	13
Major paraflagellar rod OS	B5U6T6	10	15	11
Major paraflagellar rod protein OS	Q01530	10	15	11
Paraflagellar rod protein 3, putative OS	Q4D634	10	11	10
Heat shock protein 70 OS	B5U6T4	10	10	10
Group of Uncharacterized protein OS	Q4DPV7	10	7	7
Glutamate dehydrogenase OS	O61083	10	3	6
Trichohyalin, putative OS	Q4CQV5	10	9	6
Glutamate dehydrogenase OS	K2N6Z1	10	3	5
Centrin, putative OS	Q4DQ49	10	4	4



Paraflagellar rod protein 3, putative OS	K2MCT5	9	10	10
Heat shock 70 kDa protein, mitochondrial, putative OS	Q4CVR9	9	8	9
Group of Phosphoglycerate kinase OS	Q4DNV8	9	8	7
Trans-sialidase, putative OS	Q4DVJ1	9	10	7
Uncharacterized protein OS	V5BQQ6	9	3	6
Glutamate dehydrogenase OS	Q4DWV8	9	3	5
Trypanothione reductase (Fragment) OS	Q95NP3	9	4	5
Peptidyl-prolyl cis-trans isomerase OS	Q4E4L9	9	10	5
Nascent polypeptide associated complex subunit OS	V5BDN6	9	1	2
Mucin-associated surface protein OS	V5D2E8	9	0	1
Mucin-like glycoprotein, putative OS	Q4DGK1	8	0	22
69 kDa paraflagellar rod protein, putative (Fragment) OS	Q4D0N7	8	8	8
	Q4D9H3	8	11	8
Nucleoside diphosphate kinase OS	Q4E256	8	9	7
Group of Chaperone DNAJ protein, putative OS	K2MHJ1	8	7	6
Mitochondrial RNA binding protein, putative OS	Q4DCA9	8	3	3
Mucin-associated surface protein (MASP) OS	V5CKL1	8	0	0
Mucin-associated surface protein (MASP) OS	V5B2G3	8	0	0
Pyruvate, phosphate dikinase OS	Q4E0Q0	7	8	6
Arginine kinase OS	V5BUA6	7	6	6

Arginine kinase, putative OS	Q4CWA5	7	6	6
Pyruvate, phosphate dikinase OS	Q9GN79	7	6	6
splP05456IHSP70_TRYCR Heat shock 70 kDa protein OS	splP05456IHSP70	7	4	5
Mucin TcMUCII, putative OS	Q4DGC1	7	7	5
Mucin TcMUCII, putative OS	Q4DU21	7	0	5
NAC alpha OS	Q8MUQ9	7	3	4
Putative malate dehydrogenase OS	O61084	7	4	4
Uncharacterized protein OS	Q4DCU5	7	3	4
Uncharacterized protein OS	Q4D2A8	7	5	2
Mucin-associated surface protein (MASP) OS	V5B2C2	7	0	0
Mucin-associated surface protein (MASP) OS	V5AJY1	7	0	0
Glycosomal phosphoenolpyruvate carboxykinase, putative OS	Q4D8V7	6	13	14
Mucin-associated surface protein (MASP), putative OS	Q4D843	6	7	13
Group of Elongation factor 1-alpha OS	Q4CXI1	6	7	9
TC3_70K14.4 OS	Q8T1A6	6	6	9
Group of Glucose-regulated protein 78, putative OS	Q4D620	6	9	9
Aconitate hydratase OS	Q4E5G5	6	11	8
Uncharacterized protein OS	Q4E246	6	5	7
Uncharacterized protein OS	V5BG00	6	4	7
Elongation factor 2, putative OS	Q4D5X0	6	7	7

Elongation factor 2, putative OS	Q4D3T1	6	7	7
Uncharacterized protein OS	Q4DGZ9	6	4	7
Uncharacterized protein OS	Q4DSZ8	6	9	7
Surface protein TolT, putative OS	Q4CNL2	6	7	6
Uncharacterized protein OS	Q4CPU3	6	7	6
Microtubule-associated protein Gb4, putative (Fragment) OS	Q4CKG3	6	6	6
Proteasome subunit alpha type OS	Q4D5X3	6	4	6
Heat shock protein, putative OS	Q4DI67	6	10	5
Calmodulin, putative OS	Q4E4S1	6	6	5
Mucin-associated surface protein (MASP), putative OS	Q4CUN0	6	0	5
Group of Phosphoglycerate kinase OS	V5BAG7	6	3	4
Elongation factor 1-gamma (EF-1-gamma), putative OS	Q4CXW2	6	6	4
Calpain cysteine peptidase, putative (Fragment) OS	Q4CPQ6	6	4	3
Nucleoside phosphorylase OS	V5BP86	6	6	3
Calreticulin OS	V5AMP1	6	3	3
Group of Proteasome subunit alpha type OS	Q4E4G8	6	4	3
Group of Tyrosine aminotransferase OS	Q4E4E7	6	0	2
Mucin-associated surface protein (MASP), putative OS	Q4D5C7	6	1	1
Mucin-associated surface protein (MASP) OS	V5D473	6	0	1
Surface protease GP63 OS	V5AX72	6	0	0

Mucin-associated surface protein (MASP) OS	V5CZH7	6	0	0
Mucin-associated surface protein (MASP), putative OS	Q4D845	5	4	12
Uncharacterized protein OS	K2NEG6	5	6	7
Trans-sialidase, putative OS	Q4E0D0	5	3	7
Eukaryotic translation initiation factor 5A OS	Q4E4N4	5	5	7
Group of Surface protein TolT OS	Q4CM38	5	5	5
Uncharacterized protein (Fragment) OS	K2NM62	5	4	5
Mucin TcMUCII, putative OS	Q4E1F7	5	0	5
Isocitrate dehydrogenase [NADP] OS	K2MRY2	5	2	4
Trans-sialidase OS	Q26964	5	4	4
Trans-sialidase, putative OS	Q4CTX4	5	1	4
Calpain-like cysteine peptidase, putative OS	Q4D066	5	7	4
Transaldolase OS	B6RE15	5	5	4
Mucin-associated surface protein (MASP), putative OS	Q4CVH5	5	0	4
Group of Mucin TcMUCII, putative OS	Q4CTN4	5	0	4
Phosphoglycerate kinase OS	Q4DNV8	5	4	3
Phosphoglycerate kinase OS	Q4D193	5	4	3
Trypanothione reductase OS	TYTR	5	3	3
Trypanothione reductase (Fragment) OS	Q963S4	5	3	3
Isocitrate dehydrogenase [NADP] OS	Q4E4L7	5	3	3

Uncharacterized protein OS	Q4DPV7	5	3	3
Uncharacterized protein OS	Q4DPV6	5	3	3
Glucose-regulated protein 78 OS	V5BZ53	5	3	3
Aldo-keto reductase OS	B3U4H3	5	3	3
Proteasome subunit alpha type OS	Q4D144	5	3	2
Mucin-associated surface protein (MASP) OS	V5B3C2	5	1	0
Mucin-associated surface protein (MASP) OS	V5CXB9	5	0	0
Trans-sialidase OS	V5AMH3	5	0	0
Mucin-associated surface protein (MASP), putative OS	Q4DNG3	5	2	0
Mucin-associated surface protein (MASP) OS	V5BF77	5	0	0
Mucin-associated surface protein (MASP) OS	V5BF73	5	0	0
Mucin-associated surface protein (MASP) OS	V5AQ41	5	0	0
Group of Elongation factor 1-alpha OS	Q4CRF6	4	11	8
Uncharacterized protein OS	Q4CSI2	4	4	8
C71 surface protein OS	Q6WAZ7	4	1	7
Mucin TcMUCII, putative OS	Q4DYF4	4	8	7
Mucin-associated surface protein (MASP), putative OS	Q4CS52	4	0	7
Mucin-associated surface protein (MASP), putative OS	Q4E210	4	0	7
Epsilon tubulin, putative OS	K2NGT6	4	5	6
2,3-bisphosphoglycerate-independent phosphoglycerate mutase, putative OS	Q4E122	4	3	6

Protein kinase A regulatory subunit OS	Q86RB0	4	4	5
2,3-bisphosphoglycerate-independent phosphoglycerate mutase, putative OS	K2N640	4	3	5
Uncharacterized protein (Fragment) OS	Q4DQS9	4	3	5
Glyceraldehyde-3-phosphate dehydrogenase OS	Q4DCN9	4	6	5
Proteasome subunit alpha type OS	Q4DAW0	4	3	5
Mucin TcMUCII, putative OS	Q4DXA0	4	0	5
Uncharacterized protein (Fragment) OS	Q4CY01	4	4	4
Aminopeptidase, putative OS	Q4DZJ3	4	3	4
Leucine aminopeptidase OS	A0A0M3YBC4	4	3	4
Trans-sialidase OS	Q26969	4	3	4
Mucin TcMUCII, putative OS	Q4D9S0	4	4	4
Group of 14-3-3 protein OS	V5B9L7	4	4	4
Mucin TcMUCII, putative OS	Q4E2C3	4	3	4
Flagellar calcium-binding protein, putative OS	Q4CS05	4	5	3
Flagellar calcium binding protein 3 OS	Q8MXD4	4	3	3
Carboxypeptidase OS	V5DQA0	4	2	3
3-ketoacyl-CoA thiolase, putative OS	Q4D7M6	4	5	3
Uncharacterized protein OS	Q4DX68	4	2	3
Uncharacterized protein OS	V5BHT5	4	4	3
Group of 14-3-3 protein OS	V5C116	4	4	3

RNA-binding protein, putative OS	K2MLT2	4	4	3
Mucin-associated surface protein (MASP), putative OS	Q4D521	4	0	3
Calpain cysteine peptidase, putative (Fragment) OS	Q4CS87	4	3	2
Uncharacterized protein (Fragment) OS	Q4CL51	4	2	2
Aspartate aminotransferase OS	V5BVY2	4	2	2
Aspartate aminotransferase, mitochondrial, putative OS	Q4D1Q4	4	2	2
Tryparedoxin, putative OS	Q4D1B8	4	3	2
ATP synthase subunit beta OS	Q4DTX7	4	3	2
Mucin-associated surface protein (MASP), putative OS	Q4E3E0	4	0	2
Trans-sialidase OS	V5B004	4	0	1
Mucin-associated surface protein (MASP), putative OS	Q4DYV4	4	2	1
Group of Malic enzyme OS	Q4DJ68	4	1	1
Mucin-associated surface protein (MASP) OS	V5AQA9	4	0	1
Mucin-associated surface protein (MASP) OS	V5AUI4	4	0	0
Trans-sialidase OS	V5B3S7	4	0	0
Mucin-associated surface protein (MASP) OS	V5CSE2	4	0	0
Mucin-associated surface protein (MASP) OS	V5AI98	4	0	0
Mucin-associated surface protein (MASP) OS	V5AQ54	4	0	0
Mucin TcMUCII OS	V5AM23	4	0	0
Mucin-associated surface protein (MASP) OS	V5D4V1	4	0	0

Mucin-associated surface protein (MASP) OS	V5B2F0	4	0	0
Mucin-associated surface protein (MASP) OS	V5D8B9	4	0	0
Mucin-associated surface protein (MASP) OS	V5AKT8	4	0	0
Mucin-associated surface protein (MASP), putative OS	Q4E525	3	0	11
Group of Enolase OS	V5BRU1	3	10	10
Uncharacterized protein OS	Q4CYL3	3	13	9
Uncharacterized protein OS	Q4D770	3	11	7
Uncharacterized protein OS	Q4CVX7	3	5	6
Group of Surface protein TolT OS	Q4D0C7	3	1	6
Trans-sialidase, putative OS	Q4DCY7	3	5	5
Protein kinase A regulatory subunit, putative OS	Q4DSV5	3	4	5
Aminopeptidase OS	V5D7P4	3	2	5
Uncharacterized protein OS	Q4CVJ1	3	8	5
Mucin TcMUCII, putative OS	Q4DDU7	3	2	5
Glucose-regulated protein 78, putative OS	Q4D620	3	5	4
Heat shock protein 70 OS	Q56UI2	3	5	4
Trans-sialidase, putative OS	Q4DLR5	3	4	4
Surface protease GP63, putative OS	Q4DHC2	3	0	4
Group of 90 kDa surface protein, putative OS	Q4DJL3	3	3	4
Group of NUP-1 OS	C8CHD2	3	2	4



Cystathione gamma lyase OS	V5DUQ5	3	0	4
Mucin TcMUCII, putative OS	Q4DB53	3	0	4
Uncharacterized protein (Fragment) OS	Q4D4S4	3	2	3
Heat shock 70 kDa protein, putative (Fragment) OS	Q4DAZ6	3	5	3
Cell division cycle protein OS	V5B4G8	3	3	3
Glucose-6-phosphate isomerase OS	Q4E2M9	3	2	3
Uncharacterized protein (Fragment) OS	Q4CL46	3	5	3
Uncharacterized protein OS	Q4E2Q5	3	5	3
Group of Universal minicircle sequence binding protein (UMSBP) OS	V5BU64	3	1	3
Mucin TcMUCII, putative OS	Q4E056	3	1	3
Actin OS	I6LE98	3	4	3
Group of Proteasome subunit alpha type OS	Q4DAW6	3	3	3
Group of Mitochondrial peroxidase (Fragment) OS	A0A088CGF4	3	3	3
Mucin TcMUCII, putative OS	Q4DXM6	3	0	3
Prostaglandin F2alpha synthase OS	V5BT91	3	0	3
Phosphoglycerate kinase OS	V5BAG7	3	2	2
Phosphoglycerate kinase OS	Q95PK9	3	2	2
Chaperone DNAJ protein, putative OS	K2MHJ1	3	2	2
Heat shock protein DNAJ OS	V5BFK5	3	2	2
Heat shock protein DnaJ, putative OS	Q4D832	3	2	2

Uncharacterized protein OS	V5B3K7	3	2	2
Proteasome subunit alpha type OS	Q4E4G8	3	2	2
Proteasome subunit alpha type OS	Q4DWX8	3	2	2
Mucin TcMUCII, putative OS	Q4DTB4	3	4	2
Uncharacterized protein OS	V5BBR9	3	1	2
Dihydrolipoyl dehydrogenase OS	Q4DD33	3	2	2
Mucin TcMUCII, putative OS	Q4CVM7	3	0	2
Calmodulin, putative OS	Q4CWP2	3	2	2
Group of 40S ribosomal protein S6 OS	Q4DU31	3	2	2
Group of 10 kDa heat shock protein, putative OS	Q4DFB0	3	1	2
Superoxide dismutase OS	O02615	3	1	2
Trans-sialidase, putative (Fragment) OS	Q4CKI9	3	6	1
Mucin-associated surface protein (MASP) OS	V5BBK7	3	0	1
Dynein OS	V5B145	3	1	1
Mucin-associated surface protein (MASP), putative OS	Q4DYF3	3	5	1
Glucose-6-phosphate isomerase (Fragment) OS	Q6RZZ4	3	1	1
Tyrosine aminotransferase OS	Q4E4E7	3	0	1
Tyrosine aminotransferase OS	ATTY	3	0	1
Heat shock protein OS	V5DQB4	3	1	1
Glutamamyl carboxypeptidase, putative OS	Q4CR09	3	1	1

Group of Protein kinase A catalytic subunit isoform 1, putative OS	Q4E4S9	3	2	1
Group of Histone H3, putative OS	Q4D0J9	3	1	1
Phosphomannomutase OS	Q4E4A3	3	1	1
Mucin-associated surface protein (MASP), putative OS	Q4DQS0	3	0	1
Mucin-associated surface protein (MASP) OS	V5B8G1	3	2	0
Guanine deaminase OS	V5BLN7	3	0	0
Sialidase OS	TCNA	3	0	0
Mucin-associated surface protein (MASP) OS	V5D3M1	3	0	0
Mucin-associated surface protein (MASP) OS	V5APJ7	3	0	0
Trans-sialidase OS	V5AMT0	3	0	0
Mucin-associated surface protein (MASP) OS	V5APN1	3	0	0
Trans-sialidase, putative OS	Q4DR26	3	1	0
Mucin-associated surface protein (MASP) OS	V5AIX0	3	0	0
Mucin-associated surface protein (MASP) OS	V5B7M6	3	0	0
Mucin-associated surface protein (MASP), putative OS	Q4E008	3	0	0
D-isomer specific 2-hydroxyacid dehydrogenase-protein, putative OS	Q4CU50	3	1	0
Mucin TcMUCII OS	V5AMJ3	3	0	0
Mucin-associated surface protein (MASP) OS	V5B862	3	0	0
Mucin-associated surface protein (MASP) OS	V5BF63	3	0	0
Mucin-associated surface protein (MASP) OS	V5BCA7	3	0	0

Mucin-associated surface protein (MASP) OS	V5CVV0	3	0	0
Mucin-associated surface protein (MASP) OS	V5A5A7	3	0	0
Mucin-associated surface protein (MASP) OS	V5D3A6	3	0	0
Mucin-associated surface protein (MASP) OS	V5AS95	3	0	0
Mucin-like glycoprotein OS	Q26885	3	0	0
Mucin-like glycoprotein, putative OS	Q4DVZ2	2	2	8
Isocitrate dehydrogenase [NADP] OS	Q4DG65	2	3	6
Mucin-associated surface protein (MASP), putative OS	Q4DDU8	2	2	6
Trans-sialidase, putative OS	Q4CXW0	2	4	5
Adenylosuccinate synthetase OS	K2NJB0	2	3	5
Mucin TcMUCII, putative OS	Q4D8A2	2	6	5
Mucin-associated surface protein (MASP), putative OS	Q4DZB7	2	4	5
Group of Mucin TcMUCII, putative OS	Q4DH11	2	0	5
Cytoskeleton-associated protein CAP5.5, putative (Fragment) OS	Q4CP00	2	6	4
Transitional endoplasmic reticulum ATPase, putative OS	Q4DWB5	2	3	4
Heat shock 70 kDa protein, mitochondrial, putative (Fragment) OS	Q4DXG9	2	4	4
Carboxypeptidase, putative OS	Q4E2R7	2	2	4
Antigenic protein, putative (Fragment) OS	Q4E572	2	6	4
Mucin TcMUCII, putative OS	Q4D5F4	2	4	4
Mucin TcMUCII, putative OS	Q4DDU9	2	1	4

Mucin TcMUCII, putative OS	Q4CWZ6	2	2	4
Surface protease GP63, putative OS	Q4CN42	2	1	4
Elongation factor 1-alpha OS	Q4CXI1	2	2	3
Elongation factor 1-alpha OS	H9AZH6	2	2	3
Elongation factor 1-alpha OS	K2M6L0	2	2	3
Proteasome subunit alpha type OS	Q4DIK4	2	5	3
Mucin-associated surface protein (MASP), putative OS	Q4CX27	2	4	3
p22 protein, putative OS	Q4E0T1	2	3	3
Proteasome activator protein PA26, putative OS	Q4CPR5	2	2	3
p22 protein, putative OS	Q4DG13	2	1	3
Group of Phosphotransferase OS	V5BQ43	2	3	3
Kinetoplastid membrane protein KMP-11, putative OS	Q4D7Y4	2	5	3
Proteasome subunit beta type OS	Q4E4R6	2	4	3
Group of ATP-dependent Clp protease subunit OS	V5AQ73	2	1	3
ATPase alpha subunit OS	V5AVB0	2	2	3
Surface protein TolT OS	Q4CM38	2	2	2
TolT1 OS	O97466	2	2	2
TolT3 OS	O96649	2	2	2
Mucin-associated surface protein (MASP), putative OS	Q4E1H4	2	5	2
Trans-sialidase, putative OS	Q4DQA2	2	5	2

Trans-sialidase, putative OS	Q4CRR3	2	8	2
Uncharacterized protein OS	Q4D3F7	2	3	2
Mucin-associated surface protein (MASP), putative OS	Q4E493	2	4	2
Glucose-6-phosphate isomerase OS	Q4E5N1	2	2	2
Proteasome activator protein PA26, putative (Fragment) OS	Q4D086	2	2	2
Mucin-associated surface protein (MASP), putative (Fragment) OS	Q4CNN7	2	8	2
Uncharacterized protein OS	Q4DA87	2	3	2
14-3-3 protein OS	V5B9L7	2	2	2
14-3-3 protein OS	Q6B9P3	2	2	2
Calpain-like cysteine peptidase OS	V5B5I4	2	3	2
Mucin-associated surface protein (MASP), putative OS	Q4D951	2	4	2
Universal minicircle sequence binding protein (UMSBP) OS	V5BU64	2	1	2
Universal minicircle sequence binding protein (UMSBP), putative OS	Q4D6T8	2	1	2
Succinate-CoA ligase subunit beta OS	Q4DW49	2	3	2
Dynein, putative OS	Q4DWH2	2	1	2
Proteasome subunit alpha type OS	Q4DAW6	2	1	2
Proteasome subunit alpha type OS	K2MUS2	2	1	2
Trans-sialidase, putative OS	Q4CTQ6	2	0	2
Mucin-associated surface protein (MASP), putative OS	Q4CQS4	2	4	2
85 kDa surface antigen OS	GP85	2	3	2

Mucin-associated surface protein (MASP), putative OS	Q4DVK4	2	0	2
Mucin TcMUCII, putative OS	Q4CTN4	2	0	2
Mucin TcMUCII, putative OS	Q4D8A9	2	0	2
Mucin-associated surface protein (MASP), putative OS	Q4CQD2	2	1	2
Group of ADP-ribosylation factor 1, putative OS	Q4D7Y8	2	2	2
Peptide methionine sulfoxide reductase, putative OS	Q4CSX7	2	3	2
Group of (H)-ATPase G subunit OS	V5B9V5	2	3	2
Aminopeptidase, putative OS	Q4E2R9	2	2	2
Protein mkt1 OS	V5BX20	2	2	2
Isoleucyl-tRNA synthetase OS	V5BJ49	2	1	2
Mucin TcMUCII, putative OS	Q4E1J5	2	1	2
Mucin TcMUCII, putative OS	Q4CUT4	2	1	2
Trans-sialidase, putative OS	Q4CXS5	2	3	1
Calpain-like cysteine peptidase, putative (Fragment) OS	Q4CLF8	2	2	1
Mucin-associated surface protein (MASP), putative OS	Q4CR59	2	4	1
Mucin TcMUCII, putative OS	Q4DYF2	2	2	1
Mucin TcMUCII, putative OS	Q4D8R7	2	2	1
Mucin-associated surface protein (MASP), putative OS	Q4DR50	2	1	1
Group of IgE-dependent histamine-releasing factor, putative OS	Q4CW52	2	3	1
Mucin-associated surface protein (MASP) OS	V5BBT4	2	1	1

Malic enzyme OS	Q4DJ68	2	0	1
Malic enzyme OS	V5DSI1	2	0	1
Mucin-associated surface protein (MASP), putative OS	Q4DP78	2	2	1
Trans-sialidase OS	V5BKP3	2	0	1
ATP-dependent RNA helicase, putative OS	Q4DRK9	2	2	1
Kinesin OS	V5BN65	2	1	1
Trans-sialidase, putative OS	Q4DPT3	2	1	1
Group of Hslvu complex proteolytic subunit-like, putative OS	Q4D729	2	1	1
40S ribosomal protein S14, putative OS	Q4D6I5	2	1	1
Histone H4 OS	V5BAE8	2	1	1
Group of Mucin TcMUCII OS	V5AYQ9	2	1	1
Mucin-associated surface protein (MASP) OS	V5AJ84	2	0	1
Trans-sialidase, putative OS	Q4CSI1	2	5	0
Mucin-associated surface protein (MASP), putative OS	Q4DDR2	2	2	0
Mucin-associated surface protein (MASP) OS	V5APP8	2	0	0
Mucin-associated surface protein (MASP) OS	V5AL36	2	0	0
Fumarate hydratase OS	V5BGH8	2	1	0
Mucin-associated surface protein (MASP) OS	V5AP32	2	0	0
Trans-sialidase OS	V5B172	2	0	0
Mucin-associated surface protein (MASP) OS	V5B7H5	2	0	0



Mucin-associated surface protein (MASP) OS	V5AV75	2	0	0
ATP-dependent (S)-NAD(P)H-hydrate dehydratase OS	V5BG46	2	1	0
Mucin-associated surface protein (MASP) OS	V5B8L3	2	0	0
Mucin-associated surface protein (MASP) OS	V5B8P4	2	0	0
Mucin-associated surface protein (MASP) OS	V5DEC3	2	0	0
Trans-sialidase OS	V5AMI8	2	0	0
Mucin-associated surface protein (MASP) OS	V5AZG4	2	0	0
Mucin-associated surface protein (MASP), putative OS	Q4CWA9	1	9	7
Trans-sialidase, putative OS	Q4CX14	1	3	6
Uncharacterized protein OS	Q4CTC8	1	7	5
Enolase OS	V5BRU1	1	5	5
Enolase, putative OS	Q4DZ98	1	5	5
Mitotubule-associated protein Gb4, putative (Fragment) OS	Q4CYL2	1	4	5
Trans-sialidase, putative OS	Q4E1E4	1	1	5
Guanine deaminase, putative OS	Q4D711	1	4	5
Proteasome subunit alpha type OS	Q4CYK5	1	5	5
Mucin TcMUCII, putative OS	Q4E032	1	4	5
Mucin TcMUCII, putative OS	Q4DYU8	1	2	5
Surface protease GP63, putative OS	Q4CMP1	1	3	5
Group of Mucin-associated surface protein (MASP), putative (Fragment) OS	Q4DUN7	1	0	5

Cytoskeleton-associated protein CAP5.5, putative OS	Q4D609	1	5	4
Mitotubule-associated protein Gb4, putative (Fragment) OS	Q4CTC7	1	4	4
Uncharacterized protein OS	Q4E573	1	5	4
Uncharacterized protein OS	Q4DMP7	1	5	4
Mucin TcMUCII, putative OS	Q4D8A4	1	2	4
Trans-sialidase, putative OS	Q4DTW9	1	1	4
Group of Mucin TcMUCII, putative OS	Q4DMA9	1	4	4
NADH-dependent fumarate reductase, putative OS	Q4D779	1	1	4
Mucin TcMUCII, putative OS	Q4DDU6	1	1	4
Mucin-associated surface protein (MASP), putative OS	Q4DLB2	1	0	4
Mucin TcMUCII, putative OS	Q4E3E1	1	0	4
Mucin-associated surface protein (MASP), putative OS	Q4DEC9	1	0	4
Mucin-associated surface protein (MASP), putative OS	Q4DAA7	1	0	4
Mucin TcMUCII, putative OS	Q4DXZ7	1	1	4
Mucin TcMUCII, putative OS	Q4E4X7	1	0	4
Mucin-associated surface protein (MASP), putative OS	Q4D1R7	1	0	4
Elongation factor 1-alpha OS	Q4CRF6	1	4	3
Elongation factor 1-alpha OS	H9AZH5	1	4	3
Elongation factor 1-alpha OS	B5U6U3	1	4	3
Trans-sialidase, putative OS	Q4DU07	1	2	3

Uncharacterized protein OS	V5DIG4	1	5	3
Uncharacterized protein OS	Q4DJ92	1	2	3
Calreticulin, putative OS	Q4DDX3	1	3	3
Mucin-associated surface protein (MASP), putative OS	Q4D6E3	1	6	3
Surface protein TolT OS	Q4D0C7	1	0	3
Surface protein TolT OS	Q4D0C6	1	0	3
I/6 autoantigen, putative OS	Q4DFL2	1	5	3
I/6 autoantigen, putative OS	Q4DQ44	1	2	3
DNA topoisomerase II, putative OS	K2MSC2	1	2	3
Calpain-like cysteine peptidase, putative (Fragment) OS	Q4CL00	1	2	3
Trans-sialidase, putative (Fragment) OS	Q4CR60	1	1	3
Trans-sialidase, putative OS	Q4E2C0	1	1	3
Mucin TcMUCII, putative OS	Q4E071	1	3	3
Aminopeptidase, putative (Fragment) OS	Q4DLT0	1	1	3
Mucin-associated surface protein (MASP), putative OS	Q4CPX9	1	0	3
Fructose-bisphosphate aldolase OS	Q4D0Q0	1	3	3
Mucin TcMUCII, putative OS	Q4CZ01	1	1	3
Polyadenylate-binding protein OS	K2N1D5	1	4	3
Trans-sialidase, putative OS	Q4D5F2	1	1	3
Mucin TcMUCII, putative OS	Q4DHM9	1	1	3

Mucin-associated surface protein (MASP), putative OS	Q4DQA3	1	3	3
Malate dehydrogenase (Fragment) OS	Q4D4A0	1	3	3
Surface protease GP63, putative OS	Q4DZ07	1	0	3
Mucin TcMUCII, putative OS	Q4E1Z2	1	2	3
Mucin TcMUCII, putative OS	Q4E2A8	1	3	3
Chaperonin containing T-complex protein, putative OS	Q4DWG6	1	2	3
Mucin TcMUCII, putative OS	Q4DN80	1	0	3
Mucin TcMUCII, putative OS	Q4DF67	1	1	3
6-phosphogluconate dehydrogenase, decarboxylating OS	Q6WAT4	1	2	3
Mucin TcMUCII, putative OS	Q4E2A5	1	2	3
Ribose 5-phosphate isomerase, putative OS	Q4DBP9	1	2	3
Mucin TcMUCII, putative OS	Q4D373	1	2	3
Mucin TcMUCII, putative OS	Q4D389	1	0	3
Ascorbate-dependent peroxidase, putative OS	Q4CRX7	1	1	3
Mucin-associated surface protein (MASP), putative OS	Q4DQW7	1	0	3
Mucin TcMUCII, putative OS	Q4CS53	1	0	3
Mucin TcMUCII, putative OS	Q4D1J6	1	0	3
Mucin-associated surface protein (MASP), putative OS	Q4D3A3	1	0	3
Mucin TcMUCII, putative OS	Q4D7L0	1	0	3
Mucin-associated surface protein (MASP), putative OS	Q4DJS2	1	0	3

Mucin TcMUCII, putative OS	Q4E3D5	1	0	3
Mucin-associated surface protein (MASP), putative OS	Q4DU26	1	0	3
Mucin TcMUCII, putative OS	Q4DZC5	1	0	3
Mucin-associated surface protein (MASP), putative OS	Q4CVN8	1	3	2
Uncharacterized protein OS	Q4DVF9	1	3	2
Cytoskeleton-associated protein CAP5.5 OS	V5DES7	1	3	2
Dynein heavy chain, putative (Fragment) OS	Q4CX46	1	4	2
Uncharacterized protein OS	Q4DVF8	1	2	2
Mucin-associated surface protein (MASP), putative OS	Q4DNB5	1	7	2
Trans-sialidase, putative OS	Q4DV16	1	2	2
Trans-sialidase, putative OS	Q4E063	1	1	2
Phosphotransferase OS	Q4D3P5	1	2	2
Dynein heavy chain OS	V5AWC6	1	4	2
90 kDa surface protein, putative OS	Q4DJL3	1	1	2
90 kDa surface protein, putative OS	Q4DHM3	1	1	2
Stress-induced protein sti1, putative OS	K2NE30	1	3	2
Trans-sialidase, putative OS	Q4DDR3	1	1	2
NUP-1 OS	C8CHD2	1	1	2
NUP-1 OS	Q6QR20	1	1	2
Trans-sialidase, putative OS	Q4CQP5	1	0	2

Aspartate aminotransferase OS	Q4CRK6	1	1	2
Mucin TcMUCII, putative OS	Q4DH11	1	0	2
Mucin TcMUCII, putative OS	Q4D8R3	1	0	2
Mucin TcMUCII, putative OS	Q4D8R2	1	0	2
40 kDa cyclophilin, putative OS	Q4CVB5	1	2	2
Mucin-associated surface protein (MASP), putative OS	Q4DN82	1	0	2
Mucin TcMUCII, putative OS	Q4DU44	1	3	2
Mucin-associated surface protein (MASP), putative OS	Q4CQC5	1	3	2
Group of Mucin TcMUCII, putative OS	Q4DYF7	1	3	2
Mucin-associated surface protein (MASP), putative OS	Q4E1A8	1	0	2
Mucin-associated surface protein (MASP), putative OS	Q4D463	1	1	2
Adenosine 5'-monophosphoramidase, putative OS	Q4DUX5	1	3	2
T-complex protein 1, eta subunit, putative OS	Q4E4R8	1	3	2
Group of Proteasome subunit beta type OS	Q4DW25	1	3	2
Mucin TcMUCII, putative OS	Q4DN81	1	0	2
Guanine deaminase, putative OS	Q4DUS4	1	0	2
Group of Proteasome regulatory non-ATPase subunit 3 OS	V5B0Y8	1	2	2
Group of Dynein light chain, putative OS	Q4DN14	1	2	2
Trans-sialidase, putative OS	Q4DU42	1	1	2
Mucin TcMUCII, putative OS	Q4DHM6	1	2	2

Mucin TcMUCII, putative OS	Q4DIF2	1	1	2
60S ribosomal protein L13, putative OS	K2MPX7	1	2	2
Mucin-associated surface protein (MASP), putative (Fragment) OS	Q4D4A9	1	2	2
Mucin-associated surface protein (MASP), putative OS	Q4DXN7	1	0	2
Mucin TcMUCII, putative OS	Q4D8D5	1	2	2
Mucin TcMUCII, putative OS	Q4DU09	1	2	2
Ubiquitin-like protein, putative OS	Q4CWR4	1	2	2
60S ribosomal protein L10, putative OS	K2MT82	1	1	2
Trans-sialidase, putative OS	Q4D6F8	1	0	2
Mucin-associated surface protein (MASP), putative OS	Q4E1H3	1	0	2
Mucin-associated surface protein (MASP), putative OS	Q4DGC4	1	1	2
Mucin TcMUCII, putative OS	Q4E1I8	1	1	2
Mucin TcMUCII, putative OS	Q4DFV4	1	0	2
Mucin-associated surface protein (MASP), putative OS	Q4D0E9	1	0	2
Group of 40S ribosomal protein SA OS	Q4CQ63	1	1	2
Group of Mucin TcMUCII, putative OS	Q4E206	1	0	2
Group of Purine nucleoside phosphorylase OS	Q4DZW1	1	0	2
Mucin TcMUCII, putative (Fragment) OS	Q4D384	1	0	2
Group of Thiol transferase Tc52 (Fragment) OS	Q7Z0C1	1	0	2
Mucin-associated surface protein (MASP), putative OS	Q4DYF1	1	1	2

Trans-sialidase, putative OS	Q4E026	1	0	2
Group of Putative surface antigen TASV-C1 OS	A5PGV8	1	0	2
Mucin TcMUCII, putative OS	Q4DFV7	1	0	2
Mucin TcMUCII, putative OS	Q4DXZ9	1	0	2
Mucin-associated surface protein (MASP), putative OS	Q4E4Z1	1	0	2
Group of Mucin TcMUCII, putative OS	Q4CVN9	1	0	2
Mucin TcMUCII, putative OS	Q4E5K8	1	0	2
85 kDa surface glycoprotein (Fragment) OS	A0PGC0	1	3	1
Mucin-associated surface protein (MASP), putative OS	Q4E1H5	1	5	1
Mucin-associated surface protein (MASP), putative OS	Q4DZC3	1	3	1
Mucin-associated surface protein (MASP), putative (Fragment) OS	Q4CYQ5	1	2	1
Mucin-associated surface protein (MASP), putative OS	Q4DYV1	1	6	1
Mucin-associated surface protein (MASP), putative OS	Q4E065	1	4	1
Trans-sialidase, putative OS	Q4DQW0	1	2	1
Trans-sialidase, putative OS	Q4CSG5	1	1	1
14-3-3 protein OS	V5C116	1	1	1
14-3-3 protein, putative OS	Q4DRH6	1	1	1
14-3-3 protein, putative OS	Q4DHC9	1	1	1
14-3-3 protein, putative OS	K2NW21	1	1	1
NADH-dependent fumarate reductase, putative OS	Q4CMU8	1	6	1



Mucin-associated surface protein (MASP), putative OS	Q4E1I3	1	8	1
Phosphotransferase OS	V5BQ43	1	1	1
Phosphotransferase OS	Q8ST54	1	1	1
85 kDa surface glycoprotein (Fragment) OS	A0PGC5	1	2	1
Mitochondrial peroxidase (Fragment) OS	A0A088CGF4	1	1	1
Mitochondrial peroxidase (Fragment) OS	A0A088CH35	1	1	1
Mitochondrial peroxidase (Fragment) OS	A0A088CH36	1	1	1
Mucin-associated surface protein (MASP), putative OS	Q4D4U4	1	6	1
Dynein heavy chain, putative OS	K2NDD4	1	3	1
Mucin-associated surface protein (MASP), putative OS	Q4D7K6	1	7	1
Mucin-associated surface protein (MASP), putative OS	Q4CQ23	1	1	1
Mucin-associated surface protein (MASP), putative OS	Q4DGM5	1	5	1
Trans-sialidase, putative OS	Q4DDV0	1	1	1
ATP-dependent Clp protease subunit OS	V5AQ73	1	1	1
ATP-dependent Clp protease subunit, heat shock protein 78, putative OS	Q4DTH5	1	1	1
ADP-ribosylation factor 1, putative OS	Q4D7Y8	1	1	1
ADP-ribosylation factor 1, putative OS	Q4CQM4	1	1	1
Threonyl-tRNA synthetase, putative OS	Q4DPR0	1	3	1
Mucin TcMUCII, putative OS	Q4DYF7	1	2	1
Mucin TcMUCII, putative OS	Q4DYF0	1	2	1

Trans-sialidase, putative OS	Q4CQY9	1	1	1
40S ribosomal protein S6 OS	Q4DU31	1	1	1
40S ribosomal protein S6 OS	Q4DSU0	1	1	1
10 kDa heat shock protein, putative OS	Q4DFB0	1	0	1
10 kDa heat shock protein, putative OS	Q4DFA8	1	0	1
10 kDa heat shock protein, putative OS	Q4D000	1	0	1
Mucin TcMUCII, putative OS	Q4DNP5	1	5	1
(H <sup>-</sup> )-ATPase G subunit OS	V5B9V5	1	1	1
(H <sup>+</sup> )-ATPase G subunit, putative OS	Q4DE73	1	1	1
(H <sup>+</sup> )-ATPase G subunit, putative OS	Q4CNF9	1	1	1
Aspartate aminotransferase OS	Q4D080	1	2	1
Chaperonin alpha subunit OS	V5B5Q0	1	1	1
Chaperonin alpha subunit, putative OS	Q4D0F4	1	1	1
Pyruvate kinase OS	Q4E1U3	1	1	1
Protein kinase A catalytic subunit isoform 1, putative OS	Q4E4S9	1	1	1
Protein kinase-A catalytic subunit OS	Q8WQR2	1	1	1
Aspartate aminotransferase OS	V5BSS0	1	1	1
Pyruvate kinase OS	V5C1M1	1	1	1
Dynein light chain, putative OS	Q4DN14	1	1	1
Dynein light chain, putative OS	Q4CZW3	1	1	1

Trans-sialidase, putative OS	Q4CSV1	1	1	1
Mucin-associated surface protein (MASP), putative OS	Q4CSJ9	1	2	1
Mucin-associated surface protein (MASP), putative OS	Q4DU19	1	2	1
Group of Chaperone DNAJ protein OS	V5B5S8	1	2	1
RNA helicase, putative OS	Q4D0U9	1	2	1
Hslvu complex proteolytic subunit-like, putative OS	Q4D729	1	1	1
Hslvu complex proteolytic subunit-like, putative OS	K2NJP3	1	1	1
Group of Centrin OS	V5DQ66	1	2	1
Centrin OS	V5DQ66	1	1	1
Centrin, putative OS	Q4E3T4	1	1	1
Mucin TcMUCII, putative OS	Q4DNB2	1	1	1
Trans-sialidase, putative OS	Q4D980	1	1	1
Mucin-associated surface protein (MASP), putative OS	Q4DRZ5	1	0	1
Group of splQ4D3B7IDRE21_TRYCC Anamorsin homolog 1 OS	splQ4D3B7IDRE21	1	2	1
33 kDa inner dynein arm light chain, axonemal, putative OS	K2NJ58	1	2	1
Mucin TcMUCII, putative OS	Q4DE08	1	2	1
RuvB-like helicase OS	Q4DPV3	1	1	1
Mucin-associated surface protein (MASP), putative OS	Q4DVE3	1	0	1
Mucin-associated surface protein (MASP), putative OS	Q4DBE1	1	2	1
Glutamamyl carboxypeptidase, putative OS	Q4CYZ6	1	0	1

Mucin-associated surface protein (MASP), putative OS	Q4DYU1	1	0	1
Mucin TcMUCII, putative OS	Q4E3V9	1	0	1
ATP-dependent DEAD/H RNA helicase, putative OS	Q4DIE1	1	1	1
Group of Serine/threonine protein phosphatase type 5, putative OS	Q4E1W0	1	2	1
GTP-binding nuclear protein OS	Q4DIB9	1	2	1
Mucin-associated surface protein (MASP), putative OS	Q4D6Q0	1	0	1
Peptide methionine sulfoxide reductase, putative OS	Q4DK88	1	1	1
Purine nucleoside phosphorylase OS	Q4DZW1	1	0	1
Purine nucleoside phosphorylase OS	Q7YWE5	1	0	1
Group of Histone H2B OS	Q4CTD8	1	0	1
Histone H2B OS	Q4CTD8	1	0	1
Histone H2B OS	Q4CTD7	1	0	1
Group of Short chain 3-hydroxyacyl-CoA dehydrogenase OS	V5BPS0	1	1	1
40S ribosomal protein S18, putative OS	Q4E093	1	2	1
Mucin TcMUCII, putative OS	Q4E052	1	1	1
RuvB-like helicase OS	V5B579	1	0	1
Malic enzyme OS	Q4DV37	1	0	1
ATPase ASNA1 homolog OS	ASNA	1	1	1
Fibrillarin, putative OS	Q4DYJ3	1	1	1
Group of 60S acidic ribosomal protein P0 OS	Q4E3A3	1	2	1

Mucin-associated surface protein (MASP), putative OS	Q4CUB9	1	0	1
Methionine aminopeptidase 2 OS	Q4DGA5	1	1	1
Mucin TcMUCII, putative OS	Q4E3V3	1	0	1
ATP-dependent (S)-NAD(P)H-hydrate dehydratase OS	Q4DA84	1	1	1
Putative I/6 autoantigen OS	V5D4J9	1	1	1
Elongation factor TU, putative OS	Q4DY24	1	2	1
Retrotransposon hot spot (RHS) protein OS	V5AK41	1	1	1
Mucin TcMUCII, putative OS	Q4E100	1	0	1
Small GTP-binding protein Rab1, putative OS	Q4CZR0	1	1	1
Group of Ribonucleoside-diphosphate reductase small chain OS	V5ASN2	1	0	1
Trans-sialidase OS	V5A2Q8	1	1	1
Kinesin-like protein OS	Q4DYM0	1	1	1
Mucin TcMUCII, putative OS	Q4DR59	1	0	1
Mucin-associated surface protein (MASP), putative OS	Q4DGD0	1	2	0
Trans-sialidase OS	V5AR40	1	1	0
Trans-sialidase, putative OS	Q4DTD3	1	2	0
Mucin-associated surface protein (MASP), putative OS	Q4D2L0	1	0	0
IgE-dependent histamine-releasing factor, putative OS	Q4CW52	1	1	0
IgE-dependent histamine-releasing factor, putative OS	Q4CWM1	1	1	0
Translationally controlled tumor protein (TCTP) OS	V5DBM6	1	1	0

Mucin-associated surface protein (MASP), putative OS	Q4DYE9	1	3	0
Mucin-associated surface protein (MASP) OS	V5B9D2	1	0	0
Mucin-associated surface protein (MASP) OS	V5B467	1	0	0
Mucin-associated surface protein (MASP), putative OS	Q4E1I2	1	4	0
Mucin-associated surface protein (MASP), putative OS	Q4E375	1	2	0
Histone H3, putative OS	Q4D0J9	1	0	0
Histone H3, putative OS	Q4CWE9	1	0	0
Histone H3, putative OS	Q4CZH3	1	0	0
splQ4D3B7 DRE21_TRYCC Anamorsin homolog 1 OS	splQ4D3B7 DRE21	1	1	0
splQ4DER6 DRE22_TRYCC Anamorsin homolog 2 OS	splQ4DER6 DRE22	1	1	0
Mucin-associated surface protein (MASP), putative OS	Q4E1I7	1	1	0
Mucin TcMUCII OS	V5AYQ9	1	0	0
Mucin TcMUCII OS	V5ASM5	1	0	0
Mucin-associated surface protein (MASP), putative OS	Q4DM99	1	2	0
Ribonucleoside-diphosphate reductase small chain OS	V5ASN2	1	0	0
Ribonucleoside-diphosphate reductase small chain, putative OS	Q4D6V2	1	0	0
Tubulin binding cofactor A-like protein, putative OS	Q4E253	1	1	0
splQ4DLT6 PURA1_TRYCC Adenylosuccinate synthetase 1 OS	splQ4DLT6 PURA1	0	4	6
Trans-sialidase, putative OS	Q4DV25	0	2	5
Trans-sialidase, putative OS	Q4D2W7	0	1	4

Trans-sialidase, putative OS	Q4E5U1	0	0	4
Mucin-associated surface protein (MASP), putative OS	Q4D1G4	0	0	4
Trans-sialidase, putative OS	Q4E2A1	0	1	3
Group of Paraflagellar rod component OS	O00930	0	6	3
Mucin-associated surface protein (MASP), putative OS	Q4DPK2	0	0	3
Heat shock protein, putative OS	Q4E2Q2	0	2	3
Mucin-associated surface protein (MASP), putative OS	Q4D953	0	5	3
DNAK protein, putative (Fragment) OS	Q4CWK5	0	2	3
Trans-sialidase, putative OS	Q4DS03	0	0	3
Trans-sialidase, putative OS	Q4CSS2	0	3	3
Group of Clathrin heavy chain OS	V5BJW2	0	4	3
Mucin-associated surface protein (MASP), putative OS	Q4DTW8	0	4	3
Mucin-associated surface protein (MASP), putative OS	Q4DXZ2	0	2	3
Group of Paraflagellar rod component Par4 (Fragment) OS	Q7KPR4	0	4	3
ATP-dependent 6-phosphofructokinase OS	PFKA	0	4	3
Mucin-associated surface protein (MASP), putative OS	Q4DU48	0	1	3
Mucin-associated surface protein (MASP), putative (Fragment) OS	Q4DUN7	0	0	3
Mucin-associated surface protein (MASP), putative OS	Q4D033	0	0	3
Calpain cysteine peptidase, putative OS	Q4E0D6	0	1	3
Mucin TcMUCII, putative OS	Q4CN92	0	1	3

Trans-sialidase, putative OS	Q4D6K2	0	0	3
Mucin TcMUCII, putative OS	Q4DJI1	0	2	3
Mucin-associated surface protein (MASP), putative OS	Q4E3V5	0	0	3
Group of Leucine-rich repeat protein, putative OS	Q4CLM9	0	2	3
Protein disulfide-isomerase OS	Q4E3F7	0	1	3
Trans-sialidase, putative OS	Q4CYA8	0	0	3
Mucin TcMUCII, putative OS	Q4D8S0	0	0	3
Trans-sialidase, putative OS	Q4DP77	0	0	3
Mucin TcMUCII, putative OS	Q4E2B0	0	0	3
Mucin-associated surface protein (MASP), putative OS	Q4E4Z3	0	0	3
Mucin-associated surface protein (MASP), putative OS	Q4E289	0	11	2
Trans-sialidase, putative OS	Q4E2C9	0	1	2
Paraflagellar rod component, putative OS	Q4E568	0	2	2
Uncharacterized protein OS	Q4CYI1	0	3	2
Trans-sialidase, putative OS	Q4DD62	0	1	2
Mucin-associated surface protein (MASP), putative OS	Q4DZS8	0	8	2
Mucin TcMUCII, putative OS	Q4DMA9	0	2	2
Mucin TcMUCII, putative OS	Q4D803	0	2	2
Mucin-associated surface protein (MASP), putative OS	Q4DF69	0	3	2
Mucin-associated surface protein (MASP), putative OS	Q4CS13	0	3	2



Mucin-associated surface protein (MASP), putative OS	Q4DDV1	0	5	2
Seryl-tRNA synthetase, putative OS	Q4DC68	0	2	2
Mucin-associated surface protein (MASP), putative OS	Q4DR09	0	6	2
Protein disulfide isomerase, putative OS	Q4DFA6	0	4	2
Seryl-tRNA synthetase OS	V5DSV1	0	2	2
40 kDa cyclophilin, putative OS	Q4E4G0	0	2	2
Trans-sialidase, putative OS	Q4DCG7	0	5	2
Mucin-associated surface protein (MASP), putative OS	Q4DVR8	0	2	2
Clathrin heavy chain OS	V5BJW2	0	2	2
Clathrin heavy chain OS	Q3ZMB7	0	2	2
Mucin-associated surface protein (MASP), putative OS	Q4E522	0	0	2
Trans-sialidase, putative (Fragment) OS	Q4CWB0	0	1	2
Trans-sialidase, putative OS	Q4CPX0	0	0	2
Trans-sialidase, putative OS	Q4DKJ6	0	1	2
Trans-sialidase, putative OS	Q4CSU3	0	1	2
Mucin-associated surface protein (MASP), putative OS	Q4DY06	0	2	2
Aldo/keto reductase OS	Q965C7	0	2	2
Mucin-like glycoprotein, putative OS	Q4D0C1	0	4	2
TcSTII OS	O96684	0	1	2
Group of Mucin-associated surface protein (MASP), putative OS	Q4CLV3	0	4	2

Trans-sialidase, putative OS	Q4CSU2	0	1	2
Trans-sialidase, putative OS	Q4D098	0	0	2
2-oxoglutarate dehydrogenase E1 component, putative OS	Q4CTE8	0	1	2
Kynureninase OS	Q4CYC0	0	1	2
Trans-sialidase, putative OS	Q4DTW4	0	0	2
Mucin TcMUCII, putative OS	Q4E068	0	3	2
Mucin TcMUCII, putative OS	Q4DKV9	0	1	2
Trans-sialidase, putative OS	Q4DVI7	0	1	2
Thimet oligopeptidase, putative OS	Q4CVA3	0	3	2
Mucin-associated surface protein (MASP), putative OS	Q4E455	0	0	2
Trans-sialidase, putative OS	Q4DZD4	0	0	2
2-oxoglutarate dehydrogenase E1 component, putative OS	Q4DKY2	0	1	2
Surface protease GP63, putative (Fragment) OS	Q4CMY9	0	1	2
Mucin-associated surface protein (MASP), putative OS	Q4DYU3	0	1	2
Group of Proteasome regulatory ATPase subunit 1, putative (Fragment) OS	K2NXC2	0	2	2
Glutamate dehydrogenase OS	V5B4M0	0	2	2
Trans-sialidase, putative OS	Q4DCP9	0	1	2
Mucin TcMUCII, putative OS	Q4E074	0	0	2
Adenosylhomocysteinase OS	Q4DNQ7	0	2	2
T-complex protein 1 subunit delta OS	Q4DTP9	0	2	2

Mucin TcMUCII, putative OS	Q4E0E7	0	2	2
Tcc1j12.7 OS	Q8T2Z8	0	1	2
Mucin TcMUCII, putative OS	Q4E233	0	0	2
Group of Dynamin OS	V5DTS8	0	2	2
Group of RuvB-like helicase OS	Q4D5M2	0	1	2
Mucin TcMUCII, putative OS	Q4CUJ5	0	2	2
Mucin TcMUCII, putative OS	Q4DXZ3	0	0	2
Mucin TcMUCI, putative OS	Q4DYU6	0	1	2
Mucin-associated surface protein (MASP), putative OS	Q4E033	0	0	2
Heat shock protein, putative (Fragment) OS	Q4D0L7	0	0	2
Mucin TcMUCII, putative OS	Q4E5W2	0	1	2
Group of Profilin OS	Q4CMM4	0	1	2
R27-2 protein, putative OS	Q4CRN7	0	2	2
Mucin TcMUCII, putative OS	Q4E230	0	1	2
Mucin TcMUCII, putative OS	Q4D385	0	1	2
Group of Cysteine synthase OS	V5BWY7	0	1	2
60S ribosomal protein L13a, putative (Fragment) OS	K2N4W9	0	1	2
Flagellar radial spoke component OS	V5BDZ5	0	1	2
Group of 60S ribosomal protein L6 OS	Q4DR87	0	1	2
Mucin-associated surface protein (MASP), putative OS	Q4DZC6	0	1	2

Trans-sialidase, putative OS	Q4DRK0	0	0	2
Protein phosphatase 2C, putative OS	Q4E575	0	1	2
Paraflagellar rod component OS	O00930	0	3	1
Paraflagellar rod component, putative OS	Q4DWL5	0	3	1
Trans-sialidase, putative (Fragment) OS	Q4E1H2	0	9	1
Uncharacterized protein OS	K2MDY8	0	3	1
Trans-sialidase, putative OS	Q4CUS9	0	5	1
Mucin-associated surface protein (MASP), putative OS	Q4DVW7	0	7	1
Mucin-associated surface protein (MASP), putative OS	Q4D476	0	2	1
Trans-sialidase, putative OS	Q4DQA0	0	2	1
Mucin-associated surface protein (MASP), putative OS	Q4DYV7	0	4	1
Nucleoside phosphorylase, putative (Fragment) OS	Q4DAD9	0	4	1
Mucin-associated surface protein (MASP), putative OS	Q4E380	0	1	1
Trans-sialidase, putative OS	Q4DUY7	0	1	1
Mucin-associated surface protein (MASP), putative OS	Q4E3U8	0	2	1
Mucin-associated surface protein (MASP), putative OS	Q4CSG7	0	2	1
Mucin-associated surface protein (MASP), putative OS	Q4DH73	0	2	1
Mucin-associated surface protein (MASP), putative OS	Q4D302	0	6	1
Paraflagellar rod component Par4 (Fragment) OS	Q7KPR4	0	2	1
Paraflagellar rod component Par4 OS	O46353	0	2	1

Surface protein-2 OS	Q86DL8	0	4	1
Mucin-associated surface protein (MASP), putative OS	Q4DWF9	0	2	1
Surface protease GP63, putative OS	Q4DVY6	0	2	1
Mucin-associated surface protein (MASP), putative OS	Q4DZB6	0	5	1
Mucin-associated surface protein (MASP), putative OS	Q4E1Y6	0	4	1
Fructose-bisphosphate aldolase OS	K2LYI4	0	3	1
Mucin-associated surface protein (MASP), putative OS	Q4CNK6	0	0	1
Trans-sialidase, putative OS	Q4DTC3	0	0	1
Group of Mucin-associated surface protein (MASP), putative (Fragment) OS	Q4CL65	0	5	1
Mucin-associated surface protein (MASP), putative OS	Q4E1Y0	0	1	1
Surface protease GP63, putative OS	Q4E479	0	4	1
Mucin TcMUCII, putative OS	Q4DNF8	0	0	1
Mucin-associated surface protein (MASP), putative OS	Q4D2H2	0	2	1
Mucin-associated surface protein (MASP), putative OS	Q4CLV3	0	2	1
Mucin-associated surface protein (MASP), putative OS	Q4DM12	0	2	1
Mucin-associated surface protein (MASP), putative OS	Q4CPS2	0	5	1
Group of Putative surface protein TASV-A-05 (Fragment) OS	E3P9W0	0	3	1
Putative surface protein TASV-A-05 (Fragment) OS	E3P9W0	0	1	1
Putative surface protein TASV-A-28 (Fragment) OS	E3P9X2	0	1	1
Trans-sialidase, putative OS	Q4CPW8	0	1	1

Kynureninase OS	K2P244	0	2	1
Mucin-associated surface protein (MASP), putative OS	Q4D782	0	5	1
Mucin-associated surface protein (MASP), putative OS	Q4CS02	0	0	1
Mucin-associated surface protein (MASP), putative OS	Q4DE04	0	0	1
Surface protease GP63, putative OS	Q4DVY9	0	2	1
Mucin-associated surface protein (MASP), putative OS	Q4D4B2	0	2	1
Trans-sialidase, putative OS	Q4DD57	0	0	1
Mucin TcMUCII, putative OS	Q4DU51	0	4	1
Threonyl-tRNA synthetase, putative OS	Q4D9G6	0	2	1
Mucin-associated surface protein (MASP), putative OS	Q4CTA1	0	2	1
Mucin-associated surface protein (MASP), putative OS	Q4DYU9	0	2	1
Mucin-associated surface protein (MASP), putative OS	Q4D8D6	0	4	1
Trans-sialidase, putative OS	Q4DD58	0	2	1
Mucin-associated surface protein (MASP) OS	V5ALA8	0	1	1
Proteasome regulatory non-ATPase subunit 3 OS	V5B0Y8	0	1	1
Proteasome regulatory non-ATPase subunit 3, putative OS	Q4E3B3	0	1	1
Proteasome regulatory non-ATPase subunit 3, putative OS	K2MXY3	0	1	1
Trans-sialidase, putative OS	Q4CRT3	0	1	1
Mucin-associated surface protein (MASP), putative OS	Q4D6G3	0	2	1
Mucin-associated surface protein (MASP), putative OS	Q4DXP7	0	0	1

Trans-sialidase, putative OS	Q4DYM3	0	1	1
Mucin TcMUCII, putative OS	Q4DM13	0	3	1
Trans-sialidase, putative (Fragment) OS	Q4CUV6	0	0	1
Trans-sialidase, putative OS	Q4DC15	0	2	1
Mucin-associated surface protein (MASP), putative OS	Q4DJI0	0	4	1
Mucin-associated surface protein (MASP), putative OS	Q4CUI0	0	3	1
Dihydrolipoyl dehydrogenase OS	Q4DWL8	0	1	1
Mucin-associated surface protein (MASP), putative OS	Q4E2C8	0	3	1
Trans-sialidase OS	V5BFB7	0	0	1
Calpain cysteine peptidase, putative OS	Q4DQN6	0	2	1
Trans-sialidase, putative OS	Q4DA40	0	0	1
Leucine-rich repeat protein, putative OS	Q4CLM9	0	1	1
Leucine-rich repeat protein, putative OS	Q4D4Q1	0	1	1
Trans-sialidase, putative (Fragment) OS	Q4CR17	0	1	1
DNAK protein, putative (Fragment) OS	Q4DGL0	0	1	1
Group of Putative surface protein TASV-C-18 (Fragment) OS	E3P9Z3	0	3	1
Leucyl-tRNA synthetase, putative OS	Q4CTR0	0	1	1
Proteasome regulatory ATPase subunit 1, putative (Fragment) OS	K2NXC2	0	1	1
Proteasome regulatory ATPase subunit 1, putative OS	Q4D9J1	0	1	1
Group of Succinyl-CoA ligase [GDP-forming] beta-chain OS	V5B0B5	0	1	1

Succinyl-CoA ligase [GDP-forming] beta-chain OS	V5B0B5	0	1	1
Succinyl-CoA ligase [GDP-forming] beta-chain, putative (Fragment) OS	Q4CLP3	0	1	1
Leucyl-tRNA synthetase OS	V5B774	0	1	1
Dynein intermediate chain, putative OS	Q4DRW6	0	3	1
Proteasome regulatory non-ATPase subunit, putative OS	Q4CSX5	0	3	1
Phosphomannomutase-like protein OS	V5B6A2	0	1	1
Mucin-associated surface protein (MASP), putative OS	Q4E287	0	3	1
Calmodulin, putative OS	Q4DGP9	0	3	1
Acetyltransferase component of pyruvate dehydrogenase complex OS	Q4DZT8	0	3	1
Trans-sialidase, putative OS	Q4DSG4	0	0	1
Mucin-associated surface protein (MASP), putative OS	Q4DVY2	0	2	1
Mucin-associated surface protein (MASP), putative OS	Q4CNY5	0	2	1
Group of Mucin-associated surface protein (Fragment) OS	G4V514	0	3	1
40S ribosomal protein SA OS	Q4CQ63	0	1	1
40S ribosomal protein SA OS	K2N345	0	1	1
Mucin-associated surface protein (MASP), putative OS	Q4DTW6	0	2	1
Group of Putative surface antigen TASV-A1 OS	A5PGV4	0	1	1
Mucin-associated surface protein (MASP), putative OS	Q4D9U4	0	0	1
Mucin TcMUCII, putative OS	Q4E3U7	0	0	1
Mucin TcMUCII, putative OS	Q4D264	0	1	1



Kinesin, putative OS	Q4DQP9	0	3	1
25 kDa elongation factor 1-beta OS	EF1B	0	1	1
Mucin-associated surface protein (MASP), putative (Fragment) OS	Q4CTG2	0	3	1
Mucin-associated surface protein (MASP), putative OS	Q4D8A5	0	2	1
Mucin-associated surface protein (MASP), putative OS	Q4DYV3	0	1	1
Mucin TcMUCII, putative OS	Q4D2H6	0	2	1
Translation elongation factor 1-beta, putative OS	Q4DWC3	0	1	1
Small ubiquitin protein, putative OS	Q4DSS5	0	3	1
Mucin TcMUCII, putative OS	Q4E206	0	0	1
Mucin TcMUCII, putative OS	Q4DN78	0	0	1
Mucin TcMUCII, putative OS	Q4DN75	0	0	1
Sialidase homolog OS	O61082	0	0	1
Trans-sialidase, putative OS	Q4E1F4	0	0	1
Trans-sialidase, putative OS	Q4CSG0	0	1	1
Aminopeptidase, putative OS	Q4E686	0	2	1
Mucin-associated surface protein (MASP), putative OS	Q4E234	0	2	1
60S ribosomal protein L11, putative OS	Q4CNF4	0	2	1
Mucin-associated surface protein (MASP), putative OS	Q4DCT1	0	2	1
Mucin-associated surface protein (MASP), putative OS	Q4D3W5	0	2	1
Enoyl-CoA hydratase, mitochondrial, putative OS	Q4CKX1	0	3	1

Dynamin OS	V5DTS8	0	1	1
Dynamin, putative OS	Q4E689	0	1	1
RuvB-like helicase OS	Q4D5M2	0	0	1
RuvB-like helicase OS	Q4DTV5	0	0	1
RuvB-like helicase OS	V5BQJ1	0	0	1
RuvB-like helicase OS	K2MEF1	0	0	1
Mucin TcMUCII, putative OS	Q4E463	0	1	1
Thiol transferase Tc52 (Fragment) OS	Q7Z0C1	0	0	1
Thiol transferase Tc52 (Fragment) OS	Q7Z0C3	0	0	1
Thiol-dependent reductase 1, putative OS	Q4DKI7	0	0	1
Group of Chaperone DnaJ protein, putative OS	Q4DKC8	0	1	1
Short chain 3-hydroxyacyl-CoA dehydrogenase OS	V5BPS0	0	1	1
Short chain 3-hydroxyacyl-coa dehydrogenase, putative OS	Q4DMG1	0	1	1
Profilin OS	Q4CMM4	0	1	1
Profilin OS	Q4CZF5	0	1	1
Group of Chaperonin containing t-complex protein OS	V5BL37	0	3	1
Mucin-associated surface protein (MASP), putative OS	Q4E5T5	0	0	1
Mucin-associated surface protein (MASP), putative OS	Q4CLK6	0	1	1
Mucin-associated surface protein (MASP), putative OS	Q4DVE5	0	0	1
Mucin TcMUCII, putative OS	Q4DTC0	0	2	1

Mucin-associated surface protein (MASP), putative OS	Q4DII3	0	0	1
Putative surface antigen TASV-C1 OS	A5PGV8	0	0	1
Putative surface protein TASV-C-29 (Fragment) OS	E3PA02	0	0	1
Mucin TcMUCII, putative OS	Q4DYE7	0	1	1
Trans-sialidase, putative OS	Q4D2I7	0	0	1
Mucin-like glycoprotein, putative OS	Q4D8Y3	0	2	1
Protein kinase, putative OS	Q4DYJ7	0	2	1
Flagellar radial spoke protein-like, putative OS	Q4DHQ3	0	2	1
Mucin TcMUCII, putative OS	Q4CVN9	0	0	1
Mucin TcMUCII, putative OS	Q4CNE3	0	0	1
Mucin TcMUCII, putative OS	Q4DBI3	0	2	1
Cysteine synthase OS	V5BWY7	0	1	1
Cysteine synthase, putative OS	Q4CS97	0	1	1
Dynein light chain, putative OS	Q4D5U0	0	1	1
Malic enzyme OS	Q4DV36	0	1	1
Trans-sialidase, putative OS	Q4E3G9	0	2	1
Mucin-associated surface protein (MASP), putative OS	Q4D1Z9	0	0	1
Pyridoxal kinase, putative OS	Q4D360	0	2	1
Mucin TcMUCII, putative OS	Q4E043	0	1	1
Methionyl-tRNA synthetase, putative OS	Q4D6H2	0	1	1

Eukaryotic initiation factor 4a, putative OS	K2NIX0	0	2	1
Trans-sialidase, putative OS	Q4E0J4	0	0	1
Mucin-like protein OS	Q9N2S0	0	1	1
2-oxoglutarate dehydrogenase, E2 component, dihydrolipoamide succinyltransferase, putative OS	Q4D1R9	0	2	1
Group of Mucin TcMUCII, putative OS	Q4DCZ1	0	2	1
Mucin-associated surface protein (MASP), putative OS	Q4E386	0	5	0
Surface glycoprotein Tc-85/20 (Fragment) OS	Q2VYC8	0	4	0
Mucin-associated surface protein (MASP), putative OS	Q4DHM4	0	3	0
Mucin-associated surface protein (MASP), putative OS	Q4E434	0	3	0
Trans-sialidase, putative (Fragment) OS	Q4CKG0	0	7	0
Mucin-associated surface protein (MASP), putative OS	Q4D2N7	0	3	0
Mucin-associated surface protein (MASP), putative OS	Q4DM97	0	8	0
Mucin-associated surface protein (MASP), putative OS	Q4DWE9	0	3	0
Trans-sialidase, putative OS	Q4DEK8	0	2	0
Mucin-associated surface protein (MASP), putative OS	Q4E444	0	2	0
Trans-sialidase, putative (Fragment) OS	Q4CMJ6	0	4	0
Trans-sialidase, putative OS	Q4E377	0	2	0
Mucin-associated surface protein (MASP), putative OS	Q4DI91	0	1	0
Mucin-associated surface protein (MASP), putative OS	Q4DMA1	0	6	0
Mucin-associated surface protein (MASP), putative (Fragment) OS	Q4CL65	0	3	0

Mucin-associated surface protein (MASP), putative OS	Q4D9R9	0	3	0
Mucin-associated surface protein (MASP), putative OS	Q4DAB0	0	1	0
Mucin-associated surface protein (MASP), putative OS	Q4DTB1	0	5	0
Mucin-associated surface protein (MASP), putative OS	Q4DIE7	0	1	0
Trans-sialidase, putative OS	Q4E533	0	1	0
Mucin-associated surface protein (MASP), putative OS	Q4E484	0	4	0
Proteasome subunit beta type OS	Q4DW25	0	1	0
Proteasome subunit beta type OS	Q4E0L9	0	1	0
Proteasome subunit beta type OS	V5BHX1	0	1	0
Proteasome subunit beta type OS	K2N704	0	1	0
Mucin-associated surface protein (MASP), putative OS	Q4DV29	0	3	0
Fumarate hydratase, putative OS	Q4DJH1	0	3	0
Mucin TcMUCII, putative OS	Q4DNA7	0	5	0
Mucin-associated surface protein (MASP), putative OS	Q4E442	0	1	0
Mucin-associated surface protein (MASP), putative OS	Q4D8A1	0	5	0
Mucin-associated surface protein (MASP), putative OS	Q4DGU8	0	2	0
Mucin-associated surface protein (MASP), putative OS	Q4E1H9	0	3	0
Putative trans-sialidase OS	V5AYY6	0	2	0
Mucin-associated surface protein (MASP), putative OS	Q4DBI9	0	1	0
Mucin-associated surface protein (MASP), putative OS	Q4DF33	0	3	0

Surface protease GP63, putative OS	Q4DVY4	0	2	0
Chaperone DNAJ protein OS	V5B5S8	0	1	0
Chaperone DNAJ protein, putative OS	K2NUR3	0	1	0
Co-chaperone protein OS	Q9BIX8	0	1	0
Mucin-associated surface protein (MASP), putative OS	Q4E425	0	4	0
Mucin-like protein (Fragment) OS	O15772	0	2	0
Mucin-associated surface protein (MASP), putative OS	Q4E0E6	0	2	0
Mucin TcMUCII, putative OS	Q4CZ97	0	3	0
Mucin-associated surface protein (MASP), putative OS	Q4E1F6	0	3	0
Mucin-associated surface protein (MASP), putative OS	Q4DY02	0	3	0
Putative surface protein TASV-C-18 (Fragment) OS	E3P9Z3	0	2	0
Putative surface protein TASV-C-19 (Fragment) OS	E3P9Z4	0	2	0
Mucin-associated surface protein (MASP), putative OS	Q4DD61	0	2	0
Trans-sialidase, putative OS	Q4DPD2	0	1	0
Mucin-associated surface protein (MASP), putative OS	Q4E294	0	4	0
Mucin TcMUCII, putative OS	Q4CZ92	0	3	0
Mucin-associated surface protein (MASP), putative OS	Q4DD56	0	2	0
Mucin-associated surface protein (MASP), putative OS	Q4E1Y1	0	2	0
Trans-sialidase, putative OS	Q4CQV3	0	2	0
Mucin-associated surface protein (MASP), putative OS	Q4DU08	0	3	0

Mucin-associated surface protein (MASP), putative (Fragment) OS	Q4CN90	0	4	0
Trans-sialidase, putative OS	Q4D2I1	0	1	0
Trans-sialidase (Fragment) OS	B3VSM7	0	1	0
Mucin-associated surface protein (MASP), putative (Fragment) OS	Q4CKR5	0	2	0
Mucin-associated surface protein (MASP), putative OS	Q4D8A3	0	3	0
Mucin-associated surface protein (Fragment) OS	G4V514	0	2	0
Mucin-associated surface protein (MASP), putative OS	Q4CXW1	0	2	0
Mucin TcMUCII, putative OS	Q4DIE3	0	2	0
Mucin-associated surface protein (MASP), putative OS	Q4E491	0	3	0
Serine/threonine protein phosphatase type 5, putative OS	Q4E1W0	0	1	0
Serine/threonine protein phosphatase type 5, putative OS	K2NQW9	0	1	0
Mucin-associated surface protein (MASP), putative OS	Q4DZC1	0	2	0
Mucin-associated surface protein (MASP), putative OS	Q4E1I6	0	3	0
Mucin-associated surface protein (MASP), putative OS	Q4DNA9	0	2	0
Trans-sialidase, putative OS	Q4D1A3	0	3	0
Mucin-associated surface protein (MASP), putative OS	Q4E1Z3	0	3	0
OSM3-like kinesin, putative (Fragment) OS	Q4E1M3	0	1	0
Mucin-associated surface protein (MASP), putative OS	Q4DKJ3	0	2	0
Chaperonin containing t-complex protein OS	V5BL37	0	1	0
Chaperonin containing t-complex protein, putative OS	K2MA70	0	1	0

T-complex protein 1, beta subunit, putative OS	Q4D6N0	0	1	0
OSM3-like kinesin, putative OS	K2M0V2	0	1	0
Mucin-associated surface protein (MASP), putative OS	Q4DVX2	0	3	0
Surface glycoprotein (Fragment) OS	Q26865	0	2	0
Mucin-associated surface protein (MASP), putative OS	Q4E1Z6	0	2	0
60S acidic ribosomal protein P0 OS	Q4E3A3	0	1	0
60S acidic ribosomal protein P0 OS	V5BL26	0	1	0
Mucin-associated surface protein (MASP), putative OS	Q4E1J2	0	1	0
Mucin TcMUCII, putative OS	Q4DM95	0	3	0
Mucin-associated surface protein (MASP), putative OS	Q4D6C2	0	3	0



**APPENDIX B: TcMUC II FAMILY MEMBERS IDENTIFIED IN THE TCT-SECR AND IB-4 LECTIN COLUMN FRACTIONS,  $\alpha$ -GAL(-) AND  $\alpha$ -GAL(+), FROM *T. CRUZI* COL STRAIN. VALUES ARE EXPRESSED AS AVERAGE OF NORMALIZED WEIGHTED SPECTRUM COUNTS.**

Identified Proteins	Accession Number	TCT Secr Col	$\alpha$ -Gal(-) (FT) Col	$\alpha$ -Gal(+) (EL) Col
Putative mucin TcMUCII OS	A0A2V2W2D1	0	6	39
Group of Putative mucin TcMUCII OS	A0A2V2X5V1 (+1)	0	2	27
Putative mucin TcMUCII OS	A0A2V2WR81	9	5	26
Mucin TcMUCII, putative OS	Q4CYF9	0	2	25
Putative mucin TcMUCII OS	A0A2V2W3F2	7	1	23
Putative mucin TcMUCII OS	A0A2V2W0S7	0	3	23
Putative mucin TcMUCII OS	A0A2V2VUI0	0	1	23
Putative mucin TcMUCII OS	A0A2V2WMF7	13	3	21
Mucin TcMUCII, putative OS	Q4E071	0	6	16
Putative mucin TcMUCII OS	A0A2V2WSQ6	0	3	16
Mucin TcMUCII, putative OS	Q4E2C3	0	2	16
Mucin TcMUCII, putative OS	Q4D7L0	0	0	16
Putative mucin TcMUCII OS	A0A2V2WHE6	13	3	12
Group of Mucin TcMUCII, putative OS	Q4DCZ1 (+1)	0	5	12
Putative mucin TcMUCII OS	A0A2V2VNS3	0	3	12
Mucin TcMUCII, putative OS	Q4E3U5	0	1	12
Mucin TcMUCII, putative OS	Q4E3V3	0	1	12
Group of Putative mucin TcMUCII OS	A0A2V2XGB5 (+1)	0	1	12
Mucin TcMUCII, putative OS	Q4E2B0	0	0	12
Mucin TcMUCII, putative OS	Q4DIE3	0	1	11
Mucin TcMUCII, putative OS	Q4DM06	0	0	11

Putative mucin TcMUCII OS	A0A2V2W791	0	1	10
Putative mucin TcMUCII OS	A0A2V2X2R6	7	1	8
Putative mucin TcMUCII OS	A0A2V2UYP8	0	0	8
Group of Putative mucin TcMUCII OS	A0A2V2X537 (+2)	0	0	8
Putative mucin TcMUCII OS	A0A2V2XCR2	0	2	5
Mucin TcMUCII OS	V5AN33	0	1	5
Mucin TcMUCII, putative OS	Q4DM13	7	3	4
Mucin TcMUCII, putative OS	Q4E3D1	7	1	4
Putative mucin TcMUCII OS	A0A2V2W6K6	4	2	4
Putative mucin TcMUCII OS	A0A2V2XG98	0	2	4
Putative mucin TcMUCII OS	A0A2V2WVM0	0	2	4
Mucin TcMUCII, putative OS	Q4D1J6	0	0	4
Mucin TcMUCII, putative OS	Q4CS53	0	0	4
Mucin TcMUCII, putative OS	Q4DFV4	2	0	3
Putative mucin TcMUCII OS	A0A2V2W5L6	2	0	3
Putative mucin TcMUCII OS	A0A2V2WWU0	0	0	3
Mucin TcMUCII, putative OS	Q4CZ01	0	0	1
Putative mucin TcMUCII OS	A0A2V2WUP0	2	0	0
Putative mucin TcMUCII OS	A0A2V2W6F4	0	3	0
Putative mucin TcMUCII OS	A0A2V2XHA2	0	2	0
Putative mucin TcMUCII OS	A0A2V2WCN5	0	2	0
Group of Mucin TcMUCII, putative OS	Q4CTN4 (+1)	0	2	0
Mucin TcMUCII, putative OS	Q4DIF2	0	1	0
Putative mucin TcMUCII OS	A0A2V2UPQ0	0	1	0

**APPENDIX C: MASP FAMILY MEMBERS IDENTIFIED IN THE TCT-SECR AND IN THE IB4-LECTIN COLUMN FRACTIONS,  $\alpha$ -GAL(-) AND  $\alpha$ -GAL(+), FROM *T. CRUZI* COL STRAIN. VALUES ARE EXPRESSED AS AVERAGE OF NORMALIZED WEIGHTED SPECTRUM COUNTS.**

Identified Proteins	Accession Number	TCT Secr Col	$\alpha$ -Gal(-) (FT) Col	$\alpha$ -Gal(+) (EL) Col
Mucin-associated surface protein (MASP) OS	A0A2V2W7B2	30	14	0
Group of Mucin-associated surface protein (MASP) OS	V5BF77 (+1)	20	11	2
Mucin-associated surface protein (MASP) OS	A0A2V2VRB7	7	9	0
Mucin-associated surface protein (MASP) OS	A0A2V2VF80	7	9	0
Mucin-associated surface protein (MASP) OS	A0A2V2W6S9	0	9	0
Mucin-associated surface protein (MASP) OS	A0A2V2VCX7	0	9	0
Mucin-associated surface protein (MASP) OS	A0A2V2VZS0	0	9	0
Mucin-associated surface protein (MASP) OS	A0A2V2UT67	26	8	0
Mucin-associated surface protein (MASP) OS	A0A2V2VC34	13	7	0
Mucin-associated surface protein (MASP) OS	A0A2V2VNG6	7	7	0
Group of Mucin-associated surface protein (MASP) OS	V5BBK7 (+1)	4	7	5
Mucin-associated surface protein (MASP) OS	A0A2V2V018	0	7	2
Mucin-associated surface protein (MASP) OS	A0A2V2UMB9	7	6	0
Mucin-associated surface protein (MASP) OS	A0A2V2UXX1	5	6	0
Mucin-associated surface protein (MASP) OS	A0A2V2W752	3	6	1
Mucin-associated surface protein (MASP) OS	V5BBT4	3	6	0
Mucin-associated surface protein (MASP) OS	A0A2V2UGU2	0	6	0
Mucin-associated surface protein (MASP) OS	A0A2V2V3J6	0	6	0
Mucin-associated surface protein (MASP) OS	A0A2V2US81	12	5	0
Mucin-associated surface protein (MASP) OS	A0A2V2W2Z4	7	5	0
Mucin-associated surface protein (MASP) OS	A0A2V2VMA1	0	5	4

Mucin-associated surface protein (MASP) OS	A0A2V2URT0	0	5	0
Mucin-associated surface protein (MASP) OS	A0A2V2UXG6	0	5	0
Group of Mucin-associated surface protein (MASP) OS	A0A2V2W3N4 (+1)	0	5	0
Group of Mucin-associated surface protein (MASP) OS	V5D4V1 (+1)	20	4	0
Mucin-associated surface protein (MASP) OS	A0A2V2VDP8	12	4	0
Group of Mucin-associated surface protein (MASP) OS	V5B7H5 (+1)	9	4	0
Group of Mucin-associated surface protein (MASP) OS	V5CKL1 (+1)	9	4	0
Mucin-associated surface protein (MASP) OS	A0A2V2W3L1	8	4	0
Group of Mucin-associated surface protein (MASP) OS	V5AL36 (+1)	8	4	0
Mucin-associated surface protein (MASP) OS	A0A2V2UR06	5	4	0
Mucin-associated surface protein (MASP) OS	A0A2V2V2H3	3	4	0
Mucin-associated surface protein (MASP) OS	A0A2V2W0H0	3	4	0
Mucin-associated surface protein (MASP) OS	A0A2V2V0H1	0	4	0
Mucin-associated surface protein (MASP) OS	A0A2V2VXG3	0	4	0
Mucin-associated surface protein (MASP) OS	A0A2V2VQ46	0	4	0
Mucin-associated surface protein (MASP) OS	A0A2V2W3Y6	0	4	0
Mucin-associated surface protein (MASP) OS	V5BF73	0	4	0
Mucin-associated surface protein (MASP) OS	A0A2V2VX77	0	4	0
Mucin-associated surface protein (MASP) OS	A0A2V2VW08	0	4	0
Mucin-associated surface protein (MASP) OS	V5BFX0	0	4	0
Mucin-associated surface protein (MASP) OS	A0A2V2VBN9	0	4	0
Mucin-associated surface protein (MASP) OS	A0A2V2W311	0	4	0
Mucin-associated surface protein (MASP) OS	A0A2V2VZM8	0	4	0
Mucin-associated surface protein (MASP) OS	V5B9Y3	0	4	0
Mucin-associated surface protein (MASP) OS	A0A2V2VM18	14	3	0
Group of Mucin-associated surface protein (MASP) OS	V5B2C2 (+1)	9	3	1
Mucin-associated surface protein (MASP) OS	A0A2V2W5T1	7	3	0
Mucin-associated surface protein (MASP) OS	A0A2V2W6I1	7	3	0

Mucin-associated surface protein (MASP) OS	V5BBL1	7	3	4
Group of Mucin-associated surface protein (MASP) OS	V5BBB0 (+1)	7	3	0
Mucin-associated surface protein (MASP) OS	A0A2V2V8N0	4	3	0
Mucin-associated surface protein (MASP) OS	A0A2V2W399	3	3	0
Mucin-associated surface protein (MASP) OS	A0A2V2VDA6	3	3	0
Mucin-associated surface protein (MASP) OS	A0A2V2W432	2	3	0
Mucin-associated surface protein (MASP) OS	A0A2V2VIJ8	1	3	0
Mucin-associated surface protein (MASP) OS	A0A2V2W560	1	3	0
Mucin-associated surface protein (MASP) OS	A0A2V2V1K7	1	3	0
Mucin-associated surface protein (MASP) OS	A0A2V2VQW1	0	3	8
Mucin-associated surface protein (MASP) OS	A0A2V2V826	0	3	1
Mucin-associated surface protein (MASP), putative OS	Q4DR50	0	3	2
Mucin-associated surface protein (MASP) OS	A0A2V2VQS5	0	3	0
Mucin-associated surface protein (MASP) OS	A0A2V2V3P2	0	3	0
Mucin-associated surface protein (MASP) OS	A0A2V2VBR6	0	3	0
Mucin-associated surface protein (MASP) OS	A0A2V2URE0	0	3	0
Mucin-associated surface protein (MASP) OS	A0A2V2UQX5	0	3	0
Mucin-associated surface protein (MASP) OS	V5A3C9	0	3	0
Mucin-associated surface protein (MASP) OS	A0A2V2UQD4	0	3	0
Mucin-associated surface protein (MASP) OS	A0A2V2UZD0	0	3	0
Mucin-associated surface protein (MASP) OS	A0A2V2VN01	0	3	0
Mucin-associated surface protein (MASP) OS	A0A2V2V788	0	3	0
Mucin-associated surface protein (MASP) OS	A0A2V2W529	0	3	0
Mucin-associated surface protein (MASP) OS	A0A2V2W511	0	3	0
Group of Mucin-associated surface protein (MASP) OS	A0A2V2USV3 (+1)	0	3	0
Group of Mucin-associated surface protein (MASP) OS	V5AYY5 (+1)	0	3	0
Mucin-associated surface protein (MASP) OS	A0A2V2VT61	0	3	0
Mucin-associated surface protein (MASP) OS	A0A2V2VA65	0	3	0

Mucin-associated surface protein (MASP) OS	A0A2V2VC58	0	3	0
Mucin-associated surface protein (MASP) OS	A0A2V2UYK3	0	3	0
Group of Mucin-associated surface protein (MASP) OS	V5CZJ9 (+1)	0	3	0
Mucin-associated surface protein (MASP) OS	A0A2V2W396	0	3	0
Mucin-associated surface protein (MASP) OS	A0A2V2XMK1	0	3	0
Mucin-associated surface protein (MASP) OS	A0A2V2WA36	0	3	0
Group of Mucin-associated surface protein (MASP) OS	A0A2V2UPB4 (+1)	0	3	0
Mucin-associated surface protein (MASP) OS	A0A2V2UUE1	0	3	0
Mucin-associated surface protein (MASP) OS	A0A2V2UWT9	0	3	0
Group of Mucin-associated surface protein (MASP) OS	A0A2V2XMG7 (+1)	8	2	0
Mucin-associated surface protein (MASP) OS	V5B2W7	7	2	0
Mucin-associated surface protein (MASP), putative OS	Q4D782	7	2	0
Mucin-associated surface protein (MASP) OS	A0A2V2V1F6	7	2	2
Mucin-associated surface protein (MASP) OS	A0A2V2V9K3	7	2	0
Mucin-associated surface protein (MASP) OS	A0A2V2W6F2	7	2	0
Mucin-associated surface protein (MASP) OS	A0A2V2USB3	7	2	0
Mucin-associated surface protein (MASP) OS	A0A2V2W5I4	4	2	0
Mucin-associated surface protein (MASP) OS	A0A2V2UUC3	4	2	0
Mucin-associated surface protein (MASP) OS	A0A2V2WFY4	3	2	0
Group of Mucin-associated surface protein (MASP) OS	V5D3M1 (+1)	3	2	0
Group of Mucin-associated surface protein (MASP) OS	V5AZE0 (+2)	3	2	0
Mucin-associated surface protein (MASP) OS	A0A2V2VD54	3	2	0
tr A0A2V2XI47-DECOY A0A2V2XI47-DECOY_TRYCR Mucin-associated surface protein (MASP)...	A0A2V2XI47-DECOY	2	2	0
Mucin-associated surface protein (MASP) OS	A0A2V2VXA6	2	2	0
Mucin-associated surface protein (MASP) OS	V5BCB1	2	2	0
Mucin-associated surface protein (MASP) OS	A0A2V2UQ49	1	2	0
Mucin-associated surface protein (MASP) OS	A0A2V2V132	0	2	1

Mucin-associated surface protein (MASP) OS	A0A2V2UU16	0	2	0
Mucin-associated surface protein (MASP) OS	V5DAV6	0	2	6
Mucin-associated surface protein (MASP) OS	A0A2V2VE10	0	2	0
Mucin-associated surface protein (MASP) OS	A0A2V2X238	0	2	0
Mucin-associated surface protein (MASP) OS	A0A2V2V9X2	0	2	0
Mucin-associated surface protein (MASP) OS	A0A2V2UVJ7	0	2	0
Group of Mucin-associated surface protein (MASP) OS	V5D744 (+1)	0	2	1
Group of Mucin-associated surface protein (MASP) OS	V5AZK4 (+1)	0	2	0
Mucin-associated surface protein (MASP) OS	A0A2V2VUG0	0	2	0
Mucin-associated surface protein (MASP) OS	A0A2V2V9R2	0	2	0
Group of Mucin-associated surface protein (MASP) OS	A0A2V2V7A8 (+1)	0	2	0
Mucin-associated surface protein (MASP) OS	A0A2V2USN5	0	2	0
Mucin-associated surface protein (MASP) OS	A0A2V2W2G9	0	2	0
Mucin-associated surface protein (MASP) OS	V5CJF6	0	2	0
Mucin-associated surface protein (MASP) OS	A0A2V2UXA7	0	2	0
Mucin-associated surface protein (MASP) OS	A0A2V2V191	0	2	0
Mucin-associated surface protein (MASP) OS	A0A2V2UNY3	0	2	0
Putative mucin-associated surface protein (MASP) OS	A0A2V2VT52	0	2	0
Mucin-associated surface protein (MASP) OS	A0A2V2UNJ2	0	2	0
Mucin-associated surface protein (MASP) OS	A0A2V2UWG4	0	2	0
Mucin-associated surface protein (MASP) OS	A0A2V2V087	0	2	0
Mucin-associated surface protein (MASP) OS	A0A2V2VWJ3	0	2	0
Mucin-associated surface protein (MASP) OS	A0A2V2UXX7	0	2	0
Mucin-associated surface protein (MASP) OS	V5AMK0	0	2	0
Mucin-associated surface protein (MASP) OS	A0A2V2W3J0	8	1	0
Mucin-associated surface protein (MASP), putative OS	Q4E1Z5	7	1	2
Mucin-associated surface protein (MASP), putative OS	Q4D521	7	1	4
Mucin-associated surface protein (MASP) OS	A0A2V2VZU8	4	1	0

Mucin-associated surface protein (MASP) OS	A0A2V2XKD8	3	1	1
Mucin-associated surface protein (MASP), putative OS	Q4E3V5	3	1	0
Mucin-associated surface protein (MASP) OS	A0A2V2WC30	2	1	0
Mucin-associated surface protein (MASP) OS	V5APP8	2	1	0
tr A0A2V2W3J8-DECOY A0A2V2W3J8-DECOY_TRYCR Mucin-associated surface protein (MASP)...	A0A2V2W3J8-DECOY	2	1	0
Mucin-associated surface protein (MASP) OS	A0A2V2W7A5	1	1	0
Mucin-associated surface protein (MASP) OS	A0A2V2WXA7	1	1	0
Mucin-associated surface protein (MASP) OS	A0A2V2UXZ8	1	1	0
Mucin-associated surface protein (MASP) OS	A0A2V2UT23	1	1	0
Mucin-associated surface protein (MASP) OS	A0A2V2VF83	1	1	0
Mucin-associated surface protein (MASP) OS	A0A2V2UR99	1	1	0
Mucin-associated surface protein (MASP) OS	A0A2V2VM11	1	1	0
Mucin-associated surface protein (MASP) OS	A0A2V2VQH0	1	1	0
Mucin-associated surface protein (MASP) OS	A0A2V2UT92	1	1	0
Mucin-associated surface protein (MASP) OS	A0A2V2UV69	1	1	0
Mucin-associated surface protein (MASP) OS	V5BFG7	1	1	0
Mucin-associated surface protein (MASP) OS	A0A2V2W007	1	1	0
Mucin-associated surface protein (MASP) OS	A0A2V2W375	1	1	0
Mucin-associated surface protein (MASP), putative OS	Q4D JL2	1	1	0
Mucin-associated surface protein (MASP) OS	A0A2V2VXC7	0	1	1
Mucin-associated surface protein (MASP) OS	A0A2V2VTV8	0	1	1
Group of Mucin-associated surface protein (MASP) OS	A0A2V2X5L7 (+1)	0	1	0
Mucin-associated surface protein (MASP) OS	A0A2V2XAE3	0	1	3
Mucin-associated surface protein (MASP) OS	A0A2V2V5W8	0	1	0
Mucin-associated surface protein (MASP), putative OS	Q4E380	0	1	0
Mucin-associated surface protein (MASP), putative OS	Q4DXP7	0	1	0
Mucin-associated surface protein (MASP), putative OS	Q4E493	0	1	0



Mucin-associated surface protein (MASP), putative OS	Q4E455	0	1	0
Group of Mucin-associated surface protein (MASP) OS	V5AUG7 (+1)	0	1	0
Mucin-associated surface protein (MASP) OS	V5D3A6	0	1	0
Mucin-associated surface protein (MASP) OS	A0A2V2VR09	0	1	0
Mucin-associated surface protein (MASP), putative OS	Q4CX27	0	1	0
Mucin-associated surface protein (MASP), putative OS	Q4DQA3	0	1	0
Mucin-associated surface protein (MASP), putative OS	Q4DVS8	0	1	0
Mucin-associated surface protein (MASP) OS	A0A2V2UT85	0	1	0
Group of Mucin-associated surface protein (MASP) OS	A0A2V2V1T1 (+1)	0	1	0
Group of Mucin-associated surface protein (MASP) OS	V5AJ74 (+2)	0	1	0
Group of Mucin-associated surface protein (MASP) OS	V5AQ54 (+1)	0	1	0
Mucin-associated surface protein (MASP) OS	A0A2V2W061	0	1	0
Mucin-associated surface protein (MASP) OS	A0A2V2WAR3	0	1	0
Mucin-associated surface protein (MASP) OS	V5AMY1	0	1	0
Mucin-associated surface protein (MASP) OS	V5B3Q9	0	1	0
Mucin-associated surface protein (MASP) OS	A0A2V2W9G6	0	1	0
Mucin-associated surface protein (MASP) OS	V5B331	0	1	0
Mucin-associated surface protein (MASP) OS	A0A2V2UZJ4	0	1	0
Mucin-associated surface protein (MASP) OS	A0A2V2VX98	0	1	0
Group of Mucin-associated surface protein (MASP) OS	A0A2V2XBB8 (+6)	0	1	0
Group of Mucin-associated surface protein (MASP) OS	A0A2V2VQU2 (+1)	0	1	0
Mucin-associated surface protein (MASP) OS	A0A2V2UQK0	0	1	0
Mucin-associated surface protein (MASP), putative OS	Q4E194	3	0	0
Group of Mucin-associated surface protein (MASP) OS	A0A2V2WTX4 (+1)	2	0	0
Group of Mucin-associated surface protein (MASP) OS	A0A2V2W708 (+2)	2	0	0
Mucin-associated surface protein (MASP) OS	A0A2V2VZZ1	1	0	0
Mucin-associated surface protein (MASP) OS	A0A2V2V3N3	1	0	0
Mucin-associated surface protein (MASP) OS	A0A2V2XIJ2	1	0	0

Mucin-associated surface protein (MASP) OS	A0A2V2XPF9	1	0	0
Mucin-associated surface protein (MASP) OS	A0A2V2XKW2	1	0	0
Mucin-associated surface protein (MASP) OS	A0A2V2WUL8	1	0	0
Mucin-associated surface protein (MASP) OS	A0A2V2WSD9	1	0	0
Mucin-associated surface protein (MASP) OS	A0A2V2W0A5	1	0	0
Mucin-associated surface protein (MASP) OS	V5D9L1	1	0	0
Mucin-associated surface protein (MASP), putative OS	Q4D1G4	1	0	0
Mucin-associated surface protein (MASP), putative OS	Q4D998	1	0	0
Mucin-associated surface protein (MASP) OS	A0A2V2WZX1	1	0	0
Mucin-associated surface protein (MASP) OS	A0A2V2XAR2	1	0	0
Mucin-associated surface protein (MASP) OS	A0A2V2XJI1	1	0	0
Mucin-associated surface protein (MASP), putative OS	Q4DVK4	1	0	0

**APPENDIX D: TS FAMILY MEMBERS IDENTIFIED IN TCT-SECR AND IN THE IB4-LECTIN COLUMN FRACTIONS,  $\alpha$ -GAL(+) AND  $\alpha$ -GAL(-), FROM COL STRAIN. VALUES ARE EXPRESSED AS AVERAGE OF NORMALIZED WEIGHTED SPECTRUM COUNTS.**

<b>Identified Proteins</b>	<b>Accession Number</b>	<b>TCT Secr Col</b>	<b><math>\alpha</math>-Gal(-) (FT) Col</b>	<b><math>\alpha</math>-Gal(+) (EL) Col</b>
Putative trans-sialidase, Group I OS	A0A2V2UWI0	55	41	0
Putative trans-sialidase, Group II OS	A0A2V2VAS5	54	38	0
Putative trans-sialidase, Group I OS	A0A2V2UQ56	47	37	0
Putative trans-sialidase, Group I OS	A0A2V2VQS7	46	34	0
Putative trans-sialidase, Group I OS	A0A2V2VMW6	39	33	0
Putative trans-sialidase, Group I OS	A0A2V2VZH5	13	23	0
Putative trans-sialidase, Group V OS	A0A2V2VJ94	23	20	0
Putative trans-sialidase, Group I OS	A0A2V2WSP5	28	18	3
Putative trans-sialidase, Group I OS	A0A2V2X1Q1	6	17	0
Trans-sialidase, putative OS	Q4DQ76	3	16	4
Trans-sialidase OS	V5BQA7	27	16	0
Trans-sialidase (Fragment) OS	B3VSM6	6	14	0
Putative trans-sialidase, Group I OS	A0A2V2WXL6	28	14	0
Group of Putative amidinotransferase OS	A0A2V2VUT2 (+1)	0	14	0
Trans-sialidase OS	V5AMT0	10	14	7
Trans-sialidase OS	Q26969	10	13	0
Putative trans-sialidase, Group VIII OS	A0A2V2UTK4	10	12	0
Group of Putative trans-sialidase, Group III OS	A0A2V2UVW1 (+1)	0	12	0
Putative trans-sialidase, Group I OS	A0A2V2X778	6	11	9
Putative trans-sialidase, Group V OS	A0A2V2VEF1	4	11	30
Putative trans-sialidase, Group VII OS	A0A2V2UFH4	0	11	0

Trans-sialidase, putative OS	Q4CTX4	23	10	0
Putative trans-sialidase OS	A0A2V2V3I5	12	10	0
Putative trans-sialidase, Group V OS	A0A2V2UYR0	8	10	0
Putative trans-sialidase, Group II OS	A0A2V2V0H5	19	10	0
Putative trans-sialidase, Group III OS	A0A2V2UU80	2	10	0
Putative trans-sialidase, Group VIII OS	A0A2V2UUT5	5	10	0
Putative trans-sialidase OS	A0A2V2V2Z5	13	9	0
Group of TS-193 trans-sialidase homolog protein OS	Q4R2T0 (+1)	15	9	0
Putative trans-sialidase, Group II OS	A0A2V2ULD3	6	9	18
Putative trans-sialidase, Group V OS	A0A2V2VUH3	17	8	0
Putative trans-sialidase, Group V OS	A0A2V2VF87	9	8	0
Putative trans-sialidase, Group VIII OS	A0A2V2URZ2	10	8	2
Trans-sialidase OS	V5B004	0	8	1
Putative trans-sialidase, Group II OS	A0A2V2V1F7	2	8	0
Peptidyl-prolyl cis-trans isomerase OS	Q4E4L9	0	8	1
Putative trans-sialidase, Group II OS	A0A2V2UY84	3	8	0
Putative trans-sialidase, Group II OS	A0A2V2ULK9	7	8	0
Putative trans-sialidase, Group V OS	A0A2V2V8D0	11	7	0
Putative trans-sialidase, Group V OS	A0A2V2UJV5	5	7	5
Putative trans-sialidase, Group V OS	A0A2V2UQK6	10	7	7
Putative trans-sialidase, Group V OS	A0A2V2VTX9	7	7	0
Putative trans-sialidase, Group II OS	A0A2V2UHM8	4	7	1
Trans-sialidase, putative OS	Q4DBE7	3	7	0
Trans-sialidase OS	V5AN62	2	7	0
Putative trans-sialidase, Group III OS	A0A2V2UWB4	0	7	0
Putative trans-sialidase OS	A0A2V2VLQ0	4	7	0
Putative trans-sialidase, Group VIII OS	A0A2V2VR25	20	7	0
Putative trans-sialidase, Group II OS	A0A2V2V198	0	7	0

Putative trans-sialidase, Group V OS	A0A2V2VXJ5	1	6	1
Putative trans-sialidase, Group V OS	A0A2V2V1T3	5	6	16
Putative trans-sialidase, Group V OS	A0A2V2VXJ2	1	6	4
Group of Putative trans-sialidase OS	A0A2V2XDR2 (+1)	7	6	0
Putative trans-sialidase, Group V OS	A0A2V2V1P3	1	6	0
Trans-sialidase OS	V5D006	4	6	0
Trans-sialidase, putative OS	Q4DVJ1	6	6	0
Putative trans-sialidase, Group V OS	A0A2V2VCG1	1	6	0
Putative trans-sialidase, Group II OS	A0A2V2UIK4	15	6	0
Putative trans-sialidase, Group VIII OS	A0A2V2VFP0	8	6	0
Putative trans-sialidase, Group VIII OS	A0A2V2VGF6	1	6	4
Putative trans-sialidase, Group VIII OS	A0A2V2VMX8	7	6	0
Trans-sialidase OS	V5B8Z1	0	6	1
Putative trans-sialidase, Group V OS	A0A2V2W4W1	2	5	0
Putative trans-sialidase, Group V OS	A0A2V2W442	2	5	2
Putative trans-sialidase, Group V OS	A0A2V2VXA3	4	5	11
Putative trans-sialidase, Group V OS	A0A2V2UPS0	1	5	0
Group of Putative trans-sialidase, Group II OS	A0A2V2UVV3 (+1)	8	5	0
Trans-sialidase (Fragment) OS	Q26887	3	5	0
Putative trans-sialidase, Group V OS	A0A2V2VF15	3	5	0
Trans-sialidase OS	V5B534	2	5	0
Putative trans-sialidase, Group III OS	A0A2V2UU09	0	5	0
Putative trans-sialidase, Group V OS	A0A2V2W424	1	5	0
Trans-sialidase OS	V5D3Z5	3	5	0
Group of Eukaryotic translation initiation factor 5A OS	Q4E4N4 (+1)	0	5	0
Trans-sialidase OS	V5AMH3	4	4	0
Putative trans-sialidase, Group V OS	A0A2V2VXN3	3	4	0
Trans-sialidase OS	V5CIU5	2	4	17

Putative trans-sialidase, Group V OS	A0A2V2V1I8	2	4	13
Putative trans-sialidase, Group VII OS	A0A2V2VNA5	5	4	44
Putative trans-sialidase, Group V OS	A0A2V2UJ13	1	4	1
Putative trans-sialidase, Group V OS	A0A2V2UWJ2	1	4	0
Putative trans-sialidase, Group V OS	A0A2V2W469	1	4	0
Putative trans-sialidase, Group II OS	A0A2V2UZ79	4	4	0
Trans-sialidase OS	V5A2Q8	7	4	0
Group of Putative trans-sialidase, Group II OS	A0A2V2W161 (+1)	8	4	0
Trans-sialidase OS	V5ANI3	1	4	0
Putative trans-sialidase, Group V OS	A0A2V2UPP9	1	4	0
Putative trans-sialidase, Group V OS	A0A2V2US98	0	4	0
Putative trans-sialidase, Group II OS	A0A2V2UWA9	13	4	0
Putative trans-sialidase, Group V OS	A0A2V2VCI9	1	4	0
Putative trans-sialidase, Group VIII OS	A0A2V2WQD7	3	4	0
Trans-sialidase OS	V5B4E0	0	4	0
Putative trans-sialidase, Group V OS	A0A2V2V938	1	4	0
Putative trans-sialidase, Group II OS	A0A2V2UWC5	2	4	0
Trans-sialidase OS	V5CJC4	2	4	0
Putative trans-sialidase, Group VIII OS	A0A2V2V2P3	0	4	0
Trans-sialidase OS	V5AU92	1	4	0
Putative trans-sialidase, Group V OS	A0A2V2V0J7	3	3	0
Putative trans-sialidase, Group II OS	A0A2V2W5Y9	7	3	0
Putative trans-sialidase, Group V OS	A0A2V2W9M9	2	3	0
Putative trans-sialidase, Group II OS	A0A2V2WGE5	6	3	13
Putative trans-sialidase, Group VIII OS	A0A2V2WUF2	19	3	1
Putative trans-sialidase, Group V OS	A0A2V2USE5	1	3	0
Putative trans-sialidase, Group V OS	A0A2V2UNW5	1	3	0
Putative trans-sialidase, Group V OS	A0A2V2UUV3	4	3	0

Putative trans-sialidase, Group V OS	A0A2V2WGW0	0	3	1
Trans-sialidase OS	V5ALY4	1	3	2
Trans-sialidase, putative OS	Q4D095	0	3	2
Putative trans-sialidase, Group VI OS	A0A2V2UWQ5	13	3	0
Putative trans-sialidase, Group V OS	A0A2V2UG39	1	3	0
Group of Putative trans-sialidase, Group II OS	A0A2V2W854 (+1)	7	3	0
Putative trans-sialidase, Group VI OS	A0A2V2VZR0	1	3	0
Putative trans-sialidase, Group V OS	A0A2V2UNU3	1	3	0
Putative trans-sialidase OS	A0A2V2XD07	0	3	0
Trans-sialidase, putative OS	Q4DYM3	13	3	0
Trans-sialidase, putative OS	Q4DV16	10	3	1
Trans-sialidase, putative OS	Q4D825	6	3	0
Putative trans-sialidase, Group VIII OS	A0A2V2VCK6	10	3	0
Trans-sialidase OS	V5CYK7	2	3	0
Putative trans-sialidase, Group VI OS	A0A2V2ULP2	0	3	0
Putative trans-sialidase, Group V OS	A0A2V2UT43	0	3	0
Trans-sialidase, putative (Fragment) OS	Q4DAA5	2	3	0
Trans-sialidase, putative OS	Q4DZD4	1	3	0
Putative trans-sialidase, Group V OS	A0A2V2W455	3	3	1
Trans-sialidase OS	V5AU49	0	3	10
Putative trans-sialidase, Group V OS	A0A2V2WLE1	0	3	0
Trans-sialidase, putative (Fragment) OS	K2MUC0	0	3	1
Trans-sialidase, putative OS	Q4DGZ2	0	3	0
Trans-sialidase OS	V5BBS0	7	3	0
Trans-sialidase OS	V5CIW9	0	3	0
Trans-sialidase OS	V5AT18	1	3	0
Trans-sialidase OS	V5B818	0	3	1
Trans-sialidase, putative OS	K2MUG2	7	3	0

Group of Transaldolase OS	V5BHK0 (+1)	0	3	0
Putative trans-sialidase, Group IV OS	A0A2V2V5I8	0	3	0
Putative trans-sialidase, Group V OS	A0A2V2WM98	2	2	7
Putative trans-sialidase OS	A0A2V2VNM3	5	2	2
Putative trans-sialidase OS	A0A2V2W3P7	4	2	5
Putative trans-sialidase, Group II OS	A0A2V2XE98	4	2	2
Group of Putative trans-sialidase, Group II OS	A0A2V2UMY3 (+1)	10	2	1
Trans-sialidase OS	V5AQ63	2	2	1
Putative trans-sialidase, Group V OS	A0A2V2UX92	1	2	0
Putative trans-sialidase, Group V OS	A0A2V2UJG5	4	2	0
Trans-sialidase, putative OS	Q4E2C0	1	2	1
Putative trans-sialidase OS	A0A2V2VK52	4	2	1
Putative trans-sialidase, Group VI OS	A0A2V2VU44	1	2	0
Trans-sialidase, putative OS	Q4DIE5	1	2	0
Trans-sialidase, putative OS	Q4D2W7	0	2	2
Putative trans-sialidase, Group VI OS	A0A2V2VC38	1	2	0
Putative trans-sialidase, Group V OS	A0A2V2V6R3	1	2	0
Putative trans-sialidase, Group V OS	A0A2V2UFQ4	0	2	0
Trans-sialidase OS	V5AN87	0	2	0
Trans-sialidase, putative OS	Q4D9H3	8	2	0
Trans-sialidase OS	V5API3	0	2	0
Putative trans-sialidase, Group V OS	A0A2V2XKL9	0	2	0
Trans-sialidase, putative OS	K2MP77	1	2	0
Putative trans-sialidase OS	A0A2V2XCE8	4	2	1
Trans-sialidase, putative OS	Q4CXW0	0	2	0
Putative trans-sialidase, Group II OS	A0A2V2W9S6	2	2	0
Putative trans-sialidase OS	A0A2V2VYE7	1	2	0
Putative trans-sialidase, Group II OS	A0A2V2XKQ2	4	2	0



Putative trans-sialidase, Group V OS	A0A2V2XIN0	0	2	0
Trans-sialidase, putative OS	Q4CW78	23	2	0
Putative trans-sialidase, Group VI OS	A0A2V2UX55	1	2	0
Putative trans-sialidase, Group V OS	A0A2V2VWL7	0	2	0
Putative trans-sialidase, Group II OS	A0A2V2W318	4	2	1
Trans-sialidase, putative OS	Q4D2L1	0	2	0
Trans-sialidase, putative OS	Q4DD87	0	2	0
Trans-sialidase, putative OS	Q4DEP9	0	2	0
Trans-sialidase, putative (Fragment) OS	K2PAC6	2	2	0
Putative trans-sialidase, Group II OS	A0A2V2X0R8	1	2	0
Putative trans-sialidase, Group VII OS	A0A2V2V3L7	5	2	0
Putative trans-sialidase, Group V OS	A0A2V2XMA7	0	2	0
Trans-sialidase OS	V5AUQ6	0	2	0
Trans-sialidase, putative OS	Q4D6S1	2	2	0
Putative trans-sialidase, Group VI OS	A0A2V2UXJ0	1	2	1
Putative trans-sialidase, Group V OS	A0A2V2UZ92	1	2	0
Trans-sialidase, putative OS	Q4D1E7	2	2	0
Trans-sialidase, putative OS	Q4DRK0	0	2	1
Putative trans-sialidase, Group III OS	A0A2V2WF29	0	2	10
Putative trans-sialidase, Group V OS	A0A2V2US45	0	2	0
Trans-sialidase, putative OS	Q4DVI7	1	2	1
Trans-sialidase, putative OS	K2N646	11	2	15
Trans-sialidase, putative OS	Q4CTT0	1	2	3
Group of Putative trans-sialidase OS	A0A2V2WFH7 (+1)	4	2	8
Trans-sialidase, putative OS	Q4CX14	2	2	0
Trans-sialidase, putative OS	Q4DE13	2	2	0
Putative trans-sialidase, Group VI OS	A0A2V2V1Q0	1	2	1
Group of Putative trans-sialidase, Group II OS	A0A2V2X653 (+1)	0	2	0

Aspartate aminotransferase OS	Q4CRK6	20	2	0
Putative trans-sialidase, Group VI OS	A0A2V2UXG2	0	2	0
Putative trans-sialidase, Group V OS	A0A2V2V3M2	0	2	0
Putative trans-sialidase OS	A0A2V2UYS5	0	2	0
Putative trans-sialidase, Group II OS	A0A2V2XK66	2	2	0
Trans-sialidase, putative OS	Q4DAK1	0	2	0
Trans-sialidase, putative (Fragment) OS	K2M2T7	0	2	0
Putative trans-sialidase, Group V OS	A0A2V2URS7	0	2	14
Putative trans-sialidase, Group V OS	A0A2V2VLZ3	0	2	0
Putative trans-sialidase, Group VIII OS	A0A2V2XD60	2	2	0
Putative trans-sialidase, Group VII OS	A0A2V2WLK2	0	2	3
Trans-sialidase OS	V5CHP6	0	2	0
Putative trans-sialidase, Group VIII OS	A0A2V2XFS7	0	2	1
Trans-sialidase, putative (Fragment) OS	K2NTC8	0	2	0
Trans-sialidase OS	V5B2F2	0	2	0
Trans-sialidase OS	V5AQU8	0	2	0
Putative trans-sialidase, Group II OS	A0A2V2UXB7	0	2	0
Group of Nuclear transport factor 2, putative OS	Q4CZU2 (+1)	0	2	0
Putative trans-sialidase, Group V OS	A0A2V2WG22	4	1	0
Trans-sialidase, putative OS	Q4DCY7	4	1	0
Putative trans-sialidase, Group V OS	A0A2V2XHC0	3	1	8
Putative trans-sialidase, Group V OS	A0A2V2XG34	2	1	0
Putative trans-sialidase, Group V OS	A0A2V2WNJ0	1	1	1
Putative trans-sialidase, Group II OS	A0A2V2X7F0	4	1	1
Putative trans-sialidase, Group II OS	A0A2V2X6G0	4	1	2
Trans-sialidase, putative OS	Q4DU07	2	1	7
Trans-sialidase, putative OS	Q4CQP5	6	1	9
Putative trans-sialidase, Group II OS	A0A2V2W707	4	1	0

Trans-sialidase, putative OS	Q4CZ95	4	1	0
Putative trans-sialidase, Group V OS	A0A2V2WMI6	1	1	0
Putative trans-sialidase, Group VI OS	A0A2V2WHL9	1	1	1
Putative trans-sialidase, Group V OS	A0A2V2XIH2	1	1	0
Trans-sialidase, putative OS	Q4DDR3	2	1	0
Putative trans-sialidase, Group VI OS	A0A2V2XJN6	1	1	0
Putative trans-sialidase, Group V OS	A0A2V2XAZ6	0	1	1
Trans-sialidase, putative OS	Q4DDR1	1	1	1
Putative trans-sialidase, Group VI OS	A0A2V2WWN4	1	1	1
Putative trans-sialidase, Group V OS	A0A2V2W2V7	0	1	0
Putative trans-sialidase, Group II OS	A0A2V2VTR9	2	1	1
Putative trans-sialidase, Group V OS	A0A2V2W6L0	1	1	1
Putative trans-sialidase OS	A0A2V2WJF2	1	1	0
Putative trans-sialidase, Group V OS	A0A2V2W3Y4	1	1	0
Putative trans-sialidase, Group V OS	A0A2V2V7N6	0	1	0
Putative trans-sialidase, Group II OS	A0A2V2UV35	2	1	0
Trans-sialidase, putative OS	Q4D8V4	4	1	1
Trans-sialidase, putative OS	Q4D110	7	1	0
Trans-sialidase-like protein OS	A4GWE6	2	1	0
Putative trans-sialidase, Group II OS	A0A2V2V1J2	0	1	0
Putative trans-sialidase, Group V OS	A0A2V2XIN5	1	1	0
Putative trans-sialidase, Group V OS	A0A2V2ULE5	1	1	0
Putative trans-sialidase, Group V OS	A0A2V2VSJ9	0	1	0
Putative trans-sialidase, Group V OS	A0A2V2WL79	1	1	0
Putative trans-sialidase, Group V OS	A0A2V2VY01	1	1	0
Putative trans-sialidase, Group V OS	A0A2V2XAU9	2	1	0
Putative trans-sialidase, Group VII OS	A0A2V2X3A6	0	1	0
Putative trans-sialidase, Group V OS	A0A2V2XIR1	1	1	0

Putative trans-sialidase, Group V OS	A0A2V2WE09	0	1	1
Putative trans-sialidase, Group V OS	A0A2V2UVX9	0	1	0
Putative trans-sialidase, Group II OS	A0A2V2VX80	0	1	0
Trans-sialidase, putative (Fragment) OS	K2N470	0	1	4
Putative trans-sialidase, Group II OS	A0A2V2W7M2	2	1	0
Trans-sialidase, putative OS	Q4DV17	7	1	0
Putative trans-sialidase, Group VI OS	A0A2V2UMJ7	1	1	1
Putative trans-sialidase, Group VI OS	A0A2V2VU62	1	1	0
Putative trans-sialidase, Group V OS	A0A2V2XIM4	0	1	0
Trans-sialidase OS	V5BFX6	0	1	0
Putative trans-sialidase, Group II OS	A0A2V2WJ87	0	1	0
Putative trans-sialidase, Group V OS	A0A2V2W035	0	1	0
Trans-sialidase OS	V5AJR1	2	1	4
Trans-sialidase OS	V5B1W5	1	1	0
Putative trans-sialidase, Group V OS	A0A2V2VME2	0	1	0
Trans-sialidase, putative OS	Q4CZ96	0	1	0
Putative trans-sialidase, Group V OS	A0A2V2VLZ7	1	1	8
Trans-sialidase, putative OS	K2MVG8	0	1	0
Trans-sialidase, putative OS	Q4DYC7	0	1	0
Putative trans-sialidase, Group II OS	A0A2V2XHQ4	0	1	0
Trans-sialidase, putative (Fragment) OS	K2LZP9	0	1	0
Nuclear transport factor 2, putative OS	Q4D7W2	0	1	2
Putative trans-sialidase, Group IV OS	A0A2V2WA28	0	1	0
Trans-sialidase, putative OS	Q4D5B9	0	1	0
Trans-sialidase, putative OS	Q4DUP2	1	0	0
Putative trans-sialidase, Group V OS	A0A2V2WW02	1	0	0
Trans-sialidase, putative OS	Q4DA40	2	0	0
Putative trans-sialidase, Group V OS	A0A2V2WJG4	1	0	0

Putative trans-sialidase, Group V OS	A0A2V2WKA9	1	0	0
Trans-sialidase, putative OS	Q4D6J3	0	0	15
Putative retrotransposon hot spot (RHS) protein OS	A0A2V2UJ04	0	0	1
Trans-sialidase, putative OS	Q4DH92	0	0	2
25 kDa translation elongation factor 1-beta OS	Q4CQA2	0	0	1
Phosphotransferase OS	A0A2V2WAH4	0	0	2
Trans-sialidase, putative OS	Q4DKL5	0	0	1

**APPENDIX E: GP63 FAMILY MEMBERS IDENTIFIED IN THE TCT-SECR AND IB-4 LECTIN COLUMN FRACTIONS,  $\alpha$ -GAL(-) AND  $\alpha$ -GAL(+), FROM *T. CRUZI* COL STRAIN. VALUES ARE EXPRESSED AS AVERAGE OF NORMALIZED WEIGHTED SPECTRUM COUNTS.**

Identified Proteins	Accession Number	TCT Secr	$\square$ -Gal(-)	$\square$ -Gal(+)
		Col	(FT)	(EL)
			Col	Col
Putative surface protease GP63 OS	A0A2V2VLZ0	5	20	0
Group of Putative surface protease GP63 OS	A0A2V2V4Z4 (+1)	4	10	0
Putative surface protease GP63 OS	A0A2V2VDF6	5	8	0
Putative surface protease GP63 OS	A0A2V2UG46	6	7	0
Putative surface protease GP63 OS	A0A2V2VA29	5	7	0
Putative surface protease GP63 OS	A0A2V2VBG2	3	7	0
Putative surface protease GP63 OS	A0A2V2V7L6	3	7	0
Group of Putative surface protease GP63 OS	A0A2V2WXU3 (+1)	9	6	0
Putative surface protease GP63 OS	A0A2V2UHN1	6	5	0
Surface protease GP63, putative OS	Q4DHC2	4	4	0
Putative surface protease GP63 OS	A0A2V2W180	4	4	0
Surface protease GP63, putative OS	Q4CWX0	4	4	0
Putative surface protease GP63 OS	A0A2V2WW17	4	4	0
Putative surface protease GP63 OS	A0A2V2USZ8	3	4	0
Group of Putative surface protease GP63 OS	A0A2V2W9Y8 (+1)	0	4	0
Group of Putative surface protease GP63 OS	A0A2V2W871 (+1)	13	3	0
Putative surface protease GP63 OS	A0A2V2VVN8	4	3	0
Putative surface protease GP63 OS	A0A2V2WMB5	4	3	0
Putative surface protease GP63 OS	A0A2V2WK16	4	3	0
Putative surface protease GP63 OS	A0A2V2WF49	2	3	2
Putative surface protease GP63 OS	A0A2V2VWF6	0	3	4

Surface protease GP63, putative OS	Q4CPE5	0	2	2
Surface protease GP63, putative OS	Q4DMQ1	0	2	2
Putative surface protease GP63 OS	A0A2V2V0U4	3	1	2
Putative surface protease GP63 OS	A0A2V2W129	0	1	2
Group of Putative surface protease GP63 OS	A0A2V2UT65 (+1)	0	1	2
Surface protease GP63, putative OS	Q4D7L1	0	1	2
Surface protease GP63, putative OS	Q4E479	0	1	2
Surface protease GP63 OS	V5A488	0	1	3
Putative surface protease GP63 OS	A0A2V2WU92	0	1	4
Putative surface protease GP63 OS	A0A2V2WGP4	7	0	0

**APPENDIX F: : TcMUC II FAMILY MEMBERS IDENTIFIED IN THE TCT-SECR AND IB-4 LECTIN COLUMN FRACTIONS,  $\alpha$ -GAL(-) AND  $\alpha$ -GAL(+), FROM *T. CRUZI* Y STRAIN. VALUES ARE EXPRESSED AS AVERAGE OF NORMALIZED WEIGHTED SPECTRUM COUNTS.**

Identified Proteins	Accession Number	TCT Secr Y	$\alpha$ -Gal(-) (FT) Y	$\alpha$ -Gal(+) (EL) Y
Putative mucin TcMUCII OS	A0A2V2W2D1	1	3	82
Group of Putative mucin TcMUCII OS	A0A2V2X5V1 (+1)	0	2	60
Putative mucin TcMUCII OS	A0A2V2WR81	0	1	52
Mucin TcMUCII, putative OS	Q4CYF9	0	1	39
Putative mucin TcMUCII OS	A0A2V2W0S7	0	1	35
Putative mucin TcMUCII OS	A0A2V2W3F2	0	2	35
Putative mucin TcMUCII OS	A0A2V2VUI0	0	1	27
Putative mucin TcMUCII OS	A0A2V2WMF7	0	2	27
Mucin TcMUCII, putative OS	Q4E071	0	0	26
Putative mucin TcMUCII OS	A0A2V2WSQ6	4	3	22
Mucin TcMUCII, putative OS	Q4E2C3	0	1	22
Mucin TcMUCII, putative OS	Q4D7L0	0	1	22
Group of Mucin TcMUCII, putative OS	Q4DCZ1 (+1)	0	1	22
Putative mucin TcMUCII OS	A0A2V2WHE6	0	1	22
Putative mucin TcMUCII OS	A0A2V2VNS3	0	1	22
Mucin TcMUCII, putative OS	Q4E3U5	0	2	20
Mucin TcMUCII, putative OS	Q4E3V3	0	1	19
Group of Putative mucin TcMUCII OS	A0A2V2XGB5 (+1)	0	2	15
Mucin TcMUCII, putative OS	Q4E2B0	0	2	15
Mucin TcMUCII, putative OS	Q4DIE3	0	2	15
Mucin TcMUCII, putative OS	Q4DM06	0	2	15



Putative mucin TcMUCII OS	A0A2V2W791	0	1	15
Putative mucin TcMUCII OS	A0A2V2X2R6	0	1	15
Putative mucin TcMUCII OS	A0A2V2UYP8	0	1	15
Group of Putative mucin TcMUCII OS	A0A2V2X537 (+2)	0	1	15
Putative mucin TcMUCII OS	A0A2V2XCR2	0	1	15
Mucin TcMUCII OS	V5AN33	0	1	15
Mucin TcMUCII, putative OS	Q4DM13	0	1	15
Putative mucin TcMUCII OS	A0A2V2XG98	0	1	15
Putative mucin TcMUCII OS	A0A2V2WVM0	0	0	15
Putative mucin TcMUCII OS	A0A2V2W6K6	0	0	12
Mucin TcMUCII, putative OS	Q4E3D1	0	1	10
Mucin TcMUCII, putative OS	Q4D1J6	0	0	9
Mucin TcMUCII, putative OS	Q4CS53	0	3	7
Putative mucin TcMUCII OS	A0A2V2WWU0	0	2	7
Mucin TcMUCII, putative OS	Q4DFV4	0	2	7
Putative mucin TcMUCII OS	A0A2V2W5L6	0	2	7
Mucin TcMUCII, putative OS	Q4CZ01	0	2	7
Putative mucin TcMUCII OS	A0A2V2W6F4	0	2	7
Putative mucin TcMUCII OS	A0A2V2XHA2	0	1	7
Putative mucin TcMUCII OS	A0A2V2WCN5	0	1	7
Group of Mucin TcMUCII, putative OS	Q4CTN4 (+1)	0	1	7
Mucin TcMUCII, putative OS	Q4DIF2	0	1	7
Putative mucin TcMUCII OS	A0A2V2UPQ0	0	1	7
Mucin TcMUCII, putative OS	Q4DYV6	0	1	7
Putative mucin TcMUCII OS	A0A2V2VP28	0	1	7
Putative mucin TcMUCII OS	A0A2V2WUP0	0	1	7
Mucin TcMUCII, putative OS	Q4E5W2	1	1	7
Putative mucin TcMUCII OS	A0A2V2XK83	1	1	7

Putative mucin TcMUCII OS	A0A2V2UZS3	0	1	5
Putative mucin TcMUCII OS	A0A2V2VDG1	0	1	5
Putative mucin TcMUCII OS	A0A2V2UUV8	0	0	5
Putative mucin TcMUCII OS	A0A2V2X8S8	0	3	4
Putative mucin TcMUCII OS	A0A2V2UZ94	0	3	4
Mucin TcMUCII, putative OS	Q4E056	0	1	4
Putative mucin TcMUCII OS	A0A2V2XAT0	0	1	4
Putative mucin TcMUCII OS	A0A2V2X3L4	0	2	2
Putative mucin TcMUCII OS	A0A2V2WWP4	0	1	2
Mucin TcMUCII, putative OS	Q4E4X4	0	1	2
Putative mucin TcMUCII OS	A0A2V2W3E7	0	0	2
Putative mucin TcMUCII OS	A0A2V2VX53	0	0	2
Mucin TcMUCII, putative OS	Q4E4X7	0	4	0
Mucin TcMUCII, putative OS	Q4E3E1	0	3	0
Group of Mucin TcMUCII, putative OS	Q4D803 (+1)	0	3	0
Putative mucin TcMUCII OS	A0A2V2UKD3	0	2	0
Putative mucin TcMUCII OS	A0A2V2XML1	0	2	0
Putative mucin TcMUCII OS	A0A2V2VZU2	0	2	0
Mucin TcMUCII, putative OS	Q4CX28	0	2	0
Mucin TcMUCII, putative OS	Q4DFV7	0	2	0
Putative mucin TcMUCII OS	A0A2V2VXI3	0	1	0
Putative mucin TcMUCII OS	A0A2V2W411	0	1	0
Putative mucin TcMUCII OS	A0A2V2WM81	0	1	0
Mucin TcMUCII, putative OS	Q4D8A2	0	1	0
Mucin TcMUCII, putative OS	Q4CWZ6	0	1	0
Putative mucin TcMUCII OS	A0A2V2USA7	0	1	0
Mucin TcMUCII, putative OS	Q4DQS1	0	1	0
Mucin TcMUCII, putative OS	Q4D8R2	0	1	0

Putative mucin TcMUCII OS	A0A2V2WMF2	0	1	0
Putative mucin TcMUCII OS	A0A2V2WHK8	0	1	0
Mucin TcMUCII, putative OS	Q4DN81	0	1	0
Putative mucin TcMUCII OS	A0A2V2X7I5	0	1	0
Putative mucin TcMUCII OS	A0A2V2W572	0	1	0
Putative mucin TcMUCII OS	A0A2V2W1H5	0	1	0
Mucin TcMUCII, putative OS	Q4CT04	0	1	0
Mucin TcMUCII, putative OS	Q4CUT4	0	1	0
Putative mucin TcMUCII OS	A0A2V2XAT9	0	1	0
Mucin TcMUCII, putative OS	Q4DF63	0	1	0
Putative mucin TcMUCII OS	A0A2V2XHD6	0	1	0
Putative mucin TcMUCII OS	A0A2V2W6Y7	0	1	0
Putative mucin TcMUCII OS	A0A2V2VZQ6	0	1	0
Group of Mucin TcMUCII OS	V5ASM5 (+1)	0	1	0
Putative mucin TcMUCII OS	A0A2V2UWU8	0	1	0
Putative mucin TcMUCII OS	A0A2V2UN14	0	1	0
Group of Putative mucin TcMUCII OS	A0A2V2V7J2 (+1)	0	1	0

**APPENDIX G: MASP FAMILY MEMBERS IDENTIFIED IN THE TCT-SECR AND IN THE IB4-LECTIN COLUMN FRACTIONS,  $\alpha$ -GAL(-) AND  $\alpha$ -GAL(+), FROM *T. CRUZI* Y STRAIN. VALUES ARE EXPRESSED AS AVERAGE OF NORMALIZED WEIGHTED SPECTRUM COUNTS.**

Identified Proteins	Accession Number	TCT Secr Y	$\alpha$ -Gal(-) (FT) Y	$\alpha$ -Gal(+) (EL) Y
Mucin-associated surface protein (MASP) OS	A0A2V2W7A5	1	6	0
Group of Mucin-associated surface protein (MASP) OS	A0A2V2X5L7 (+1)	0	6	0
Mucin-associated surface protein (MASP) OS	A0A2V2VCX7	0	5	0
Mucin-associated surface protein (MASP) OS	A0A2V2WF02	0	5	0
Group of Mucin-associated surface protein (MASP) OS	V5BF77 (+1)	4	4	0
Mucin-associated surface protein (MASP) OS	A0A2V2W7B2	2	4	0
Mucin-associated surface protein (MASP) OS	A0A2V2VC34	0	4	0
Mucin-associated surface protein (MASP) OS	A0A2V2WC30	0	4	0
Mucin-associated surface protein (MASP) OS	A0A2V2W752	1	3	0
Mucin-associated surface protein (MASP) OS	A0A2V2US81	0	3	0
Group of Mucin-associated surface protein (MASP) OS	V5BBK7 (+1)	0	3	0
Mucin-associated surface protein (MASP) OS	A0A2V2VRB7	0	3	0
Mucin-associated surface protein (MASP) OS	A0A2V2W3E2	0	3	0
Mucin-associated surface protein (MASP) OS	A0A2V2WP56	0	3	0
Mucin-associated surface protein (MASP), putative OS	Q4E1Y4	0	3	0
Mucin-associated surface protein (MASP) OS	A0A2V2X2N1	0	3	0
Mucin-associated surface protein (MASP), putative OS	Q4D953	0	3	0
Group of Mucin-associated surface protein (MASP) OS	A0A2V2XGK1 (+1)	0	3	0
Mucin-associated surface protein (MASP), putative OS	Q4CVH5	0	3	0
Mucin-associated surface protein (MASP), putative OS	Q4CQC5	0	3	0
Mucin-associated surface protein (MASP) OS	A0A2V2V8I6	0	3	0

Mucin-associated surface protein (MASP), putative OS	Q4E1H4	0	3	0
Mucin-associated surface protein (MASP) OS	A0A2V2WA58	0	3	0
Mucin-associated surface protein (MASP) OS	A0A2V2X4B4	0	3	0
Mucin-associated surface protein (MASP) OS	A0A2V2UR06	0	2	0
Mucin-associated surface protein (MASP) OS	A0A2V2UXX1	1	2	0
Mucin-associated surface protein (MASP) OS	A0A2V2WFY4	1	2	0
Mucin-associated surface protein (MASP) OS	A0A2V2V2H3	0	2	0
Mucin-associated surface protein (MASP) OS	A0A2V2UT67	0	2	0
Group of Mucin-associated surface protein (MASP) OS	V5D4V1 (+1)	0	2	0
Mucin-associated surface protein (MASP) OS	A0A2V2W0H0	0	2	0
Mucin-associated surface protein (MASP) OS	A0A2V2WXA7	0	2	0
Mucin-associated surface protein (MASP) OS	A0A2V2XIJ2	0	2	0
Mucin-associated surface protein (MASP) OS	A0A2V2XPF9	0	2	0
Group of Mucin-associated surface protein (MASP) OS	V5CKL1 (+1)	0	2	0
Mucin-associated surface protein (MASP) OS	A0A2V2V018	0	2	0
Mucin-associated surface protein (MASP) OS	A0A2V2UGU2	2	2	0
Mucin-associated surface protein (MASP), putative OS	Q4E1Z5	0	2	0
Mucin-associated surface protein (MASP) OS	A0A2V2W6S9	0	2	0
Group of Mucin-associated surface protein (MASP) OS	A0A2V2XMG7 (+1)	0	2	0
Mucin-associated surface protein (MASP), putative OS	Q4DR50	0	2	0
Mucin-associated surface protein (MASP) OS	A0A2V2VZS0	0	2	0
Mucin-associated surface protein (MASP) OS	A0A2V2W2Z4	0	2	0
Mucin-associated surface protein (MASP) OS	A0A2V2UU16	2	2	0
Mucin-associated surface protein (MASP) OS	A0A2V2W560	0	2	0
Mucin-associated surface protein (MASP), putative OS	Q4D521	0	2	0
Mucin-associated surface protein (MASP) OS	A0A2V2VXG3	0	2	0
Mucin-associated surface protein (MASP) OS	A0A2V2VE10	0	2	0
Mucin-associated surface protein (MASP) OS	A0A2V2VDA6	0	2	0

Mucin-associated surface protein (MASP), putative OS	Q4E3U8	0	2	4
Mucin-associated surface protein (MASP) OS	A0A2V2UVJ7	0	2	0
Mucin-associated surface protein (MASP) OS	A0A2V2VN01	0	2	0
Mucin-associated surface protein (MASP) OS	A0A2V2V3J6	0	2	0
Mucin-associated surface protein (MASP) OS	A0A2V2V788	0	2	0
Mucin-associated surface protein (MASP) OS	A0A2V2V9R2	0	2	0
Mucin-associated surface protein (MASP) OS	A0A2V2XM77	0	2	0
Mucin-associated surface protein (MASP), putative OS	Q4CX27	0	2	0
Mucin-associated surface protein (MASP), putative OS	Q4DQA3	0	2	0
Mucin-associated surface protein (MASP) OS	A0A2V2W137	0	2	0
Mucin-associated surface protein (MASP) OS	A0A2V2XMK1	0	2	0
Mucin-associated surface protein (MASP) OS	A0A2V2WL91	0	2	0
Mucin-associated surface protein (MASP), putative OS	Q4CWA9	0	2	0
Mucin-associated surface protein (MASP) OS	A0A2V2XIP9	0	2	0
Mucin-associated surface protein (MASP), putative OS	Q4D839	0	2	0
Mucin-associated surface protein (MASP) OS	A0A2V2X4Z6	0	2	0
Mucin-associated surface protein (MASP), putative OS	Q4E468	0	2	0
Mucin-associated surface protein (MASP), putative OS	Q4CQD2	0	2	0
Mucin-associated surface protein (MASP) OS	A0A2V2WUK7	0	2	0
Mucin-associated surface protein (MASP) OS	A0A2V2WM66	0	2	0
Mucin-associated surface protein (MASP), putative OS	Q4E3E0	0	2	0
Group of Mucin-associated surface protein (MASP) OS	A0A2V2XBB8 (+6)	0	2	0
Mucin-associated surface protein (MASP) OS	A0A2V2XAG0	0	2	0
Group of Mucin-associated surface protein (MASP) OS	A0A2V2X506 (+1)	0	2	0
Mucin-associated surface protein (MASP), putative OS	Q4D4U0	0	2	0
Mucin-associated surface protein (MASP) OS	A0A2V2W0R7	0	2	0
Mucin-associated surface protein (MASP) OS	A0A2V2X2Y8	0	2	0
Mucin-associated surface protein (MASP), putative (Fragment) OS	Q4CNN7	0	2	0

Mucin-associated surface protein (MASP) OS	A0A2V2WXU6	0	2	0
Mucin-associated surface protein (MASP), putative OS	Q4DT31	0	2	0
Group of Mucin-associated surface protein (MASP) OS	V5B7H5 (+1)	2	1	0
Mucin-associated surface protein (MASP) OS	A0A2V2VDP8	1	1	0
Mucin-associated surface protein (MASP), putative OS	Q4E3V5	2	1	0
Mucin-associated surface protein (MASP) OS	A0A2V2VIJ8	1	1	0
Group of Mucin-associated surface protein (MASP) OS	V5D3M1 (+1)	2	1	0
Mucin-associated surface protein (MASP), putative OS	Q4E194	0	1	0
Mucin-associated surface protein (MASP) OS	A0A2V2VM18	0	1	0
Mucin-associated surface protein (MASP) OS	V5BBT4	0	1	0
Mucin-associated surface protein (MASP) OS	A0A2V2W3L1	0	1	0
Mucin-associated surface protein (MASP) OS	A0A2V2UT23	0	1	0
Group of Mucin-associated surface protein (MASP) OS	V5AL36 (+1)	0	1	0
Mucin-associated surface protein (MASP) OS	A0A2V2XKW2	0	1	0
Mucin-associated surface protein (MASP) OS	A0A2V2WUL8	0	1	0
Mucin-associated surface protein (MASP) OS	A0A2V2WSD9	0	1	0
Mucin-associated surface protein (MASP) OS	A0A2V2W0A5	0	1	0
Mucin-associated surface protein (MASP) OS	A0A2V2W5T1	0	1	0
Mucin-associated surface protein (MASP) OS	A0A2V2W3J0	1	1	0
Mucin-associated surface protein (MASP) OS	A0A2V2W5I4	0	1	0
Mucin-associated surface protein (MASP) OS	A0A2V2VF80	0	1	0
Mucin-associated surface protein (MASP) OS	A0A2V2W399	0	1	0
Group of Mucin-associated surface protein (MASP) OS	V5B2C2 (+1)	0	1	0
Mucin-associated surface protein (MASP) OS	A0A2V2VQW1	0	1	0
Mucin-associated surface protein (MASP) OS	V5B2W7	0	1	0
Mucin-associated surface protein (MASP) OS	A0A2V2VXC7	0	1	0
Mucin-associated surface protein (MASP) OS	A0A2V2V826	0	1	0

tr A0A2V2XI47-DECOY A0A2V2XI47-DECOY_TRYCR Mucin-associated surface protein (MASP)...	A0A2V2XI47-DECOY	0	1	0
Mucin-associated surface protein (MASP) OS	A0A2V2V0H1	0	1	0
Mucin-associated surface protein (MASP), putative OS	Q4D782	0	1	0
Mucin-associated surface protein (MASP) OS	A0A2V2V1F6	0	1	0
Mucin-associated surface protein (MASP) OS	A0A2V2W6I1	0	1	0
Mucin-associated surface protein (MASP) OS	A0A2V2V9K3	0	1	0
Mucin-associated surface protein (MASP) OS	A0A2V2VQS5	0	1	0
Mucin-associated surface protein (MASP) OS	A0A2V2V3P2	0	1	0
Mucin-associated surface protein (MASP) OS	A0A2V2VNG6	0	1	0
Mucin-associated surface protein (MASP) OS	A0A2V2W6F2	0	1	0
Mucin-associated surface protein (MASP), putative OS	Q4E1Y9	0	1	4
Mucin-associated surface protein (MASP) OS	A0A2V2VBR6	0	1	0
Mucin-associated surface protein (MASP) OS	A0A2V2UT92	0	1	0
Mucin-associated surface protein (MASP) OS	A0A2V2UV69	0	1	0
Mucin-associated surface protein (MASP) OS	V5BBL1	0	1	0
Mucin-associated surface protein (MASP) OS	A0A2V2UMB9	0	1	0
Mucin-associated surface protein (MASP) OS	A0A2V2URE0	0	1	0
Mucin-associated surface protein (MASP) OS	V5BFG7	0	1	0
Mucin-associated surface protein (MASP) OS	A0A2V2VQ46	0	1	0
Mucin-associated surface protein (MASP) OS	A0A2V2VMA1	0	1	0
Group of Mucin-associated surface protein (MASP) OS	A0A2V2WTX4 (+1)	0	1	0
Mucin-associated surface protein (MASP), putative OS	Q4D1G4	0	1	0
Mucin-associated surface protein (MASP), putative OS	Q4D998	0	1	0
Group of Mucin-associated surface protein (MASP) OS	V5BBB0 (+1)	0	1	0
Mucin-associated surface protein (MASP) OS	A0A2V2UQX5	0	1	0
Mucin-associated surface protein (MASP) OS	A0A2V2V1K7	0	1	0
Mucin-associated surface protein (MASP), putative OS	Q4DJL2	0	1	0



Mucin-associated surface protein (MASP) OS	V5A3C9	0	1	0
Mucin-associated surface protein (MASP) OS	A0A2V2XAE3	0	1	0
Mucin-associated surface protein (MASP) OS	A0A2V2X238	0	1	0
Mucin-associated surface protein (MASP) OS	A0A2V2URTO	0	1	0
Mucin-associated surface protein (MASP) OS	A0A2V2UQD4	0	1	0
Mucin-associated surface protein (MASP) OS	A0A2V2V9X2	0	1	0
Mucin-associated surface protein (MASP) OS	A0A2V2UXG6	0	1	0
Mucin-associated surface protein (MASP) OS	A0A2V2V5W8	0	1	0
Mucin-associated surface protein (MASP) OS	A0A2V2VD54	0	1	0
Group of Mucin-associated surface protein (MASP) OS	A0A2V2W3N4 (+1)	0	1	0
Mucin-associated surface protein (MASP) OS	V5BF73	0	1	0
Mucin-associated surface protein (MASP) OS	A0A2V2UZD0	0	1	0
Group of Mucin-associated surface protein (MASP) OS	V5D744 (+1)	0	1	0
Mucin-associated surface protein (MASP) OS	A0A2V2VX77	0	1	0
Mucin-associated surface protein (MASP), putative OS	Q4E380	0	1	0
Mucin-associated surface protein (MASP), putative OS	Q4DXP7	0	1	0
Mucin-associated surface protein (MASP), putative OS	Q4E493	0	1	0
Group of Mucin-associated surface protein (MASP) OS	V5AZK4 (+1)	0	1	0
Mucin-associated surface protein (MASP) OS	A0A2V2VW08	0	1	0
Mucin-associated surface protein (MASP) OS	A0A2V2USB3	0	1	0
Mucin-associated surface protein (MASP), putative OS	Q4E455	0	1	0
Mucin-associated surface protein (MASP) OS	V5BFX0	0	1	0
Group of Mucin-associated surface protein (MASP) OS	V5AUG7 (+1)	0	1	7
Mucin-associated surface protein (MASP) OS	V5D3A6	0	1	0
Mucin-associated surface protein (MASP) OS	A0A2V2W529	0	1	0
Mucin-associated surface protein (MASP) OS	A0A2V2VBN9	0	1	0
Mucin-associated surface protein (MASP) OS	A0A2V2W311	0	1	0
Group of Mucin-associated surface protein (MASP) OS	A0A2V2USV3 (+1)	0	1	0

Mucin-associated surface protein (MASP) OS	A0A2V2WZX1	0	1	0
Mucin-associated surface protein (MASP) OS	A0A2V2VT61	0	1	0
Mucin-associated surface protein (MASP) OS	A0A2V2WB84	0	1	0
Mucin-associated surface protein (MASP) OS	A0A2V2XBD0	0	1	0
Mucin-associated surface protein (MASP) OS	A0A2V2XAR2	0	1	0
Mucin-associated surface protein (MASP), putative OS	Q4CSJ9	0	1	0
Group of Mucin-associated surface protein (MASP) OS	A0A2V2V7A8 (+1)	0	1	0
Mucin-associated surface protein (MASP) OS	A0A2V2XJI1	0	1	0
Mucin-associated surface protein (MASP) OS	A0A2V2XC70	0	1	0
Mucin-associated surface protein (MASP) OS	A0A2V2XCN3	0	1	0
Mucin-associated surface protein (MASP) OS	A0A2V2UYK3	0	1	0
Mucin-associated surface protein (MASP), putative OS	Q4E1A8	0	1	0
Mucin-associated surface protein (MASP) OS	A0A2V2VZM8	0	1	0
Mucin-associated surface protein (MASP) OS	V5B9Y3	0	1	0
Mucin-associated surface protein (MASP) OS	A0A2V2XM45	0	1	0
Mucin-associated surface protein (MASP) OS	A0A2V2WUI5	0	1	0
Group of Mucin-associated surface protein (MASP) OS	V5AJ74 (+2)	0	1	0
Mucin-associated surface protein (MASP) OS	A0A2V2W061	0	1	0
Group of Mucin-associated surface protein (Fragment) OS	G4V514 (+4)	0	1	0
Mucin-associated surface protein (MASP) OS	A0A2V2WAR3	0	1	0
Mucin-associated surface protein (MASP), putative OS	Q4DGU9	0	1	0
Group of Mucin-associated surface protein (MASP) OS	A0A2V2UPB4 (+1)	0	1	0
Mucin-associated surface protein (MASP) OS	V5B3Q9	0	1	0
Mucin-associated surface protein (MASP) OS	A0A2V2W9G6	0	1	0
Group of Mucin-associated surface protein (MASP) OS	A0A2V2USP5 (+4)	0	1	0
Mucin-associated surface protein (MASP) OS	A0A2V2W1L6	0	1	0
Mucin-associated surface protein (MASP) OS	A0A2V2UWT9	0	1	0
Mucin-associated surface protein (MASP) OS	A0A2V2X979	0	1	0

Mucin-associated surface protein (MASP) OS	A0A2V2W8U1	0	1	0
Mucin-associated surface protein (MASP) OS	A0A2V2V087	0	1	0
Mucin-associated surface protein (MASP) OS	A0A2V2W6J7	0	1	0
Mucin-associated surface protein (MASP) OS	A0A2V2W6N8	0	1	0
Mucin-associated surface protein (MASP), putative OS	Q4DGB8	0	1	0
Mucin-associated surface protein (MASP) OS	A0A2V2UU89	0	1	0
Mucin-associated surface protein (MASP), putative (Fragment) OS	Q4CLC5	0	1	0
Mucin-associated surface protein (MASP), putative OS	Q4DN82	0	1	0
Mucin-associated surface protein (MASP), putative OS	Q4DE04	0	1	0
Mucin-associated surface protein (MASP), putative OS	Q4CS03	0	1	0
Mucin-associated surface protein (MASP) OS	A0A2V2XKD8	1	0	0
Mucin-associated surface protein (MASP) OS	A0A2V2UQ49	1	0	0

**APPENDIX H: TS FAMILY MEMBERS IDENTIFIED IN TCT-SECR AND IN THE IB4-LECTIN COLUMN FRACTIONS,  $\alpha$ -GAL(-) AND  $\alpha$ -GAL(+), FROM Y STRAIN. VALUES ARE EXPRESSED AS AVERAGE OF NORMALIZED WEIGHTED SPECTRUM COUNTS.**

<b>Identified Proteins</b>	<b>Accession Number</b>	<b>TCT Secr Y</b>	<b><math>\alpha</math>-Gal(-) (FT) Y</b>	<b><math>\alpha</math>-Gal(+) (EL) Y</b>
Putative trans-sialidase, Group I OS	A0A2V2UW10	20	10	7
Trans-sialidase, putative OS	Q4DA40	18	10	0
Trans-sialidase, putative OS	Q4DTW4	0	10	0
Trans-sialidase, putative OS	Q4DH92	0	10	0
Putative trans-sialidase, Group VI OS	A0A2V2WHL9	0	8	0
Trans-sialidase, putative OS	Q4DCY7	2	8	0
Trans-sialidase, putative OS	Q4DIN1	0	8	0
Group of Putative trans-sialidase, Group II OS	A0A2V2W854 (+1)	9	7	0
Putative trans-sialidase, Group V OS	A0A2V2WG22	2	7	0
Putative trans-sialidase, Group V OS	A0A2V2WM98	10	7	0
Putative trans-sialidase, Group VII OS	A0A2V2X3A6	1	7	0
Trans-sialidase OS	Q26969	11	7	0
Trans-sialidase, putative OS	Q4D9H3	17	7	0
Group of Putative trans-sialidase OS	A0A2V2XDR2 (+1)	8	6	0
Putative trans-sialidase, Group I OS	A0A2V2WSP5	9	6	0
Putative trans-sialidase, Group II OS	A0A2V2XE98	0	6	0
Putative trans-sialidase, Group V OS	A0A2V2VJ94	3	6	0
Trans-sialidase, putative OS	Q4DVJ1	3	6	0
Group of Putative trans-sialidase, Group II OS	A0A2V2X653 (+1)	4	5	0
Putative trans-sialidase OS	A0A2V2VNM3	3	5	0
Putative trans-sialidase OS	A0A2V2VK52	3	5	0

Putative trans-sialidase OS	A0A2V2WFX7	0	5	0
Putative trans-sialidase OS	A0A2V2WB08	0	5	0
Putative trans-sialidase, Group I OS	A0A2V2X1Q1	8	5	0
Putative trans-sialidase, Group I OS	A0A2V2WXL6	9	5	0
Putative trans-sialidase, Group II OS	A0A2V2VAS5	8	5	11
Putative trans-sialidase, Group II OS	A0A2V2W9S6	1	5	0
Putative trans-sialidase, Group V OS	A0A2V2XHC0	1	5	0
Putative trans-sialidase, Group V OS	A0A2V2WNJ0	10	5	0
Trans-sialidase (Fragment) OS	B3VSM6	7	5	0
Trans-sialidase, putative OS	Q4DQ76	6	5	0
Trans-sialidase, putative OS	Q4CTX4	9	5	0
Trans-sialidase, putative OS	Q4CX14	4	5	0
Putative trans-sialidase OS	A0A2V2XD07	1	4	0
Putative trans-sialidase, Group I OS	A0A2V2UQ56	6	4	0
Putative trans-sialidase, Group II OS	A0A2V2X7F0	8	4	0
Putative trans-sialidase, Group II OS	A0A2V2X6G0	4	4	0
Putative trans-sialidase, Group II OS	A0A2V2XKQ2	9	4	0
Putative trans-sialidase, Group II OS	A0A2V2V1J2	8	4	0
Putative trans-sialidase, Group II OS	A0A2V2X5M9	6	4	0
Putative trans-sialidase, Group II OS	A0A2V2WZJ7	6	4	0
Putative trans-sialidase, Group II OS	A0A2V2XLR9	0	4	0
Putative trans-sialidase, Group V OS	A0A2V2XG34	1	4	0
Putative trans-sialidase, Group V OS	A0A2V2VXJ5	2	4	0
Putative trans-sialidase, Group V OS	A0A2V2W9M9	5	4	0
Putative trans-sialidase, Group V OS	A0A2V2VEF1	2	4	0
Putative trans-sialidase, Group V OS	A0A2V2XMA7	3	4	0
Trans-sialidase, putative OS	Q4E2C0	0	4	0
Trans-sialidase, putative OS	Q4CXW0	7	4	0

Trans-sialidase, putative OS	Q4DTW9	0	4	0
Trans-sialidase, putative OS	Q4D8V4	11	4	0
Group of TS-193 trans-sialidase homolog protein OS	Q4R2T0 (+1)	8	3	0
Putative trans-sialidase, Group I OS	A0A2V2VQS7	9	3	0
Putative trans-sialidase, Group I OS	A0A2V2X778	6	3	0
Putative trans-sialidase, Group I OS	A0A2V2VZH5	8	3	0
Putative trans-sialidase, Group II OS	A0A2V2W707	9	3	0
Putative trans-sialidase, Group II OS	A0A2V2VX80	0	3	0
Putative trans-sialidase, Group II OS	A0A2V2WJ87	1	3	0
Putative trans-sialidase, Group V OS	A0A2V2VF87	2	3	0
Putative trans-sialidase, Group V OS	A0A2V2XAZ6	0	3	0
Putative trans-sialidase, Group V OS	A0A2V2XAU9	0	3	0
Putative trans-sialidase, Group VII OS	A0A2V2WLK2	1	3	0
Trans-sialidase, putative OS	Q4CZ95	0	3	0
Trans-sialidase, putative OS	Q4DBE7	0	3	0
Trans-sialidase, putative OS	Q4DV16	8	3	0
Trans-sialidase, putative OS	Q4E0C8	0	3	0
Group of Putative trans-sialidase, Group II OS	A0A2V2W161 (+1)	6	2	0
Putative trans-sialidase OS	A0A2V2V2Z5	1	2	0
Putative trans-sialidase OS	A0A2V2V3I5	1	2	0
Putative trans-sialidase, Group I OS	A0A2V2VMW6	5	2	0
Putative trans-sialidase, Group II OS	A0A2V2ULD3	1	2	0
Putative trans-sialidase, Group II OS	A0A2V2VTR9	4	2	0
Putative trans-sialidase, Group II OS	A0A2V2UWA9	3	2	0
Putative trans-sialidase, Group II OS	A0A2V2W318	3	2	0
Putative trans-sialidase, Group II OS	A0A2V2WFJ2	0	2	0
Putative trans-sialidase, Group II OS	A0A2V2XHQ4	0	2	0
Putative trans-sialidase, Group II OS	A0A2V2X219	0	2	0

Putative trans-sialidase, Group III OS	A0A2V2UU80	1	2	0
Putative trans-sialidase, Group V OS	A0A2V2V8D0	2	2	0
Putative trans-sialidase, Group V OS	A0A2V2UJV5	1	2	0
Putative trans-sialidase, Group V OS	A0A2V2UYR0	1	2	0
Putative trans-sialidase, Group V OS	A0A2V2UQK6	2	2	0
Putative trans-sialidase, Group V OS	A0A2V2VXN3	1	2	0
Putative trans-sialidase, Group V OS	A0A2V2W442	1	2	0
Putative trans-sialidase, Group V OS	A0A2V2VXA3	0	2	0
Putative trans-sialidase, Group V OS	A0A2V2VXJ2	0	2	0
Putative trans-sialidase, Group V OS	A0A2V2UWJ2	0	2	0
Putative trans-sialidase, Group V OS	A0A2V2WGW0	1	2	0
Putative trans-sialidase, Group V OS	A0A2V2WMI6	1	2	0
Putative trans-sialidase, Group V OS	A0A2V2XIH2	2	2	0
Putative trans-sialidase, Group V OS	A0A2V2UFQ4	3	2	0
Putative trans-sialidase, Group V OS	A0A2V2VCG1	0	2	0
Putative trans-sialidase, Group V OS	A0A2V2US98	1	2	0
Putative trans-sialidase, Group V OS	A0A2V2W424	0	2	0
Putative trans-sialidase, Group V OS	A0A2V2WKA9	0	2	0
Putative trans-sialidase, Group VII OS	A0A2V2VNA5	1	2	0
Putative trans-sialidase, Group VIII OS	A0A2V2UTK4	0	2	0
Putative trans-sialidase, Group VIII OS	A0A2V2VGF6	0	2	0
Trans-sialidase OS	V5B004	0	2	0
Trans-sialidase OS	V5AMT0	0	2	0
Trans-sialidase, putative OS	Q4DU07	1	2	0
Trans-sialidase, putative OS	Q4CQP5	1	2	0
Trans-sialidase, putative OS	Q4D2W7	3	2	0
Trans-sialidase, putative OS	Q4DDR1	0	2	0
Trans-sialidase, putative OS	Q4DYM3	3	2	0

Trans-sialidase, putative OS	Q4D825	1	2	0
Trans-sialidase, putative OS	Q4DEP9	1	2	0
Trans-sialidase, putative OS	Q4DZD4	3	2	0
Trans-sialidase, putative OS	Q4DRK0	2	2	0
Trans-sialidase, putative OS	Q4DVI7	1	2	0
Trans-sialidase, putative OS	Q4DV17	0	2	0
Trans-sialidase, putative OS	Q4CSS2	0	2	0
Trans-sialidase, putative OS	Q4DYC7	0	2	0
Trans-sialidase, putative OS	Q4DKL5	0	2	0
Group of Putative trans-sialidase OS	A0A2V2WFH7 (+1)	0	1	0
Group of Putative trans-sialidase, Group II OS	A0A2V2UMY3 (+1)	6	1	0
Group of Putative trans-sialidase, Group II OS	A0A2V2UVV3 (+1)	2	1	0
Group of Putative trans-sialidase, Group II OS	A0A2V2XD71 (+1)	0	1	0
Group of Putative trans-sialidase, Group III OS	A0A2V2UVW1 (+1)	1	1	0
Putative trans-sialidase OS	A0A2V2WJF2	0	1	0
Putative trans-sialidase OS	A0A2V2XCE8	3	1	0
Putative trans-sialidase, Group II OS	A0A2V2W5Y9	3	1	0
Putative trans-sialidase, Group II OS	A0A2V2WGE5	1	1	0
Putative trans-sialidase, Group II OS	A0A2V2UHM8	1	1	0
Putative trans-sialidase, Group II OS	A0A2V2V0H5	0	1	0
Putative trans-sialidase, Group II OS	A0A2V2V1F7	5	1	0
Putative trans-sialidase, Group II OS	A0A2V2UZ79	0	1	0
Putative trans-sialidase, Group II OS	A0A2V2UV35	3	1	0
Putative trans-sialidase, Group II OS	A0A2V2UIK4	0	1	0
Putative trans-sialidase, Group II OS	A0A2V2X0R8	1	1	0
Putative trans-sialidase, Group II OS	A0A2V2UWC5	0	1	0
Putative trans-sialidase, Group II OS	A0A2V2V198	0	1	0
Putative trans-sialidase, Group II OS	A0A2V2W7M2	0	1	0



Putative trans-sialidase, Group II OS	A0A2V2UXB7	0	1	0
Putative trans-sialidase, Group III OS	A0A2V2UWB4	1	1	0
Putative trans-sialidase, Group III OS	A0A2V2UU09	1	1	0
Putative trans-sialidase, Group III OS	A0A2V2WF29	5	1	0
Putative trans-sialidase, Group IV OS	A0A2V2WA28	0	1	0
Putative trans-sialidase, Group V OS	A0A2V2V0J7	1	1	0
Putative trans-sialidase, Group V OS	A0A2V2W4W1	0	1	0
Putative trans-sialidase, Group V OS	A0A2V2V1T3	1	1	0
Putative trans-sialidase, Group V OS	A0A2V2V1I8	1	1	0
Putative trans-sialidase, Group V OS	A0A2V2UJI3	1	1	0
Putative trans-sialidase, Group V OS	A0A2V2VTX9	1	1	0
Putative trans-sialidase, Group V OS	A0A2V2UPS0	0	1	0
Putative trans-sialidase, Group V OS	A0A2V2VUH3	0	1	0
Putative trans-sialidase, Group V OS	A0A2V2V1P3	2	1	0
Putative trans-sialidase, Group V OS	A0A2V2USE5	1	1	0
Putative trans-sialidase, Group V OS	A0A2V2UNW5	4	1	0
Putative trans-sialidase, Group V OS	A0A2V2UX92	0	1	0
Putative trans-sialidase, Group V OS	A0A2V2UUV3	1	1	0
Putative trans-sialidase, Group V OS	A0A2V2UG39	5	1	0
Putative trans-sialidase, Group V OS	A0A2V2W469	0	1	0
Putative trans-sialidase, Group V OS	A0A2V2VF15	0	1	0
Putative trans-sialidase, Group V OS	A0A2V2W6L0	0	1	0
Putative trans-sialidase, Group V OS	A0A2V2UNU3	0	1	0
Putative trans-sialidase, Group V OS	A0A2V2W3Y4	0	1	0
Putative trans-sialidase, Group V OS	A0A2V2UPP9	0	1	0
Putative trans-sialidase, Group V OS	A0A2V2WJG4	0	1	0
Putative trans-sialidase, Group V OS	A0A2V2VWL7	0	1	0
Putative trans-sialidase, Group V OS	A0A2V2XIN5	0	1	0

Putative trans-sialidase, Group V OS	A0A2V2ULE5	0	1	0
Putative trans-sialidase, Group V OS	A0A2V2WL79	0	1	0
Putative trans-sialidase, Group V OS	A0A2V2UT43	1	1	0
Putative trans-sialidase, Group V OS	A0A2V2W455	0	1	0
Putative trans-sialidase, Group V OS	A0A2V2XIR1	0	1	0
Putative trans-sialidase, Group V OS	A0A2V2WE09	0	1	0
Putative trans-sialidase, Group V OS	A0A2V2XIM4	0	1	0
Putative trans-sialidase, Group VI OS	A0A2V2UWQ5	0	1	0
Putative trans-sialidase, Group VI OS	A0A2V2VU44	0	1	0
Putative trans-sialidase, Group VI OS	A0A2V2VZR0	0	1	0
Putative trans-sialidase, Group VI OS	A0A2V2WWN4	0	1	0
Putative trans-sialidase, Group VI OS	A0A2V2UX55	1	1	0
Putative trans-sialidase, Group VI OS	A0A2V2ULP2	0	1	0
Putative trans-sialidase, Group VI OS	A0A2V2UXJ0	0	1	0
Putative trans-sialidase, Group VI OS	A0A2V2VU62	0	1	0
Putative trans-sialidase, Group VII OS	A0A2V2V3L7	1	1	0
Putative trans-sialidase, Group VII OS	A0A2V2UFH4	1	1	0
Putative trans-sialidase, Group VIII OS	A0A2V2WUF2	4	1	0
Putative trans-sialidase, Group VIII OS	A0A2V2URZ2	0	1	0
Putative trans-sialidase, Group VIII OS	A0A2V2WQD7	3	1	0
Putative trans-sialidase, Group VIII OS	A0A2V2XD60	0	1	0
Putative trans-sialidase, Group VIII OS	A0A2V2XFS7	2	1	0
Trans-sialidase (Fragment) OS	Q26887	3	1	0
Trans-sialidase OS	V5AMH3	0	1	0
Trans-sialidase OS	V5CIU5	3	1	0
Trans-sialidase OS	V5D006	2	1	0
Trans-sialidase OS	V5AN62	1	1	0
Trans-sialidase OS	V5B534	2	1	0

Trans-sialidase OS	V5AN87	1	1	0
Trans-sialidase OS	V5CYK7	1	1	0
Trans-sialidase OS	V5B4E0	0	1	0
Trans-sialidase OS	V5AU49	3	1	0
Trans-sialidase OS	V5CJC4	1	1	0
Trans-sialidase OS	V5CIW9	0	1	0
Trans-sialidase OS	V5BFX6	0	1	0
Trans-sialidase OS	V5AJR1	0	1	0
Trans-sialidase OS	V5AT18	0	1	0
Trans-sialidase OS	V5AQU8	0	1	0
Trans-sialidase-like protein OS	A4GWE6	0	1	0
Trans-sialidase, putative (Fragment) OS	Q4DAA5	2	1	0
Trans-sialidase, putative OS	Q4D095	3	1	0
Trans-sialidase, putative OS	Q4DDR3	1	1	0
Trans-sialidase, putative OS	Q4DIE5	0	1	0
Trans-sialidase, putative OS	Q4D110	0	1	0
Trans-sialidase, putative OS	Q4D2L1	0	1	0
Trans-sialidase, putative OS	Q4DD87	2	1	0
Trans-sialidase, putative OS	Q4D6S1	4	1	0
Trans-sialidase, putative OS	Q4DE13	0	1	0
Trans-sialidase, putative OS	Q4DGZ2	0	1	0
Trans-sialidase, putative OS	Q4CZ96	0	1	0
Trans-sialidase, putative OS	Q4D6J3	0	1	0
Trans-sialidase, putative OS	K2MUG2	0	1	0
Trans-sialidase, putative OS	Q4D5B9	0	1	0
Putative trans-sialidase OS	A0A2V2W3P7	1	0	0
Putative trans-sialidase, Group V OS	A0A2V2WW02	1	0	0
Putative trans-sialidase, Group V OS	A0A2V2V938	4	0	0

Putative trans-sialidase, Group V OS	A0A2V2VSJ9	2	0	0
Putative trans-sialidase, Group V OS	A0A2V2V3M2	1	0	0
Putative trans-sialidase, Group VI OS	A0A2V2XJN6	1	0	0
Putative trans-sialidase, Group VI OS	A0A2V2UXG2	1	0	0
Putative trans-sialidase, Group VIII OS	A0A2V2UUT5	1	0	0
Putative trans-sialidase, Group VIII OS	A0A2V2V2P3	1	0	0
Trans-sialidase OS	V5BQA7	3	0	0
Trans-sialidase OS	V5A2Q8	1	0	0
Trans-sialidase OS	V5ANI3	3	0	0
Trans-sialidase OS	V5B2F2	1	0	0
Trans-sialidase, putative (Fragment) OS	K2N470	1	0	0
Trans-sialidase, putative (Fragment) OS	K2M2T7	1	0	0
Trans-sialidase, putative OS	Q4DUP2	1	0	0
Trans-sialidase, putative OS	Q4D1E7	1	0	0

**APPENDIX I: GP63 FAMILY MEMBERS IDENTIFIED IN THE TCT-SECR AND IN THE IB4-LECTIN COLUMN FRACTIONS,  $\alpha$ -GAL(-) AND  $\alpha$ -GAL(+), FROM *T. CRUZI* Y STRAIN. VALUES ARE EXPRESSED AS AVERAGE OF NORMALIZED WEIGHTED SPECTRUM COUNTS.**

Identified Proteins	Accession Number	TCT Secr	$\alpha$ -Gal(-)	$\alpha$ -Gal(+)
		Y	(FT)	(EL)
			Y	Y
Putative surface protease GP63 OS	A0A2V2WGP4	6	6	0
Putative surface protease GP63 OS	A0A2V2XEP8	6	5	0
Putative surface protease GP63 OS	A0A2V2W180	4	4	0
Putative surface protease GP63 OS	A0A2V2VVN8	3	4	0
Putative surface protease GP63 OS	A0A2V2WK16	3	4	0
Group of Putative surface protease GP63 OS	A0A2V2WXU3 (+1)	8	4	0
Putative surface protease GP63 OS	A0A2V2VEX2	4	3	0
Putative surface protease GP63 OS	A0A2V2VBH2	4	3	0
Putative surface protease GP63 OS	A0A2V2UG46	3	3	0
Surface protease GP63, putative OS	Q4DHC2	4	3	0
Putative surface protease GP63 OS	A0A2V2WMB5	3	3	0
Putative surface protease GP63 OS	A0A2V2WW17	4	3	0
Putative surface protease GP63 OS	A0A2V2UHN1	4	2	0
Surface protease GP63, putative OS	Q4CWX0	3	2	0
Putative surface protease GP63 OS	A0A2V2VBG2	3	2	0
Putative surface protease GP63 OS	A0A2V2VLZ0	0	2	0
Putative surface protease GP63 OS	A0A2V2V7L6	0	2	0
Putative surface protease GP63 OS	A0A2V2VDF6	0	1	0
Putative surface protease GP63 OS	A0A2V2VA29	0	1	0
Group of Putative surface protease GP63 OS	A0A2V2W871 (+1)	0	1	0

Group of Putative surface protease GP63 OS	A0A2V2V4Z4 (+1)	0	1	0
Group of Putative surface protease GP63 OS	A0A2V2W9Y8 (+1)	0	1	0

**APPENDIX J: : TcMUC II FAMILY MEMBERS IDENTIFIED IN THE TCT-SECR AND IB-4 LECTIN COLUMN FRACTIONS,  $\alpha$ -GAL(-) AND  $\alpha$ -GAL(+), FROM *T. CRUZI* CLB STRAIN. VALUES ARE EXPRESSED AS AVERAGE OF NORMALIZED WEIGHTED SPECTRUM COUNTS.**

Identified Proteins	Accession Number	TCT Secr	$\alpha$ -Gal(-)	$\alpha$ -Gal(+)
		CLB	(FT)	(EL)
			CLB	CLB
Putative mucin TcMUCII OS	A0A2V2WR81_TRYCR	2	5	49
Cluster of Mucin TcMUCII, putative OS	Q4E056_TRYCC [3]	3	4	41
Cluster of Mucin TcMUCII, putative OS	Q4CZ01_TRYCC [2]	3	3	37
Mucin TcMUCII, putative OS=	Q4CYF9_TRYCC	2	2	33
Cluster of Mucin TcMUCII, putative OS=	Q4CVM7_TRYCC [6]	4	11	28
Mucin TcMUCII, putative OS	Q4D1J6_TRYCC	2	1	25
Cluster of Putative mucin TcMUCII OS	A0A2V2W2D1_TRYCR [3]	2	2	21
Mucin TcMUCII, putative OS	Q4DIF2_TRYCC	1	1	21
Mucin TcMUCII, putative OS	Q4DKJ4_TRYCC (+1)	1	1	21
Mucin TcMUCII, putative OS	Q4DM13_TRYCC	0	0	21
Putative mucin TcMUCII OS	A0A2V2XHF8_TRYCR	1	1	20
Putative mucin TcMUCII OS	A0A2V2W0T6_TRYCR	0	0	17
Putative mucin TcMUCII OS	A0A2V2XH36_TRYCR	2	0	17
Putative mucin TcMUCII OS	A0A2V2WWP4_TRYCR	2	4	16
Putative mucin TcMUCII OS	A0A2V2WUP0_TRYCR	0	3	16
Putative mucin TcMUCII OS	A0A2V2XGB5_TRYCR	0	2	16
Putative mucin TcMUCII OS	A0A2V2WHE6_TRYCR	0	1	16
Cluster of Putative mucin TcMUCII OS	A0A2V2W6K6_TRYCR [3]	3	2	16
Putative mucin TcMUCII OS	A0A2V2XIF6_TRYCR	2	5	16
Putative mucin TcMUCII OS	A0A2V2W6Q1_TRYCR	0	0	8
Mucin TcMUCII, putative OS	Q4E463_TRYCC	0	0	8

Mucin TcMUCII, putative OS	Q4DXZ9_TRYCC	1	1	8
Mucin TcMUCII, putative OS	Q4CMK8_TRYCC	1	0	8
Mucin TcMUCII, putative OS	Q4E3V3_TRYCC	0	0	8
Cluster of Mucin TcMUCII, putative OS	Q4DU44_TRYCC [2]	0	1	0
Cluster of Mucin TcMUCII, putative OS	Q4E3E1_TRYCC [3]	1	7	0
Cluster of Mucin TcMUCII, putative OS	Q4DTB6_TRYCC [2]	0	0	0
Cluster of Putative mucin TcMUCII OS	A0A2V2W6F4_TRYCR [4]	1	1	0
Cluster of Putative mucin TcMUCII OS	A0A2V2W0S8_TRYCR [3]	1	0	0
Cluster of Putative mucin TcMUCII OS	A0A2V2X7L6_TRYCR [3]	0	1	0
Cluster of Putative mucin TcMUCII OS	A0A2V2X8S8_TRYCR [2]	3	2	0
Cluster of Putative mucin TcMUCII OS	A0A2V2WM81_TRYCR [3]	0	1	0
Putative mucin TcMUCII OS	A0A2V2W5L6_TRYCR	1	4	0
Putative mucin TcMUCII OS	A0A2V2W8B5_TRYCR	1	0	0
Putative mucin TcMUCII OS	A0A2V2W3F2_TRYCR	0	1	0
Putative mucin TcMUCII OS	A0A2V2X8C2_TRYCR	0	1	0
Putative mucin TcMUCII OS	A0A2V2X4V6_TRYCR	1	1	0
Putative mucin TcMUCII OS	A0A2V2X3L4_TRYCR	0	1	0
Putative mucin TcMUCII OS	A0A2V2X537_TRYCR (+2)	0	4	0
Putative mucin TcMUCII OS	A0A2V2V976_TRYCR	0	1	0
Putative mucin TcMUCII OS	A0A2V2XML1_TRYCR	0	1	0
Putative mucin TcMUCII OS	A0A2V2WYV2_TRYCR	0	2	0
Putative mucin TcMUCII OS	A0A2V2WSK9_TRYCR (+1)	1	0	0
Putative mucin TcMUCII OS	A0A2V2WSQ6_TRYCR (+1)	2	7	0
Putative mucin TcMUCII OS	A0A2V2WXB6_TRYCR	0	1	0
Putative mucin TcMUCII OS	A0A2V2WRR3_TRYCR	1	0	0
Putative mucin TcMUCII OS	A0A2V2WQY3_TRYCR (+2)	2	1	0



Putative mucin TcMUCII OS	A0A2V2WMF2_TRYCR	1	1	0
Mucin TcMUCII, putative OS	Q4CWZ6_TRYCC	2	0	0
Mucin TcMUCII, putative OS	Q4CX28_TRYCC	1	0	0
Mucin TcMUCII, putative OS	Q4DXA0_TRYCC	0	1	0
Mucin TcMUCII, putative OS	Q4DIE3_TRYCC	2	6	0
Mucin TcMUCII, putative OS	Q4DP79_TRYCC	1	0	0
Mucin TcMUCII, putative OS	Q4D7L0_TRYCC	0	1	0
Mucin TcMUCII, putative OS	Q4DFV4_TRYCC	1	1	0
Mucin TcMUCII, putative OS	Q4DFV7_TRYCC	1	1	0
Mucin TcMUCII, putative OS	Q4DJR8_TRYCC	1	0	0
Mucin TcMUCII, putative OS	Q4CS53_TRYCC	1	0	0
Mucin TcMUCII, putative OS	Q4E4X7_TRYCC	2	6	0
Mucin TcMUCII, putative OS	Q4E2B0_TRYCC	2	2	0
Mucin TcMUCII, putative OS	Q4E2C3_TRYCC	1	1	0
Mucin TcMUCII, putative OS	Q4DM06_TRYCC	0	1	0

**APPENDIX K: MASP FAMILY MEMBERS IDENTIFIED IN THE TCT-SECR AND IN THE IB4-LECTIN COLUMN FRACTIONS,  $\alpha$ -GAL(-) AND  $\alpha$ -GAL(+), FROM *T. CRUZI* CLB STRAIN. VALUES ARE EXPRESSED AS AVERAGE OF NORMALIZED WEIGHTED SPECTRUM COUNTS.**

Identified Proteins	Accession Number	TCT Secr	$\alpha$ -Gal(-)	$\alpha$ -Gal(+)
		CLB	(FT)	(EL)
			CLB	CLB
Cluster of Mucin-associated surface protein (MASP) OS	A0A2V2W7A5_TRYCR [10]	3	10	0
Cluster of Mucin-associated surface protein (MASP) OS	A0A2V2WXA7_TRYCR [26]	2	10	0
Cluster of Mucin-associated surface protein (MASP) OS	A0A2V2WP56_TRYCR [5]	1	8	0
Cluster of Mucin-associated surface protein (MASP), putative OS	Q4D9A4_TRYCC [2]	2	8	0
Mucin-associated surface protein (MASP) OS	A0A2V2XJW9_TRYCR	1	7	0
Mucin-associated surface protein (MASP), putative OS	Q4D521_TRYCC	1	6	0
Cluster of Mucin-associated surface protein (MASP) OS	A0A2V2W3E2_TRYCR [17]	2	5	0
Cluster of Mucin-associated surface protein (MASP), putative OS	Q4DX99_TRYCC [22]	2	5	0
Mucin-associated surface protein (MASP) OS	A0A2V2W137_TRYCR	1	3	0
Mucin-associated surface protein (MASP) OS	A0A2V2X5L7_TRYCR (+1)	1	2	0
Mucin-associated surface protein (MASP) OS	A0A2V2XIH9_TRYCR (+1)	0	2	0
Mucin-associated surface protein (MASP), putative OS	Q4DT31_TRYCC	0	2	0
Mucin-associated surface protein (MASP), putative OS	Q4E1Y4_TRYCC	0	2	0
Mucin-associated surface protein (MASP), putative OS	Q4CVH5_TRYCC	0	2	0
Mucin-associated surface protein (MASP), putative OS	Q4E3E0_TRYCC	1	2	0

Mucin-associated surface protein (MASP), putative OS	Q4CVA6_TRYCC	0	2	0
Cluster of Mucin-associated surface protein (MASP) OS	A0A2V2XAR2_TRYCR [21]	1	2	0
Cluster of Mucin-associated surface protein (MASP) OS	A0A2V2XPL1_TRYCR [2]	0	2	0
Cluster of Mucin-associated surface protein (MASP) OS	A0A2V2XG47_TRYCR [3]	1	2	0
Cluster of Mucin-associated surface protein (MASP), putative OS	Q4CX27_TRYCC [11]	1	2	0
Cluster of Mucin-associated surface protein (MASP), putative OS	Q4DE04_TRYCC [13]	1	2	0
Cluster of Mucin-associated surface protein (MASP), putative OS	Q4DXA2_TRYCC [2]	0	2	0
Cluster of Mucin-associated surface protein (MASP), putative OS	Q4D4B2_TRYCC [2]	0	2	0
Cluster of Mucin-associated surface protein (MASP), putative OS	Q4E493_TRYCC [15]	2	2	0
Cluster of Mucin-associated surface protein (MASP), putative OS	Q4CR59_TRYCC [2]	1	2	0
Mucin-associated surface protein (MASP) OS	A0A2V2WD41_TRYCR	0	1	0
Mucin-associated surface protein (MASP) OS	A0A2V2WA58_TRYCR	1	1	0
Mucin-associated surface protein (MASP) OS	A0A2V2W7Y9_TRYCR	1	1	0
Mucin-associated surface protein (MASP) OS	A0A2V2W5V7_TRYCR	0	1	0
Mucin-associated surface protein (MASP) OS	A0A2V2XA41_TRYCR	0	1	0
Mucin-associated surface protein (MASP) OS	A0A2V2X506_TRYCR (+1)	0	1	0
Mucin-associated surface protein (MASP) OS	A0A2V2XAV0_TRYCR	1	1	0
Mucin-associated surface protein (MASP) OS	A0A2V2X4B4_TRYCR	0	1	0
Mucin-associated surface protein (MASP) OS	A0A2V2V8I6_TRYCR	1	1	0
Mucin-associated surface protein (MASP) OS	A0A2V2XKJ8_TRYCR	0	1	0
Mucin-associated surface protein (MASP) OS	A0A2V2WTH1_TRYCR	1	1	0

Mucin-associated surface protein (MASP), putative OS	Q4CSJ9_TRYCC	0	1	0
Mucin-associated surface protein (MASP), putative OS	Q4E455_TRYCC	2	1	0
Mucin-associated surface protein (MASP), putative OS	Q4DLD3_TRYCC	0	1	0
Mucin-associated surface protein (MASP), putative OS	Q4DYF1_TRYCC	0	1	0
Mucin-associated surface protein (MASP), putative OS	Q4E194_TRYCC	0	1	0
Mucin-associated surface protein (MASP), putative OS	Q4DU24_TRYCC	0	1	0
Mucin-associated surface protein (MASP), putative OS	Q4E3E7_TRYCC	0	1	0
Mucin-associated surface protein (MASP), putative OS	Q4DR50_TRYCC	0	1	0
Mucin-associated surface protein (MASP), putative OS	Q4DZS8_TRYCC	0	1	0
Mucin-associated surface protein (MASP), putative OS	Q4DGC2_TRYCC	1	1	0
Mucin-associated surface protein (MASP), putative OS	Q4CQC5_TRYCC	1	1	0
Cluster of Mucin-associated surface protein (MASP) OS	A0A2V2WCW7_TRYCR [5]	0	1	0
Cluster of Mucin-associated surface protein (MASP) OS	A0A2V2WWT4_TRYCR [5]	0	1	0
Cluster of Mucin-associated surface protein (MASP) OS	A0A2V2WYN7_TRYCR [3]	0	1	0
Cluster of Mucin-associated surface protein (MASP) OS	A0A2V2XM03_TRYCR [2]	0	1	0
Cluster of Mucin-associated surface protein (MASP), putative (Fragment) OS	Q4CNN7_TRYCC [2]	1	1	0
Cluster of Mucin-associated surface protein (MASP), putative OS	Q4D843_TRYCC [3]	1	1	0
Cluster of Mucin-associated surface protein (MASP), putative OS	Q4D953_TRYCC [6]	0	1	0
Mucin-associated surface protein (MASP) OS	A0A2V2VR30_TRYCR	1	0	0
Mucin-associated surface protein (MASP) OS	A0A2V2XMK1_TRYCR	1	0	0
Mucin-associated surface protein (MASP), putative OS	Q4DQ99_TRYCC	1	0	0
Mucin-associated surface protein (MASP), putative OS	Q4DQW7_TRYCC	1	0	0

Cluster of Mucin-associated surface protein (MASP) OS	A0A2V2XM45_TRYCR [4]	2	0	0
---	-------------------------	---	---	---

**APPENDIX L: TS FAMILY MEMBERS IDENTIFIED IN TCT-SECR AND IN THE IB4-LECTIN COLUMN FRACTIONS,  $\alpha$ -GAL(-) AND  $\alpha$ -GAL(+), FROM CLB STRAIN. VALUES ARE EXPRESSED AS AVERAGE OF NORMALIZED WEIGHTED SPECTRUM COUNTS.**

Identified Proteins	Accession Number	TCT Secr	$\alpha$ -Gal(-)	$\alpha$ -Gal(+)
		CLB	(FT)	(EL)
			CLB	CLB
Cluster of Putative trans-sialidase, Group II OS	A0A2V2W9S6_TRYCR [175]	5	70	0
Cluster of Trans-sialidase, putative OS	Q4DVJ1_TRYCC [6]	5	16	0
Cluster of Trans-sialidase, putative OS	Q4CTX4_TRYCC [2]	0	8	0
Trans-sialidase, putative OS	Q4DV16_TRYCC	0	3	0
Cluster of Trans-sialidase OS	Q26969_TRYCR [20]	1	2	0
Cluster of Trans-sialidase, putative OS	Q4DH92_TRYCC [2]	0	1	0
Cluster of Trans-sialidase, putative OS	Q4DV17_TRYCC [2]	0	1	0
Cluster of Trans-sialidase, putative OS	Q4E026_TRYCC [2]	1	1	0
Putative trans-sialidase, Group V OS	A0A2V2WW02_TRYCR	0	1	0
Trans-sialidase, putative OS	Q4CQL8_TRYCC	0	1	0
Trans-sialidase, putative OS	Q4D9H3_TRYCC	0	1	0
Cluster of Trans-sialidase, putative OS	Q4DA40_TRYCC [71]	1	0	0

**APPENDIX M: GP63 FAMILY MEMBERS IDENTIFIED IN THE TCT-SECR AND IN THE IB4-LECTIN COLUMN FRACTIONS,  $\alpha$ -GAL(-) AND  $\alpha$ -GAL(+), FROM *T. CRUZI* CLB STRAIN. VALUES ARE EXPRESSED AS AVERAGE OF NORMALIZED WEIGHTED SPECTRUM COUNTS.**

Identified Proteins	Accession Number	TCT Secr	$\alpha$ -Gal(-)	$\alpha$ -Gal(+)
		CLB	(FT)	(EL)
			CLB	CLB
Cluster of Putative surface protease GP63 OS	A0A2V2XEP8_TRYCR [2]	2	1	0
Cluster of Putative surface protease GP63 OS	A0A2V2VVN8_TRYCR [15]	1	1	0
Cluster of Putative surface protease GP63 OS	A0A2V2WME9_TRYCR [34]	0	1	0

## VITA

Nasim Karimi Hosseini was born in July 29 1981, in Mashhad, Iran. She graduated from Islamic Azad University, Shahroud in 2002 with AAC in Medical Laboratory Science. She worked in Emergency laboratory of Mashhad Ghaem Hospital, as a Laboratory technician from 2002 to 2003. She also worked in Mashhad Aria Laboratory as in sections of Hematology, Parasitology, and Reception from 2003 to 2010, while she achieved her BSc in Medical Laboratory science at Mashhad Pirapezeshki University in 2009. She also worked in Mashhad Nezhadhossein Laboratory as in Immunology, Biochemistry, and Parasitology sections for one year from 2009. She achieved her MSc in Immunobiology at Universiti Putra Malaysia (UPM) in 2014. Afterwards, she worked as a research assistant for three months at University Kebangsaan Malaysia in Social sciences and Humanity field. She was accepted by the doctoral program in Biological Sciences at the University of Texas at El Paso (UTEP), 2015. She has been teaching since then in Topics in study of life I, Molecular cell biology, and Immunology. She has been awarded Frank B. Cotton Trust Scholarship, Office of Scholarships, UTEP, 2017 and 2018, participated in several conferences: Oral presenter: NeuroFair 2013 symposium, UPM 2013, Poster presenter: 9th International Symposium on Antimicrobial Agents & Resistance, 2013, 3M thesis presenter: UPM, 2013, Poster presentation: at Gordon Research Conference (GRC), 2018, Poster presentation: at GRC, and GRS, 2019. Also, she has published two manuscripts as first author and two as co-author. She has seven more under review as first- and co-author to be published soon.

Permanent address: 6941 Bruce Bissonette Dr.

El Paso, Texas, 79912

This dissertation was typed by Nasim Karimi Hosseini and edited by Dr. Igor C. Almeida.